Effect of elevated CO_2 on marine bacterioplankton and biogeochemical processes

Michael Joseph Maguire

A thesis submitted to Newcastle University in partial fulfilment of the requirements for the degree of

Doctor of Philosophy

AUTHORS DECLARATION

I am the sole author of this thesis and have consulted all of the references cited either in full or abstract form. The work reported was all carried out by myself, with the exception of that performed by other members of the consortia in the Bergen mesocosm project as acknowledged within the text.

None of the work discussed in this thesis has previously been submitted for a higher degree. This programme of advanced study was financed with the aid of a studentship from the Natural Environment Research Council.

Michael Maguire

Table of Contents

List of Figures

List of tables.

List of equations

List of abbreviations

AAnPs	aerobic anoxygenic phototrophs
ADP	adenosine diphosphate
AMO	ammonia monooxygenase enzyme
amoA	ammonia monooxygenase gene
ANOVA	analysis of variance
ANOSIM	analysis of similarities
AOB	ammonia oxidising bacteria
AT	adenosine thymine
ATP	adenosine triphosphate
BLAST	basic local alignment search tool
BLASTn	BLAST search nucleotide sequences
BLASTx	BLAST search protein sequences
bp	base pair
C	centigrade
CA	carbonic anhydrase
CCM	carbon concentrating mechanisms
cDNA	complementary DNA
CO	Carbon monoxide
CO_2(aq)	dissolved carbon dioxide
CO_2	carbon dioxide
CO_3^{2-}	carbonate
Ct	threshold cycle
D	day
DGGE	denaturing gradient gel electrophoresis
DMS	dimethyl sulphide
DMSP	dimethylsulphoniopropionate
DOM	dissolved organic matter
DNA	deoxyribonucleic acid
dNTP	deoxynucleotide triphosphate
DIC	dissolved inorganic carbon
DIN	dissolved inorganic nitrate
DOC	dissolved organic carbon
dsDNA	double stranded DNA
EDTA	ethylenediaminetetraacetic acid
g	gram
GC	guanine cytosine
gDNA	genomic DNA
HAB	harmful algal bloom
$HCO3^-$	bicarbonate
Hr	hour
IPCC	Intergovernmental Panel on Climate Change
ISAMS	integrated science assessment model
KEGGs	Kyoto encyclopaedia of genes and genomes
l	litre
kg	kilogram
L	log
m	metre
M	molar
MDA	multiple displacement amplification

MEGAN	metagenome analyzer
mg	milligram
MG-RAST	metagenomic rapid annotation by subsystems technology
ml	millilitre
mol	moles
Mya	million years ago
N	number
NADP+	oxidised nicotinamide adenine dinucleotide phosphate
NADPH	reduced nicotinamide adenine dinucleotide phosphate
ng	nanogram
nm	nanometre
Ω	saturation state of seawater for a mineral
OTU	operational taxonomic unit
pCO_2	partial pressure of carbon dioxide
PCR	polymerase chain reaction
PeECE	Pelagic ecosystem CO_2-enrichment study
pers. comm.	personal communication
pH	potentiometric hydrogen ion concentration
pKa	logarithmic measure of the acid dissociation constant
PIC	particulate inorganic carbon
pmol	picomoles
POC	particulate organic carbon
POM	particulate organic matter
PSI	photosystem 1
PSII	photosystem 2
ppm	parts per million
qRT-PCR	quantitative reverse transcription polymerase chain reaction
RCF	relative centrifugal force
RDP	ribosomal database project
RNA	ribonucleic acid
rrn operon	rRNA gene regions
rRNA	ribosomal RNA
rpm	revolutions per minute
RuBisCO	ribulose-1,5-bisphosphate carboxylase/oxygenase
s	second
SDS	sodium dodecyl sulphate
SEM	Scanning Electron Microscopy
SET	lysis buffer
sp.	Species
SRES	Special report on Emissions Scenarios
SYBR	fluorescent dye for staining nucleic acid
STAMP	statistical analysis of metagenomic profiles
t	time
Taq	DNA polymerase from Thermus aquaticus
TAE	buffer containing a mixture of Tris base, acetic acid and EDTA
T_m	melting temperature
tris	Tris (hydroxymethyl) aminomethane
µatm	microatmophere
µg	microgram
µl	microlitre
µm	micrometre
µM	micromole per litre

UV	Ultra Violet
WGA	Whole Genome Amplification
3GP	glyceraldehyde 3-phosphate
16S rRNA	prokaryotic small subunit rRNA

Acknowledgements

I would like to express my sincere gratitude to Prof Ian Head for his constant support, supervision and above all patience throughout this project. Ian was especially thorough in reading and constructively criticising the early drafts of this thesis. Many thanks also to Dr Neil Gray for his academic guidance and practical advice throughout the study period.

Fellow students and staff at Newcastle University where I undertook this work, were supportive and often an important source of academic, practical and administrative knowledge. Some of those particularly helpful during my research include Dr Angie Sherry, Dr Casey Hubert, Dr Russell Davenport, Mr Ian Waite and Mr Richard Swainsbury.

I am indebted to all those involved in the mesocosm experiment in Bergen, Norway for making the experiment both a great experience and a success in particularly, Dr Ian Joint for his leadership of the experiment and especially Dr Andy Whiteley for his practical advice with my experiments.

I acknowledge with thanks financial support from the Natural Environment Research Council (UK).

Abstract

It has been established that ocean acidification will adversely affect calcifying organisms but little is known about its effects on bacterioplankton and the biogeochemical processes which they catalyse. In this thesis, the impact these changes may have on microbialy driven processes is assessed through a mesocosm experiment conducted in a Norwegian fjord near Bergen in May 2006. Three mesocosms were bubbled with $CO_{2(g)}$ to simulate the predicted future conditions of rising atmospheric CO_2 concentrations (~760ppm, pH ~7.8), while another three were treated as controls and bubbled with ambient air to represent present day conditions (~380ppm, pH ~8.15). The mesocosms were amended with nitrate and phosphate [16:1] to stimulate a phytoplankton bloom and scientific measurements and analyses were conducted over a 23 day period. At the peak of the phytoplankton bloom chlorophyll-a concentration was ~34% higher under ambient CO_2 conditions compared to the high CO_2. This was reflected in the flow cytometry results which showed a significant decrease of coccolithophorid and picoeukaryote cell numbers in the high CO_2 treatment. Analysis of 16S rRNA gene clone libraries supported by qPCR data revealed that elevated CO_2 resulted in a sharp decline in *Roseobacter*-like bacteria from the *Alphaproteobacteria* which are significant consumers of the algal osmolyte dimethylsulphoniopropionate (DMSP). Stable isotope probing using ^{13}C labelled sodium bicarbonate revealed that the assimilation of dissolved inorganic carbon by *Roseobacter*-like bacteria is more prevalent than previously thought making them major contributors to global CO_2 fixation. Furthermore, metagenomic analysis of the ambient and high CO_2 libraries revealed a significant decrease in genes coding for DMSP demethylase in the high CO_2 metagenome. This gene is responsible for the catabolism of DMSP resulting in the eventual release of methanethiol, a source of reduced sulfur for marine bacteria. However, DMSP degradation may proceed down an alternate route known as the lyase pathway resulting in the release of the climatically active gas dimethylsulfide (DMS). In conclusion, the findings of this study strongly suggest that the subsequent decline in Roseobacter species will shift the balance in the degradation of DMSP in favour of the alternate lyase pathway resulting in increased production of DMS and a decrease in the concentration of methanethiol. It is believed that the consequent loss of fixed sulfur will affect ocean productivity and that global climate patterns may change due to the scattering of solar radiation by increased atmospheric sulfur.

1. Introduction

1.1 Ocean acidification

Ocean acidification is a term used to describe the direct consequence of increasing levels of atmospheric carbon dioxide (CO_2) altering the chemistry of the oceans. According to the National Oceanic and Atmospheric Administration (NOAA) atmospheric CO_2 levels have risen from 280 ppm in the 1700s to the current concentration of 398.0 ppm (February 2014). This increase is governed by two major anthropogenic forcing factors, the burning of fossil fuel for industrial processes and changes in farming practices such as land clearance for livestock (Raupach *et al.*, 2007). Atmospheric CO_2 levels are now at their highest for at least the past 650,000 years when they were between 180 to 300 ppm (Siegenthaler *et al.*, 2005, IPCC, 2007). This increase is now having a profound impact on global temperature as CO_2 retains infrared heat that would normally be radiated back into space and as a consequence the planet is getting warmer. According to the NASA Earth Observatory the global average surface temperature rose 0.6 to 0.9 °C between 1906 and 2005 (Riebeek, 2010) while climate model projections predict a further rise in global temperature of between 1.8 to 4.0 °C by the end of 2100 (IPCC, 2007).

Approximately one-third of the anthropogenic carbon emissions released have been absorbed by the oceans (Sabine *et al.*, 2004) which is expected to rise to ~90% by the end of the millennium (Archer *et al.*, 1998, Kleypas *et al.*, 2006). Currently, the oceans are absorbing around 22 million metric tons of CO_2 per day (Feely *et al.*, 2008) which has decreased seawater pH by 0.1 units since the industrial revolution (Feely *et al.*, 2004; Sabine *et al.*, 2004, Orr *et al.*, 2005). However, since the units on the pH scale are logarithmic this equates to a 33% increase in hydrogen ion (H^+) concentration which is expected to increase as ocean acidification models predict a further decrease in pH of 0.3–0.4 pH units by the end of the century (Houghton *et al.*, 2001).

1.2 Climate models

In 1992 the Intergovernmental Panel on Climate Change (IPCC) devised six emission scenarios (IS92a to f) based on assumptions regarding population growth,

social and economic development, land use, energy use and technological advances (Houghton *et al.*, 1992). IS92a and IS92b are middle of the range scenarios using a combination of fossil fuel and renewable energy resources with no new emission polices being implemented. IS92c and IS92d are best case scenarios with the high cost of gas and oil promoting investment in renewable energy. IS92e and IS92f are worse case scenarios with high population and plentiful fossil fuel availability leading to less investment in renewable energy. Of the proposed emission scenarios, IS92a has been widely accepted as a plausible framework in order to assess future uncertainties regarding greenhouse gas emission. Under the IS92a scenario, the population rises to 11.3 billion by 2100 with economic growth averaging 2.3% annually between 1990 and 2100. A mixture of conventional and renewable energy sources are used with CO_2 from burning fossil fuels increasing from 7.4 Gt in 1990 to 20.3 Gt in 2100, increasing atmospheric CO_2 concentration from 354 ppm to 723 ppm (Figure 1.1).

The IS92a scenario has been used in numerous climate model studies and is often referred to as the "business-as- usual" scenario. A recommendation by the 1994 IPCC evaluation of the usefulness of the IS92 scenarios stated that, "due to the high degree of uncertainty regarding future climate change, analysts should use the full range of IS92 emissions as input to climate models rather than a single scenario". The review concluded that the mere fact of IS92a being an intermediate or central CO_2 emissions scenario at the global level does not equate it with being the most likely scenario.

In 2000, the IPCC released a new set of scenarios in its third assessment report (Special Report on Emissions Scenarios - SRES) to analyse how driving forces could influence future emission outcomes and assess associated uncertainties (IPCC, 2000). Initially, four storylines (A1, A2, B1 and B2) were created which combined two sets of opposing tendencies: one set varying between strong economic values and strong environmental values, the other set between increasing globalization and increasing regionalization (IPCC, 2000). From these storylines, 40 equally valid scenarios were developed of which six were chosen to represent the uncertainties of future greenhouse

gas emissions. The six scenario groups (A1FI, A1B, A1T, A2, B1, B2) encompass demographic change, social and economic development and technological advances.

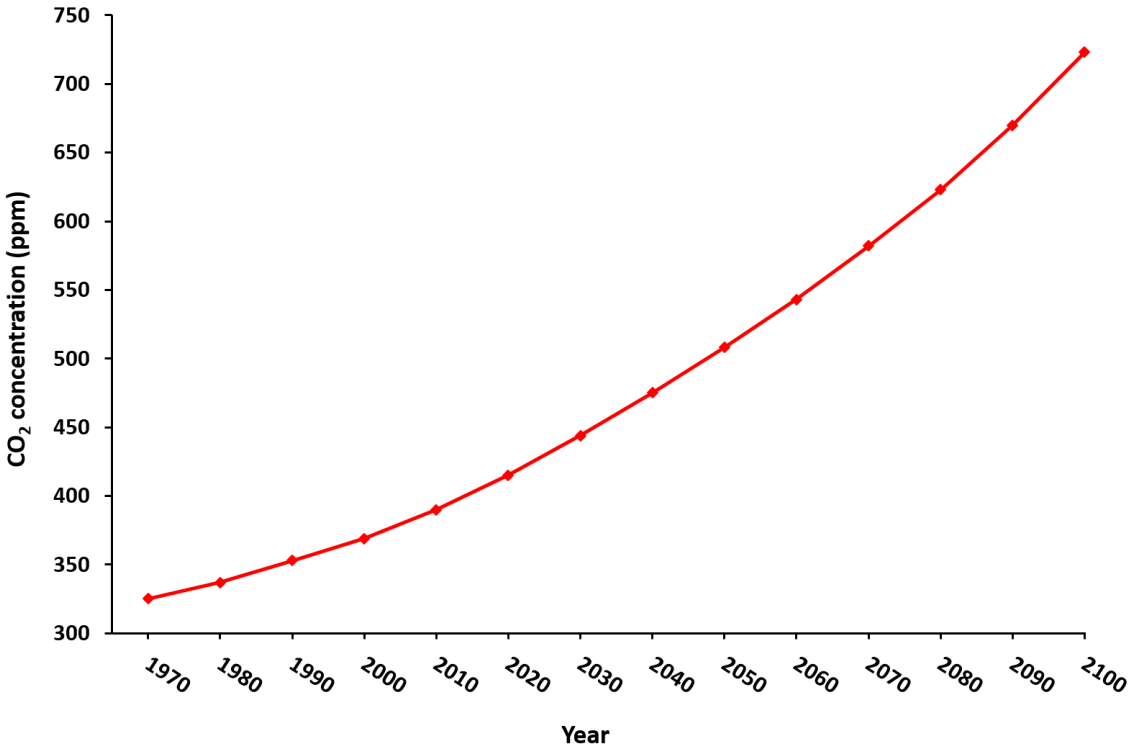

Figure 1.1 Projected CO_2 emissions for the IS92a "business as usual" scenario

The A1 scenarios depict a future world of rapid economic growth, a global population which peaks in the middle of the century to 9 billion then declines thereafter and the introduction of new efficient technologies. The A1 subgroups can be distinguished by their technological emphasis: fossil fuel intensive (A2F1), non-fossil energy sources (A1T) and a balance emphasis across all energy sources (A1B).

The A2 scenario describes a heterologous world of independently operating nations with an underlying theme of self-reliance and local identity. Populations are

continuously increasing reaching 15 billion by 2100. Economic development is regionally orientated and technological changes are more fragmented and slower than other scenarios.

The B1 scenario assumes continuing globalization and economic growth with the population rising to 9 billion by 2050 and then gradually declining. This world is more integrated and ecologically astute with emphasis on global solutions to economic, social, and environmental sustainability.

The B2 scenario shows a world with a continuously increasing global population reaching 10.5 billion by 2100. This emphasis of this scenario is based on local and regional development rather than global solutions to economic, social and environmental stability. Technological changes are more diverse than A1 and B1 scenarios though they are less rapid and more fragmented.

Based on the Integrated Science Assessment Model (ISAM) (Jain *et al.*, 1994) the projected 2100 atmospheric CO_2 levels for the emission scenarios range from 549 ppm (B1) to 970 ppm (A1FI) (Figure 1.2). This will greatly influence the global mean temperature which is predicted to increase in all scenarios ranging from 1.9 °C to 3.3 °C leading to a rise in sea level of between 55 – 70 cm (Strengers *et al.*, 2004).

The IPCC fifth assessment report dealing with the physical basis of climate change was released in September 2013 (Stocker *et al.*, 2013). To ensure accuracy the report was subjected to three rounds of reviews by academic and governmental reviewers worldwide in order to establish an objective and balanced assessment. The report stated that each of the last three decades had been progressively warmer than preceding decades since observations began in 1850. Human activities can account for all the observed warming (with a 95% certainty) and there is no evidence of a significant contribution from natural sources. As a consequence, sea level rise will proceed at a faster rate than what has been observed during the past 40 years with global sea rise from 2081 – 2100 being between 26 cm (low estimate) and 82cm (high estimate) depending on greenhouse emissions.

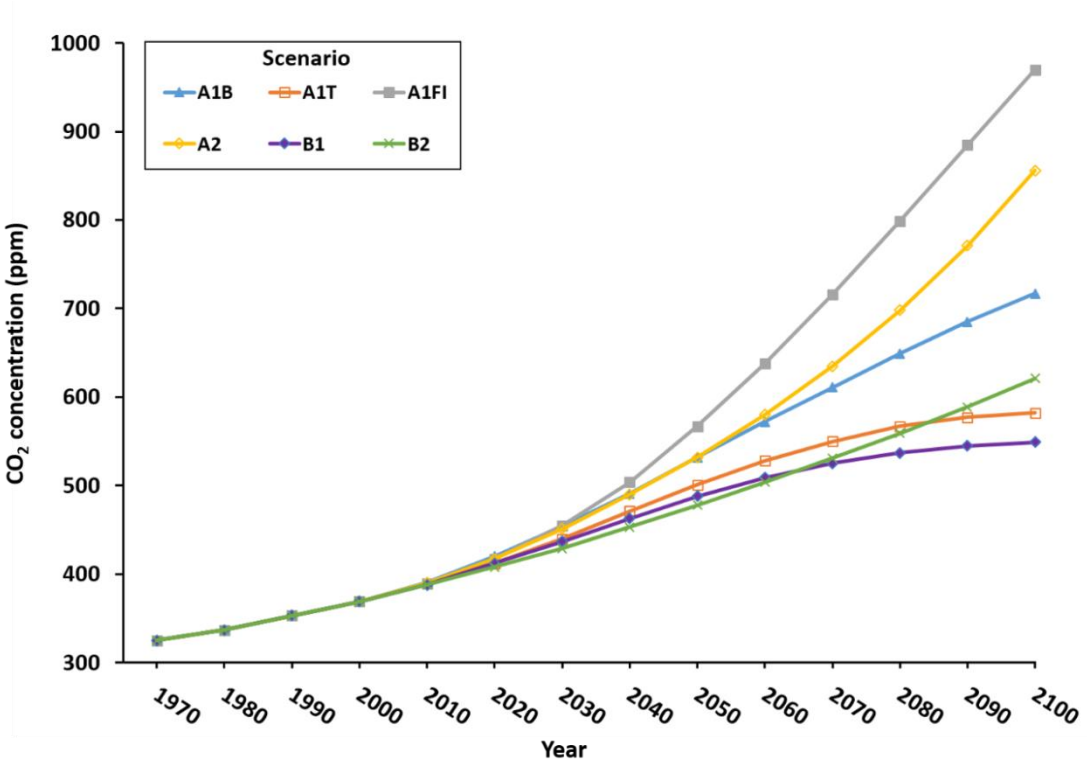

Figure 1.2 Predicted increase in atmospheric CO_2 concentration of six SRES scenarios using the ISAM carbon cycle model.

1.3 Carbon dioxide (CO_2)

Carbon dioxide is a colourless, odourless, non-flammable liquid gas which is heavier than air and soluble in water. The primary source of CO_2 is from volcanic emissions, mid-ocean ridges and degassing of unerupted magma beneath volcanoes. Global estimates of annual volcanic CO_2 output have been calculated at 0.26 Gt with minimum and maximum global estimates of 0.18 – 0.44 Gt per annum (Marty and Tolstikhin, 1998). This is a relatively modest output in comparison to the CO_2 emissions of light vehicles (3.0 Gt per year) and cement production (1.4 Gt per year) (Gerlach, 2011). In fact, volcanic CO_2 emissions are comparable to two dozen 1000 mega-watt coal-fired power stations which is approximately 2% of the world's coal-fired electricity generating capacity (Gerlach, 2011).

1.3.1 The carbon cycle

The carbon cycle is a sequence of events where atmospheric CO_2 exchanges rapidly with terrestrial systems and the oceans. In terrestrial ecosystems, plants use water and sunlight to assimilate CO_2 and convert it into organic carbon in a process known as photosynthesis. Carbon compounds are then transferred through the food chain to heterotrophic organisms via the consumption of plant biomass. Carbon (in the form of CO_2) is then returned to the atmosphere via respiration pathways of autotrophic and heterotrophic organisms or by the burning of organic matter such as forest fires and land clearance. Alternatively, it can be stored in the soil until it is returned to the atmosphere via soil respiration, washed into rivers and oceans or until it is available as fossil fuel for future combustion. Terrestrial carbon storage primarily occurs in forests with the sum of carbon living in terrestrial biomass and soils being three times greater than the CO_2 in the atmosphere (Dean and Gorham, 1998).

After the lithosphere, the oceans contain the greatest amount of carbon in the world sequestering 20 – 35% of anthropogenic CO_2 (Khatiwala *et al.*, 2009). Atmospheric CO_2 continuously exchanges with oceanic CO_2 in order to reach a state of equilibrium between the atmosphere and surface waters. Consequently it is the oceans which determine atmospheric CO_2 concentration, not vice versa (Falkowski *et al.*, 2000). However, the buffering capacity of the ocean is not finite as the availability of carbonate ions (CO_3^{2-}) will eventually limit how much bicarbonate (HCO_3^-) can be formed thereby decreasing the ability of the surface oceans to absorb CO_2 (Egleston *et al.*, 2010). The majority of anthropogenic CO_2 is found in the upper ocean with approximately 30% found at depths shallower than 200 m and almost 50% at depths above 400 m (Sabine *et al.*, 2004). CO_2 is more soluble in cold saline waters with the North Atlantic being a particularly strong sink region accounting for more than 40% of the global ocean CO_2 uptake (Takahashi *et al.*, 2002). In winter, these cold waters which are heavily enriched with dissolved organic carbon (DIC) sink to the ocean depths and flow southwards across the equator where they eventually enter the Antarctic circumpolar current. Here they mix with other deep water masses and move northwards filling the deep waters into the

Pacific and Indian oceans (Schmittner *et al.*, 2013). This mechanism of physical mixing known as the solubility pump is balanced when the waters from the ocean interior are brought back to the warm surface waters, decades to several hundred years later (Falkowski *et al.*, 2000).

In contrast, phytoplankton assimilate CO_2 or HCO_3^- via photosynthesis in order to promote the synthesis of organic compounds (equation 1.1). This mechanism known as the biological pump reduces the partial pressure of CO_2 in surface waters thereby promoting the absorption of atmospheric CO_2.

$$6CO_2 + 6H_2O + \text{light energy} \longrightarrow C_6H_{12}O_6 + 6O_2 \qquad [1.1]$$

After cell death the fixed CO_2 sinks into the interior of the ocean or is released as particulate organic carbon (POC) where the majority is oxidized through heterotrophic respiration and recirculated to the surface as DIC. The remaining organic carbon sinks to abyssal depths (4,000 – 6,000 m) and a small fraction reaches the deep ocean sediments where it can be buried for millennia (Solomon *et al.*, 2007). The biological pump is responsible for reducing the current atmospheric CO_2 concentration by 150 – 200 ppm as it exports approximately 11 – 18 Gt of organic carbon per year from surface water to the ocean interior (Falkowski *et al.*, 2000).

Phytoplankton also influence the carbon cycle by precipitating inorganic carbon as calcium carbonate ($CaCO_3$) for the formation of calcareous skeletons (calcification). This leads to a reduction in surface ocean DIC relative to the deep ocean and as a consequence is known as the carbonate cycle. There are two main forms of calcium carbonate which can be differentiated by their mineral structure and different solubility properties. Planktonic foraminifera and coccolithophores secrete shells made of calcite, whereas pteropods form shells made of aragonite which is ~50% more soluble in seawater than calcite (Mucci, 1983). Marine biogenic calcification is closely coupled to photosynthesis and respiration with $CaCO_3$ production being mostly limited to the upper photic zone (Brownlee and Taylor, 2002). Photosynthetic assimilation of CO_2 enhances calcification by shifting the carbonate equilibrium towards carbonate and increasing pH,

thereby increasing the saturation state of $CaCO_3$ (Gao *et al.*, 1993). Conversely, respiration acts in the opposite manner decreasing ocean pH and the saturation state of $CaCO_3$ thereby hampering the calcification process (De Beer and Larkum, 2001). Calcification is a major oceanic process through which carbon is stored in the open ocean, shallow seas and in sediments (Frankignoulle *et al.*, 1995). In the precipitation reaction the sum total of DIC is reduced but the remaining carbon is repartitioned resulting in $CO_{2(aq)}$ thereby increasing pCO_2 in the surface ocean (Ridgwell and Zeebe, 2005) For each mol of $CaCO_3$ precipitated, 0.6 mol of CO_2 is produced (equation 1.2) reducing seawater total alkalinity (TA) by two equivalents (Gattuso *et al.*, 1995).

$$Ca^{2+} + 2HCO_3^- \longrightarrow CaCO_3 + CO_2 + H_2O \qquad [1.2]$$

Conversely, the dissolution of $CaCO_3$ during rock weathering results in decreasing pCO_2 in the surface ocean (equation 1.3).

$$CO_2 + H_2O + CaCO_3 \longrightarrow Ca^{2+} + 2HCO_3^- \qquad [1.3]$$

Although the formation and burial of $CaCO_3$ provides a net sink for carbon, it is the balance between calcification and photosynthesis that determines whether calcifying organisms act as a sink (absorbing CO_2) or as a source of CO_2 to the atmosphere (Barker *et al.*, 2003). Calcifying organisms play an import ecological role in marine ecosystems which is evident from the vast calcite deposits found in geological records (Van de Waal *et al.*, 2013). The majority of $CaCO_3$ production is carried out by pelagic foraminifera and coccolithophores though coccolith calcite dominates the $CaCO_3$ in sediments as it dissolves less rapidly than foraminifera calcite (Broecker and Clark, 2009).

1.3.2 Greenhouse effect of CO_2

CO_2 is only one of several greenhouse gases in our atmosphere which include methane, ozone, nitrous oxide, halocarbons and water vapour. The primary effect of greenhouse gases is increased absorption of thermal radiation from the earth's surface thereby increasing the air temperature of the troposphere. Radiative forcing is a measure

of the influence a factor has in altering the balance of incoming and outgoing energy in the earth's atmosphere expressed in watts per square meter (W/m^2). The largest contribution of total radiative forcing caused by greenhouses gasses (excluding water vapour) is CO_2 which in 2011 was 1.68 W/m^2 (Figure 1.3). It was stated in the IPCC summary report for policy makers (Stocker *et al.*, 2013) that:

"Warming of the climate system is unequivocal and since the 1950s, many of the observed changes are unprecedented over decades to millennia. The atmosphere and ocean have warmed, the amounts of snow and ice have diminished, sea level has risen, and the concentration of greenhouse gases have increased".

Currently, the total level of radiative forcing is 2.3 W/m^2 which taking into account the surface area of the earth ($5.0x10^{14}$ m^2) gives a total warming effect of approximately 1150 terawatts – more than 76 times the worlds average rate of energy consumption which is currently about 15 terawatts.

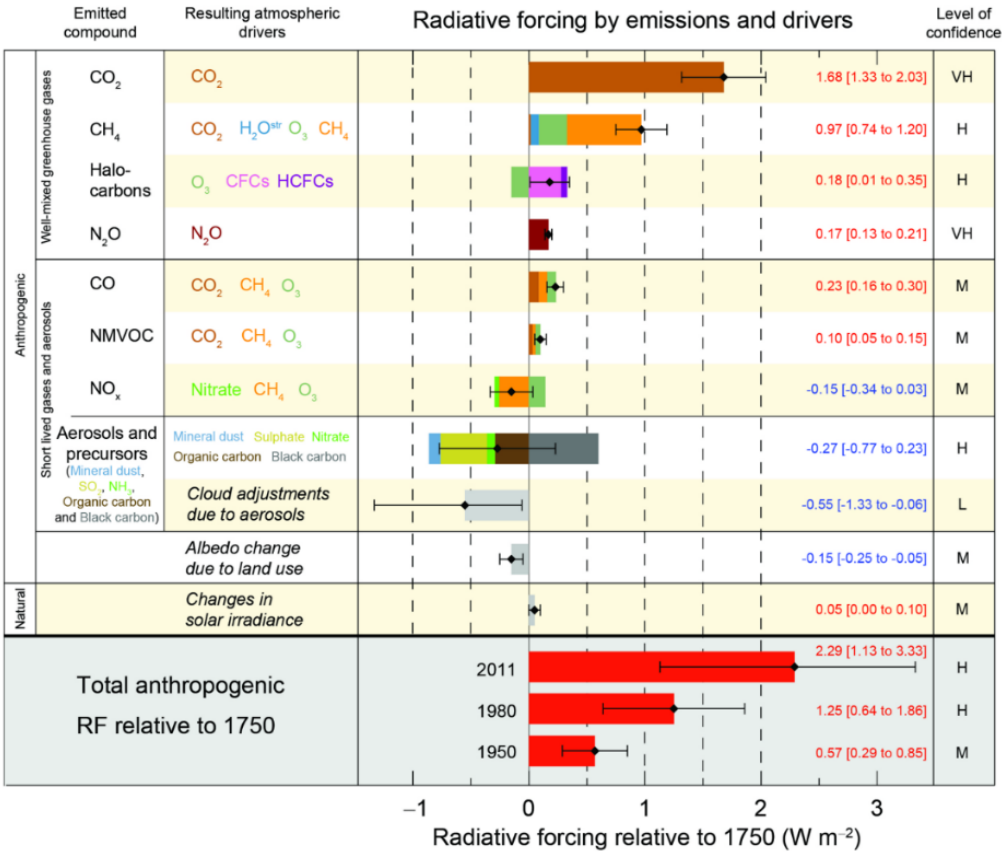

Figure 1.3 Radiative forcing estimates in 2011 relative to 1750 for the main drivers of climate change. Values are global average radiative forcing (RF14), partitioned according to the emitted compounds or processes that result in a combination of drivers. The best estimates of the net radiative forcing are shown as black diamonds with corresponding uncertainty intervals; the numerical values are provided on the right of the figure, together with the confidence level in the net forcing (VH – very high, H – high, M – medium, L – low, VL – very low). Figure obtained from IPCC (2013) Summary for Policymakers.

1.4 Impact of anthropogenic CO_2 on seawater carbonate chemistry

The inorganic carbon system is the most important chemical equilibria in the ocean as it is largely responsible for regulating the pH of seawater (Fabry *et al.*, 2008). Dissolved inorganic carbon is present in seawater in three forms; aqueous carbon dioxide, ($CO_{2(aq)}$) bicarbonate ions (HCO_3^-) and carbonate ions (CO_3^{2-}) all of which can interchange rapidly with each other to maintain chemical equilibrium (Johnson, 1982). When CO_2 dissolves in seawater, carbonic acid (H_2CO_3) is formed (equation 1.4). H_2CO_3 immediately dissociates releasing bicarbonate (HCO_3^-) and a proton (H^+)

(equation 1.5). Conversely, HCO_3^- can dissociate to carbonate ions and a proton (H^+) (equation 1.6). Both equations (1.5 and 1.6) have produced protons thereby reducing ocean pH. In an attempt to balance the equilibrium between HCO_3^- and CO_3^{2-} the excess H^+ is neutralized by interacting with carbonate ion to form another bicarbonate (equation 1.7).

$$CO_{2(aq)} + H_2O \rightleftarrows H_2CO_{3(aq)} \quad [1.4]$$

$$H_2CO_3 \rightleftarrows HCO_3^- + H^+ \quad [1.5]$$

$$HCO_3^- \rightleftarrows CO_3^{2-} + H^+ \quad [1.6]$$

$$CO_3^2 + H^+ \rightleftarrows HCO_3^- \quad [1.7]$$

Due to the natural buffering capacity of the ocean, absorption of CO_2 does not always result in the production of H^+ and a decrease in pH as CO_2 can be neutralized by reacting with CO_3^{2-} resulting in the production of $2HCO_3^-$ (equation 1.8).

$$CO_{2(aq)} + CaCO_3 + H_2O \rightleftarrows 2HCO_3^- + Ca^{2+} \quad [1.8]$$

The buffering capacity of the ocean is therefore dependent on the concentration of CO_3^{2-} and can be progressively reduced as more CO_2 is added to the system and CO_3^{2-} is consumed (Barker and Ridgwell, 2012). Due to the influx of anthropogenic CO_2 the carbonate system is rapidly changing leading to an increase of carbonic acid and bicarbonate ion concentration while decreasing the pH and carbonate ion concentration (Zeebe and Wolf-Gladrow, 2001). Currently, (pH 8.07) 91% of ocean DIC is in the form of bicarbonate ions, 8% is carbonate ions and 1% is carbonic acid. However, as more CO_2 is absorbed ocean pH will decrease further and the balance between the three DIC species will change (Figure 1.4). As a consequence, a decrease in ocean pH predicted by the SRES A2 scenario (pH 7.65 by 2100) would result in a 300% increase in carbonic acid concentration, a 9% increase in bicarbonate ion concentration and a 56% decrease in carbonate (Caldeira and Wickett, 2005, Royal Society, 2005).

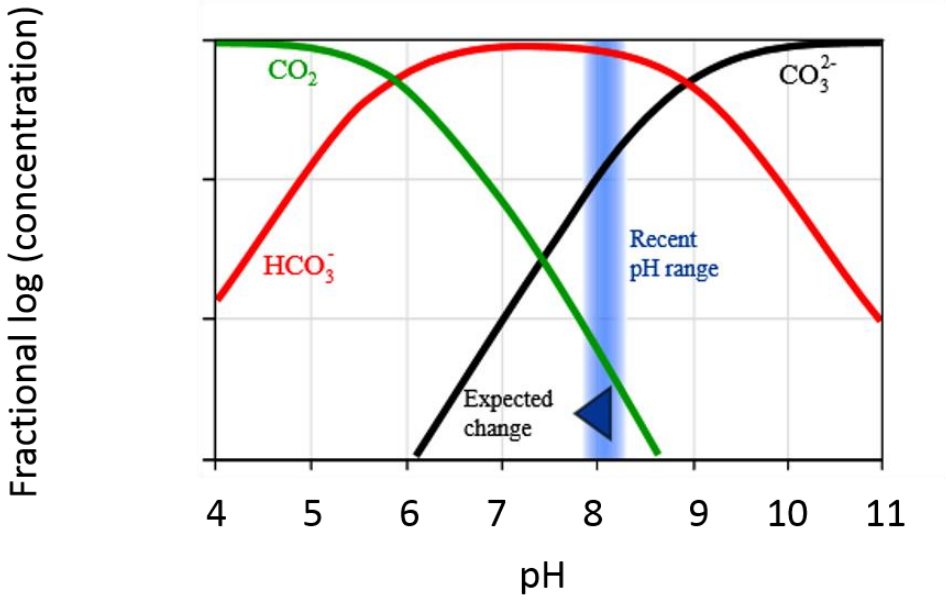

Figure 1.4 Bjerrum plot depicting the inter-relationship of relative proportions of carbonate species and pH. The shaded region indicates the narrow variation of pH observed at the present due to regional and seasonal factors Royal society (2005).

1.4.1 Impact of anthropogenic CO_2 on calcification

Calcium carbonate ($CaCO_3$) is a fundamental building block for numerous marine organisms which are critical for maintaining the biological diversity of the oceans. Organisms on higher trophic levels (including humans) rely on marine calcifiers for nutrition, shelter and their contribution in numerous biogeochemical cycles. For example, calcareous phytoplankton and zooplankton form the basis of the food chain for numerous commercial fish species and play crucial roles in carbon and sulfur cycles. Bivalve mollusks such as oysters, mussels, scallops and clams are economically important with the global harvest of shellfish estimated at 10 – 13 billion USD and representing 13 – 16% of total global seafood consumption (Parker *et al.*, 2013). Coral reefs which secrete copious amounts of calcium carbonate are among the most diverse and productive of marine ecosystems proving feeding grounds and nursery areas for marine species. Furthermore, they protect coastal regions by acting as natural breakwaters which dissipate wave energy and prevent coastal erosion.

However, calcium carbonate can also dissolve in seawater if the concentration of carbonate and calcium ions is below a critical level known as the saturation state. The saturation state of seawater in respect to calcite (Ω_{Calc}) and aragonite (Ω_{Arag}) can be defined as the product of the concentrations of dissolved calcium and carbonate ions in seawater divided by their product at equilibrium (equation 1.9).

$$\Omega_{Calc} = \frac{[Ca^{2+}]\,[CO_3^{2-}]}{K_{Calc}} \quad \text{and} \quad \Omega_{Arag} = \frac{[Ca^{2+}]\,[CO_3^{2-}]}{K_{Arag}} \qquad [1.9]$$

Where K_{Calc} and K_{Arag} ($mol^2\ Kg^{-2}$) are the apparent stoichiometric solubility products of calcite and aragonite in seawater. In the ocean Ca^{2+} is only weakly affected by the precipitation and dissolution of carbonate minerals and does not vary by more than 1.5%. Therefore, the degree of saturation of seawater in respect to calcite and aragonite is determined by variations in ratio of CO_3^{2-} from their respective stoichiometric solubility product (Feely *et al.*, 2004). Marine organisms that produce $CaCO_3$ inhabit regions above the calcite saturation horizon, where $CaCO_3$ can exist in solid form. In regions where Ω_{Calc} or Ω_{Arag} is > 1 seawater is supersaturated and the formation of shell is favoured. However if seawater is undersaturated ($\Omega < 1$) it is corrosive and calcium carbonate will dissolve. It is therefore highly probable that ocean acidification will decrease the saturation state of $CaCO_3$ and raise the saturation horizon closer to the surface. Acidification events are already appearing with seasonal upwells of undersaturated seawater with respect to aragonite ($\Omega < 1$) along the California coastline at pH 7.75 (Feely *et al.*, 2008).

Natural variability in ocean pH is also observed due to the changes in biological activities such as calcium carbonate precipitation and dissolution, nutrient utilization, respiration and photosynthesis (Schulz and Riebesell, 2013). Changes in seawater pH may also seasonal, differing from region to region with the highest variability being observed in low buffered eutrophic regions such as the Baltic Sea (Thomsen *et al.*, 2010).

The degree of severity that ocean acidification will have on calcification will depend largely on the form of mineral precipitated. It is expected, at least in the short term that calcitic plankton such as coccolithophorids and foraminifera will fare better as calcite undersaturation is predicted to lag behind that of aragonite by 50 – 100 years (Orr *et al.*, 2005). In fact, several research studies have reported that certain coccolithophores species fare better under elevated CO_2 conditions with increased calcification and net primary production (Iglesias-Rodriguez *et al.*, 2008; Shi *et al.*, 2009, Fukuda *et al.*, 2014).

Pteropods, the major planktonic producers of aragonite are found in high densities in polar and sub Polar Regions. Although they constitute only 6.5% of the total abundance density of grazers in the Southern Ocean, aragonite production constitutes 12% of the total carbon flux worldwide (Berner and Honjo, 1981). Pteropods are also important prey for larger zooplankton with some marine gastropods (e.g. Clione) preying exclusively on them. Fish, squid and birds also consume pteropods and they are a major food source for juvenile salmon (Hunt *et al.*, 2008; Karnovsky *et al.*, 2008, Mackas and Galbraith, 2011).

Laboratory experiments investigating the effects of ocean acidification in pteropods found they precipitate lower rates of $CaCO_3$, (Comeau *et al.*, 2010) exhibit shell malformation (Comeau *et al.*, 2010) and shell dissolution (Orr *et al.*, 2005) at reduced pH. However, similar results have recently been observed when analyzing freshly caught specimens from the Southern Ocean (Bednarsek *et al.*, 2012). The region sampled had a shallow aragonite saturation horizon ($\Omega Arag \approx 1$ at a depth of 200 m) due to upwelling of undersaturated deep waters combining with the upper mixed surface layer. Analysis of pteropod morphology revealed that juvenile specimens showed severe levels of dissolution over their entire shells, indicating that the periostracum (outer layer of the shell) provided little or no protection (Figure 1.5). Scanning electron microscopy (SEM) revealed that the amount of dissolution was comparable to a laboratory experiment in which pteropods were subjected to an 8 day incubation in aragonite saturation levels of 0.94 – 1.12. The researchers concluded that the detrimental effects

on calcification were partially due to oceanic absorption of anthropogenic CO_2 which is already impacting marine species long before aragonite undersaturation levels are reached (Bednarsek *et al.*, 2012).

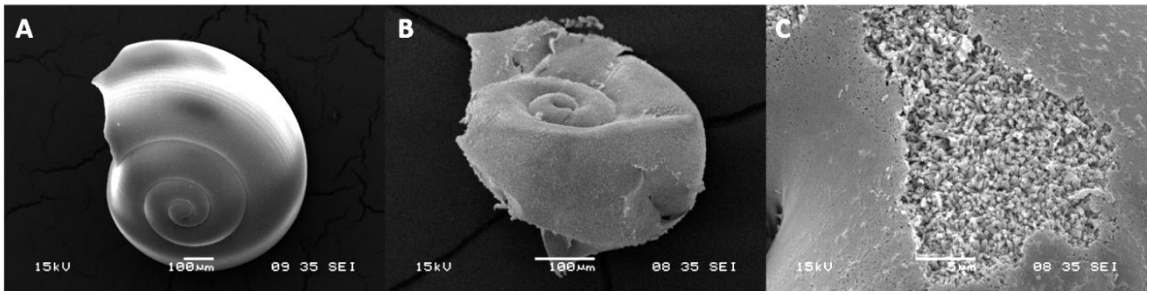

Figure 1.5 SEM images of juvenile pteropod *L. helicina antarctica* showing; intact organism without any shell dissolution, (A) dissolution and fragmentation of entire shell (B) dissolution of crossed-lamellar matrix (C). Periostracum has been removed from images B and C in order to show different levels of dissolution. Bednarsek *et al* (2012).

Although pteropods do not necessarily die as a direct result of their shells dissolving, it does increase their vulnerability to predation and infection which may reduce their numbers significantly (Comeau *et al.*, 2010). Therefore, the actual consequences of ocean acidification is that it will most likely alter the structure and productivity of primary and secondary planktonic producers which in turn affects the productivity of all other organisms in higher trophic levels. Biogeochemical cycles may also be compromised as pteropods play an important role in the carbonate cycle by balancing alkalinity budgets (Betzer *et al.*, 1984) and by their contribution to the vertical carbon flux (Francois *et al.*, 2002). Key processes in the sulfur cycle are conducted by calcareous marine phytoplankton as they assimilate sulfate from seawater and reduce it to a form that can be easily assimilated by other microorganisms at a less energetic cost (Kiene *et al.*, 1999; Simó, 2001, Malin, 2006). They also provide an important link between oceanic and atmospheric sulfur cycles through the release of dimethylsulfide (Lovelock *et al.*, 1972).

1.4.2 Other biological responses to ocean acidification

Primary production essentially supports all life in the ocean by converting inorganic carbon to organic carbon via photosynthesis. In the ocean, photosynthesis is mostly conducted by free-living phytoplankton such as coccolithophores, diatoms, dinoflagellates and cyanobacteria that inhabit the euphotic zone (Falkowski *et al.*, 1998). At the current surface ocean (pH ~8.07), CO_2 accounts for less than 1% in pelagic waters and it has been suggested that its supply can limit photosynthetic carbon fixation (Raven, 1993, Riebesell *et al.*, 1993). Furthermore, RuBisCO the key enzyme in carbon fixation has a low affinity for CO_2 and therefore its uptake is inefficient when concentrations are low. However, some phytoplankton species can alternately assimilate HCO_3^- and convert it to $CO_{2(aq)}$ via the enzyme carbonic anhydrase (Kaplan and Reinhold, 1999). In addition to carbonic anhydrase, numerous phytoplankton species possess carbon concentrating mechanisms (CCMs) which increase intracellular CO_2 concentrations to support photosynthetic carbon fixation (Nimer and Merrett, 1996; Iglesias-Rodriguez *et al.*, 1998, Giordano *et al.*, 2005). Naturally, these mechanisms come at an energetic cost to the organism and therefore elevated CO_2 could be beneficial to some phytoplankton species as it would reduce the metabolic cost of acquiring inorganic carbon and increase carbon fixation (Rost *et al.*, 2003; Riebesell, 2004, Engel *et al.*, 2005). It has been speculated that elevated CO_2 concentrations will have negligible effects on phytoplankton species which possess CCMs (McMinn, 2011, Brussaard *et al.*, 2013). However, at high CO_2 concentrations CCMs do not function correctly and they are expected to be down regulated when external CO_2 levels reach the required saturation state of RuBisCO (Chen and Gao, 2003; Rost *et al.*, 2003, Wu *et al.*, 2008, Hopkinson *et al.*, 2010). Numerous studies have been conducted to ascertain if elevated CO_2 increases primary production or growth, though the results have been controversial with the majority being conducted in the laboratory and therefore not accurately reflecting the natural environment (Wu *et al.*, 2008). Some investigations have shown positive responses to elevated CO_2 (Riebesell *et al.*, 1993; Hein and Sand-Jensen, 1997, Schippers *et al.*, 2004, Wu *et al.*, 2010) while others have shown negative or neutral responses (Fu *et al.*, 2007; Feng *et al.*, 2008, Gao *et al.*, 2012, Rokitta and Rost, 2012).

Although it is generally accepted that increased CO_2 can stimulate growth in some phytoplankton species it seems to be very species specific, dependent on the cells capability to actively assimilate HCO_3^- or CO_2 or the differing efficiencies in CCMs (Rost *et al.*, 2008, Wu *et al.*, 2008).

Hypercapnia is a condition where body fluid pH rapidly decreases due to excess carbon dioxide in the blood. As the oceans absorb more CO_2 it diffuses across biological membranes and equilibrates in intra and extracellular spaces dissolving in bodily fluids to form H^+ and HCO_3^- thereby decreasing internal pH. Marine organisms employ several mechanisms to regulate their internal pH: passive buffering of intra and extracellular compartments, active proton transport and metabolic production and consumption of protons (Michaelidis *et al.*, 2005). However, taxa with low buffering capacity that are less adept at controlling intracellular pH under elevated CO_2 conditions are likely to be more susceptible to extinction from hypercapnia (Knoll *et al.*, 2007, Kiessling and Simpson, 2011). Organisms with high metabolic lifestyles such as teleost fish and cephalopods are expected to be better equipped to cope with future ocean acidification as they possess more efficient acid-base regulation systems than invertebrates (Perry and Gilmour, 2006; Gutowska *et al.*, 2008, Widdicombe and Spicer, 2008, Melzner *et al.*, 2009). However, recent studies have found that elevated CO_2 can affect larval survival and growth in the estuarine fish *Menidia beryllina* (Baumann *et al.*, 2012) and produce severe tissue damage in larval Atlantic cod (Frommel *et al.*, 2012). Further effects include, diminished olfactory (Munday *et al.*, 2009, Dixson *et al.*, 2010) and auditory ability, (Simpson *et al.*, 2011) increased embryonic abnormalities, egg loss, visual hypersensitivity (Forsgren *et al.*, 2013) and enhanced otolith growth in larval white sea bass (Checkley *et al.*, 2009). In conclusion, it can be said that any organism exposed to pH values higher than which they evolved will require more energy for internal pH regulation thereby reducing energy available for maintenance, growth and reproduction (Williamson *et al.*, 2013).

Ocean acidification is not a singular consequence of anthropogenic CO_2 and it is the synergistic effects of other environmental factors which will place multiple stressors

on organic physiologies and biogeochemical cycles. The majority of anthropogenic CO_2 has been absorbed by the ocean changing the carbonate system and decreasing seawater pH. Most of the energy flux from greenhouse gases is absorbed by the ocean causing warming which results in stratification of the upper ocean and changes in ocean mixing and ventilation (Plattner *et al.*, 2002). Consequently, this will reduce the oxygen and nutrient supply to the euphotic layer inducing nutrient stress on phytoplankton species (Bopp *et al.*, 2001; Keeling *et al.*, 2010, Helm *et al.*, 2011). Investigating a single consequence of elevated CO_2 is inadequate as biological differences may differ with additional stressors (Kroeker *et al.*, 2010). Therefore a more combined approach is required which focuses on the consequences of elevated CO_2 in response to the collective stressors of warming, acidification, deoxygenation and reduced primary productivity.

1.5 Other biological responses to ocean acidification

In the documentary "An inconvenient" truth, Al Gore states that the correlation between earth's average global temperature and the concentration of carbon dioxide in the atmosphere irrefutably demonstrates that carbon dioxide drives global warming. This statement however caused controversy with climate change skeptics who rebuked Gores statement as during the late Ordovician period CO_2 concentrations were higher during periods of glaciation (Chapter 3 section 3.1). However, carbon dioxide is not the only driver of climate change and there are numerous other internal and external forcing mechanisms.

1.5.1 Internal forcing mechanisms

Volcanic eruptions inject large quantities of fragmented mantle material into the upper atmosphere. The volcanic pollutants are primarily gases such as CO_2, H_2O, N_2 SO_2 and H_2S which affect the energy balance of the atmosphere by reflecting incoming solar radiation back into space. Studies investigating the volcanic eruption of Mount Pinatubo in the Philippines in 1991 found that global warming was delayed for several years after the eruption do to the cooling effects of the aerosols (Robock, 2002). Furthermore, a statistical association between volcanic activity and global temperatures

has been established which found evidence of high volcanic activity occurring within the period known as the little ice age and low volcanic activity during the medieval warm period (Hammer *et al.*, 1980).

The ocean is a major driver of the climate as it redistributes heat around the planet through a process known as thermohaline circulation (Figure 1.6). Originating in the North Atlantic, wind driven cooling evaporates the warm surface seawater of the Gulf Stream increasing salinity (and density) causing it sink to the deep ocean. The dense seawater then becomes part of the North Atlantic Deep Water (NADW) where it flows southward towards Antarctica joining the Antarctic Circumpolar Current. The mixed currents flow past South Africa and Australia and then head northwards to the Pacific where they become warmer and fresher. The waters then flow up through the South Atlantic towards the tropics and return back to the North Atlantic. It is the transport of heat into the North Atlantic that moderate's climate in North-western Europe and keeps the regions around Iceland and Southern Greenland free of sea ice (Vellinga and Wood, 2002). However, temperature changes due to global warming are predicted to affect wind patterns and intensities altering ocean currents and upwellings (Pierce *et al.*, 2006, D'Orgeville and Peltier, 2009). Oceanographers have already identified five hotspots worldwide in which strengthening winds have driven ocean currents beyond their normal boundaries (Wu *et al.*, 2012). Global warming has also been attributed to wind oscillations accompanied by a southward shift in the jet stream which delayed seasonal upwelling winds by a month. As a consequence, numerous anomalies were observed in marine ecosystems of Northern California with decreases in chlorophyll-a and nutrients of 50% and 30% respectively, a reduction in mussels and barnacles of 83% and 66% respectively and increased near shore surface water temperatures 2°C warmer than normal (Barth *et al.*, 2007).

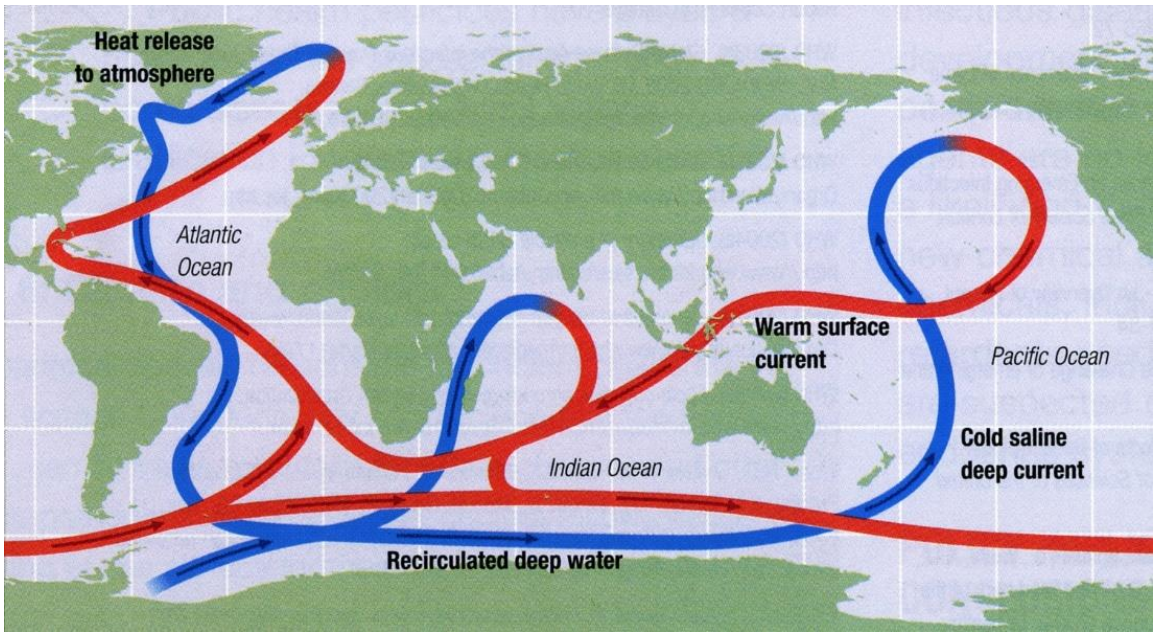

Figure 1.6 Schematic of global oceanic thermohaline circulation. Blue lines are deep cold-water flow while red lines are warmer surface flow IPCC (2001).

The earth's surface consists of a number of plates which are in constant motion due to the internal dynamics of the earth. Plate tectonics is the interaction between these plates which involves both horizontal and vertical motions of the earth's crust. There are basically three types of interactions; divergence, where two plates separate and new lithospheric crust is created by molten rock, subduction where two plates converge and the denser plate moves under the other into the mantle and where two plates slide past each other without divergence or subduction. The consequence of plate tectonics is that distribution of the land masses is continually changing which has an important effect on the spatial heterogeneity of the Earth's energy balance via differences in the albedos (reflectivity) and thermal properties (DeConto, 2009). The arrangement of the continents can significantly alter ocean circulation which regulates the climate through latitudinal heat transport and impacts atmospheric CO_2 via primary productivity and the biological pump. Climate can also be influenced by the elevation of continents and the formation of mountains as atmospheric temperature decreases with height by 6.5°C per kilometre (Petty, 2008). Consequently, high elevations can dramatically influence the climate

system as snow and ice tend to accumulate in these regions increasing surface albedo and cooling.

1.5.2 External forcing mechanisms

Milankovitch cycles are periodic orbital variations of the earth which influence the amount of energy received by the sun. Milankovitch, a Serbian mathematician theorized that these orbital variations determined climatic patterns and were crucial factors in the initiation of ice ages (Milankovitch, 1941). The three orbital forcing mechanisms of Milankovitch cycles are eccentricity, obliquity and precession. Eccentricity, describes the path of the earth around the sun which oscillates between circular and nearly circular with two periodicities of approximately 96,000 and 413,000 years (Berger, 1976). Obliquity, describes the tilt of the earth relative to the plane of its orbit which ranges from 22.1° to 24.5° with a periodicity of 41,000 years. Currently, the axis of rotation for the earth is tilted at 23.5° in respect to its orbital plane around the sun. Precession describes the motion of the Earth's axis of rotation which does not point towards a fixed direction in the sky through time. This is due to the Earth's equatorial bulge (by the gravitation pull of the sun and moon) causing the axis to gyrate like the spinning of a wobbling top, with a periodicity of 19,000–23,000 years (Campisano, 2012). Based on these oscillations, Milankovitch predicted that ice ages would peak every 100,000 and 41,000 years, with additional "blips" every 19,000 to 23,000 years. This association has been partly verified by long term proxy temperature data though the seminal work of Hays *et al* (1976) who found a correlation between changes in the Earth's orbital geometry and the succession of Quaternary ice ages (Hays *et al.*, 1976). However, there is strong evidence to suggest that additional feedback mechanisms are also required as orbital forcing mechanisms alone cannot account for the observed climatic variations over the past 2 million years (Hoyle, 1981, Berger, 2012).

1.6 Mass extinctions and climate change

In the last 3.5 billion years approximately 4 billion species have evolved on the earth of which 99% are now extinct (Novacek, 2001). All mass extinctions are

ultimately caused by changes in the climate, either by rapid global cooling, rapid global warming or rapid fluctuations of both warming and cooling (Twitchett, 2006). Climate change influences abiotic and biotic factors effecting species distribution, habitat selection and species interactions.

Abiotic factors are the non-living physical components of an ecosystem which influence physiological tolerances such as air/water temperature, water availability, nutrients, sea level, salinity and the amount of sea ice. Conversely, biotic factors are the living components of an ecosystem and how they interact with each other as a result of food availability, competition and predation. Climate change can severely alter abiotic factors which determine the biotic factors living in a particular habitat. There is evidence to suggest that warming could alter the capacity of ecosystems to absorb CO_2. In terrestrial systems there is a strong correlation between temperature and increased soil respiration (Knorr *et al.*, 2005; Arnone *et al.*, 2008, Bond-Lamberty and Thomson, 2010, Flanagan, 2013) and it has been suggested as the oceans warm their ability to sequester CO_2 will be reduced (Rivkin and Legendre, 2001; Del Giorgio and Duarte, 2002, López-Urrutia *et al.*, 2006). Global warming has been shown to affect the metabolic balance between photosynthetic CO_2 fixation and respiratory release of CO_2 back into the ecosystem (Yvon-Durocher *et al.*, 2010). This was demonstrated using a combination of theoretical projections and mesocosm studies which simulated the global warming predictions for 2100 (IPCC, 2007). The results revealed that ecosystem respiration increased at a faster rate than primary production in response to warming, reducing carbon sequestration by 13% (Yvon-Durocher *et al.*, 2010).

The distribution of organisms is a sensitive indicator of climate change (Hughes, 2000). The dinoflagellate *Ceratium trichoceros* is known for its sensitivity to temperature in terms of biogeography (Dodge and Marshall, 1994). Prior to 1970 this species was only found in the warmer waters off the south coast of the UK but due to increases in sea water temperature it has now been able to extend its range to the west of Scotland and parts of the North Sea (Hays *et al.*, 2005). In 1999 the Pacific diatom *Neodenticula seminae* was observed in the Labrador Sea for the first time in 800,000

years and has since recolonized the northern North Atlantic (Reid *et al.*, 2007). This was due to melting of Arctic sea ice which allowed the waters of North Pacific to flow into the North Atlantic (Reid *et al.*, 2007). At this stage it is unclear what impact (if any) the introduction of new phytoplankton species will have on the endemic planktonic community.

Several mesocosm studies have revealed that phytoplankton biomass is negatively affected by increasing temperature (Müren *et al.*, 2005; Sommer and Lengfellner, 2008, Lassen *et al.*, 2010). This has been corroborated by the examination of chlorophyll-a data spanning the period 1899-2008 which revealed a decline in global phytoplankton biomass estimated at 1% per year (Boyce *et al.*, 2010). The decline has been attributed to rising sea surface temperatures which promote stratification and changes in deep water circulation that limit nutrient fluxes into the euphotic zone.

There have been five major mass extinction events on earth: at the end of the Ordovician, Devonian, Permian, Triassic and Cretaceous periods (Table 1.1). There is no single common cause for these extinctions, although all are associated with evidence of climate change and temperature variations (Wignall, 2005, Twitchett, 2006). Analysis of fossil records of the past 520 million years against estimates of low latitude sea surface temperature for the same period have revealed a correlation between temperature and global biodiversity (Mayhew *et al.*, 2008). The study found that four out of the five mass extinctions events are associated with rapid global warming (Figure 1.7). The exception was the Ordovician extinction ~443 million years ago which has been linked to rapid global cooling caused by massive glaciation and a reduction in sea level (Sheehan, 2001). Although, a bolide impact is the accepted theory for the Cretaceous extinction which resulted in a nuclear winter lasting several months, (Alvarez *et al.*, 1980, Pollack *et al.*, 1983) CO_2 levels increased to 2,300 ppm within 10,000 years of the impact which raised the global temperature by ≈7.5°C (Beerling *et al.*, 2002) (Chapter 3 section 3.1).

Table 1.1 Five mass extinction events and proposed causes adapted from Barnosky et al, (2011).

Extinction event	Myr	Extinct genera (%)	Extinct species (%)	Proposed cause
Ordovician	443	57	86	Onset of alternating glacial and interglacial episodes; repeated marine transgressions and regressions. Uplift and weathering of the Appalachians affecting atmospheric and ocean chemistry.
Devonian	359	35	75	Global cooling (followed by global warming), possibly tied to the diversification of land plants, with associated weathering and the drawdown of global CO_2. Evidence for widespread deep-water anoxia and the spread of anoxic waters by transgressions.
Permian	251	56	96	Siberian volcanism. Global warming. Spread of deep marine anoxic waters. Elevated H_2S and CO_2 concentrations in both marine and terrestrial realms. Ocean acidification.
Triassic	200	47	80	Activity in the Central Atlantic Magmatic Province (CAMP) thought to have elevated atmospheric CO_2 levels, which increased global temperatures and led to a calcification crisis in the world oceans.
Cretaceous	65	40	76	A bolide impact in the Yucatan peninsula is thought to have led to a global cataclysm and caused rapid cooling. CO_2 spike just before extinction caused by Deccan volcanism or bolide impact accompanied by global warming; ocean acidification, eutrophication, anoxic episodes and decreased primary production

There are indications that the collapse of primary production is a key proximate cause of extinction (Twitchett, 2006). It has been proposed that several mass extinction events were the consequence of a collapse in marine primary productivity, such as the Permian, (Twitchett, 2001, Rampino and Caldeira, 2005) Triassic (Ward *et al.*, 2001) and Cretaceous (Zachos *et al.*, 1989). The Permian event was the greatest mass extinction ever recorded in earth history with 96% of marine life and 70% of terrestrial life becoming extinct in approximately 60,000 years (Burgess *et al.*, 2014). Interestingly, all three mass extinctions (Permian, Triassic and Cretaceous) share common features, a short lived perturbation of the carbon cycle followed by a rise in atmospheric pCO_2 and temperature, ocean acidification, anoxia and rapid extinction (10s of thousands of years) (Zachos *et al.*, 2008; Schulte *et al.*, 2010, Blackburn *et al.*, 2013, Burgess *et al.*, 2014).

If we lose the species that are currently on the critically endangered category we will propel the world to a state of mass extinction which has only been observed five times in the last 540 million years (Barnosky *et al.*, 2011). During the Permian extinction the oceans would have undergone dramatic acidification and temperature rises of 10°C in approximately 60,000 years representing a ~1°C increase per 6,000 years (Burgess *et al.*, 2014). In their 5th assessment report, (AR5) the IPCC predict that by the end of the century the global temperature could rise by 1.7°C (best case scenario) to 4.8°C (worst case scenario). The oceans will continue to warm with the top 100 m expecting to rise by 0.3°C - 2°C by the end of the century. Polar ice, snow cover and glaciers will continue to shrink increasing average sea level by 26 – 98 cm (Stocker *et al.*, 2013). Even the lowest estimates of ocean warming (~0.3°C per century) equate to a 10°C rise in only 3,330 years which is 18 times faster than the temperature rise of the Permian extinction. At this rate, many organisms may be unable to adapt quickly enough to the rapidly changing environment and will therefore become extinct. The paleontological definition of mass extinction is the disappearance of over 75% of species in geological time of less than 2 million years (Barnosky *et al.*, 2011). The current projection for species level extinction due to climate change is 18% minimal range, 24% medium range and 35% maximum range by 2050 (Thomas *et al.*, 2004).

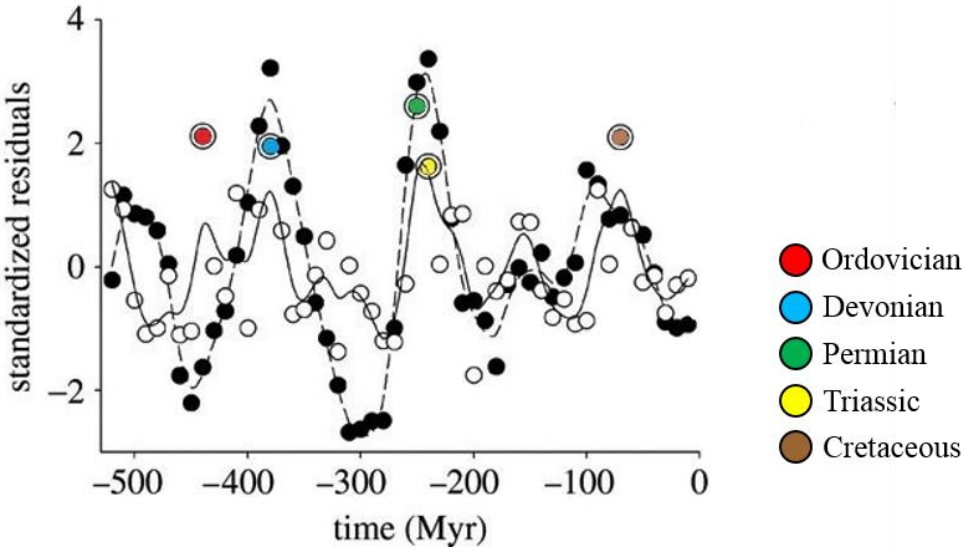

Figure1.7 Positive association between extinction rate and temperature residuals across a time series. Closed circles and dashed lines represent temperature and open circles and continuous lines extinction rates. Large coloured symbols represent periods of mass extinction in order of decreasing age. Adapted from Mayhew *et* al (2008).

1.7 Research Aims and objectives

There have been numerous studies investigating the sensitivity of phytoplankton species to ocean acidification but few concerning the effects of elevated CO_2 on bacterial communities. The 2005 Royal Society report on ocean acidification stated that "Although their physiology suggests that they will respond to increased CO_2 in the surface oceans and to decreased pH, there are few data available to demonstrate any responses" (Royal Society, 2005). Bacteria associated with oceanic algal blooms are acknowledged to play important roles in carbon, nitrogen, and sulfur cycling and microbial dynamics seem to be coupled to the development of the phytoplankton bloom (González *et al.*, 2000, Allgaier *et al.*, 2008). It is hypothesized that ammonia oxidising bacteria (AOB) will be particularly influenced by increased atmospheric CO_2 due to the increase in ocean acidity and the decreased availability of ammonia which is pH dependent. These bacteria play a key role in the nitrification process by converting ammonia (NH_3) to nitrite (NO_2^-) and are therefore essential to all life in the oceans.

The aim of this study is to investigate the effects of CO_2 driven ocean acidification on microbial composition and diversity by testing the following hypotheses:

Hypothesis I: Marine bacterial diversity will change in response to seawater pH

Hypothesis II: Decreasing seawater pH will alter biogeochemical cycling of carbon nitrogen and sulfur.

These hypotheses will be tested by long term mesocosm studies using variable pH values maintained by the artificial introduction of CO_2 ranging from 760 – 280 parts per million. Molecular and metagenomic studies will be used to determine the differential effects of elevated CO_2 on bacterial communities and the possible consequences on biogeochemical cycles.

2. Materials and Methods

2.1 Experimental design

The aim of this experiment was to simulate the environment of a high CO_2 world as predicted by the "Business as usual" scenario IS92a of the IPCC (IPCC, 2001). This was conducted in the context of ocean acidification which is likely to affect bacterial populations and marine biogeochemical cycles. To test the effect of increased atmospheric CO_2 a field experiment was conducted at the Marine Biological Station of the University of Bergen, Norway (Raunefjorden, 60.27 N 5.22E). This tidal fjord on the North Sea is influenced by the Baltic current making salinity variable. Water temperature during the experiment varied between 8 – 11^{o}C due to the warm and sunny weather in the early part of May 2006.

The experiment consisted of 6 polyethylene enclosures (ca. 12m ^{3}) which were moored to a raft 200 m offshore from the field station. The bags were filled with unfiltered fjord water and amended with nutrients to stimulate a phytoplankton bloom. Seawater pCO_2 was manipulated via aeration with CO_2 enrichment or ambient air to achieve two different CO_2 levels. All the bags were covered with transparent hoods in order to maintain the CO_2 balance and to allow the transmission of photosynthetically active radiation (PAR) at wavelengths utilized by phytoplankton. CO_2 was introduced into the system in two phases of the experiment: Phase 1 (pre-bloom) used to determine the response of phytoplankton to reduced pH and Phase 2 (post-bloom) investigated the bacterial response to increased CO_2 following the phytoplankton bloom.

The separation of DNA from putative chemoautotrophic bacteria was achieved by stable isotope probing (SIP). Eight x 4 L high density polyethylene carboys (Nalge Nunc International, Denmark) were used as incubation vessels for the SIP experiments which were painted black to reduce the proliferation of phototrophic organisms.

Sampling of the mesocosms took place daily at 9 am from the 6th – 23rd May (Day 1 – 18) 2006. SIP experiments commenced on 13th May (Day 8) when seawater was withdrawn from the mesocosms and placed into allocated dark incubation bottles. Sampling of the bottles was over a five day period on days 9, 10, 11 and 13 for phase 1

and days 16, 17 18 and 20 for phase 2. The samples were taken at 3 pm in both phases of the experiment (Table 2.1).

Table 2.1 Schematic representation of the Bergen mesocosm experiment showing sampling days and the 2 phases (pre/post bloom) of the experiment.

Actual date	Mesocosm day	Dark incubations	Phase
6th May	1		
7th May	2		
8th May	3		
9th May	4		
10th May	5		Phase 1
11th May	6		
12th May	7		
13th May	8	Phase 1 bottles filled	
14th May	9	1	
15th May	10	2	
16th May	11	2	
17th May	12		
18th May	13	5	
19th May	14		
20th May	15	Phase 2 bottles filled	Phase 2
21st May	16	8	
22nd May	17	9	
23rd May	18	10	
24th May	End		
25th May	End	12	

2.1.1 pCO_2, Total alkalinity and pH

pCO_2, total alkalinity (TA) and pH analyse were conducted by Dr D. Bakker, University of East Anglia (UEA). pCO_2 was measured using a UEA built CO_2 instrument with infrared detection (Wanninkhof and Thoning, 1993, Hopkins *et al.*, 2009). TA was determined by potentiometric titration with a Vindta system (Versatile Instrument for the Determination of Total inorganic carbon and titration Alkalinity). Mesocosm pH was calculated from measured and extrapolated total alkalinity (TA) and pCO_2 measurements

by Dr Dorothee Bakker, University of East Anglia, using the computer program CO2SYS (Lewis *et al.*, 1998).

2.1.2 DMSPp and DMS

Particulate dimethylsulphoniopropionate (DMSPp) and dimethylsulfide (DMS) analysis was conducted by Dr F.E Hopkins from the University of East Anglia. DMSPp was measured by headspace analysis on a Shimadzu GC-2020 with flame photometric detector. DMS samples were analysed using a Shimadzu GC-14B with flame photometric detector (Hopkins *et al.*, 2009).

2.1.3 Analytical flow cytometry

Flow cytometric counts of absolute concentrations of bacterioplankton, Synechococcus, Prochlorococcus, and algae were enumerated by Dr A.S Whiteley (Centre for Ecology and Hydrology (CEH) Oxford) using a Becton Dickinson FACSort flow cytometer equipped with an air-cooled blue light laser at 488 nm.

2.1.4 Chlorophyll- a

Chlorophyll-a concentrations were determined by Dr K. Crawfurd, University of Dundee using two methods. Fluorometrically (performed on site) using a Turner fluorometer and high performance liquid chromatography (HPLC) analysis conducted at Plymouth Marine Laboratory (PML). The acetone extractions gave complete datasets for each mesocosm whereas the HPLC data was less complete providing no data for mesocosms M3 and M4. The HPLC data were uploaded into the Bergen database and was the dataset used in this study.

2.1.5 Primary production and nutrients

Primary productivity of the phytoplankton community and nutrient concentrations were measured by Dr I. Joint of PML. Primary productivity was determined by the assimilation of radioactive ^{14}C sodium bicarbonate ($NaH^{14}CO_3$) into organic matter by phytoplankton and measured on a scintillation counter. Dissolved nutrient concentrations were measured (nitrate, nitrite and phosphate) using colorimetric methods.

Further details about the measurements and samples taken by other members of the Bergen mesocosm consortium may be obtained from Dr Ian Joint, Plymouth Marine Laboratory (I.Joint@pml.ac.uk).

2.2 Experimental Set–up

2.2.1 Mesocosms

On 2nd May 2006 six mesocosms (2 m diameter, 3.5 m deep and 0.5m above the surface) were filled with ~ 11,000 L of unfiltered water collected from the fjord at a depth of 2 m. Throughout the duration of the experiment water inside each enclosure was circulated from a depth of 3m to the surface at a rate of 1000 L per day.

To assess the effect of high CO_2 in the future oceans, the mesocosms were divided into two treatments. Mesocosms M1-M3 were designated high CO_2 and were manipulated to simulate the possible climatic conditions of the year 2100 where predicted atmospheric CO_2 is ~750 ppm and seawater pH 7.8. Mesocosms M4-M6 were designated as ambient CO_2 and maintained the conditions of the present day (380 ppm, pH 8.1. On the 3rd May water in mesocosms M1-M3 was aerated with air enriched with CO_2 using flow meters to a target level of 760 ppm. pH was constantly monitored throughout the process using a standard pH meter and electrode which was later verified by Dr D. Bakker (UEA) from the pCO_2 and TA measurements. After 3 days the aeration ceased when the high CO_2 mesocosms reached CO_2 concentrations of 744 ppm and pH

7.7. The atmospheric concentration in the head space was maintained at its target level of 760 ppm by daily flushing with high CO_2. The present day mesocosms (M4-M6) were treated identically except they were aerated with ambient air.

On the 6th May (Day 1) after the first water samples were taken, nutrients were added to the mesocosms to stimulate the development of a phytoplankton bloom to a final concentration of 1.25 μmol l^{-1} phosphate and 16 μmol l^{-1} nitrate. Mesocosms M2 and M5 (high and ambient CO_2 respectively) were treated with ^{15}N-labelled nitrate in order to detect nitrogen fixation activity (University of Stirling).

After the peak of the phytoplankton bloom the high CO_2 mesocosms had returned to a near ambient state and therefore it was necessary to repeat the aeration process on day 10 (15th May). In this instance, only mesocosms M1, M2, M5 and M6 were aerated whereas M3 and M4 received no further treatment to establish the effects of the aeration process on the system. Sampling commenced the following day and continued until the end of the mesocosm experiment on day 18 (23rd May).

2.2.2 SIP incubations

Prior to the commencement of the experiment the dark incubation bottles were acid washed with 10% HCl for 3 hours and rinsed with filtered (0.2 μm) fjord water. Mesocosms M1, M3 (high CO_2) and M4, M6 (ambient CO_2) were each allocated two incubation bottles designated ^{13}C and ^{12}C to which were added 0.68 g of ^{13}C labelled sodium-bicarbonate (99 atom%; Cambridge Isotope laboratories, MA) at a final concentration of 2.02 mM, whereas controls (^{12}C) received 0.68 g (2 mM) of unlabelled sodium bicarbonate (Figure2.1). The incubation bottles were filled with seawater withdrawn from their allocated mesocosm on day 8 (13th May) and suspended from a line in the fjord to incubate for 24hrs prior to sampling.

This procedure was repeated for the phase 2 incubations when the bottles were re-filled from the same mesocosms on day 15 (20th May).

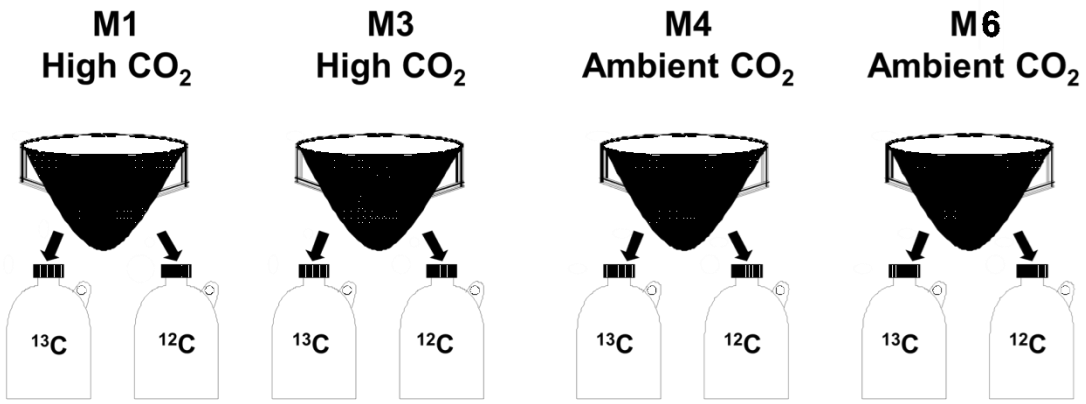

Figure 2.1 Schematic representations of the allocation of dark incubation bottles

2.2.3 Sampling

Seawater was withdrawn from each mesocosm via a 5 litre bucket attached to a nylon cord. Samples were transferred from the bucket to 25 litre containers which were immediately stored in a cold room at 4 ºC in the dark until required for further analysis.

1 L of water was withdrawn from each dark incubation bottle at four time points over a 5 day period for each phase of the experiment. After each bottle was sampled it was immediately reattached onto its line and suspended back into the fjord. From the 1 L of seawater obtained, 20 ml was taken for flow cytometry and pH measurements. Due to time restraints it was not possible to perform pH measurements in the same manner as the mesocosms. Therefore, bottle pH was measured using a Mettler Toledo MP220 pH meter, calibrated with pH 4, 7 and 10 standards. The remaining water was filtered through a 5 µm polycarbonate filter (Whatman) and then a 0.2 µm Sterivex filter (Millipore) which was then sealed at both ends with parafilm. The filters were then immediately stored at - 80°C.

2.3 DNA extraction

DNA was extracted using a method derived from (Somerville *et al.*, 1989) and (Murray *et al.*, 1998). After completely thawing the Sterivex unit, 1.6 ml of SET lysis buffer (40 mM EDTA pH 8, 50 mM Tris-HCl pH 9, 0.75 M sucrose) and 180 µl of fresh lysozyme solution (10 mg/ml) were added via the inlet port using a 2.5-ml syringe with a 25G x 5/8" needle. After sealing the ends of the unit using parafilm the contents were mixed by inversion and incubated in a Hybaid rotary oven (Thermo Scientific) for 30 minutes at 37°C. After the incubation period, 200 µl of 10% (m/v) sodium dodecyl sulfate (SDS) and 55 µl proteinase K (20 mg/ml) was added and the filter unit was incubated at 55°C for a further 2 hours. The lysate was withdrawn from the Sterivex unit via the inlet port using a 5 ml syringe. To remove any residual DNA the unit was washed with 1 ml of SET lysis buffer and incubated for a further 15 minutes in the rotary oven at 55^{o}C. The remaining wash buffer was removed and pooled with the initial lysate.

Nucleic acid was purified from the lysate using the phenol:chloroform:isoamyl alcohol (25:24:1) method in heavy 15 ml Phase lock tubes (Eppendorf, Hamburg, Germany) according to the manufacturer's instructions. This method increases the recovery of nucleic acid by trapping the organic and aqueous phases between the Phase Lock Gel (PLG). The barrier is sufficiently durable that the upper aqueous phase (containing the nucleic acid) can be recovered by simply decanting into a new tube. The method utilizes the density differences between the phases with the organic layer having higher density than the PLG and aqueous phase and the PLG having higher density than the aqueous phase. Separation is achieved by mixing equal amounts of lysate with phenol:chloroform:isoamyl alcohol in phase lock tube and centrifuge for 10 minutes at 1500 g.

Approximately 2 ml of aqueous phase from each PLG tube was decanted into a 10-ml Oakridge tube. 5 µl of a 20 µg/µl^{-1} glycogen solution (Roche, Basel, Switzerland), 0.5 volumes of 7.5 M ammonium acetate and two volumes of 95% (v/v) ice-cold ethanol were added to the tube to precipitate the DNA. Ethanol precipitation was carried out overnight at -20°C. Samples were centrifuged at 48 000 x *g* to pellet the nucleic acid,

washed twice with 80% (v/v) ethanol, air dried for 30 min at room temperature, and dissolved in 140 µl of sterile UV-treated molecular biology grade water (Sigma-Aldrich). Finally, one unit of RNase A (Qiagen) was added to the DNA preparation and incubated at room temperature for 30 minutes.

The concentration and quality of the DNA was assessed using a NanoDrop ND-1000 spectrophotometer (NanoDrop Technologies).

2.4. Polymerase chain reaction (PCR)

PCR was conducted using a G-Storm GS1 thermal cycler (GRI, Essex, UK). Reactions were carried out in a 50 µl volume containing 1 µl of template DNA, 10 pmol each of the forward and reverse primers (Thermo Scientific, Germany), 2 units of Biotaq™ DNA polymerase (Bioline, London, UK), 1×NH_4 buffer (670mM Tris-HCl pH 8.8, 160mM $(NH_4)_2SO_4$) (Bioline, London, UK), 1.5 mM $MgCl_2$ (Bioline, London, UK), 10 nmol of each deoxyribonucleoside triphosphate and molecular biology grade water (Sigma-Aldrich). A negative control which consisted of sterile water in place of template DNA was included in each PCR reaction (Erlich *et al.*, 1991). All samples were serially diluted in a ten–fold dilution series to determine the optimum sample concentration required for amplification. PCR was conducted using the cycling parameters in Table 2.2.

Table 2.2 Summary of PCR conditions the primer pairs used in this study

Primers	Initial denaturation	Denaturation	Annealing	Extension	No of cycles	Final extension
pA/pH (Edwards et al. 1989)	3 min, 95ºC	1 min, 95ºC	1mins, 55ºC	1 min 72ºC	45	10 min 72ºC
Primer 2/3 (Muyzer et al. 1993)	3 min, 95ºC	1 min, 95ºC	1 min 65ºC reduce 1º every 2nd cycle until 55 ºC	1 min 72ºC	20 followed by 5 cycles at 55ºC	10 min 72ºC
A20f/U1492r (DeLong 1992)	5 min, 94ºC	1.5 min, 94ºC	30 sec, 55ºC	1 min 72ºC	30	7 min 72ºC
***amoA*1f/2r** (Rotthauwe et al. 1997)	5 min, 94ºC	1 min, 94ºC	1min 57ºC	1.5 min 72ºC	42	10 min 72ºC
amoA 23f/616r (Tourna et al. 2008)	3 min, 95ºC	45 sec, 95ºC	1mins, 55ºC	1 min 72ºC	30	15 min 72ºC
CTO189f/654r (Kowalchuk et al. 1997)	3 min, 95ºC	1 min, 95ºC	1 min, 57ºC	1 min 72ºC	35	10 min 72ºC
pUCf/r	3 min, 95ºC	1 min, 95ºC	1 min, 57ºC	1 min 72ºC	30	10 min 72ºC
RBf1/RBr2 (This study)	7 min, 95ºC	45 sec, 95ºC	45 min, 60ºC	45 sec 72ºC	40	10 min 72ºC
FBf1/FBr2 (This study)	7 min, 95ºC	45 sec, 95ºC	45 sec, 59ºC	45sec, 72ºC	40	10 min 72ºC
U1048/1371 Neil Gray (unpublished)	7 min, 95ºC	45sec, 95ºC	45 sec, 61ºC	45 sec, 72ºC	40	10 min 72ºC

2.4.1 PCR of bacterial and archaeal 16S rRNA gene fragments

PCR amplification of bacterial 16S rRNA gene fragments was performed using primer pA (5′-AGAGTTTGATCCTGGCTCAG-3’) and pH (5’-AAGGAGGTGATCCAGCCGCA-3’) (Edwards *et al.*, 1989). A nested PCR approach was taken for samples which required DGGE analysis. The first round of amplification was conducted using the bacterial 16S rRNA primers pA/pH followed by the amplification of the variable V3 region using primer 2 (5’-ATTACCGCGGCTGCTGG-3’) and primer 3 (5’-CGCCCGCCGCGCGCGGCGGGCGGGGCGGGGGCACGGGGGGCCTACGGGAGGCAGCAG-3’) (Muyzer *et al.*, 1993). Primer 3 contained a 40 bp GC clamp (underlined). Amplification of the V3 region was achieved using DyNAzyme™ II DNA polymerase (Finnzyme, Keilaranta,, Finland) due its high purity and the ability to amplify templates which are GC rich. This resulted in increased amplification and a clean negative control which was not consistently observed when Biotaq™ DNA polymerase was used for nested amplification using broad specificity primers.

Betaproteobacterial ammonia-oxidizer 16S rRNA gene fragments were amplified using primer CTO189f (5’-GAGRAAAGYAGGGGATCG-3’) and CTO654r (5’-CTAGCYTTG TAGTTTCAAACGC-3’) (Kowalchuk *et al.*, 1997).

Archaeal 16S rRNA gene fragments were amplified using primer A20f, (5’-TTCCGGTTGATCCYGCCRG-3’) and primer U1492r, (5’-GGTTACCTTGTTACGACTT-3’) (DeLong, 1992).

2.4.2 PCR analysis of bacterial and archaeal amoA genes

Amplification of the bacterial ammonia monooxygenase α-subunit gene (*amoA*) was performed using primer *amo*A-1f (5’-GGGGTTTCTACTGGTGGT-3’) and primer *amo*-2r (5’-CCCCTCKGSAAAGCCTTCTTC-3’) (Rotthauwe *et al.*, 1997).

The Archaeal amoA gene was amplified using primer *amoA*-23f (5′-ATGGTCTGGCTWAGACG -3′) and primer *amoA*-616r (5′-GCCATCCATCTGTATGTCCA-3′) (Tourna *et al.*, 2008) .

2.4.3 qPCR analysis

Abundance and dynamics of specific bacterial groups were determined by quantitative real time PCR (qPCR). qPCR reactions comprised iQ Supermix (10 µl) (100 mM KCl, 40 mM Tris-HCl, pH 8.4, 0.4 mM each DNTPs, 50 U/ml iTaq DNA polymerase, 6 mM $MgCl_2$), PCR primers (1 µl of 10 pmoles μl^{-1} each), DNA template (3 µl), SYBR Green (0.2 µl per reaction of 100 × diluted from 10 000 × concentrate) and sterile water made up to a final volume of 20 µl. qPCR reactions were carried out in optical-grade 96-well plates with a iQ5 thermocycler (Bio-Rad) using the cycling conditions given in Table 2.3. Optimal annealing temperatures were determined for primers designed to target *Rhodobacteraceae*, *Flavobacteriaceae* and total bacteria (Table 2.2) by performing a temperature gradient PCR with annealing temperatures in the range of 55°C to 70°C. The universal bacterial primers contained deoxyinsosinetriphosphate (I) which is a nucleoside triphosphate that indiscriminately pairs with adenine, thymine, guanine or cytosine. Genes in experimental samples were quantified with reference to external standards. Cloned target genes were used to prepare known amounts of standard to prepare standard curves. The cloned genes were amplified using vector specific primers (pUCf/pUCr) and 4 x 45 µl PCR reactions were pooled and purified using a QIAquick PCR purification kit (Qiagen) to remove residual primers and dNTPs. The amount of target DNA was quantified using NanoDrop ND-1000 spectrophotometer (NanoDrop Technologies) and the concentration of genes in the standard was quantified on the basis of the molecular mass of the amplified DNA fragment and 10 fold serial dilutions were prepared to give a range of concentrations from 10^1 to 10^8 genes per microlitre. Standard curves were generated by plotting the cycle threshold (C_T) values of qPCR reactions performed on 16S rRNA gene standards containing 10^8 to 10^1 genes per µl against the log starting quantity of 16S rRNA gene in the reaction. All samples were analysed in duplicate.

Table 2.3 Primers used in quantitative PCR

Primer	Sequence	Target
RBf1	(5'-AGG GGG TTA GCG TTG TTC GG-3')	*Rhodobacteraceae*
RBr2	(5'-ACC TCA GCG TCA GTA TCG AG-3')	*Rhodobacteraceae*
FBf1	(5'-GAG GAA CCT TAC CAG GGC TT-3')	*Flavobacteriaceae*
FBr2	(5'-AGGACGTAAGGGCCGTGATG-3')	*Flavobacteriaceae*
U1048f	(5'-GTG ITG CAI GGI IGT CGT CA-3')	*Bacteria*
U1371r	(5'-ACG TCI TCC ICI CCT TCC TC-3')	*Bacteria*

2.5 Design of PCR primers

The PRIMROSE software package (Ashelford *et al.*, 2002) was used to design 16S rRNA gene primer sets for 2 dominant families of bacteria (*Rhodobacteraceae* and *Flavobacteriaceae*) detected in 16S rRNA gene clone libraries. Primers were generated using the 16S rRNA sequences from the clone libraries and associated sequences obtained from the Ribosomal Database project II (http://rdp.cme.msu.edu/). All primer sets were designed using the default settings of the PRIMROSE program. The number of target and non-target matches of the primers was tested *in silico* using the Probe match function within the RDP-II database.

2.6 Agarose gel electrophoresis

All gels were prepared with 1 x TAE **(**40mM Tris Acetate, and 1.0mM EDTA, pH 8.3.) containing 1.6 µl ethidium bromide (10 mg/ml^{-1}) in a 100 ml gel. Samples were loaded with 0.2 volume of loading buffer (8% [w/v] Ficol; 6M urea; 0.01% [w/v] bromophenol blue) and electrophoresed at a constant 100 volts for 1 hr. DNA molecular weight markers (HyperLadder II, Bioline, London, UK) were run on all gels to estimate the size of the PCR products obtained. Nucleic acids were visualized using a Fluor-S Multiimager (Bio-Rad, Hercules, CA, USA) at 320 nm.

2.7 DGGE analysis

DGGE analysis was conducted using the D-Gene denaturing gradient gel electrophoresis system (Bio-Rad Laboratories, Hercules, CA, USA). Polyacrylamide gels (10% w/v polyacrylamide; 0.75 mm thick; 16 x16 cm) were run in 1 x TAE buffer (40 mM Tris-acetate, 1 mM EDTA, pH 8.3). A denaturant gradient ranging from 30% - 55% of urea and formamide (100% denaturant is 40% (v/v) formamide, 7M urea in 1 x TAE) was used. Approximately 20 µl of PCR product obtained using primers 2/3 (233bp) was loaded per well and the gels were run at 60 °C for 4.5 hrs at a constant 200 volts. Gels were stained for 30 min in SYBR green (Sigma, Poole, UK; diluted 1/1000 in 1 x TAE) and visualized using a Fluor-S Multiimager (Bio-Rad).

2.8 Statistical analysis of DGGE gels

DGGE images were analysed using Bionumerics version 3.5, (Applied Maths, Kortrijk, Belgium). Reference markers (PCR products amplified from cloned 16S rRNA genes) were used as a normalization standard to ensure gel-to-gel comparability. Band positions were detected automatically and the band assignments were checked manually to validate the results. Quantitative comparison of the similarity between DGGE profiles was done using the Pearson correlation coefficient. Similarities were displayed graphically as a dendrogram using the unweighted pair-group method with arithmetic mean (UPGMA) algorithm so that potential clustering patterns could be observed.

2.9 Excision and Sequencing of DGGE bands

Prominent bands from the DGGE gels were excised using sterile scalpel blades and resuspended in 30 µl of UV treated molecular biology grade water (Sigma-Aldrich). After an overnight incubation at 4 °C, 2 µl of the elutant was used as DNA template for PCR amplification with the original primers using the reaction conditions outlined in Table 2.1. 5 µl from each PCR reaction was ran on a 0.7% w/v agarose gel to validate the PCT reaction. The remaining PCR products were purified using ExoSAP-IT (GE Healthcare, Buckinghamshire, UK) following the recommended protocol of the manufacturer. Between 40 and 50 ng of the PCR product was used for sequencing (with

the corresponding forward primer) using the BigDye Terminator v3.1 Cycle Sequencing Kit and an ABI Prism 3730xl DNA sequencer (Applied Biosystems). The resulting sequences were compared to the GenBank database using BLAST to identify the nearest neighbours.

2.10 Cloning and Sequencing of gene fragments

Two samples (1 high CO_2, 1 ambient CO_2) were characterised using cloning and sequence analysis. A total of 8 clone libraries were constructed (4 libraries from each sample) using the following primer sets: Bacteria 16S rRNA (pA/pH), Archaeal 16S rRNA (A20/U1492r), Betaproteobacterial AOB 16S rRNA (CTO189f/654r) and Bacterial *amo*A (*amo*1f/2r). Prior to cloning all amplicons of the correct size were gel-purified using a QIAquick gel extraction kit (Qiagen). Samples were cloned using a TOPO TA cloning kit with one shot TOP10 chemically competent *E. coli* cells (Invitrogen Corporation, Carlsbad, CA) according to the manufacturer's instructions. The resulting transformed cells were aseptically plated on to fresh LB ampicillin plates and incubated overnight at 37ºC. Individual colonies were randomly chosen and amplified by PCR using the vector-specific primers pUCf. (5'-GTT TTC CCA GTC ACG AC-3') and pUCr (5'-CAG GAA ACA GCT ATG AC-3'). Unwanted primers and dNTPs were removed from the amplified inserts with ExoSAP-IT (GE Healthcare, Buckinghamshire, UK). Sequencing with the pUC f primer was acheived using BigDye Terminator v3.1 Cycle Sequencing Kit and an ABI Prism 3730 DNA sequencer (Applied Biosystems). Grouping of 16S rRNA gene clone library sequences was performed using the FastGroup program (Yu *et al.*, 2006). Clone sequences were compared to the GenBank database using BLASTN to identify the nearest neighbours.

For a more rigorous analysis nearly full length 16S rRNA gene sequences were obtained from the Bacterial 16S rRNA gene libraries by sequencing each clone using four primers (Table 2.4). Only clones containing sequences which were present more than 3 times in each library were used to obtain full length sequences. The resulting 16S rRNA sequences were assembled using BioEdit version 7.0.8.0 (Hall, 1999) by aligning the sequences against the 16 rRNA gene of *E. coli* K12.

Table 2.4 Summary of sequencing primers

Primer	Seqeunce	Reference
pD	(5′-CAG CAG CCG CGG TAA TAC-3′)	
pD-reverse	(5′-GTA TTA CCG CGG CTG CTG-3′)	(Lane *et al.*, 1985)
pE-reverse	(5′-CCG TCA ATT CCT TTG AGT TT-3′)	
pH	(5′-AAG GAG GTG ATC CAG CCG CA-3′)	(Edwards *et al.*, 1989)

2.11 Phylogenetic analysis

Phylogenetic analysis of full length bacterial 16S rRNA gene sequences was computed using Molecular Evolutionary Genetics Analysis version 4 (MEGA 4) (Tamura *et al.*, 2007). Sequences were aligned using the alignment editor of the program and alignments were manually corrected with gaps and ambiguously aligned regions excluded from further analyses. Phylogenetic trees were constructed based on the neighbor-joining (NJ) method (Saitou and Nei, 1987) and the minimum evolution (ME) method (Rzhetsky and Nei, 1992). Both these methods begin with input data in the form of a matrix specifying the distance between each pair of taxa, except that ME method further improves the initial NJ tree by post processing. Subsequent analysis for robustness of the resulting NJ and ME trees was achieved using bootstrap analysis (500 samplings from sequence data).

2.12 Purification of ^{13}C-DNA from SIP experiments

^{13}C-DNA from stable isotope probing experiments was separated from ^{12}C-DNA using CsCl density gradient centrifugation. Approximately 4 µg of genomic DNA from each sample incubated with $H^{13}CO_3^-$ was added to gradient buffer (0.1 M Tris HCl pH 8.0, 0.1 M KCI, 1 mM EDTA) to give a total volume of 1380 µl. This was mixed in a 15 ml Falcon tube (Corning) with 5.5 ml of 7.163M caesium chloride (density 1.88 g/ml) to give a final density of 1.725 g/ml. The amount of gradient buffer/DNA mix to add to the CsCl solution was calculated using the following formula:

Gradient buffer and DNA solution volume (ml) = (CsCl stock solution density - desired final density) x volume of CsCl stock solution added x 1.52

Specify the volume of the CsCl solution at 5.5 ml (volume of tube used in ultracentrifugation). The stock solution density is 1.88 g ml^{-1} and the final density should be 1.725 g ml^{-1}.

The solution was then added to a 6 ml Quick-Seal Polyallomer ultracentrifuge tube (Beckman Coulter Palo Alto, CA, USA) and sealed with a cordless tube topper ensuring that the tube was completely filled to eliminate air bubbles. The sealed tubes were placed in an NVT 65 rotor (Beckman Coulter) ensuring that they were balanced to within 0.02 g. Centrifugation was conducted at 60,000 rpm (345,830 x *g)* under vacuum, with maximum acceleration and no braking at 20 °C for 35.40 hr using an Optima L-100 XP ultracentrifuge (Beckman Coulter). After centrifugation the gradients were fractionated into twenty eight 200-µL fractions by displacement using a Beckman fraction recovery system supplying molecular biology grade mineral oil to the top of the tube using a syringe pump (KD Scientific, MA, USA). Gradients and ultracentrifugation conditions were initially calibrated with 4 µg of DNA extracted from a pure culture of *E. coli M165* grown in a minimal medium with ^{13}C labelled glucose. The gradients were achieved as previously described except that 100 µl of ethidium bromide (10 mg/ml^{-1}) was added in order to visualize the separation of the heavy and light bands. The tube was then used as a positive control in every centrifuge run to determine the success of the isopycnic separation prior to fractionation.

To establish which fractions contained the $^{13}C/^{12}C$ DNA, 5 µl from each aliquot was run on a 0.7 % (w/v) agarose gel for 1 hr at 100 volts and visualized using a Fluor-S Multiimager (Bio-Rad, Hercules, CA, USA).Aliquots which tested positive for the presence of DNA were pooled together into ^{13}C and ^{12}C fractions. The resulting DNA from both fractions was precipitated with 20 µg glycogen and two volumes of polyethylene glycol (30% PEG 6000 and 1.6 M NaCl) and dissolved in 20 µl UV treated

molecular biology grade water (Sigma-Aldrich). Separation and purification of $^{13}C/^{12}C$ was conducted in triplicate to test reproducibility.

2.13 Whole-genome amplification of environmental DNA

Whole genome amplification was carried out on selected samples to obtain microgram quantities of DNA from initial nanogram concentrations to provide sufficient DNA for pyrosequencing (Section 2.14). Samples were subjected to multiple displacement amplification (MDA) using GenomiPhi V2 DNA amplification kit (GE Healthcare, Buckinghamshire, UK). Briefly 1 µl of DNA template (~10 ng) was mixed with 9 µl of GenomiPhi buffer solution which was incubated for 3 minutes at 95 ºC. After cooling the reaction on ice for 2 minutes the random hexamers and phi29 polymerase were added (9 and 1 µl respectively) and the sample was incubated for a further 1.5 hours at 30 ºC followed by 10 minutes at 65 ºC to inactivate the phi29 polymerase. The resulting DNA was visualized by agarose gel electrophoresis using lambda EcoR1/HindIII markers (ABgene, surrey, UK) and purified using DNeasy Blood & Tissue Kit (Qiagen). Quantification of the DNA was achieved using a NanaDrop ND-1000 spectrophotometer (NanoDrop Technologies).

2.14 454 Sequencing

454 sequencing was employed to analyse the metagenomes of one of the high and one of the ambient CO_2 samples which were judged to be representative based on the reproducibility of 16S rRNA gene-based DGGE analysis. The two samples for analysis were first amplified using MDA in order to obtain the 6 – 8 µg of DNA required for this method. Sequencing was carried out on 2 x 1/8 of a sequencing plate by the Advanced Genomic Facility, University of Liverpool using a 454 GS FLX sequencer (Branford, CT, USA). The GS FLX instrument is capable of generating 100 million bp of sequence in approximately 250 bp reads in a 7.5 hour run. Briefly, the DNA was mechanically sheared into smaller fragments and sequence specific A and B adaptors were ligated. The DNA was then captured on beads via the adaptor sequence and clonally amplified by emulsion PCR, generating millions of copies of template per bead. The beads were then

loaded individually into wells on a picotiter plate along with other beads coated in enzymes required for pyrosequencing. DNA nucleotides (dATP. dGTP, dCTP, dTTP) were then flowed sequentially over the plate and light signals released upon base incorporation which are detected by a CCD camera. The presence of luminescence and its signal intensity determines the read.

2.15 Analysis of metagenomic data

Metabolic reconstruction and phylogenetic classification of the metagenomes was performed using the MG-RAST server (Meyer *et al.*, 2008) which annotates metagenomes without the need of sequence assembly or phylogenetic markers. The raw sequence data in fasta format were uploaded onto the server (http://metagenomics.nmpdr.org/) where each dataset was given a unique ID and duplicate sequences were removed. The sequences were automatically screened for protein encoding genes using BLASTX (Altschul *et al.*, 1997) against the SEED none-redundant database (Overbeek *et al.*, 2005) and against rRNA databases such as GREENGENES (DeSantis *et al.*, 2006) and the Ribosomal Database Project (RDP) (Cole *et al.*, 2009) using BLASTN. Phylogenetic and functional reconstructions are then derived from the data which is used to generate the metabolic potential of the sample. Rarefaction curve plots and alpha diversity are also calculated to determine species richness. The curve plots the total number of distinct species annotations as a function of the number of sequences sampled, while alpha diversity is a single number which summarizes the distribution of species-level annotations in a sample.

The results can be viewed via a web based interface which allows interrogation of datasets for comparative analysis studies against other metagenome datasets and fully annotated genomes within the database.

In addition to MG-RAST the metagenome data were analysed using the Metagenome Analyzer (MEGAN) software (Huson *et al.*, 2007). MEGAN is a computer program which allows interactive analysis of large metagenomic datasets. The programs main approach is to parse and analyse the results of a BLAST comparison using

BLASTN, BLASTX or BLASTP against the NCBI-NT, NCBI-NR or other genome specific databases. Therefore a pre-processing step is required where the sequences must be compared to a database and retrieved as BLAST-out files which can then imported into the MEGAN. At start-up, MEGAN loads the complete NCBI taxonomy, currently containing 350,000 taxa, which can be interactively explored using the tree-navigation feature. This database is then compared to the sequence results in the BLAST-out file and a new interactive tree is produced containing the taxonomy of the new dataset from kingdom to species level. Physiological features associated with each read-assigned organism are also provided and COGs (Clusters of Orthologous Groups of proteins) are mapped and displayed in graphical format.

2.16 Statistical analysis

Mann – Whitney, ANOVA and Chi Square tests were carried out using Minitab® (Minitab statistical software, release 15.1.0.0, State College, Pennsylvania**)** The statistical degree of significance was set at a *P* value of <0.05. Statistical analysis of the community composition of ambient and high CO_2 clone libraries was compared using webLIBSHUFF version 0.96 (Henriksen, 2004) (http://libshuff.mib.uga.edu). WebLIBSHUFF is a web based version of the Libshuff program (Singleton *et al.*, 2001) which compares 16S rRNA gene clone libraries to determine if they differ significantly. ClustalW and DNADIST program available in the Bio Edit software package (Hall, 1999) were utilised to construct a distance matrix that was used as an input in the webLIBSHUFF program. WebLIBSHUFF compares libraries based on their coverage (the extent the library represents the total population –homologous coverage curve) and the number of sequences in one library that are not found in the second library (heterologous coverage). Heterologous coverage is calculated over a range of evolutionary distances (values ranging from 0.0 to 0.5 in increments of 0.01) to obtain a coverage curve. The difference between the 'heterologous coverage' curve and the homologous coverage curve is calculated using the Cramér-von Mises test (Pettitt, 1976). The Monte Carlo test then compares the libraries by shuffling sequences between them to determine if both libraries were likely sampled from the same population.

3. Effects of elevated CO_2 and reduced pH on marine microbial communities

3.1 Introduction

The biology of this planet is the direct result of the chemistry of our oceans. All life on earth evolved from single-celled microorganisms which lived in the primitive oceans some 3.8 billion years ago. Consequently the marine ecosystem is an important reservoir of the Earth's biological diversity which plays an important role in our economic and cultural systems. Covering approximately 71% of the Earth's surface the oceans are responsible for regulating climate and play a vital role in numerous biogeochemical cycles such as carbon, nitrogen, sulfur and silicon. Most of Earth's oxygen is produced by phytoplankton in the sea (Mitchell, 2010), and currents such as the North Atlantic drift exert a strong influence on the climate of the coastal regions of northwest Europe (Allaby and Garratt, 2002). Phytoplankton are microscopic (0.4 to 200 μm diameter) unicellular algae that drift in the upper sunlit layers of the ocean. They represent ~1% of the Earth's photosynthetic biomass though are responsible for more than 45% of the planets annual primary production (Field *et al.*, 1998). Consequently they form the base of the marine food web on which, with the exception of hydrothermal vent communities, all marine life is dependent. As phytoplankton represent the keystone of the food chain their abundance and proliferation has profound consequences on the fishing industry both in the commercial sector and in small scale/subsistence fishing communities where fish are essential for survival. Worldwide, approximately 1 billion people are dependent on fish in their diet and they contribute up to 50% of total animal protein intake in many developing countries such as Bangladesh, Cambodia, Equatorial Guinea, French Guiana, the Gambia, Ghana, Indonesia and Sierra Leone (Food and Agriculture Organization, 2008). Furthermore, phytoplankton represent the single largest contributor to net oxygen production and play a vital role in regulating atmospheric CO_2 by incorporating it into biomass. This is especially significant today in the post industrial revolution era when the concentration of atmospheric CO_2 is increasing at an unprecedented rate as a direct result of burning fossil fuels and massive deforestation.

Global warming is one of the consequences of climate change caused by accumulation of greenhouse gases in the atmosphere that produce a positive radiative forcing by trapping long wave solar radiation. Global warming and ocean acidification are a direct consequence of an increase in greenhouse gases such as carbon dioxide, methane, nitrous oxide and trifluoromethane. Though carbon dioxide is considered a trace gas in the atmosphere (0.03%), based on its concentration, it is the major greenhouse gas in the atmosphere (excluding water vapour) with a current concentration of 386.3 ppm (Blasing and Smith, 2010). In contrast, methane the second most abundant greenhouse gas is only 1.7 ppm though it is a more potent gas per unit than carbon dioxide (Khalil, 1999). The total radiative forcing (extra heat energy) in the atmosphere since pre-industrial 1750 is 2.43 W/m^2. Of this total, methane contributes 20% of the radiative forcing with 0.48 W/m^2 which proportionally (due to concentration) contributes more than carbon dioxide at 1.66 W/m^2 (Forster *et al.*, 2007). Since 1751 approximately 337 billion tons of carbon have been released into the atmosphere primarily from the burning of fossil fuels and cement production (Boden *et al.*, 2010). As a direct result of these emissions the average global temperature has increased by 0.7 °C in the past 100 years with a global average sea level rise of 1.8 mm per year over the period 1993 to 2003 (IPCC, 2007).

The uptake of CO_2 by the ocean is a direct response to rising atmospheric CO_2 concentration in which the partial pressure of CO_2 is equilibrated across the air-water interface. In essence, the ocean directly mediates against climate change by sequestering anthropogenic CO_2 thus reducing the effects of global warming (McNeil, 2006). This results in what is known as ocean acidification, a process in which the carbonate chemistry of seawater is altered by the addition of CO_2 resulting in an increase in hydrogen ion concentration and a decrease in pH. Since the beginning of the industrial revolution the pH of the ocean has declined from 8.2 to 8.1 and this trend is expected to continue if CO_2 emissions go unabated. The term “ocean acidification” is therefore a misnomer and in reality the oceans are becoming less alkaline rather than becoming acidic *per se*. The phrase was coined by the atmospheric scientist Ken Caldeira in a 2003

Nature paper to add impact to his research (Caldeira and Wickett, 2003) since then it has been adopted by climate scientists as it adds gravitas to a very real and serious threat.

In the oceans, dissolved inorganic carbon (DIC) exists in 3 forms and their proportions are reflected in the pH of the seawater. These forms are (I) aqueous CO_2 and carbonic acid (H_2CO_3), (II) Bicarbonate (HCO_3^-) and (III) Carbonate ion (CO_3^{2-}) Under current ocean conditions (pH 8.1) approximately 90% of the inorganic carbon is bicarbonate, 9% is carbonate ion, and only 1% is dissolved CO_2 (Millero *et al.*, 2002). In seawater dissolved CO_2 (aq) combines with H_2O producing carbonic acid. Both CO_2 (aq) and carbonic acid exist in equilibrium in water however carbonic acid is weak and can quickly dissociate resulting in the production of bicarbonate and hydrogen ions (H^+) which decreases the pH of the water making it slightly more acidic. Bicarbonate can also dissociate to carbonate and H^+ but this is dependent on pH, the more alkaline the solute the greater the dissociation.

Carbonate system - aqueous speciation:

CO_2 (aq) + H_2O <=> H_2CO_3 (Carbonic acid)

H_2CO_3 <=> HCO_3^- + H^+ (Bicarbonate)

HCO_3^- <=> CO_3^{-2} + H^+ (Carbonate ion)

The carbonate buffer system allows the ocean to adjust to the addition of CO_2 without large scale change in pH. As seawater becomes more acidic (due to increased CO_2) the system counters by altering the proportions of bicarbonate and carbonate thus reducing the amount of H^+ and stabilizing the pH. However, the concentrations of CO_2 and carbonate are inversely related, increasing one reduces the concentration of the other. Therefore increased CO_2 decreases the relative concentration of carbonate which in turn impairs the process of calcification, with important implications for calcifying marine organisms.

It is anticipated that over the next century atmospheric CO_2 concentrations will continue to decrease ocean pH and the concentration of carbonate ions, that marine calcifying organisms require to build their skeletons and shells, will decrease. Currently the calcium carbonate of such organisms does not dissolve due to the fact that the oceans are supersaturated with calcium (Ca^{2+}) and carbonate ions. It is anticipated however that the decrease in carbonate ions will eventually reach a point where the rate of calcium carbonate erosion exceeds production. This would have a detrimental effect on reef building organisms as they deposit calcium carbonate in the form of aragonite which is the easiest form of calcium carbonate to dissolve when carbonate concentrations decrease.

Sceptics of climate change have pointed out that there have been periods in Earth's history when CO_2 levels were considerably higher than today while at the same time there was widespread glaciation (McClintock, 2009). There is unequivocal evidence for a period of glaciation during the late Ordovician (Royer, 2006) with CO_2 data close to this period suggesting high CO_2 concentrations ~5600 ppm (Yapp and Poths, 1992, Yapp and Poths, 1996). However, it is unclear exactly what the CO_2 levels were at the time of the event as the single proxy record spans a period of almost 7 million years which includes a known global warming event. Furthermore, solar output was around 4% lower than current values and as a consequence the CO_2 threshold for initiating glaciation would be higher (Royer, 2006). The CO_2-ice threshold for the present-day Earth is 500 ppm but global climate models have predicted a CO_2-ice threshold for the late Ordovician of 2240 and 3920 ppm (Poussart *et al.*, 1999, Herrmann *et al.*, 2003). Paradoxically, there were periods when CO_2 was considerably lower than it is today and yet the climate was actually warmer than the present. The Medieval Warm Period (~800-1300 AD) was one such event which was marked by an increase in temperature (1.2–1.4°C) and rainfall (+10%) in pre-industrial Europe (Lamb, 1965). Research conducted by Trouet (Trouet *et al.*, 2009) has found a positive North Atlantic Oscillation (NAO) mode during the medieval climate anomaly. The NAO is a large scale seesaw in atmospheric mass between the subtropical high and the polar low. A Positive NAO results in warm and wet winters in Europe and cold and dry winters in

northern Canada and Greenland whereas a negative NAO brings cold air to Europe and milder winter temperatures to Canada and Greenland.

CO_2 is not the only driver of climate and there are numerous climate forcing mechanisms which influence the energy balance of the planet. Climate forcing is an imposed perturbation of the Earth's energy balance with space, (Hansen *et al.*, 1998) and as a consequence the climate is "forced" to change. Forces which influence climate change can be broken down into extraterrestrial and terrestrial with the terrestrial forces being further subdivided into natural and man-made. The primary forcing mechanisms are as follows; orbital variation (Milankovitch cycles), plate tectonics, thermohaline circulation, volcanic activity and surface albedo (Chapter 1 section 1.5).

The most significant extraterrestrial forcing event occurred 65 Mya resulting in a mass extinction of at least 46% of genera (Keller, 2005). It has been hypothesised that the bolide impact at Chicxulub on the Yucatán Peninsula, Mexico resulted in the transfer of ~ 4,600 Gt of carbon into the atmosphere (Beerling *et al.*, 2002). This was followed by a dramatic rise in atmospheric CO_2 concentration which rose from 350–540 ppm between the Late Cretaceous and the Early Tertiary to a pCO_2 of 2,300 ppm within 10,000 years of the impact, raising global temperatures by as much as 7.5 Celsius. Beerling and his team calculated the pCO_2 using the inverse relationship between the stomatal index (SI) which is the proportion of epidermal cells that have stomatal pores in fossil leaves of gingkoes and ferns that grew around the time of the dinosaurs' demise. The number of stomatal pores reflects the atmospheric CO_2 concentration, the fewer the pores, the higher the pCO_2 level. The equation was derived from both CO_2 enrichment experiments and historical archives of gingko leaves collected over a 200 year period and calibrated using CO_2 data between 1837 and 1964. Beerling refuted the alternate hypothesis that the increase in CO_2 was the result of massive volcanic activity in the Deccan traps of south west India by simulating volcanic CO_2 emissions over a 2 million year period. The results revealed no significant increase in atmospheric pCO_2 because the input of volcanic CO_2 was only a small fraction of the background production which could be easily absorbed by the ocean. The rise of pCO_2 to 2,300 ppm would have been

an additional stress to ecosystems already perturbed by the "impact winter" predicted by Alvarez (Alvarez *et al.*, 1980) in which dust from the impact stayed in the atmosphere for several years blocking the sun and suppressing photosynthesis. Consequently the mass extinction of marine and terrestrial organisms at the end of the Cretaceous-Tertiary period was not instantaneous and several species including the dinosaurs took several thousand years to become extinct. It is estimated that approximately 90% of all marine calcareous nanoplankton became extinct resulting in a "Strangelove" ocean where ocean productivity was severely reduced for at least 0.5 Myr (Zachos *et al.*, 1989). There are 2 pieces of evidence which substantiate the disturbance of the marine biosphere by this event. First, the mass extinction of marine calcareous nanoplankton was reflected in a reduction of $CaCO_3$ deposition at the Cretaceous-Tertiary Boundary (KTB) (Arthur *et al.*, 1987) and second the negative $\delta^{13}C$ value of planktonic carbonate at the KTB of approximately 2‰ compared to those below the boundary (Corfield, 1994; Kaiho *et al.*, 1999, Arens and Jahren, 2000, Maruoka *et al.*, 2007). Photosynthetic plankton preferentially assimilate the light isotope of carbon (^{12}C) leaving the surrounding water enriched with the heavier ^{13}C. Therefore any carbonate precipitated from this water will be enriched in^{13}C and will have a positive $\delta^{13}C$ value. Essentially, the more positive the $\delta^{13}C$, the greater the primary production while a negative $\delta^{13}C$ can be interpreted as evidence for a reduction (or shutdown) of marine primary production (Hsu, 1980).

Analysis of carbonate sediments can therefore provide a record of the changing primary productivity through time. The Yucatan Peninsula is a sedimentary terrace of calcium carbonate (chalk) formed from the shells of coccolithophorid algae which were laid down in the early Cretaceous (Latin *Creta* meaning chalky) period. The area also includes significant amounts of calcium sulfate which upon impact of the bolide caused the release of sulfur dioxide into the atmosphere. It is hypothesized that the sulfur dioxide reacted in the atmosphere with water and oxygen to form sulfuric acid which rained down making the waters of the upper ocean corrosive to calcium carbonate shells (D'Hondt *et al.*, 1994; D'Hondt *et al.*, 1996, Pope *et al.*, 1997, Pope *et al.*, 1998). This acidification event would have only lasted one or two years as the upper ocean would have eventually mixed with the waters from the ocean depths restoring the chemistry

equilibrium. Consequently phytoplankton with shells constructed from silica survived the extinction event whereas it took 500,000 years before new species of calcium carbonate producing plankton evolved and 20 million years to recover to pre-extinction levels of species diversity (Caldeira, 2007, Riebesell, 2007).

Nearly half of all the anthropogenic CO_2 produced in last 200 years has been absorbed by the oceans resulting in a drop in pH of 0.1 units which equates to a 30% increase in the concentration of hydrogen ions (Royal Society, 2005) . Currently the oceans are absorbing about one tonne of anthropogenic CO_2 per year for each person on the planet (IPCC, 2001) further reducing pH. It is hypothesised that today's CO_2 emissions may be even more detrimental to ocean chemistry than the sulfuric acid rain which fell 65 million years ago (Caldeira, 2007). Although these effects were probably more extreme the actual acidification event itself was only short lived lasting only a couple of years. Unfortunately, the current level of ocean acidity is irreversible during our lifetime and it is anticipated that it will take tens of thousands of years for ocean chemistry to revert back to pre-industrial levels (Royal Society, 2005) until then the oceans are expected to become more acidic as carbon dioxide levels continue to rise.

In this study I examined the impact of rising CO_2/reduced pH on both phytoplankton and bacterioplankton and evaluated the possible consequences for marine ecosystems and processes. To this end an 18 day perturbation experiment was conducted in a Norwegian fjord which simulated the pCO_2 and pH conditions of the future high CO_2 world of 2100 as predicted by the IPCC (IPCC, 2001). Bacteria and phytoplankton were enumerated daily throughout the experiment along with pCO_2 and pH measurements in order to assess the effects of elevated CO_2 on the microbial populations. Chlorophyll-*a* concentrations were measured to monitor the evolution of the phytoplankton bloom coupled with trace gas analysis (DMS, DMSP). Comparative analysis of the data from high and ambient CO_2 treatments was then conducted to assess the effects of CO_2-driven ocean acidification. The data provided the overall context for the detailed microbial community analyses that was conducted subsequently (Chapter 3 to Chapter 6).

3.2 Methods

3.2.1 Mesocosm experiment

The mesocosm experiment was conducted at the Espeland Marine Biological Station, Bergen, Norway in May 2006. 6 x 1100 L mesocosms were deployed approximately 200 m from the shore and filled with unfiltered seawater water pumped directly from the fjord. The experiment was divided into 2 different treatments; mesocosms 1, 2 and 3 (M1-M3) were designated as high CO_2 (~pH 7.8) while mesocosms 4, 5 and 6 (M4-M6) were designated as ambient CO_2 (~pH 8.1). This was achieved by aerating the mesocosm for 2 days with either CO_2 or air and flushing the headspace thereafter. Once the desired conditions had been attained nutrients in the form of phosphate and nitrate were added to all the mesocosms (initial concentrations: 1.25 µmol l^{-1} phosphate; 16 µmol l^{-1} nitrate) in order to induce a phytoplankton bloom. Due to phytoplankton growth reducing CO_2 concentration to near ambient levels in the high CO_2 mesocosms, the acidification process was repeated a second time on the evening of day 10 (15th May). In this instance only two mesocosms were bubbled overnight with CO_2 (M1 & M2) and two with air (M5 & M6). Mesocosms M3 and M4 were left untreated and used as a control experiment to ascertain if the bubbling process itself affected the ecology of the mesocosms. Therefore the experiment had two phases; phase 1 (pre-bloom) which ran from the 6 – 15th May (Day 1 – Day 10) and phase 2 (post bloom) which ran from 16 – 23rd May (Day 11 – Day 18).

Mesocosm water samples were taken daily at 9 am throughout phase 1 and phase 2 of the experiment with the exception of 17th May when due to technical difficulties no samples were taken. 25 L of seawater was withdrawn from each mesocosm and filtered through GF/A filters to remove large eukaryotes and the filtrate was collected onto 0.2 µm Durapore membranes for further molecular analysis. Approximately 20 ml was retained to enumerate absolute concentrations of phytoplankton and bacterioplankton using a Becton Dickinson FACSort flow cytometer. All flow cytometric analyses were conducted by Dr Andrew Whiteley, CEH Oxford. pH

and pCO_2 was also measured and the development of phytoplankton bloom was monitored by measuring the chlorophyll-a concentration. pH and pCO_2 were determined by Dr Dorothee Bakker (University of East Anglia) and chlorophyll-a was determined Dr K. Crawfurd, (University of Dundee).

3.2.2 Bottle incubations

In order to study the effects of elevated CO_2 on chemoautotrophic bacteria seawater was sub sampled from mesocosms M1, M3, M4 and M6 and placed into 2 x 4L dark incubation bottles which were amended with either 0.68 grams of ^{13}C sodium bicarbonate or ^{12}C sodium bicarbonate. These were designated bottles B1, B3, B4 and B6 with each designation having a ^{13}C and ^{12}C equivalent. Every mesocosm was allocated its specific set of incubation bottles (i.e. Bottles B1$^{13}C/^{12}C$ allocated to mesocosm M1). Bottle incubations were prepared for both phases of the experiment on day 8 (phase 1) and then again on day 15 (phase 2). The bottles were incubated by suspending them in the fjord and sampling commenced after 24 hours.

Dark incubation bottles were sampled daily at 3 pm on days 9, 10, 11 and 13 in phase 1 and days 16, 17, 18 and 20 in phase 2 of the experiment. Approximately 1 L of seawater was withdrawn from each bottle of which 20 ml was used for flow cytometry and to measure pH.

3.2.3. Statistical analysis

To determine large scale treatment effects and identify samples for further molecular analysis statistical analyses was conducted on all data generated using the software package Minitab® 15. Due to the small sample size of some of the datasets non-parametric analyses was conducted using the Mann-Whitney U Test (Mann and Whitney, 1947). This test compares the medians of two groups to suggest whether both samples come from the same population or not which is advantageous in groups that may be skewed as the medians remain unaffected by outliers.

All data generated as part of the NERC Bergen mesocosm project were deposited in the Bergen mesocosm data repository and made available to all participants http://nebc.nerc.ac.uk/bergendb

3.3 Results and discussion

3.3.1 Effect of CO_2 on pH in mesocosms and bottle incubations

Data for 2 high CO_2 (M1 & M2) and 2 ambient CO_2 (M5 &M6) mesocosms are presented here as these treatments remained constant throughout the entire experiment. The dark incubation data presented were obtained from bottles B1 ($^{13}C/^{12}C$) and B6 ($^{13}C/^{12}C$) which were prepared from seawater obtained from M1 and M6 respectively. No incubations were prepared from the remaining two mesocosms (M2 and M5) due to the fact they were amended with ^{15}N labelled nitrate which may have interfered with the ^{13}C labelling of the chemoautotrophic bacteria in the subsequent SIP analyses (Chapter 5, section 5.2).

At the start of the experiment (day 0) the average pH of mesocosms M1-M3 was 8.06. However, due to the introduction of CO_2 (750 µatm) the pH decreased and by day 1 of the experiment it averaged pH 7.81±0.003. In contrast, mesocosms M4-M6 averaged pH 8.14 which was similar to the fjord (pH 8.19). A steady increase in pH was observed in both treatments throughout phase 1 of the experiment due to the uptake of CO_2 by the increasing phytoplankton biomass (Figure 3.1A). Phase 2 of the experiment commenced on day 11 after the reintroduction of CO_2 into M1, M2 and ambient air into M5, M6. On this occasion, mesocosms M3 and M4 were left to equilibrate in order to ascertain if the bubbling had any effect on bacterial community composition.

It has been argued that the relationship between atmospheric CO_2 and ocean pH is unconvincing as a non-linear response is observed when plotting pH changes against atmospheric carbon dioxide partial pressure (Marsh, 2008, Doney *et al.*, 2009).

However, a linear relationship was clearly observed if the pCO_2 data is transformed to a logarithmic scale so that both scales (pCO_2 and pH) are consistent (Figure 3.1B).

In the bottle incubations there were no significant differences in pH observed between the labelled and unlabelled treatments in the high and ambient incubation from both phases of the experiment ($P > 0.05$; Mann Whitney U Test; Figure 3.1C). However, significant difference were observed in pH between the ambient and high CO_2 dark incubations in phase 1 ($P=<0.01$; Mann Whitney U Test) and phase 2 ($P=<0.01$; Mann Whitney U Test) of the experiment (Figure 3.1C). Furthermore, the pH in the incubations was considerably lower than in the mesocosms from which the bottles were prepared due to the exclusion of light which reduced the uptake of CO_2 via photosynthesis.

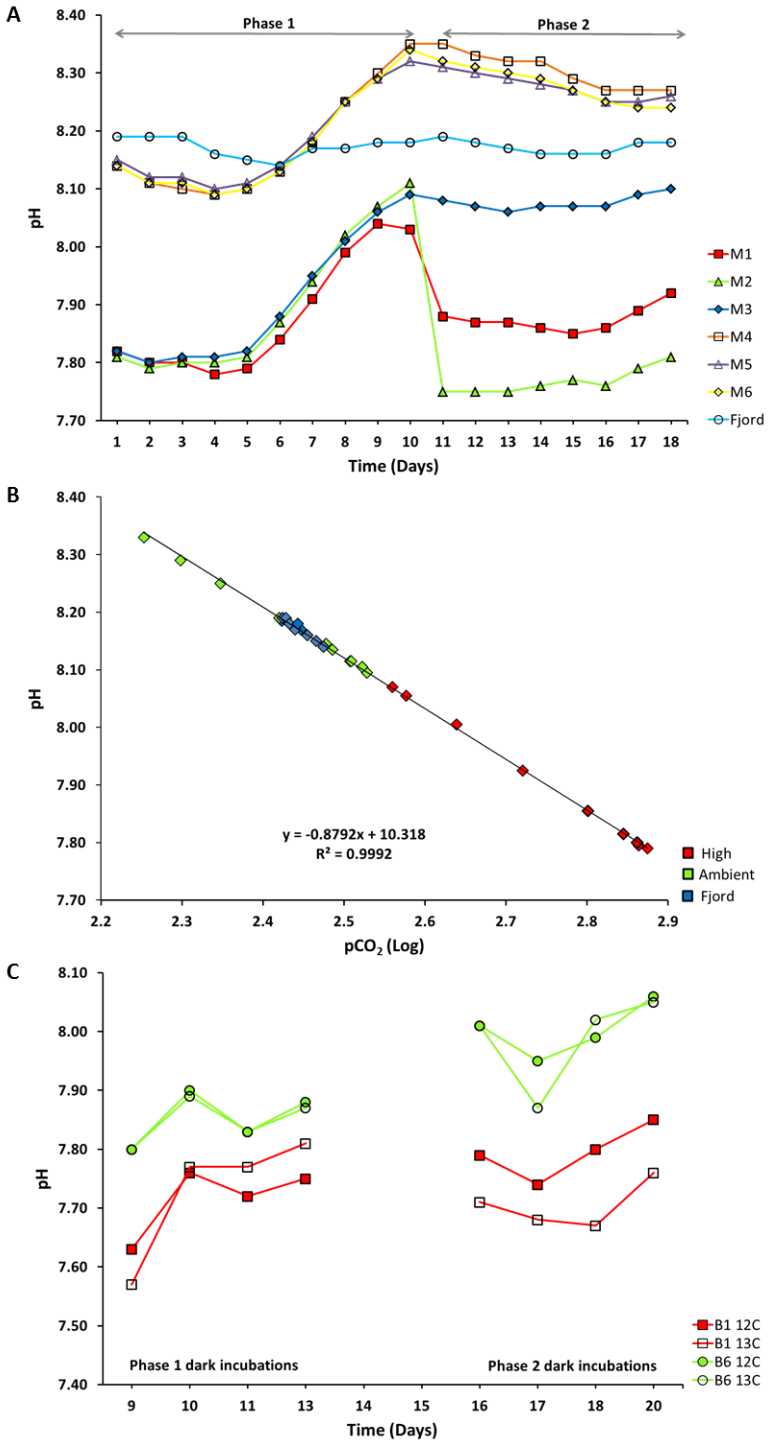

Figure 3.1 pH of mesocosms M1-M3, (high CO_2) M4 -M6 (ambient CO_2) and the fjord for the entire duration of the experiment (A). Negative linear correlation between the partial pressure of atmospheric CO_2 and pH during phase 1 of the experiment (B). pH values for ^{13}C and ^{12}C dark incubation bottles with B1 the high CO_2 treatment and B6 the ambient CO_2 treatment (C).

3.3.2 Bloom development

The addition of phosphate and nitrate at the start of the experiment led to the development of a pronounced algal bloom in all the mesocosms which reached its peak around day 8. Chlorophyll-a concentration (Figure 3.2) at its peak, was ~34% higher under ambient CO_2 conditions (10.41 ± 1.14 $\mu g/l^{-1}$ chlorophyll-a) compared to high CO_2 conditions (6.87 ± 3.33 $\mu g/l^{-1}$ chlorophyll-a). Chlorophyll-a concentration continued to decline throughout phase 2 but slowly increased due to a minor secondary bloom between days 15-18. Statistically, there was no significant difference in chlorophyll-a concentration between the treatments at the peak of the bloom on day 8 (P=0.24; Mann Whitney U Test). However, in the same study Hopkins (Hopkins *et al.*, 2009) using the acetone extraction dataset found that chlorophyll-a concentrations were significantly lower under high CO_2 conditions if data from the whole period between days 5 - 12 is considered (P=0.021; Two sample t test).

A significant decrease in primary productivity of 27.3% was observed in the high CO_2 mesocosms M1 and M2 compared to the ambient CO_2 mesocosms M5, M6 between days 6 to 8 (P=0.03; Mann Whitney U Test). During this period the daily average primary productivity was 599±36 mg C m^{-2} d^{-1} in the high CO_2 treatments while in the ambient CO_2 treatment it averaged 824±61 mg C m^{-2} d^{-1}. Primary productivity was calculated using the ^{14}C technique which measures the assimilation of bicarbonate into organic matter (Joint and Pomroy, 1983).

The development of the algal bloom coincided with the depletion of nutrients however early observations indicated that the rate of nutrient depletion was slower in the high CO_2 treatment compared to that of the ambient CO_2 treatment (Figure 3.3). However, the difference was not statistically significant in either nitrate (P= 0.60; Mann Whitney U Test) or phosphate (P= 0.79; Mann Whitney U Test) between the treatments. In the high CO_2 treatment, the average depletion rate of nitrate (Figure 3.3A) was 0.076 ±0.05 µmol/l/hr, while in the ambient CO_2 treatment the average depletion rate was 0.072 ±0.01 µmol/l/hr. Conversely, phosphate depletion rates were 0.0043 ±0.0037

µmol/l/hr in the high CO_2 treatment and 0.0044 ±0.0014 µmol/l/hr in the ambient CO_2 treatment (Figure 3.3B).

3.3.3 Bacterioplankton Dynamics

No significant differences were observed in total bacterial abundance between the high and ambient CO_2 mesocosms in phase 1 of the experiment (P=0.14). Bacterial numbers slowly increased in both treatments during this phase peaking on day 6 in the high CO_2 treatment with 4.80 ±0.02x10^6 cells/ml and on day 9 in the ambient CO_2 treatment with 5.68 ±0.97x10^6 cells/ml after which they remained relatively steady until phase 2 of the experiment commenced on day 11 (Figure 3.4A).

In phase 2 of the experiment bacterial numbers initially rose in both treatments reaching their peak on day 14 in the high CO_2 mesocosms with 1.15 ±0.19x10^7 cells/ml and on day 16 in ambient CO_2 mesocosms with 1.04 ±0.09x10^7 cells/ml. After these peaks, cell numbers decreased rapidly in the high CO_2 treatment to a final concentration of 1.72 ±0.49x10^6 cells/ml whereas cell numbers in the ambient CO_2 mesocosms decreased gradually to 8.10 ±2.8x10^6 cells/ml (Figure 3.4A). No statistical difference was observed in bacterial numbers at the beginning of phase 2 of the experiment (P=0.43; Mann-Whitney U test) however a significant difference was observed after day 14 (P= 0.03) when bacterial cell numbers declined rapidly in the high CO_2 mesocosms.

Similar results were obtained from the dark incubation bottles (Figure 3.4B) with cell numbers indicating no significant difference between the treatments in phase 1 of the experiment (P=0.37) but a significant difference was observed between the high and ambient CO_2 treatments in phase 2 of the experiment (P=<0.01). It was also established that there was no significant difference in bacterial cell abundance between ^{13}C and ^{12}C-bicarbonate amended incubation bottles within the same treatments (P = >0.1).

It was observed that in the dark incubations the bacterial cell counts in phase 2 of the experiment were considerably lower in the high CO_2 treatment (Figure 3.4B). The average bacterial cell count over the 5 day incubation period (^{13}C and ^{12}C) was 3.85 $\pm 0.33 \times 10^6$ cells/ml in the ambient CO_2 treatment whereas in the high CO_2 treatment it had decreased by 81.9% to 6.97 $\pm 0.52 \times 10^5$ cells/ml. This is has been attributed to a decrease in primary production (lower phytoplankton biomass) in the high CO_2 treatment during phase 1 of the experiment which is reflected in the chlorophyll-a concentrations (Figure 3.2.) during the peak of the bloom. This can be further substantiated by the fact that in the high CO_2 treatments at the peak of the bloom (~day 8) cell numbers of Synechococcus (Figure 3.7A), large picoeukaryotes (Figure 3.8A), cryptophytes (Figure 3.9A), nanoeukaryotes (3.9B) and coccolithophores (Figure 3.10) were lower than that of the ambient CO_2 treatments.

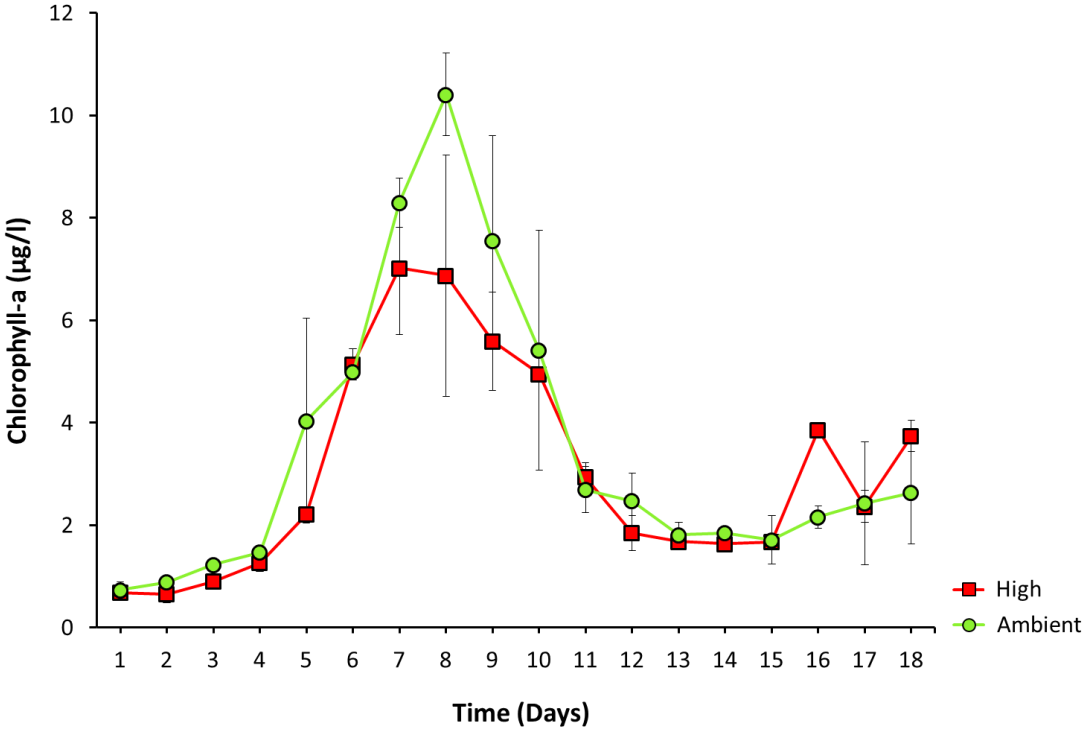

Figure 3.2 Temporal evolution of mean chlorophyll-a concentration (±s.e., n=2) of high CO_2 (M1&M2) and ambient CO_2 (M5& M6) treatments indicating the development and eventual demise of the phytoplankton bloom in phase 1 of the experiment.

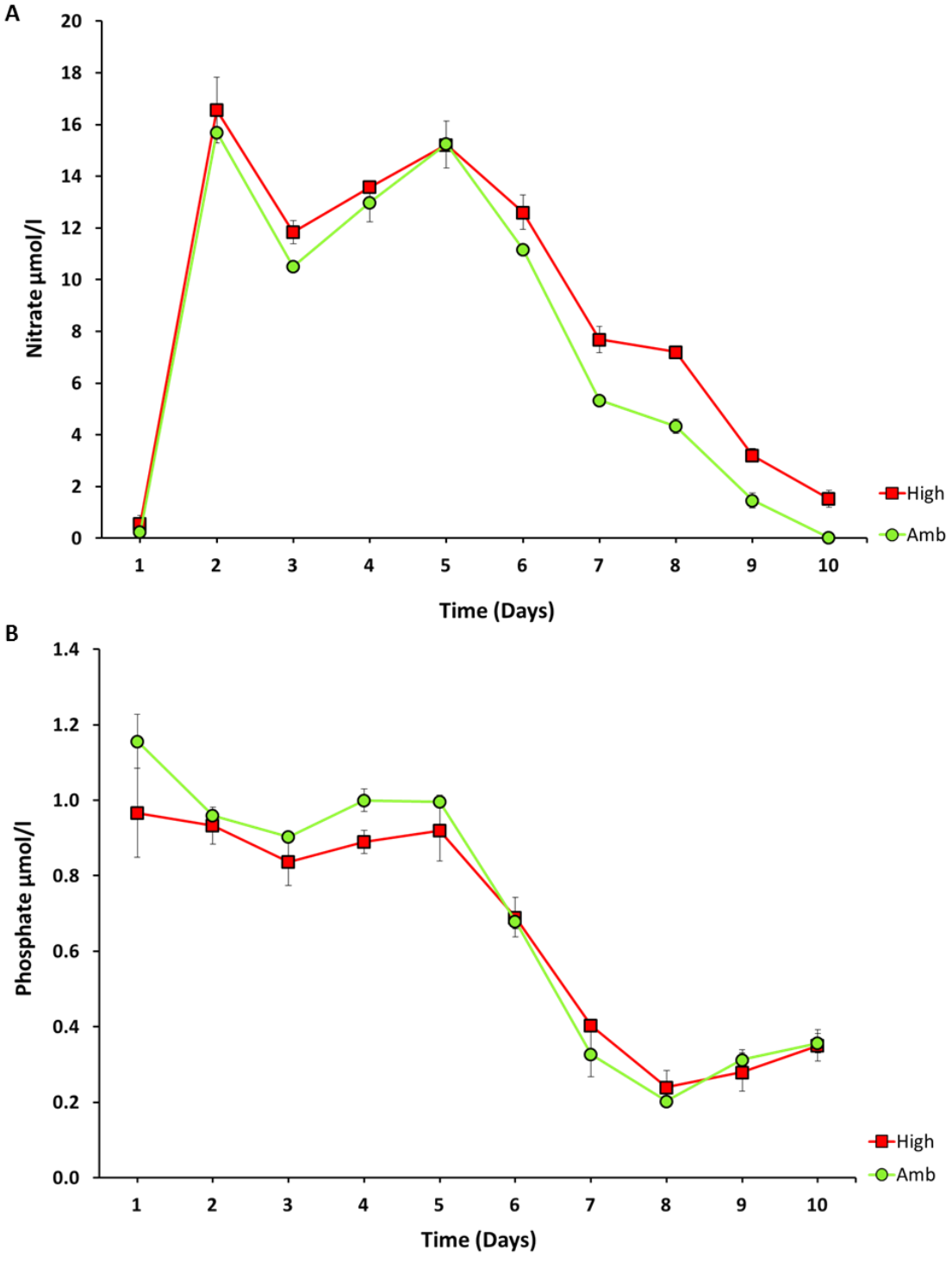

Figure 3.3 Temporal changes in nutrient availability of nitrate (A) and phosphate (B). Concentrations were derived from the mean average concentration (µmol/l) of M1, M2, M3 (high CO_2 mesocosms) and M4, M5, M6 (ambient CO_2 mesocosms) (±s.e., n=3).

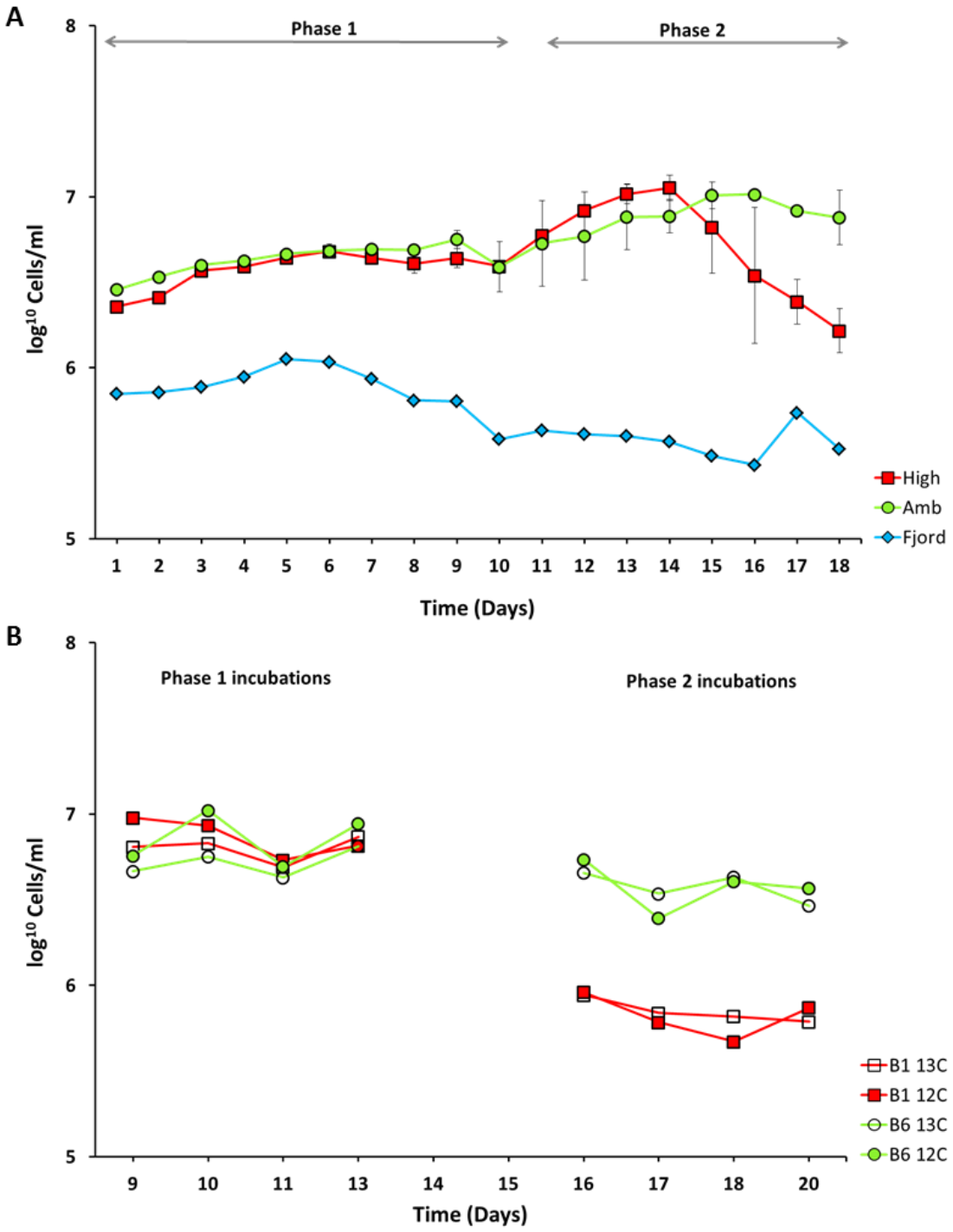

Figure 3.4 Temporal variability of total bacterial abundance (± s.e., n=2) in mesocosms with high and ambient CO_2 treatments in comparison to the fjord, (A). Variability of total bacterial abundance in the dark incubation bottles subject to high CO_2 (B1) and ambient CO_2 (B6) treatments (B).

Heterotrophic bacteria were also enumerated by flow cytometry represented by high nucleic acid (HNA) and low nucleic acid (LNA) bacterial cell counts. Traditionally HNA cells have been regarded as dynamic members of the bacterial assemblage which are actively growing (Gasol *et al.*, 1999) whereas LNA cell are regarded as inactive, dead or cell fragments (Lebaron *et al.*, 2001). These two groups can be discriminated by flow cytometry by differences in their side scatter (inner cell complexity) and fluorescence (emission wavelength). However, using a combination of flow cytometry and the incorporation of labelled amino acids [^{3}H] leucine and [^{35}S] methionine Zubkov *et al* (2001) discovered that bacterioplankton in the LNA group were just as metabolically active as members in the HNA group. Furthermore, the groups were phylogenetically identified by fluorescent in situ hybridization (FISH). The HNA- hs (high scatter) group was dominated by the *Roseobacter* clade of the *Alphaproteobacteria* with the *Gammaproteobacteria* representing ≤10% of the cells while the HNA-ls (low scatter) group was dominated by the *Cytophaga-Flavobacterium* cluster. A higher phylogenetic characterization of the LNA group was not determined as only a weak signal in approximately 10 – 20% of the cells was observed for the SAR86 probe (*Gammaproteobacteria*). It was determined that this was due to additional diversity within the sample which was not covered by the set of probes used in the FISH analysis (Zubkov *et al.*, 2001). However, the characterization of the LNA group was addressed several years later which revealed it was dominated by the SAR 11 clade (Mary *et al.*, 2006). The only cultured representative of this group Pelagibacter ubique, strain HTCC1062 has the smallest genome (1,308,506 bp) of any cell known to replicate independently (Giovannoni *et al.*, 2005). Therefore even when this bacterium is replicating its nucleic acid content would still be significantly smaller than a member of the marine *Roseobacter* clade whose genomes vary from 3.5 – 5.3 Mb (Tang *et al.*, 2010).

The mesocosm HNA and LNA bacterial cell counts (Figure 3.5A/B) showed a similar pattern to that of the total bacterial counts (Figure 3.4A). Both indicated no significant treatment differences in cell numbers for phase 1 or the start of phase 2 of the experiment but differences were observed in the latter half of phase 2 when cell numbers

declined rapidly in the high CO_2 treatments (P=0.031, HNA; P=<0.001, LNA). The largest decrease was observed in the HNA group which declined from 4.32 ±0.92x 10^6 to 4.16 ±2.29x10^5 cells/ml (-90.4%) between days 14 and 18 whereas the LNA decreased from 1.16 ±0.05x10^6 to 4.0 ±0.1x10^5 cells/ml (-65.5%) during the same period. These results strongly suggest that both bacterial groups were affected, either directly or indirectly by the elevated CO_2 treatment, though the effects were more pronounced in the HNA group. It is uncertain if such decreases in cell numbers are permanent or just temporary changes in which the community is able to physiologically adapt in a relatively short time.

In the dark incubation bottles no significant differences were observed in either HNA or LNA cell numbers from phase 1 of the experiment P=>0.5 (Figure 3.6A/B). However, a significant treatment response was observed in both HNA and LNA cell numbers in phase 2 of the experiment (P = < 0.01 for both HNA & LNA). As there was little fluctuation in cell numbers within each treatment an average was obtained for each pair of incubation bottles (^{13}C & ^{12}C). Over the 5 day incubation period the HNA bacteria averaged 2.68 ±0.25x10^6 cells/ml in the ambient CO_2 incubations and 4.31 ±0.23x10^5 cells/ml in the high CO_2 incubation whereas the LNA bacteria averaged 1.06 ±0.08x10^6 cells/ml in the ambient CO_2 incubation and 2.35 ±0.29x10^5 cells/ml in the high CO_2 incubation. Cell numbers were lower in both the HNA and LNA bacteria in the high CO_2 incubations by 83.9% and 77.8% respectively, consistent with the mesocosm data.

The abundance of the cyanobacterium *Synechococcus* gradually increased during the entire experiment in both the ambient and high CO_2 mesocosms (Figure 3.7A). In the high CO_2 treatment cell numbers rose from 1.73 ±0.006x10^3 cells/ml on day 1 to 1.88 ±0.59x10^4 cells/ml on day18 whereas cell numbers in the ambient CO_2 treatments rose from 2.34 ±0.04x 10^3 cells/ml on day 1 to 3.17 ±0.07x10^4 cells/ml on day 18. No significant differences were observed in cell numbers between the treatments (P = 0.21) in phase 1 of the experiment, however a difference was observed in phase 2 (P=0.002).

Synechococcus cell numbers gradually decreased in both treatments of the dark incubations (Figure 3.7B). As light is essential for all obligate phototrophs the demise of *Synechococcus* and all phytoplankton species analysed in the dark bottle incubations was expected. For this reason no statistical analysis was conducted on any phytoplankton species in the dark incubations as long as their numbers were declining. In this instance the mean cell concentration (^{13}C &^{12}C) on the first day of sampling (day 9) was 1.59 $\pm$0.34x10^4 cells/ml decreasing to 1.02 $\pm$0.07x10^4 cells/ml in the ambient CO_2 incubations and 8.66 $\pm$0.21x10^3 cells/ml decreasing to 4.42 $\pm$0.71x10^3 cells/ml in the high CO_2 incubations.

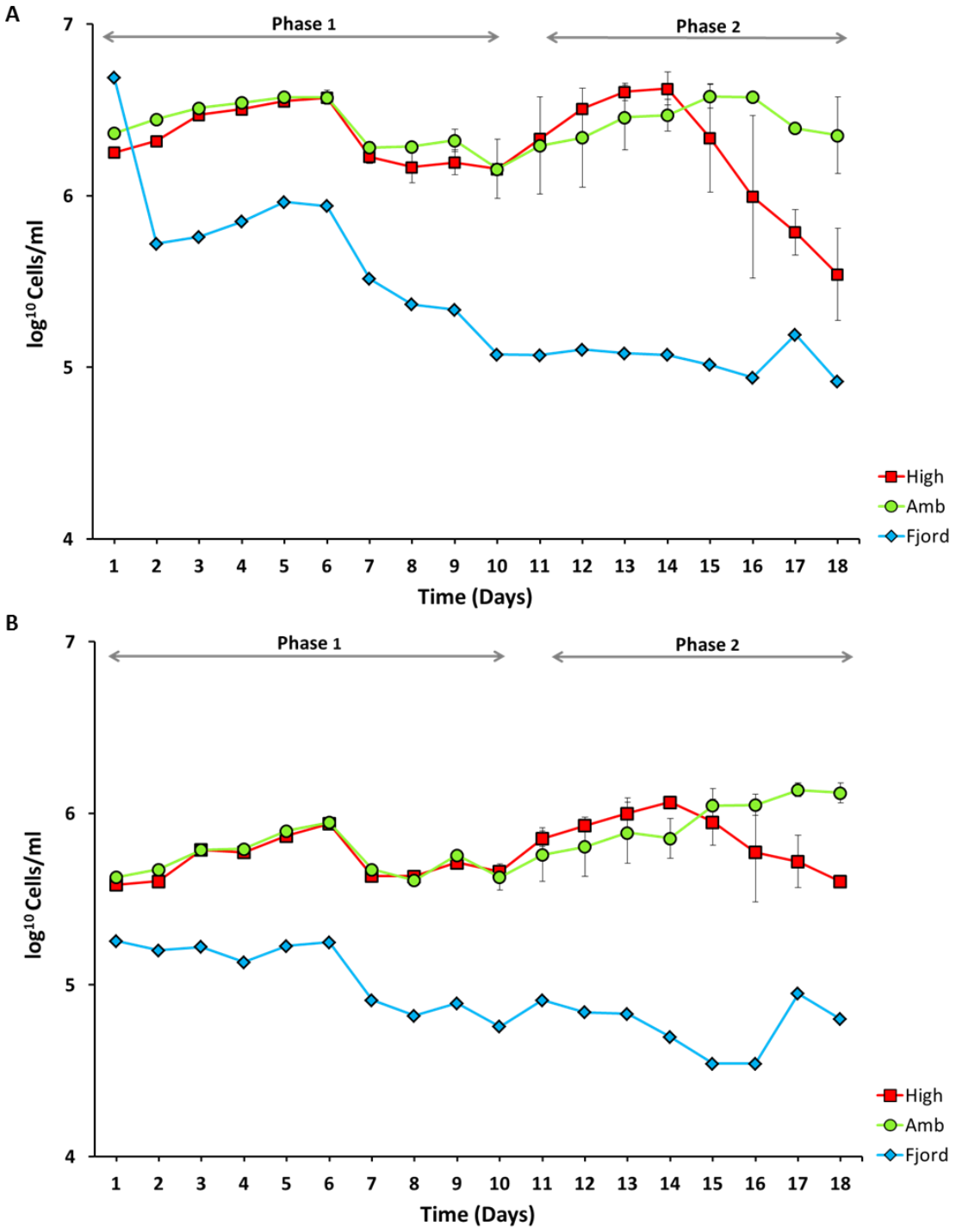

Figure 3.5 Temporal variability in log mean (± s.e., n=2) of cell abundance for HNA (A) and LNA heterotrophic bacteria (B) in both treatments and the fjord during the entire duration of the experiment.

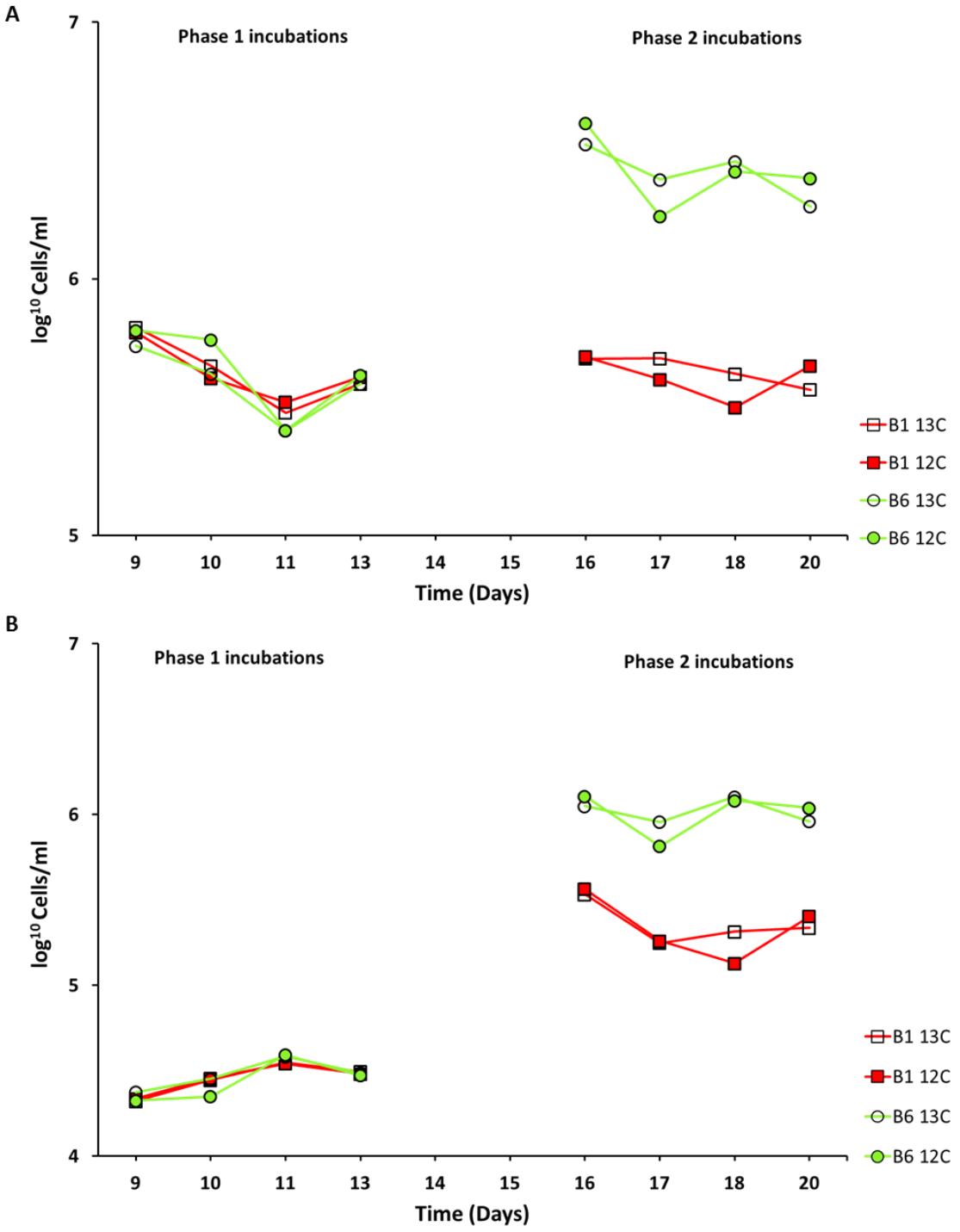

Figure 3.6 Concentration of HNA heterotrophic bacteria (A) and LNA heterotrophic bacteria (B) for the dark bottle incubations. Bottles were filled from their allocated mesocosm (M1= B1) 24 hours prior to the first sampling and incubated in the fjord to simulate mesocosm conditions.

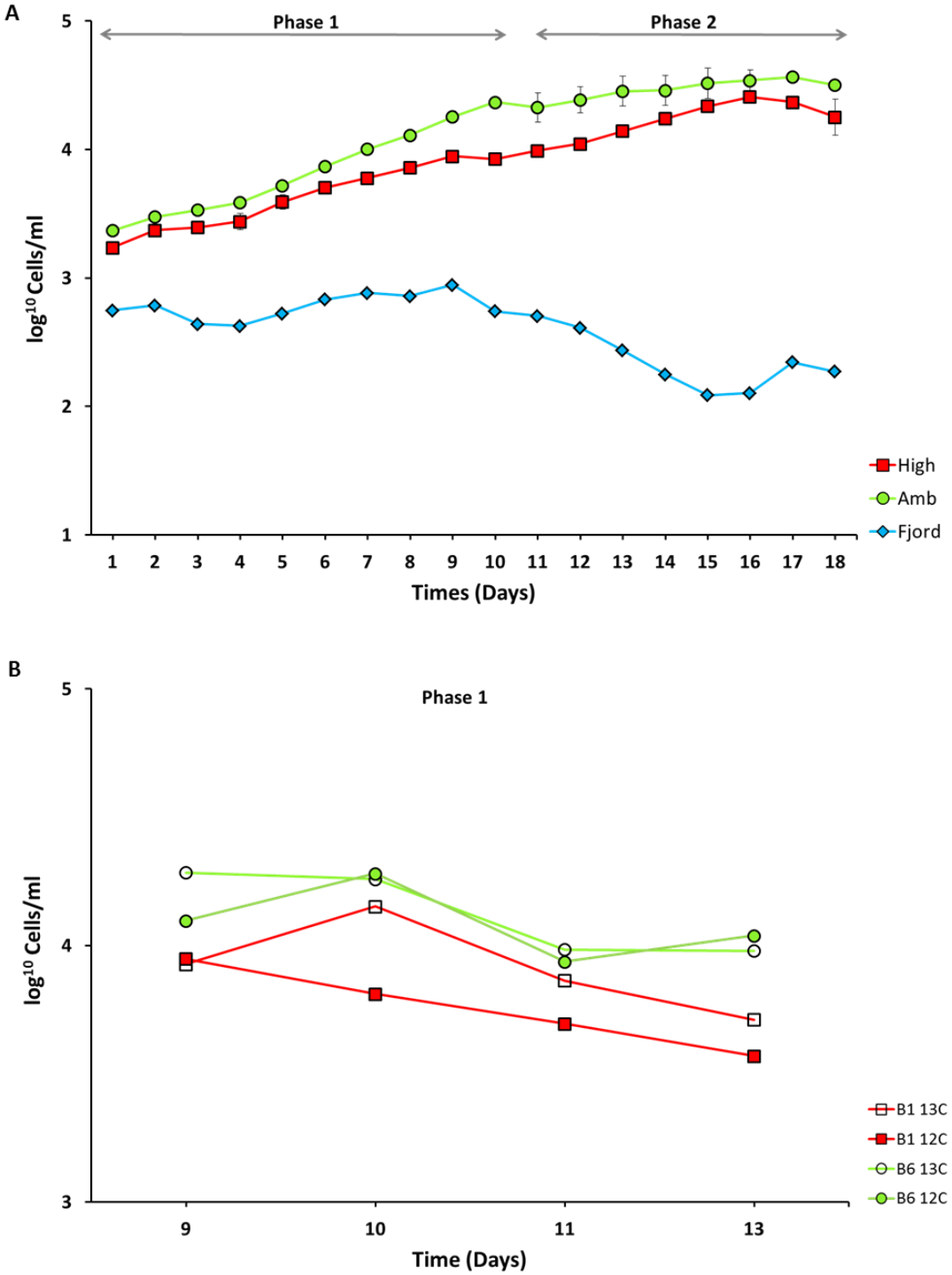

Figure 3.7 Cell concentrations of the photosynthetic bacteria Synechococcus for the mesocosms and fjord for the entire duration of the experiment (A) and for the dark bottle incubations for phase 1 of the experiment (B). Flow cytometry analysis was not conducted for photosynthetic organisms in the dark bottle incubations from phase 2 of the experiment.

3.4 Phytoplankton Dynamics

The phytoplankton population in both treatments was dominated numerically by picoeukaryotes, whereas cryptophytes, prymnesiophytes (including coccolithophores) and other flagellates of uncertain taxonomic affiliations made the greatest contributions to phytoplankton biomass (Hopkins *et al.*, 2009).

3.4.1 Picoeukaryotes

A substantial fraction of the picoplankton biomass consists of small unicellular photosynthetic algae, known collectively as picoeukaryotes. They are found throughout the photic zone at concentrations between 10^2 and 10^4 cells/ml and are of ecological importance as they can produce blooms which affect the whole ecosystem (Bricelj and Lonsdale, 1997, Massana *et al.*, 2004). Though they are subject to a high grazing mortality they can be responsible for ~75% of net carbon production in some coastal areas (Worden *et al.*, 2004). The class Prasinophyceae dominates the picoeukaryotes of which *Micromonas pusilla* has been described in several marine studies as the principal component of the picoplankton assemblage (Not *et al.*, 2004; Zhu *et al.*, 2005, Marie *et al.*, 2006, Worden, 2006).

For analysis of the Bergen mesocosm samples the flow cytometry data categorized picoeukaryotes into 2 size fractions (large and small), however these were not identified taxonomically.

Under high CO_2 conditions numbers of large picoeukaryotes were significantly lower than in the ambient CO_2 treatments ($P=0.019$) throughout the entire experiment (Figure 3.8A). Taken independently, significant differences were only observed in phase 1 ($P=0.049$) of the experiment but not for phase 2 ($P=0.16$). This discrepancy was due to the secondary bloom which commenced ~ day 15 (Figure 3.2) that resulted in both the high and ambient CO_2 treatments having similar cell numbers during the final days of the experiment. However, between days 11 to 15 in phase 2 the large picoeukaryotes were

significantly more abundant under ambient CO_2 conditions (P=0.0013; Mann-Whitney U test).

In the ambient CO_2 treatment large picoeukaryotes reached their peak on day 10 with 2.33 ±1.08x10^4 cells/ml. In contrast, cell number in the high CO_2 treatment peaked the previous day (day 9) with 6.97 ±0.008x10^3 cells/ml. These results show that large picoeukaryote cell abundance in the high CO_2 treatment was ~70% lower compared to the ambient CO_2 which is significant when one considers that picoeukaryotes in general can be the main net primary producers of the phytoplankton assemblage accounting for up to 32.05 ±1.31 µg C L^{-1} d^{-1} produced and 28.31 ±2.61 µg C L^{-1} d^{-1}consumed in some marine systems (Worden *et al.*, 2004).

Small picoeukaryotes numerically dominated the photosynthetic eukaryotes examined during this study (Figure 3.8B). Cell numbers rose quickly in the high CO_2 treatment peaking on day 7 with 4.65 ±0.93x10^4 cells/ml while at the same time cell numbers in the ambient CO_2 mesocosms were 52.3% lower with 2.22 ±0.35x10^4 cells/ml. However a rapid decline in cell numbers was observed in the high CO_2 treatment after it peaked on day 7 while cell numbers in the ambient CO_2 treatment continued to rise despite lower concentrations of nitrate and phosphate at this time (6.15 ±0.23 µmol/l and 0.24 ±0.04 µmol/l, high CO_2 treatment) and (4.33 ±0.2 µmol/l and 0.20 ±0.008 µmol/l, ambient CO_2 treatment). In contrast, peak cell abundance in the ambient CO_2 treatment was recorded on day 10 with 5.10 ±1.42x10^4 cells/ml. No statistical difference was observed between the treatments in phase 1of the experiment (P=0.086). However, statistical analysis of phase 2 of the experiment did reveal a significant difference between the treatments (P=≤0.01) which can be attributed to the rapid decline of cell numbers in the high CO_2 treatment in contrast to the ambient CO_2 treatment (Figure 3.8B).

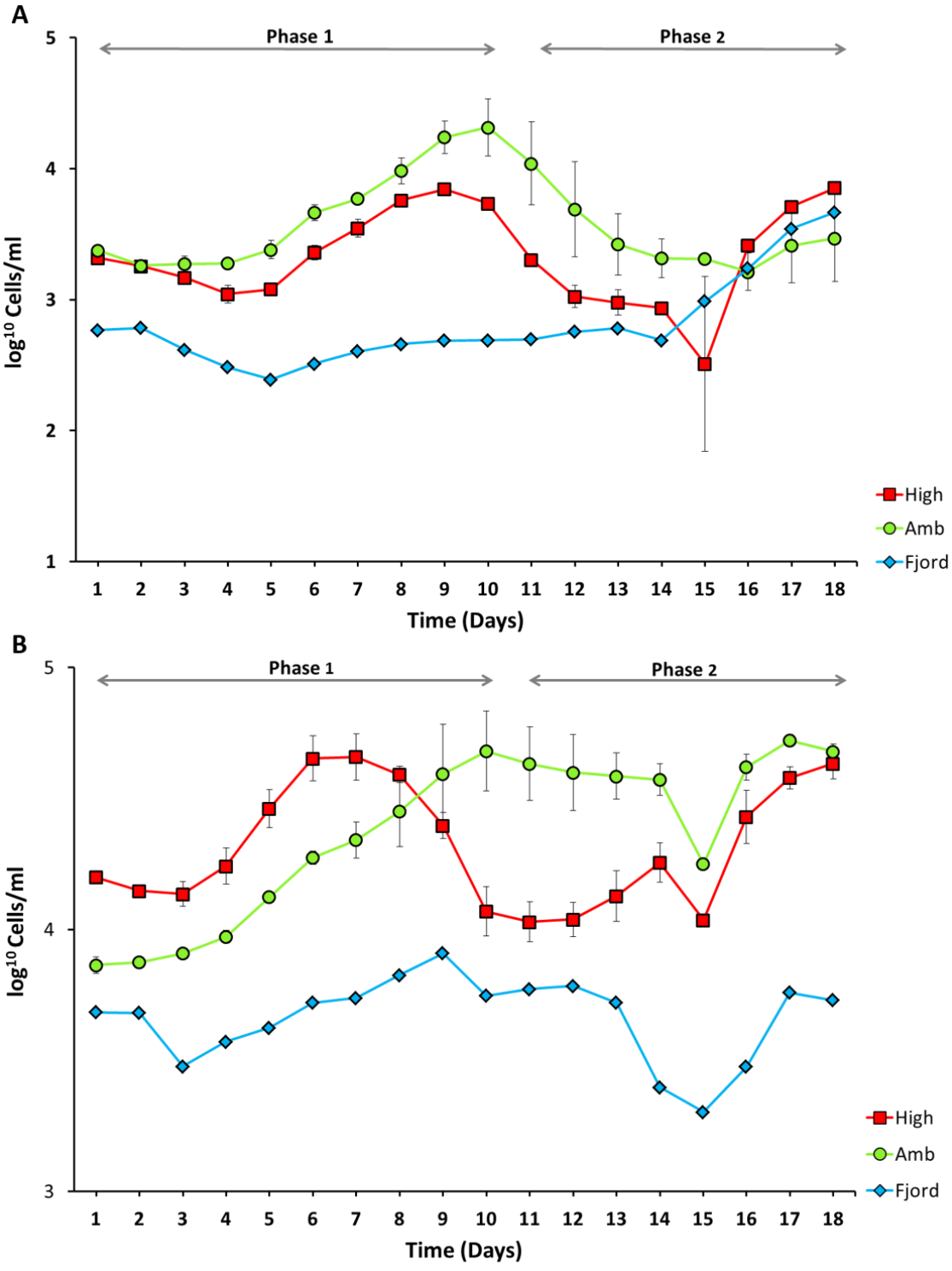

Figure 3.8 Temporal variability in log mean (± s.e., n=2) of cell abundance for large picoeukaryotes (A) and Small picoeukaryotes in both treatments and the fjord (B.)

Meakin and Wyman (2011) as part of this Bergen mesocosm experiment, employed a combination of ribulose-bisphosphate carboxylase gene (*rbcL*) clone libraries and quantitative PCR to explore shifts in the picoeukaryote community in response to elevated CO_2 (Meakin and Wyman, 2011). In this instance they analysed two closely related species, *Micromonas pusilla* and *Bathycoccus prasinos* for the first 8 days of the experiment and found that they responded very differently to the high CO_2 treatment. *Micromonas* abundance was significantly higher under high CO_2 treatment between days 0 – 3 (days 1 - 4 this study) reaching a ~23 fold increase by day 7 with $1.55 \pm 0.76 \times 10^5$ copies ml^{-1} in the high CO_2 treatment compared to $6.88 \pm 3.08 \times 10^3$ copies ml^{-1} in the ambient CO_2 treatment. *Bathycoccus* was found at similar numbers in both treatments but dominated the community under ambient conditions.

These results seem contrary to the flow cytometry data for the same time period as Meakin and Wyman's (2011) analysis (days 1 - 8) as the abundance of large picoeukaryotes was significantly higher in the ambient CO_2 treatment in phase 1 of the experiment and no significant difference between the treatments was observed in the small picoeukaryotes during the same period. While studying the growth rates of picoplankton in coastal systems Moran (Morán, 2007) found that the average length of a large picoeukaryote was 1.94 µm while a small picoeukaryote was ~1.31 µm. The size of *Bathycoccus prasinos* is estimated to be ~1.5 – 2.5 µm (Eikrem and Throndsen, 1990) while *Micromonas pusilla* is 1 – 3 µm (Manton and Parke, 1960). It is therefore reasonable to assume that *Micromonas* and *Bathycoccus* would be detected in both the large and small picoeukaryote cell fractions and taken independently the cytometry data would not necessarily reflect the results reported by Meakin and Wyman (2011). However, based on the average cell diameter of *Micromonas* (~1.5 µm) it is possible to speculate that the majority of this species would be present in the small picoeukaryote fraction whereas *Bathycoccus* with a larger average cell diameter (2.0 µm) would be present in the large picoeukaryote fraction.

Analysis of small picoeukaryote cell numbers over the 8 day period described by Meakin and Wyman (2011) revealed that cell numbers were actually higher in the high

CO_2 treatment (Figure 3.8B) but statistically the significance was minimal (P=0.05; Mann Whitney U Test). However, statistical analysis of days 1- 4 did reveal a significant difference (P=0.030; Mann Whitney U Test) in cell numbers between the treatments lending support to Meakin and Wyman (2011) observation that *Micromonas*-like rbcL concentrations consistently increased over a 4 day period in the high CO_2 mesocosms.

With the exception of the small picoeukaryotes, all the cytometric cell counts in this study have commenced (day 1) with similar cell numbers in both treatments. This exception seems to strongly suggest that some picoeukaryotes are able to proliferate under elevated CO_2 conditions. *M. pusilla* has been shown to have a growth rate of 1.3 diversions per day which occurs mainly during the dark period with approximately one doubling from dusk to dawn (DuRand *et al.*, 2002). If elevated CO_2 increased the growth rate of *M. pusilla* over and above that reported by DuRand *et al* (2002) then it should be reflected in the day 1 cell counts as CO_2 was introduced into the mesocosms two days prior to the commencement of sampling, providing adequate time for cell numbers to differentiate between the treatments. It is therefore conceivable that *M. pusilla* was mostly confined to the small picoeukaroyotic fraction as this could account for the increase in cell numbers in the elevated CO_2 treatment from days 1 - 7 thus supporting the findings of Meakin and Wyman (2011).

3.4.2 Cryptophytes

Cryptophytes are unicellular biflagellate cells, most of which are photosynthetic. They have a cell length of 3-50 µm and possess two types of light harvesting complexes containing phycobiliproteins or chlorophyll-a which permit photosynthesis to function with high efficiency under limited irradiance (Hammer *et al.*, 2002). Cryptophytes may form blooms, but are different from toxin-producing dinoflagellates or cyanobacteria as they are not known to cause harm (Pedrós-Alió *et al.*, 1987).

No significant differences were observed between cryptophyte cell numbers in the high and ambient CO_2 treatments during phase 1 of the mesocosm experiment

(P=0.42) (Figure 3.9A). Cell numbers gradually rose in both treatments peaking on day 9 in the high CO_2 mesocosms at 3.72 $\pm$0.89x10^2 cells/ml and on day 10 in the ambient CO_2 mesocosms with 5.68 $\pm$3.27x10^2 cells/ml. A significant difference between the treatments was observed in phase 2 of the experiment (P=0.04) due to cryptophyte cell numbers in in high CO_2 treatment declining earlier than those of the ambient CO_2 treatment.

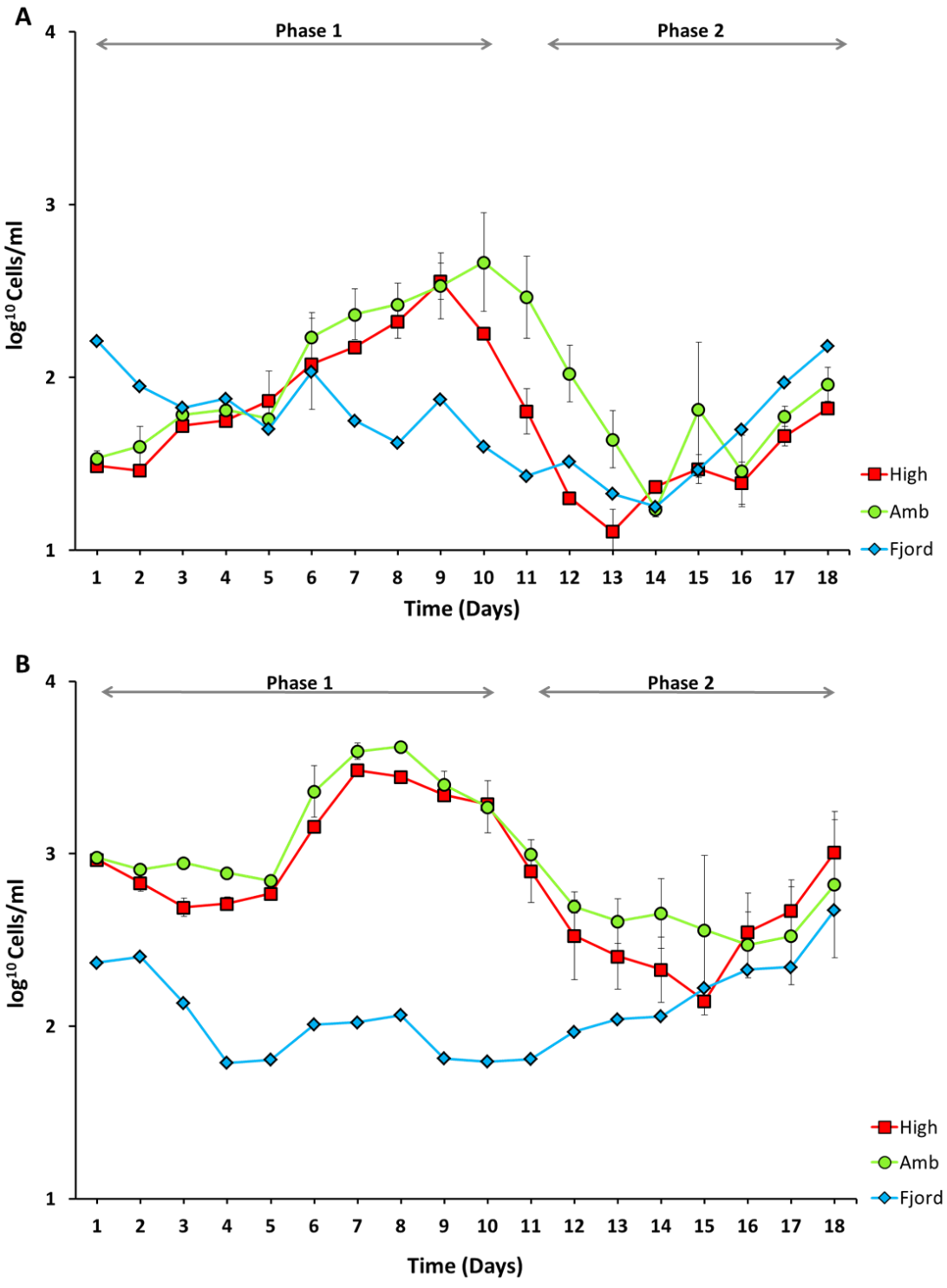

Figure 3.9 Temporal variability in log mean (± s.e., n=2) of cell abundance for cryptophytes (A) and nanoeukaryotes (B) in both treatments and the fjord.

3.4.3 Nanoeukaryotes

Nanoeukaryotes (2 – 20 μm) are in general 10 times less abundant than picoeukaryotes in phytoplankton assemblages and are mainly associated with two main groups of algae, the Dinophyta and the Prymnesiophyta (Marie *et al.*, 2010).

Cell numbers in the high CO_2 treatment were slightly lower than those of the ambient CO_2 treatment throughout both phases of the experiment with the exception of the last 3 days of the secondary bloom (Figure 3.9B). As a result, no significant difference between the treatments in either phase 1 or phase 2 of the experiment was observed ($P>0.5$).

3.4.4 Coccolithophorids

Coccolithophorids comprise a family of calcite-producing Prymnesiophytes that contribute a significant fraction of deep-sea oozes and chalks in the open ocean, contributing up to 80% of the total precipitated $CaCO_3$ (Fabry, 1989). There are approximately two hundred described species of coccolithophorids (Jordan and Green, 1994) but only two, *Emiliania huxleyi* and *Gephyrocapsa oceanica* are known to produce seasonal blooms (Iglesias-Rodriguez *et al.*, 2002).

The abundance of coccolithophorids was significantly lower under high CO_2 conditions in both phases of the experiment ($P=\leq 0.01$) (Figure 3.10). Cell numbers were consistently higher in the ambient CO_2 treatment throughout the entire experiment peaking on day 9 with a mean of $2.99 \pm 0.18 \times 10^3$ cells/ml. Cell abundance in the high CO_2 treatment also peaked on day 9 with $8.88 \pm 0.79 \times 10^2$ cells/ml which is 70.3% less that its ambient CO_2 counterpart. However, the largest treatment difference was observed on day 10 when cell numbers in both treatments crashed due to nutrient depletion (Figure 3.3). In this instance, cell abundance in the high CO_2 treatment was 82.1% lower than the ambient CO_2 treatment with $2.79 \pm 0.65 \times 10^2$ cells/ml compared to $1.56 \pm 0.49 \times 10^3$ cells/ml.

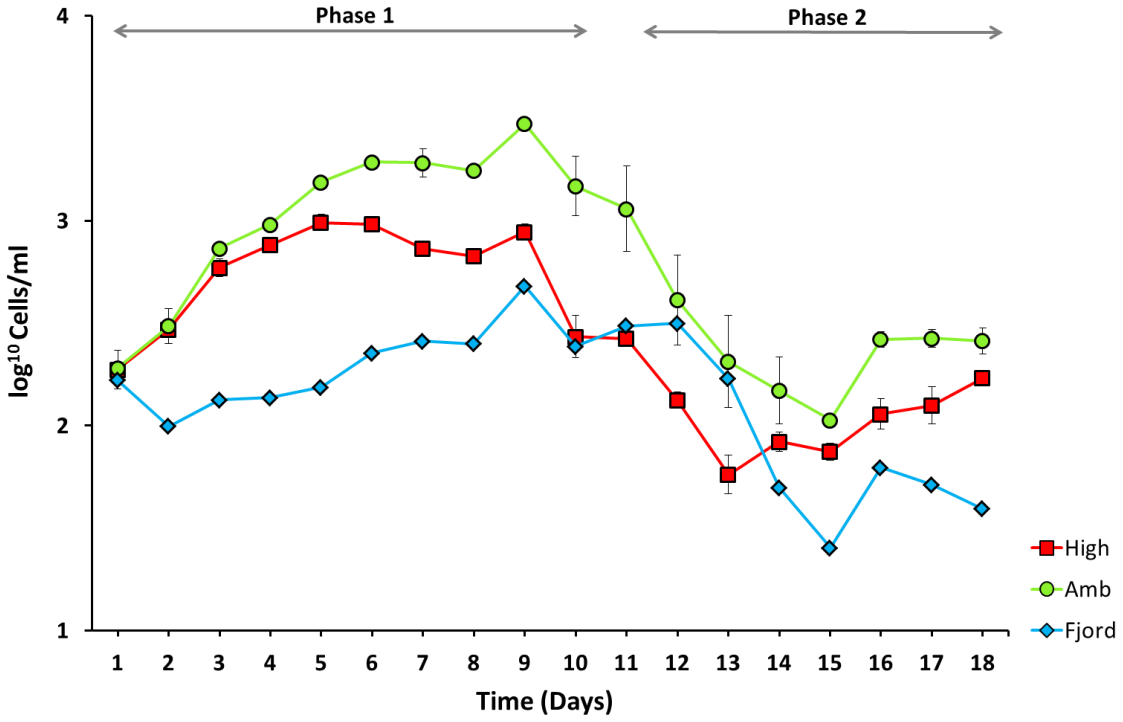

Figure 3.10 Temporal variability in log mean (± s.e., n=2) of cell abundance for Coccolithophorids in both treatments and the fjord.

This was the only phytoplankton group analysed in which cell numbers in both treatments reached their peak cell densities at the same time. In the other phytoplankton groups analysed maximum cell abundance was always achieved in the high CO_2 treatments 1 – 3 days prior to the ambient CO_2 treatment. This lag pattern was reflected in the chlorophyll-a data that indicated the maximum chlorophyll-a concentration was reached on day 7 in the high CO_2 treatment and day 8 in the ambient CO_2 treatment.

E. huxleyi is known to reach concentrations over 1.0×10^6 cells/ml producing blooms up to 250,000 km^2 in area which can be detected via satellite (Holligan *et al.*, 1993). Furthermore, *E. huxleyi* blooms can influence how much CO_2 is assimilated in their vicinity (Holligan *et al.*, 1993, Robertson *et al.*, 1994) and precipitate several thousand tonnes of $CaCO_3$ in each bloom event (De Vrind-de Jong and De Vrind, 1997). These extensive blooms can result in large fluxes of DMS into the atmosphere (Malin *et*

al., 1993) as *E. huxleyi* contains DMSP-lyase isozymes which cleave DMSP to DMS (Steinke *et al.*, 1998).

Results of mesocosm studies conducted in Norway 2005 (PeECE III) suggest that a doubling of CO_2 (~ 750 ppm) leads to a 26% increase in the emission of DMS, whereas a tripling of CO_2 (1150 ppm pCO_2) leads to only an 18% increase in DMS emissions (Wingenter *et al.*, 2007). However, it was not determine if the increase in DMS emissions was due to the response of the phytoplankton to elevated CO_2 or due to increased lysis or viral attack. Using different statistical methods applied to the same data another member of the PeECE III group concluded that there was no statistical difference in DMS emissions for the same increase in CO_2 (Vogt *et al.*, 2007), suggesting that the response of DMS emissions to changes in CO_2 levels is not unequivocally established.

In this current study Hopkins *et al* (2009) reported a significant reduction in DMS concentration under elevated CO_2 conditions at the peak of the bloom ($P<0.001$; Two sample t-test). By the end on the experiment (23rd May) DMS concentrations were reduced 3 fold in the high CO_2 treatment. However, it must be noted that the post bloom analysis of Hopkins *et al* (2009) was based on mesocosms M3 and M4 which were portrayed as high and ambient CO_2 respectively. For phase 2 of the experiment (post bloom) mesocosms M3 and M4 were not re-bubbled with CO_2 and ambient air (respectively) in order to establish the effects of bubbling in the system. Consequently, at the start of phase 2, the true high CO_2 mesocosms (M1 and M2) had an average CO_2 concentration of 823 µatm and pH values of 7.9 and 7.7 respectively, whereas the CO_2 concentration of M3 was 358 µatm and pH 8.1 (Hopkins *et al.*, 2009). However, Hopkins *et al* (2009) reasoned that M3 could still be considered a high CO_2 perturbation as its CO_2 concentration was on average 80 µatm higher than in the ambient CO_2 treatments plus they wanted to give priority to the unbubbled mesocosms as trace gases are driven out of the water phase by aeration.

As the ecological and biogeochemical importance of coccolithophores has become recognized numerous studies have been conducted to ascertain their response to ocean acidification. Of particular interest is the decrease in the saturation of calcium carbonate which makes it harder for calcifying organisms to precipitate their mineralized cell walls. The results of several studies are conflicting, with one group stating that calcification and net primary production in the coccolithophore species *Emiliania huxleyi* is significantly increased by high CO_2/reduced pH (Iglesias-Rodriguez *et al.*, 2008) while another study reported reduced calcification in *Emiliania huxleyi* (Riebesell *et al.*, 2000). Both studies used different methods to reduce the pH of seawater. Iglesias-Rodriguez *et al*., employed a similar method to the one used in this study, bubbling seawater with CO_2 until the desired pH was achieved whereas Riebesell *et al*. (2000) added either an acid or base to seawater to mimic future/past ocean pH. Ocean acidification is the net result of an increase in CO_2 (aqueous) and HCO_3^-, accompanied by a decrease of CO_3^{2-} and pH. The acid/base method for manipulating seawater pH does not realistically simulate an ocean acidification event as it not accompanied by changes in the bicarbonate ion. For this reason the experimental design of Iglesias-Rodriguez was superior to that of Riebesell *et al* (2000) however, this too was flawed as it did not include temperature as one of its parameters. Ocean acidification is the direct result of climate change facilitated by the synergistic effects of increased atmospheric CO_2 and rising temperature. It is therefore only logical that all experiments designed to simulate the future carbonate system should include these parameters.

Riebesell *et al* (2000) suggested that because increased CO_2 decreases the calcium saturation state (thereby allowing calcite to dissolve) organisms such as *E. huxleyi* may show reduced calcification or malformation in their coccoliths (Riebesell *et al.*, 2000). However, examination of *E. huxleyi* morphology using scanning electron microscopy (SEM) revealed no significant differences in either the size or shape of the coccoliths (figure 3.11).

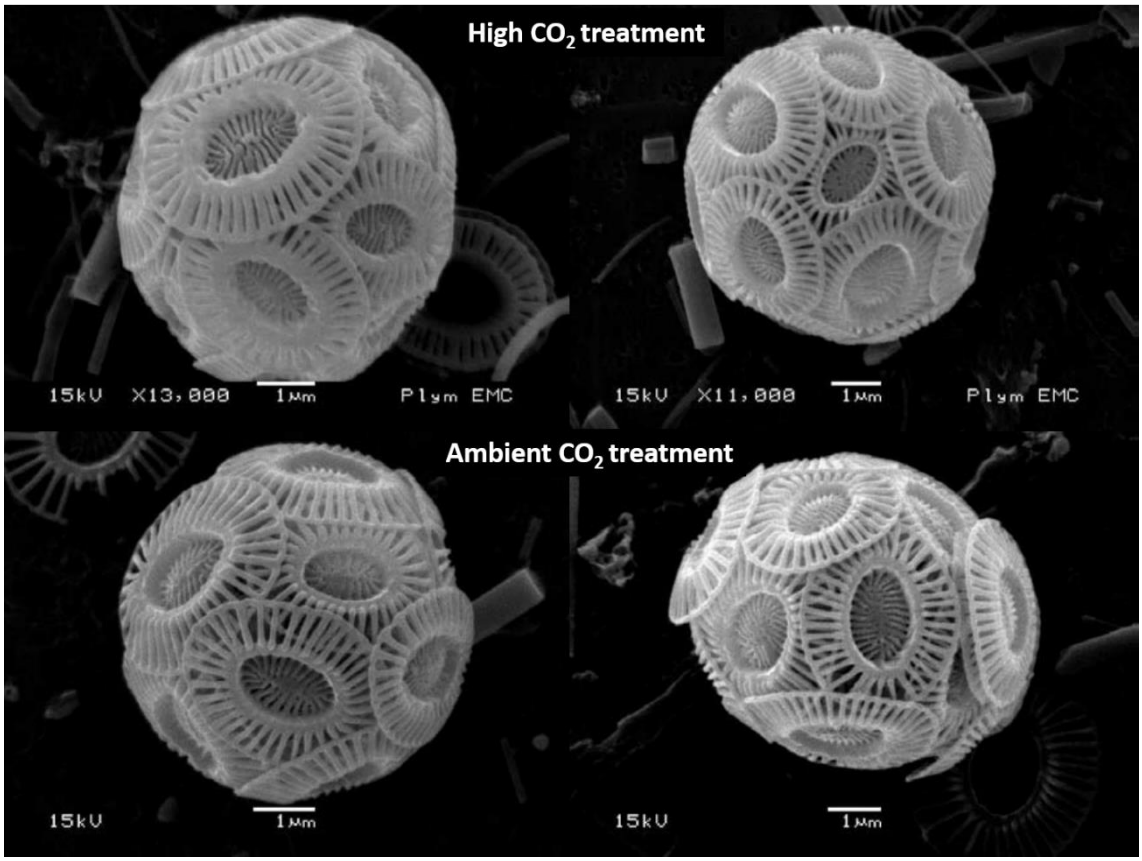

Figure 3.11 SEM images of Emiliania huxleyi from mesocosms M1 (high CO_2) and M6 (ambient CO_2) sampled on day 3 of the experiment. Photograph courtesy of Dr K. Crawfurd, Plymouth marine laboratory.

Calcification was measured using the alkalinity anomaly method based on the fact that when a calcifying organism produces a mole of calcium carbonate, total alkalinity is decreased by two moles (Chisholm and Gattuso, 1991). Although changes in total alkalinity were observed these differences when normalized to the change in cell number during exponential growth revealed no significant difference between the treatments (P=0.07; ANOVA). Furthermore, the calcite saturation state Ω_{Cal} (the thermodynamic potential for calcite to form or to dissolve) was measured in both treatments. At saturation states below 1 $CaCO_3$ will dissolve unless the production rate is greater than dissolution. Saturation states peaked on day 10 for the high CO_2 treatments and day 11 for the ambient CO_2 treatment when they were 3 (±0.2) and 4.7 (±0.1) respectively and at no point did it fall below 1 (Crawfurd, 2010).

Although there is much speculation regarding the effects of elevated CO_2 on calcifying organisms the function of calcification in some groups of phytoplankton is still not fully understood (Paasche, 2002). It was originally hypothesised that the cell covering layer of coccoliths of species such as *Emiliania huxleyi* served as protection against predatory grazing whereas the "trash can" hypothesis speculates that calcification serves as a mechanism to facilitate the use of bicarbonate in photosynthesis (Young, 1994). The benefit of this mechanism is that during the process of calcification CO_2 is released that can be used directly in photosynthesis which may be beneficial when CO_2 is limited. There is however compelling evidence to refute this hypothesis. Firstly, photosynthesis can continue when calcification ceases, such as when cells are grown in calcium free media (Paasche, 1964). Secondary, non-calcifying *Emiliania huxleyi* are capable of directly assimilating bicarbonate, implying that it is not required for calcification (Rost and Riebesell, 2004). Thirdly, calcification is an inefficient method of obtaining CO_2 as it has been observed that the rate of photosynthesis decreases with decreasing CO_2 concentration despite an associated increase in calcification rate (Riebesell *et al.*, 2000). Calcification in coccolithophores is neither a prerequisite for photosynthesis nor is it particularly effective in mitigating CO_2 limitation (Riebesell, 2004). Therefore calcification rates cannot be used as a predictive indictor for assessing primary productivity in a future high CO_2 world**.**

Several studies have indicated that elevated CO_2 increases phytoplankton growth and/or primary production. Gordillo *et al* (2003) studied CO_2 induced growth of the chlorophyte *Dunaliella viridis* at ambient CO_2 (350 ppm) and high CO_2 (10,000 ppm) at different nitrate concentrations: high (5 mM) and low (0.5 mM). CO_2 enrichment had no effect on photosynthesis in the low nitrate cultures. However, in the high-N cultures it increased by 114% in comparison to the control (non-manipulated air and high nitrate). Furthermore, cell biomass tripled in the high nitrate cultures with ~$6.0x10^7$ cells/ml at high CO_2 in contrast to the non-CO_2 enriched cultures with ~$2.0x10^7$ cells/ml. Gordillo *et al* (2003) concluded from this work that the effects of high CO_2 are nitrogen dependent as the observed acclimation involves the light harvesting machinery and nutritional metabolism (Gordillo *et al.*, 2003). Feng *et al* (2009) observed that coccolithophorid

abundance was 5 fold higher in greenhouse conditions (16°C and 690 ppm CO_2) compared to ambient CO_2 (12°C and 390 ppm CO_2) while calcification was significantly decreased. Furthermore, the high coccolithophorid abundance in the greenhouse conditions was accompanied by the highest $DMSP_p$ concentrations. It was suggested that the combined effects of high CO_2 and temperature alter community structure by selecting for phytoplankton species that have a high CO_2 requirement (Feng *et al.*, 2009). Egge *et al* (2009) reported increased primary production rates in elevated CO_2 in the latter stages of a mesocosm experiment when phytoplankton growth had become nutrient limited. Similar to the work of Feng *et al* (2009) it was proposed that the observed effects were associated with changes in species composition (diatoms to flagellates) due to elevated CO_2 and/or nutrient limitation (Egge *et al.*, 2009).

Phytoplankton production is generally not expected to respond to elevated atmospheric CO_2 because it is rarely limiting to growth (Low-DÉCarie *et al.*, 2011). Freshwater systems are usually in equilibrium with the atmosphere and may even be supersaturated in CO_2 due to the degradation of organic matter by heterotrophic bacteria (Duarte and Prairie, 2005). In marine systems CO_{2aq} is generally lower in the ocean's euphotic zone than in deeper waters as a result of photosynthetic consumption. Large phytoplankton blooms may leave transient patches of CO_2 depleted surface seawater that may persist for several weeks until it is replenished by the physical exchange of dissolved inorganic carbon (DIC) from the deep sea and/or by air-sea exchange (Reinfelder, 2011). Consequently, many marine phytoplankton species have evolved inorganic carbon concentrating mechanisms (CCMs) for the active transport of CO_2 and/or HCO_3^- enabling them to grow in the presence of low concentrations of CO_2 by utilizing bicarbonate transporters and CO_2 traps to generate high intracellular concentrations of DIC. The enzyme associated with CCMs is carbonic anhydrase (CA) which catalyses the reversible dehydration of HCO_3 to CO_{2aq} thereby raising the concentration of CO_{2aq} either at the cell surface or internally close to the site of CO_2 fixation. Naturally there is an energetic cost to organisms possessing CCMs as they require ATP for the active transport of carbon plus sufficient nitrogen, sulfur and micronutrients for the biosynthesis of DIC transporters and associated proteins. Thus the

ability to express CCMs in natural environments may be determined by nutrient and light availability (Engel *et al.*, 2008). It has been speculated that algae which possess weak or lack CCMs may show enhanced growth rates under elevated CO_2 conditions whereas those with a high CCM activity would be relatively unaffected (Beardall and Giordano, 2002). This was proven experimentally by Clark and Flynn (2000) who cultivated a range of phytoplankton species in a closed system in order to examine their growth responses to elevated DIC concentrations. The results revealed that *Stichococcus bacillaris* which had been reported as having no CCM activity (Munoz and Merrett, 1989) showed a 15 – 20% increase in growth rate at elevated DIC concentrations whereas the growth rates of *Phaeodactylum tricornutu,* a species known to possess a CCM remained relatively similar (Clark and Flynn, 2000).

The results of this experiment suggest that CO_2 concentrations may be a selective environmental factor in determining the evolution of marine phytoplankton species (Raven *et al.*, 2008). If this assumption is correct then one would expect the future oceans of 2100 to be populated by organisms such as coccolithophorids and dinoflagellates which have a low CO_2 affinity. Coccolithophorids are capable of utilising HCO_3^- as a source of inorganic carbon for photosynthesis however they have a low level of CA activity which is not regulated by CO_2 concentration (Rost *et al.*, 2003). Dinoflagellates on the other hand are the only oxygenic photoautotrophs with form II RuBisCO which has the lowest carboxylation/oxygenation specificity factor among eukaryotic phytoplankton (Morse *et al.*, 1995, Whitney and Andrews, 1998). The fact that both these organisms rose to dominance during a period of variable, but relatively high atmospheric CO_2 (1,000 – 2,000 ppm) in the Mesozoic period (Retallack, 2001, Falkowski *et al.*, 2004) suggests that these organisms may be better adapted to a future high CO_2 world than more recently evolved species.

Although *M. pusilla* has an efficient CCM, it is only induced when CO_2 levels have fallen below 4 µM (0.18 ppm) (Iglesias-Rodriguez *et al.*, 1998), while water in equilibrium with air contains around 12–15 µM CO_2 (~0.66 ppm) at 18°C, depending on salinity (Beardall and Giordano, 2002). This would suggest that *M. pusilla* would

proliferate in a high CO_2 environment as it would utilize less energy for growth (and require less nutrients) as its CCM mechanisms would be virtually redundant.

Flow cytometry analysis showed a decrease in cell numbers in the high CO_2 treatments for all the phytoplankton groups analysed compared to their ambient CO_2 counterparts. Analysis of mean peak cell numbers from all six mesocosms (M1-M3, high CO_2 and M4-M6, ambient CO_2) showed that the response to elevated CO_2 varied between the groups with the large picoeukaryotes being the most adversely affected (Table 3.1). Large picoeukaryotes cell numbers were four fold greater in the ambient CO_2 treatments whereas small picoeukaryotes showed little response to elevated CO_2 with average cell numbers decreasing by 11.4%. Coccolithophores cell numbers were also affect by elevated CO_2 decreasing by ~45% in the high CO_2 mesocosms which is similar to the biomass decrease of autotrophic dinoflagellates (~51%) reported by Hopkins *et al* (2009) for this study. Since both these organism rose to dominance in the Mesozoic period when atmospheric CO_2 was considerably higher than the present it is possible that these decreases are a temporal stress response to elevated CO_2 and that cell numbers may eventually be restored due to genetic variability and short generation times (Lohbeck *et al.*, 2012). Although the evidence suggests that elevated CO_2 effects phytoplankton growth, statistically none of the observed decreases were significant (Mann Whitney U Test).

Table 3.1 Mean and maximum cell numbers (± s.e., n=3) of phytoplankton enumerated by flow cytometry. Data were calculated from the means of mesocosms M1-M3 (high CO_2 treatment) and M4-M5 (ambient CO_2) during the bloom period (phase 1) of the experiment. The day each group attained maximum cell concentration is also shown with phytoplankton groups arranged according to effect response (percentage decrease).

Organism	Treatment	Cell abundance (cells/ml)	Day of peak abundance	Percentage decrease
Large picoeukaryotes	Ambient CO_2	$2.65\pm0.69 \times 10^4$	Day 9	74.2%
	High CO_2	$6.85\pm0.13 \times 10^3$	Day 10	
Synechococcus	Ambient CO_2	$2.11\pm0.21 \times 10^4$	Day 9	63.6%
	High CO_2	$7.69\pm0.11 \times 10^3$	Day 10	
Coccolithophores	Ambient CO_2	$2.86\pm0.16 \times 10^3$	Day 9	44.7%
	High CO_2	$1.58\pm0.69 \times 10^3$	Day 9	
Cryptophytes	Ambient CO_2	$5.85\pm1.9 \times 10^2$	Day 9	43.8%
	High CO_2	$3.29\pm0.66 \times 10^2$	Day 10	
Nanoeukaryotes	Ambient CO_2	$4.08\pm0.16 \times 10^3$	Day 7	19.9%
	High CO_2	$3.27\pm0.22 \times 10^3$	Day 8	
Small picoeukaryotes	Ambient CO_2	$5.35\pm1.03 \times 10^4$	Day 7	11.4%
	High CO_2	$4.74\pm0.54 \times 10^4$	Day 10	

3.5 Conclusions

The results of the Bergen mesocosm experiment revealed a significant reduction in primary production (~27.3%) in the elevated CO_2 treatments that are associated with a reduction in seawater pH. This was shown on the basis of lower chlorophyll-a concentration under high CO_2 conditions (Figure 3.2) and a reduction of cell numbers in all the phytoplankton groups analysed including the parsinophytes which dominated primary productivity in the system. Although chlorophyll-a concentrations were not statistically different in this analysis other researchers (Hopkins *et al.*, 2009) using a more complete dataset did show a significant difference between the treatments (P=0.021; Two sample t test). Because primary productivity was significantly reduced in the high CO_2 treatment and the fact that the chlorophyll-a analysis was conducted using an incomplete dataset I concur with the results presented by Hopkins *et al* (2009) showing a significant decrease in chlorophyll-a concentration in the elevated CO_2 treatment.

The negative effects of elevated CO_2 were predominantly observed in the post bloom phase of the experiment (phase 2) with the exception of the coccolithophorids which showed a significant decrease in cell numbers under elevated CO_2 conditions throughout the entire experiment.

During the pre-bloom phase of the experiment (phase 1) elevated CO_2/reduced pH had no effect on bacterial abundance in the mesocosms. However, following the crash of the algal bloom a significant treatment effect was observed with lower bacterial numbers in the high CO_2 mesocosms compared to the ambient CO_2 mesocosms. This difference can be attributed to the significant decrease in primary productivity under elevated CO_2 conditions thereby reducing algal-derived organic carbon and phytoplankton exudates such as DMSP. Therefore, the response of heterotrophic bacteria to altering CO_2 concentrations is linked to phytoplankton abundance and diversity rather than a direct effect of reduced pH

Similar results were obtained from the dark incubation bottles which were filled from the mesocosms in both phases of the experiment. No treatment effects were observed in phase 1 of the dark incubations, with similar bacterial cell numbers in both treatments. Significant differences were observed for the phase 2 dark incubations with bacterial cell numbers being lower in the high CO_2 treatment compared to those of the ambient CO_2 treatment.

Due to the complexity of marine systems no definitive answer can yet be given regarding the effects of elevated CO_2 on all the microbial groups analysed in this study. The results suggest that the effects of elevated CO_2 on primary productivity vary between taxa and with the availability of nutrients. This is supported by the fact that significant treatment differences were observed mostly in the nutrient deplete phase of the experiment (phase 2). However, another explanation may be that elevated CO_2 increases grazing activity in heterotrophic dinoflagellates reducing phytoplankton numbers. Heterotrophic dinoflagellates are known to feed on an array of prey species such as phytoplankton, heterotrophic bacteria and mixotrophic dinoflagellates (Jeong *et al.*,

2007). This has been observed in another mesocosm study in which elevated CO_2 significantly stimulated the grazing rate and the growth rate of heterotrophic dinoflagellates resulting in the production of between 60 – 80% more DMS compared to the control mesocosms (Kim *et al.*, 2010). In this study, heterotrophic dinoflagellates biomass increased by 8% with 33.2 *g* Cm^{-3} in mesocosm M1 (high CO_2) compared to 30.6 g Cm^{-3} in mesocosm M6 (ambient CO_2) (Hopkins *et al.*, 2009).

The oceans of the future are likely to be the result of the synergistic effects of increased CO_2, increased temperature, increased solar irradiance and a decrease in pH. Most of these parameters were not included in this experiment and therefore it is extremely difficult to predict their effects on microbial assemblage diversity and function. It is hypothesised that increasing global temperature will stimulate stratification of the water column causing nutrient limitation in surface waters (Behrenfeld *et al.*, 2006, Beardall *et al.*, 2009). I speculate that the combination of elevated CO_2 and reduced pH will result in a significant decline in both primary production and bacterial cell abundance disrupting major biogeochemical pathways.

4. Effects of CO_2 driven ocean acidification on microbial community composition

4.1 Introduction

It is estimated that there are approximately 10^{29} bacterial cells in the oceans (Whitman *et al.*, 1998) which is more than the number of stars in the known universe (10^{22}-10^{24}). Because they represent such a large fraction of the marine biomass, bacteria dominate the flux of energy and biologically important chemical elements in the ocean (Pomeroy *et al.*, 2007). As a result, the uptake of organic matter by heterotrophic bacteria is a major carbon-flow pathway, and its variability can change overall patterns of carbon flux (Azam and Malfatti, 2007). In the euphotic zone community respiration is dominated by heterotrophic bacteria that convert organic carbon back to CO_2 thereby decreasing the ocean's CO_2 uptake capacity (Rivkin and Legendre, 2001). The coupling of phytoplankton production and heterotrophic bacteria is via labile dissolved organic matter (DOM) a carbon rich substance released by phytoplankton due excess photosynthetic carbon fixation (Larsson and Hagström, 1979, Fogg, 1983). DOM is the largest ocean reservoir of reduced carbon containing more than 200 times the carbon inventory of marine biomass (Hansell, 2009). It is mostly produced by photosynthetic phytoplankton in the surface ocean and becomes available either by direct exudation (Bjornsen, 1988) or indirectly via viral lysis, sloppy feeding or the rupture of algae cells in the late phase of a phytoplankton bloom (Middelboe *et al.*, 1995; Gobler *et al.*, 1997, Berges and Falkowski, 1998, Nagata, 2000).

The release of DOM is regarded as both a sink for the newly fixed carbon (sequestration) (Flynn *et al.*, 2008) and also supports the microbial loop (Azam *et al.*, 1983, Fasham *et al.*, 1999) where it serves as a substrate for heterotrophic microbial populations and as a source of nitrogen and phosphorus to autotrophs (Hansell, 2009). Phytoplankton assemblages strongly influence bacterioplankton community structure and succession (Cunliffe *et al.*, 2009) due to the variability of the molecular composition of the exudates depending on phytoplankton species and nutrient availability (Myklestad, 1995; Puddu *et al.*, 2003, Lau *et al.*, 2007). Algal classes differ substantially in their biochemical composition, in terms of C/N/P ratios and in terms of relative proportions of cellular protein, fatty acids, and nucleic acids (Pinhassi *et al.*, 2004). Several studies have been conducted to investigate if specific algal groups are associated with certain

species of bacterioplankton (Van Hannen *et al.*, 1999; Hold *et al.*, 2001, Schäfer *et al.*, 2002, Pinhassi *et al.*, 2004, Grossart *et al.*, 2005) all of which observed species specific phytoplankton-bacterioplankton coupling. It was further speculated that algal diversity is inextricably linked to bacterial diversity in order to process the plethora of extracellular substances and organic carbon produced by different phytoplankton species (Schäfer *et al.*, 2002). Therefore, shifts in phytoplankton community structure may not only affect primary production (increase/decrease) but also disrupt phytoplankton-bacterial coupling by changing DOM bioavailability (De Kluijver *et al.*, 2010).

Changes in carbonate chemistry also alter the concentration, speciation and oxidation states of major inorganic nutrients (Zeebe and Wolf-Gladrow, 2001). A study by Huesemann *et al* (2002) showed a reduction in nitrification rates at elevated CO_2 and reduced pH, due to a shift in the ratio of ammonia (NH_3) to ammonium (NH_4^+) which is reduced with decreasing pH (Zeebe and Wolf-Gladrow, 2001; Huesemann *et al.*, 2002, Bell *et al.*, 2007). This would have a profound impact on chemoautotrophic ammonia-oxidizing bacteria and archaea such as *Nitrosomonas* or *Nitrosopumilus* which obtain their energy from the oxidation of ammonia to nitrite which is the first step in the nitrification process. Altered bioavailability of nutrients may also impact phytoplankton growth and community structure as different phytoplankton groups have a preference for different nitrogen species (Dortch, 1990; Tamminen, 1995, Berg *et al.*, 2003, Howard *et al.*, 2007). Therefore, organisms such as *Prochlorococcus* would proliferate in an environment that has a low nitrate and high ammonium concentration (Moore *et al.*, 2002) while diatoms that are better adapted to high nitrate and low ammonium and account for up to 40% of marine primary production may decline (Dortch, 1990; Sarthou *et al.*, 2005, Gehlen *et al.*, 2011).

Bacterioplankton are often classified into two assemblages, free-living bacteria (FLB) and particle–associated bacteria (PAB). PABs are often larger, more abundant and functionally more active than FLB in the same location (Caron *et al.*, 1982, Acinas *et al.*, 1997). They experience different substrate availabilities (Ayo *et al.*, 2001) and grazing pressures (Langenheder and Jurgens, 2001, Artolozaga *et al.*, 2002) than their

free living counterparts and appear to be phylogenetically distinct from FLB communities in marine environments (DeLong *et al.*, 1993, Acinas *et al.*, 1997). Species abundance and diversity is regulated by substrate requirements and the availability of particles in seawater (Grossart *et al.*, 2003). Algal cells are a major source of particulate organic matter during a phytoplankton bloom and also provide a rich carbon source for heterotrophic bacteria via algae exudates. Members of the *Cytophaga–Flavobacterium* (CF) cluster of the Cytophaga–Flavobacterium–Bacteroides group have been shown to be important members of PAB communities (DeLong *et al.*, 1993; Manz *et al.*, 1996, Rath *et al.*, 1998) possibly due to their gliding motility and ability to degrade macromolecules (Shewan and McMeekin, 1983, Cottrell and Kirchman, 2000). In contrast, *Alpha-* and *Gammaproteobacteria* typically dominate free-living marine bacterial communities (Fandino *et al*., 2001; Simon *et al*., 2002, Grossart *et al*., 2005). It is however difficult to distinguish between FLB and PAB communities since many chemotactic species show the ability to frequently attach and detach from particles (Kiørboe *et al.*, 2002).

Aerobic anoxygenic phototrophs (AAnPs) are photoheterotrophic bacteria that are widely distributed in the marine environment. They are genetically diverse containing representatives from *Alph-, Beta-* and *Gamma*-subclasses of *Proteobacteria* (Beja *et al.*, 2002, Yutin *et al.*, 2005) and their fast growth, metabolic diversity and high abundance suggests that they play a significant role in biogeochemical cycles (Kolber *et al.*, 2001, Koblížek *et al.*, 2007). Several studies have suggested that AAnPs are able to alternate between a free-living or particle associated lifestyle depending on environmental conditions (Waidner and Kirchman, 2007; Lami *et al.*, 2009, Cottrell *et al.*, 2010). Furthermore, a close correlation between AAnP abundance and chlorophyll-*a* has been observed, indicating the requirement of AAnPs for dissolved organic carbon produced by phytoplankton (Sieracki *et al.*, 2006, Zhang and Jiao, 2007).

Members of the marine *Roseobacter* clade of *Alphaproteobacteria* are among the most abundant and ecologically relevant marine bacteria that mediate key biogeochemical processes. They are broadly distributed across diverse marine

environments but their abundance is often highest near phytoplankton blooms or in association with organic particles suggesting cell-surface interactions (Dang and Lovell, 2000; Riemann *et al.*, 2000, Rink *et al.*, 2007, Slightom and Buchan, 2009). Their physiological traits include aerobic anoxygenic photosynthesis, dimethylsulphoniopropionate (DMSP) degradation, carbon monoxide oxidation and the degradation of aromatics (González *et al.*, 1999; Wagner-Dobler and Biebl, 2006, Moran *et al.*, 2007, Brinkhoff *et al.*, 2008). Furthermore, several *Roseobacter* species have been found to possess antibacterial capabilities (Bruhn *et al.*, 2007) to inhibit non-*Roseobacter* species and also algicidal activity (Riclea *et al.*, 2012) suggesting an antagonistic relationship between certain *Roseobacter* species and phytoplankton. A number of molecular mechanisms and morphological features allow some *Roseobacter* species to attach to a phytoplankton cell in order to have access to DOM and DMSP. Swimming motility and chemotaxis allow the bacteria to position themselves close to the surface of the algal cell in readiness for the transition from a motile to a sessile lifestyle (Miller *et al.*, 2004; Miller and Belas, 2006, Belas *et al.*, 2009). This transition includes loss of flagella, formation of adhesive fimbrial low-molecular-weight protein (Flp) pili and biofilm formation (Slightom and Buchan, 2009, Geng and Belas, 2010). It is unknown if this relationship is mutually beneficial to the host species though another member of the *Roseobacter* clade *Silicibacter* sp. strain TM1040 has been shown experimentally to enhance the growth of the DMSP producing dinoflagellate *Pfiesteria piscicida* (Miller and Belas, 2006). Therefore, this can be described as a true symbiotic relationship as both organisms benefit from the interaction.

Bacteria and microalgae have extremely high diversity, fast growth rate and dominate marine primary production and nutrient cycling and as such act as sensitive indicators of ecosystem status and changes which translates into altered microbial community structure and function (Paerl *et al.*, 2002). In this study the population dynamics of bacterioplankton taxa during a nutrient induced phytoplankton bloom was followed and differences in the bacterioplankton communities in relation to CO_2 conditions levels were assessed. Seawater mesocosm studies were used to manipulate CO_2 in a complex ecosystem and facilitated the monitoring of microbial activity in a

controlled environment. CO_2 or air was introduced into the mesocosms at 2 time periods, pre-bloom (phase 1) and post bloom (phase 2) of the experiment. Analysis of non-photosynthetic and chemoautotrophic bacteria was achieved using dark incubation bottles incubated in situ in the field mesocosms. Changes in microbial community composition were investigated using PCR-DGGE of 16S rRNA genes, the construction of 16S rRNA gene clone libraries and qPCR analysis of predominant groups of bacteria identified from the DGGE and clone library analysis. The experiment included some treatments with ^{13}C-labelled bicarbonate which were included to detect chemoautotrophs. The results of the experiments with ^{13}C-labelled bicarbonate are reported in chapter 5.

4.2 Methods

Mesocosm setup, preparation of dark-incubation bottles, sampling regime and DNA extraction methodology is fully described in chapter 2. Briefly, DNA was extracted from water samples obtained from dark incubation bottles on days 9, 10, 11 and 13 of the mesocosm experiment (now referred to as day 1, 2, 3, 5 for dark incubation experiment) and days 16, 17, 18 and 20 (now referred to as day 8, 9, 10, 12) (Table 4.1).

Table 4.1 Key stages of the mesocosm experiment showing the sampling regime of the dark incubation bottles in both phases of the experiment.

Date/mesocosm day	Mesocosms	Dark incubations
13th May (8)	Phytoplankton bloom	Phase 1 bottles filled
14th May (9)		1
15th May (10)	Reintroduction of CO_2/air	2
16th May (11)	Phase 2 of experiment	2
17th May (12)		
18th May (13)		5
19th May (14)		
20th May (15)		Phase 2 bottles filled
21st May (16)		8
22nd May (17)		9
23rd May (18)	Mesocosm sampling ended	10
24th May (19)		
25th May (20)		12

Polymerase chain reaction (PCR) with a range of primer sets was used to amplify 16S rRNA genes from bacteria, archaea and two ammonia oxidizing genera of *Betaproteobacteria, Nitrosomonas* and *Nitrosospira* (Edwards *et al.*, 1989; DeLong, 1992, Kowalchuk *et al.*, 1997). Initial PCR amplification of the DNA using primers specific for archaeal 16S rRNA genes produced extremely weak bands when viewed on an agarose gel. In order to generate high quality DNA template and increase yield, 5 µl of the DNA extracted from the dark-incubated bottles was used as template in whole genome amplification (WGA). Specific primers were also used which targeted the alpha-subunit gene of ammonia monooxygenase (*amoA*) in bacteria (Rotthauwe *et al.*, 1997) and archaea (Tourna *et al.*, 2008). PCR reactions which produced either weak or no products were repeated using DNA that was subjected to whole genome amplification (WGA) to increase the abundance of targeted genes. This method has been previously used to enable the amplification of microbial DNA from low biomass samples (González *et al.*, 2005) The bacterial 16S rRNA gene fragments were analyzed by denaturing gradient gel electrophoresis (DGGE) and the profiles were examined using Bionumerics version 3.5, (Applied Maths, Kortrijk, Belgium) to allow statistical comparison of the microbial communities from each treatment. Using the similarity matrix produced from the DGGE profiles a statistical test for the pairwise comparison of clusters recovered in the analysis was computed by analysis of similarity (ANOSIM) (Clarke, 1993) using the software PRIMER 6 (PRIMER-E Ltd, Plymouth, UK).

On the basis of the DGGE analysis specific samples were chosen for further analysis by cloning and sequencing of 16S rRNA gene fragments to determine the phylogenetic affiliations of the microbial species. In addition, primers were designed to specifically target the dominant bacterial families observed in the samples. These were used for quantitative PCR (qPCR) to determine the abundance of key bacterial taxa in relation to CO_2 levels.

Comparison of bacterial 16S rRNA gene clone libraries (ambient and high CO_2) was tested using webLIBSHUFF version 0.96 (Singleton *et al.*, 2001) (http://libshuff.mib.uga.edu), which incorporates the coverage formula of Good (1953)

to generate homologous and heterologous coverage curves (Good, 1953). The measured distance between curves was calculated using the Cramér-von Mises test statistic (Pettit, 1982). Distance matrices submitted webLIBSHUFF were generated using the DNADIST program of BioEdit version 7.0.8.0 (Hall, 1999) using the Jukes and Cantor (1968) model for establishing nucleotide substitution rates.

Briefly, a homologous coverage curve is plotted by grouping the sequences from community X (C_X) as the percentage of sequences in X that are not singletons. C_X increases with distance until the maximum distance of 1 is reached when there are no singletons remaining. The homologous coverage curve is compared with a heterologous coverage curve, by comparing the sequences in X with those from another community Y. Heterologous library coverage (C_{XY}) is calculated as the fraction of sequences that are in X and also in Y. The Cramer–von Mises statistic (Pettit, 1982) is used to calculate the distance between the two curves. To determine if the two communities are significantly different, the sequences are randomly shuffled between two samples in 999 replicate trials and the Cramer–von Mises statistic is calculated for each trial. A P-value is calculated from the fraction of trials in which the real value is greater than the random values.

Abundance and dynamics of specific bacterial groups was determined by quantitative real time PCR (qPCR) using primers designed to target *Rhodobacteraceae*, *Flavobacteriaceae* and total bacteria. Genes in experimental samples were quantified with reference to external standards. Cloned target genes were used to prepare a known range of standard concentrations from 10^1 to 10^8 genes per microlitre.

4.3 Results and discussion

Primers targeting both bacterial 16S rRNA genes and bacterial *amoA* were successful in amplifying their target genes in all samples from the high and ambient CO_2 treatments. However, CTO primers (Kowalchuk *et al.*, 1997) designed to amplify the currently recognized betaproteobacterial ammonia oxidizer 16S rRNA genes only yielded PCR products in the high CO_2 treatments. PCR amplification of the archaeal 16S

rRNA gene using the WGA DNA as template produced amplicons in all samples analysed however, no PCR products were obtained from any of the samples using the archaeal *amoA* primers using either the original or WGA DNA.

4.3.1 The effect of elevated CO_2 on bacterial communities during a phytoplankton bloom (mesocosm experiment phase 1)

To investigate bacterial community composition a nested PCR approach was taken in which near full-length 16S rRNA genes were used as template DNA for PCR amplification of the hypervariable V3 region of the 16S rRNA gene using primers 2/3 (Muyzer *et al.*, 1993). Identification of organisms represented by DGGE bands was accomplished by excising the prominent bands from stained DGGE gels and extracting the DNA. The eluted DNA was then reamplified and sequenced.

The DGGE profiles from phase 1 of the experiment revealed that the bacterial communities in both high and ambient CO_2 incubations were characterized by a small number of dominant bands (Figure 4.1). In addition, communities from bottles treated with ^{13}C or ^{12}C bicarbonate were also similar, indicating that the labeled bicarbonate did not have a major effect on the bacterial community composition. Sequencing of DGGE bands revealed that the bacterial community was dominated by *Roseobacter* species from the family *Rhodobacteraceae* within the *Alphaproteobacteria* (14 out of 16 bands sequenced) with a smaller contribution from members of the family *Flavobacteriaceae* within the phylum *Bacteroidetes* (2 of 16 bands sequenced; Figure 4.1). Examination of the gels did not indicate a relationship between changes in bacterial community structure with changes in CO_2 concentration as both the high and ambient CO_2 profiles were highly similar. However, it must be noted that these samples were obtained at the height of the phytoplankton bloom which may not have allowed sufficient time for the bacterioplankton community to respond as phytoplankton-bacterioplankton coupling may be characterized by the succession of phytoplankton followed by bacterioplankton after a temporal lag (Piontek *et al.*, 2012) which was observed in this study. The presence of *Roseobacter* species may be the direct result of their high motility and high chemotaxis

in the presence of DMSP (Kiørboe *et al.*, 2002) of which they are the primary consumers, while *Bacteroidetes* are important consumer of high molecular weight (HMW) DOM which is released during the senescent stage of the bloom (Chrost and Faust, 1983, Kirchman, 2002).

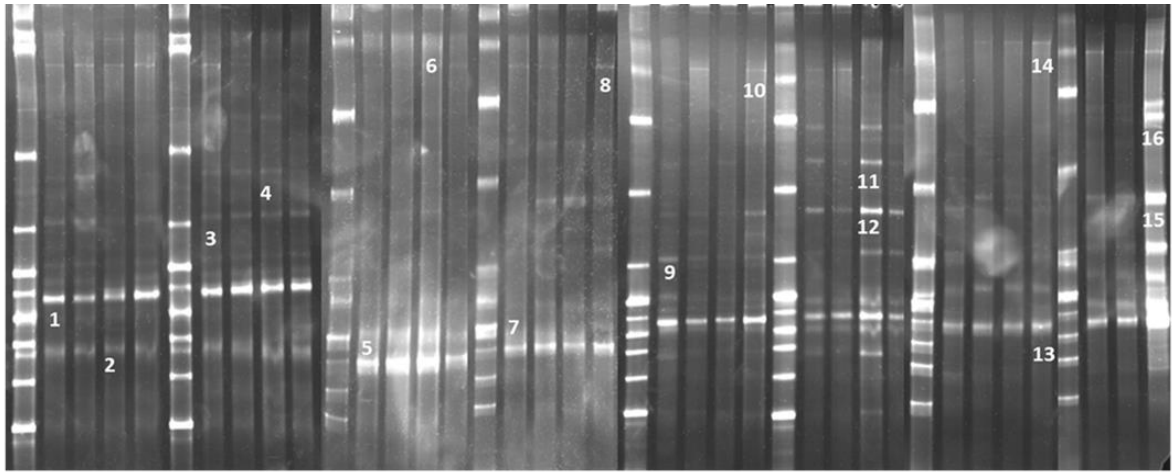

Band	NCBI ID	Band	NCBI ID
1	Uncultured Roseobacter sp. clone 2 E1 (99%)	9	Uncultured Roseobacter sp. clone C146500027 (96%)
2	Rhodobacteraceae bacterium enrichment culture clone PSHTC-015 (97%)	10	Rhodobacteraceae bacterium Hel1 33 108 (97%)
3	Uncultured Roseobacter sp. clone C146Chl242 (99%)	11	Uncultured Flavobacteriaceae bacterium clone C139001323 (90%)
4	Uncultured Roseobacter sp. clone 2 E1 (98%)	12	Uncultured Polaribacter sp. clone SV1264 (92%)
5	Uncultured Thalassobacter sp. clone M3N23 (95%)	13	Uncultured Rhodobacteraceae bacterium clone M3N70 (95%)
6	Rhodobacteraceae bacterium Hel1 33 108 (99%)	14	Uncultured Roseobacter sp. clone 2 E1 (89%)
7	Uncultured Thalassobacter sp. clone M3N23 (99%)	15	Uncultured Roseobacter sp. clone 2 E1 (97%)
8	Rhodobacteraceae bacterium Hel1 33 108 (100%)	16	Uncultured Roseobacter sp. clone 2 E1 (93%)

Figure 4.1 Denaturing gradient gel electrophoresis analysis of PCR-amplified 16S rRNA gene fragments from phase 1 of the dark incubation experiment. Bands indicated by numbers below them were excised and sequenced with the identities reported in the table below. High CO_2 incubations are represented by bottles B1 ($^{13}C/^{12}C$ respectively) and B3 ($^{13}C/^{12}C$ respectively) while ambient CO_2 incubations are represented by bottles B4 ($^{13}C/^{12}C$ respectively) and B6 ($^{13}C/^{12}C$ respectively). Bottle B6 on day 4 is from the ^{13}C incubation only and unmarked lanes are marker ladders.

4.3.2 The effect of elevated CO_2 on bacterial communities following a phytoplankton bloom (mesocosm experiment phase 2)

Phase 2 dark incubation bottles were prepared with water from the mesocosms sampled 7 days after the peak of the phytoplankton bloom in contrast to the phase 1 dark incubation bottles that were prepared at the peak of the bloom on day 8. Phase 2 of the experiment commenced with a second treatment of CO_2-enriched or ambient air into the appropriate mesocosms. Analysis of the DGGE profiles from the bacterial communities revealed that in phase 2 incubations the bacterial communities were more complex than in phase 1 (Figure 4.2). The communities showed a much more even distribution of bands and were not dominated by a single group of organisms (Figure 4.2)

The major phylotypes identified in phase 2 of the experiments were related to *Flavobacteria*, *Aureimarina, Cellulophaga*, (*Flavobacteriaceae*) and *Roseobacter*, (*Rhodobacteraceae*). Members of the SAR11 cluster within the *Alphaproteobacteria*, were also detected in the DGGE gel of phase 2 which were not observed in the phase 1 DGGE gel (Figure 4.2).

Cluster analysis was performed on the DGGE profiles from the phase 2 experiment using Bionumerics software (Applied Maths, Kortrijk, Belgium). This revealed that the communities in the dark incubations prepared from ambient and high CO_2 mesocosms were distinct (Figure 4.3). Furthermore, the bacterial communities in bottles treated with ^{12}C and ^{13}C bicarbonate were similar (Figure 4.3) demonstrating that the labelled bicarbonate did not affect the bacterial community composition. The similarity of the profiles was calculated on the basis of the Pearson correlation coefficient and clustering was done with the unweighted pair group method using arithmetic average (UPGMA) clustering algorithm.

ANOSIM analysis demonstrated that the differences in the communities from ambient and high CO_2 bottles were significant ($P= 0.003$, $R=1$) but there was no significant difference between the ^{13}C and ^{12}C profiles ($P = 1$, $R = -0.27$)

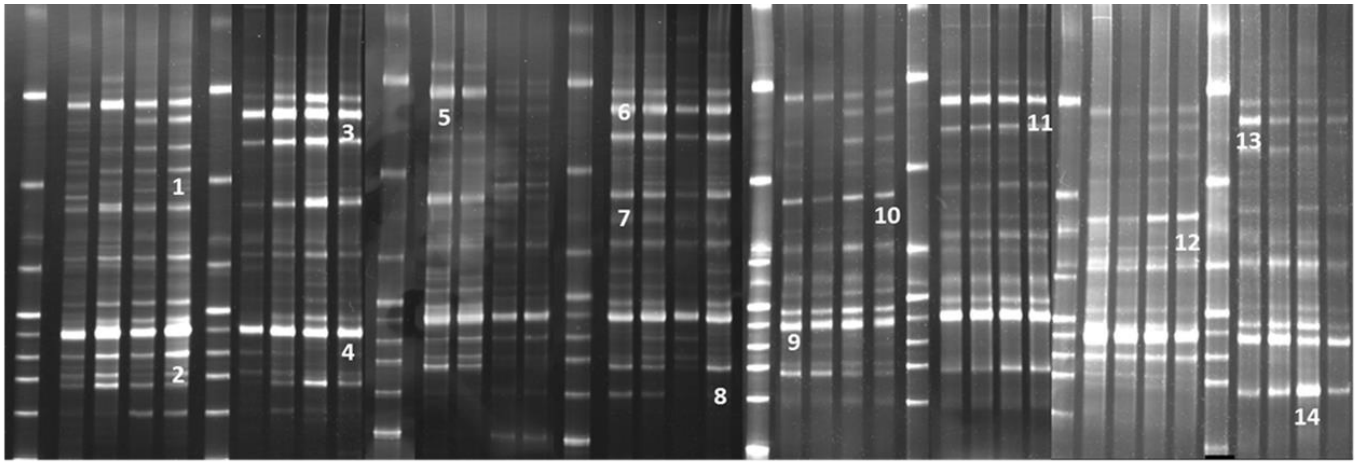

Band	NCBI ID	Band	NCBI ID
1	Uncultured Roseobacter sp. clone 2 E1(94%)	8	Rhodobacteraceae bacterium JN-1 (98%)
2	Uncultured Flavobacteriaceae bacterium clone Klon157-MesoI (95%)	9	Uncultured Flavobacteriaceae bacterium clone C139001323 (95%)
3	Uncultured SAR11 cluster alpha proteobacterium clone C146ChI095 (99%)	10	Uncultured Aureimarina sp. clone SV1302 (98%)
4	Uncultured Cellulophaga sp. clone F1C36 (91%)	11	Uncultured Flavobacteriaceae bacterium clone 0306_MLB77 (87%)
5	Uncultured Flavobacteriia bacterium (93%)	12	Uncultured SAR11 cluster alpha proteobacterium clone SWB9A1-07 (99%)
6	Uncultured Flavobacteria bacterium clone SIMO-2802 (90%)	13	Uncultured Aureimarina sp. clone SV1302 (96%)
7	Uncultured Roseobacter sp. clone 2 E1 (99%)	14	Uncultured Roseobacter sp. clone C114500429 (99%)

Figure 4.2 Denaturing gradient gel electrophoresis analysis of PCR-amplified 16S rRNA gene fragments from phase 2 of the dark incubation experiment. Bands indicated by numbers below them were excised and sequenced with the identities reported in the table below. High CO_2 incubation are represented by bottles B1 ($^{13}C/^{12}C$ respectively) and B3 ($^{13}C/^{12}C$ respectively) while ambient CO_2 incubations are represented by bottles B4 ($^{13}C/^{12}C$ respectively) and B6 ($^{13}C/^{12}C$ respectively). Unmarkeed lanes are bacterial standard markers.

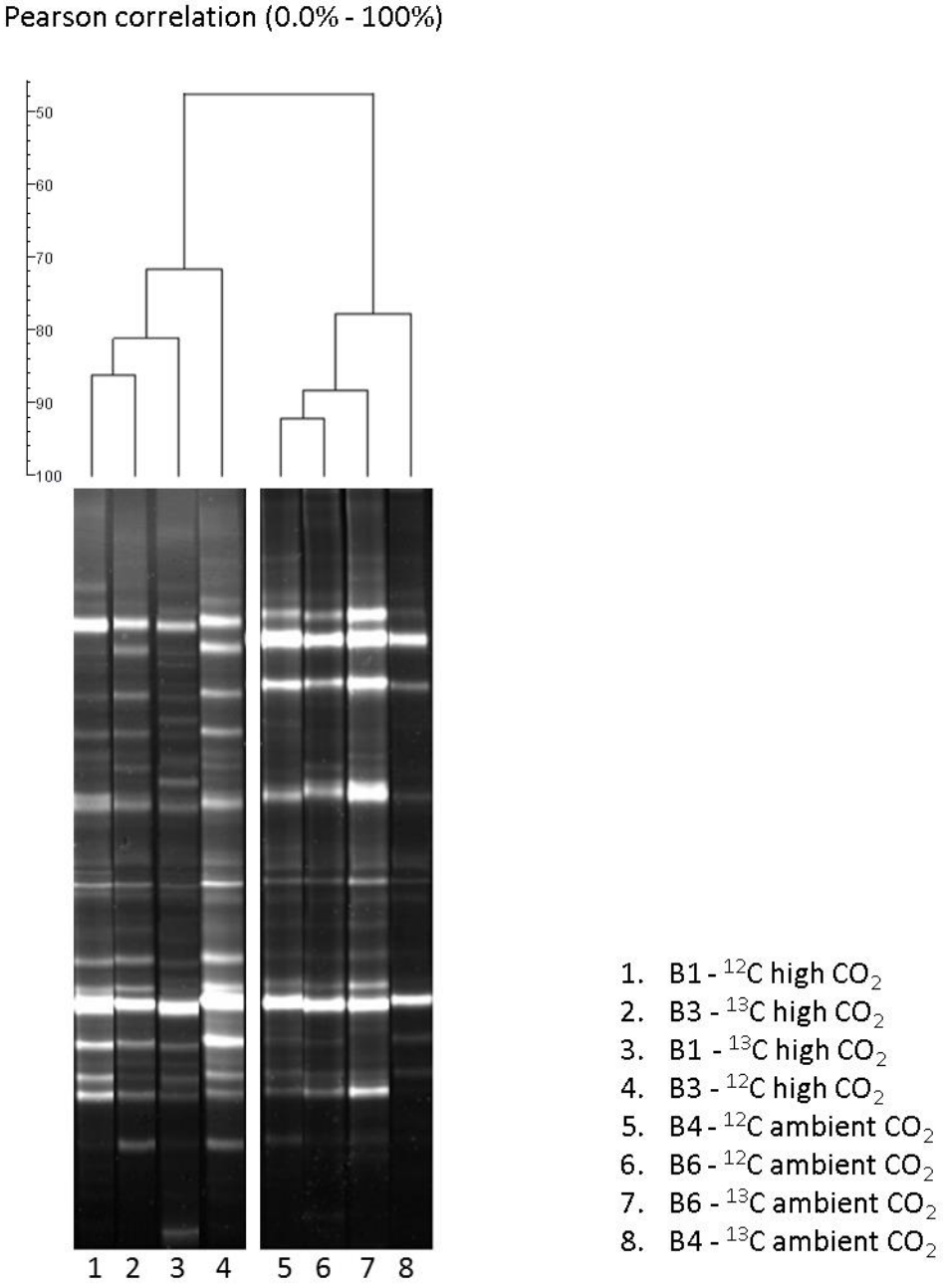

Figure 4.3 Hierarchical cluster analysis of phase 2 (day 5) DGGE profiles using UPGMA clustering of Pearson correlations. Distinct grouping of the high and ambient CO_2 treatments is apparent however it must be emphasised that only B1 incubations (derived from mesocosm M1) were subjected to high CO_2 in both phases of the experiment whereas the B3 incubations were subjected to the high CO_2 treatment in phase 1 only.

It was evident from the DGGE analysis that there was a greater bacterial complexity in the phase 2 incubations (post bloom) compared to phase 1 (bloom). This was anticipated as at the peak of a phytoplankton bloom DOC levels are relatively low

and only when the bloom collapses is DOC released in to the surrounding environment (due to the breakdown of algal cells). The influx of DOC stimulates bacterial growth which is corroborated by the correlation between heterotrophic bacteria and chlorophyll-a levels observed in several studies (Azam *et al.*, 1983; Linley *et al.*, 1983, Bird and Kalff, 1984). Furthermore, distinct changes in bacterial community structure between the ambient and high CO_2 treatments were observed in phase 2 of the experiment which was not evident in phase 1. Based on these results 16S rRNA gene clone libraries were constructed from day 9 of the phase 2 incubations. Seven clone libraries were constructed in total using the following target genes and primers: bacterial 16S rRNA genes (primers pA and pH) (Edwards *et al.*, 1989) archaeal 16S rRNA genes (primers A20f and U1492r) (DeLong, 1992) betaproteobacterial ammonia oxidizer 16S rRNA genes (primer CTO 189f and 654r) (Kowalchuk *et al.*, 1997) and the bacterial ammonia monooxygenase alpha subunit gene (primers amoA 1f and amoA 2r) (Rotthauwe *et al.*, 1997). A betaproteobacterial ammonia oxidizer 16S rRNA genes16S rRNA gene clone library could not be constructed for the ambient CO_2 treatment as PCR reactions with the CTO primers were negative. Therefore, only 3 libraries were constructed for this treatment while the high CO_2 treatment had 4 libraries. After sequencing selected clones from each library, identification of the nearest relative sequence was obtained from the GenBank database using the basic local alignment search tool (BLAST) at the NCBI website (Altschul *et al.*, 1990).

Both the archaeal 16S rRNA gene libraries (ambient CO_2 & high CO_2) contained only sequences which were identified as 18S rRNA gene fragments. A closer examination of primers A20F/U1492R used in the construction of these libraries revealed that this primer set was an exact match for the 18S rRNA gene of several species of fungi and more importantly uncultured chlorophyte (green alga). A possible explanation of this result is that the specificity of the primers was compromised to some degree due to the fact that the mesocosms contained a high proportion of eukaryotic algae and that one of the primers was universal (U1492R) with a broad specificity which apparently targeted a large number of 18S rRNA gene fragments.

The results of the bacterial 16S rRNA gene clone library analysis (Table 4.2) revealed that the ambient CO_2 clone library was dominated by sequences from two bacterial phyla, *Bacteroidetes* (60.3%) and *Proteobacteria* (21.5%). The high CO_2 clone library was also dominated by sequences from the same phyla, *Bacteroidetes* (80.5%) and *Proteobacteria* (12.2%), however in this instance the relative abundance of the two phyla was different. A closer examination of both libraries revealed a shift in composition within the *Proteobacteria*, with the proteobacterial sequences from the ambient CO_2 clone library consisting of sequences entirely from the *Rhodobacteraceae* within the class *Alphaproteobacteria*. In contrast, the *Proteobacteria* represented in the high CO_2 clone library were more diverse with sequences most closely related to *Pelagibacter ubique* HTCC1062 within the SAR11 Clade (6.1%), *Psychromonas* within the class *Gammaproteobacteria* (3.7%) and *Rhodobacteraceae* (2.4%).

The presence of *Pelagibacter ubique* in the high CO_2 library suggests that the high CO_2 mesocosms were less rich in DOC compared to the ambient CO_2 mesocosm. This is consistent with the reduction in primary productivity observed in the high CO_2 treatments (Chapter 3 section 3.3.2). *Pelagibacter ubique* is found in pelagic oceanic ecosystems where it replicates efficiently in low DOC habitats due to its specialized metabolism which is optimized to survive at very low nutrient levels. Although it is an extremely small bacterium (0.15 x 0.6 µm) this results in a large surface area to volume ratio which has evolved to absorb trace nutrients from the open ocean water and its genome encodes for a very high proportion of transport proteins. A study by Sowell *et al* (2008) investigating microbial survival in oligotrophic environments revealed that SAR 11 cells express abundant transport proteins to maximize nutrient uptake activity. Using capillary liquid chromatography (LC)-tandem mass spectrometry to detect microbial proteins in surface samples from the Sargasso Sea they discovered that 67% of the total spectra for SAR 11 were associated with transport functions (Sowell *et al.,* 2008). In contrast, when the same approach was applied to other Gram-negative bacteria, only 4%–11% of spectra matched to transport proteins (Adkins *et al.*, 2006; Callister *et al.*, 2006, Ding *et al.*, 2006, Hixson *et al.*, 2006, Elias *et al.*, 2008). Furthermore there is strong evidence to suggest that *Pelagibacter ubique* is able to produce ATP in the

absence of exogenous carbon sources using proteorhodopsin (proteins that can function as light-dependent proton pumps) thus enabling it to maintains cell functions during periods of carbon starvation (Steindler *et al.*, 2011).

Table 4.2 Phylogenetic assignment of three clone libraries of partial 16S rRNA and *amoA* gene sequences prepared from ambient and high CO_2 dark incubations.

Library	*Representative sequences	Clone frequency	**Organism ID/Nearest neighbour	Identity	No of sequences
Bacterial 16S rRNA					
Ambient CO_2					
	C05	35.5%	*Uncultured Bacteroidetes bacterium* clone 1D10	99%	33
	B02	12.9%	*Uncultured alpha proteobacterium* clone M0-Ar2-P4E06	99.2%	12
	F04	11.8%	*Uncultured Flavobacteria bacterium*, clone Vis_St3_32	100%	11
	C07	7.5%	*Uncultured Bacteroidetes bacterium* clone M0-Ar7-P2F03	99.4%	7
	G07	3.2%	*Uncultured Bacteroidetes bacterium* clone D4861	97.1%	3
	H10	2.15%	*Uncultured Rhodobacteraceae bacterium* clone F4C03	99.3%	2
	E02	2.15%	*Roseobacter sp.* ARK9990	97%	2
	A08	2.15%	*Uncultured Bacteroidetes bacterium* clone 1D10	96.6%	2
	G04	2.15%	*Uncultured Bacteroidetes bacterium* clone 1D10	94.9%	2
	D06	2.15%	*Uncultured alpha proteobacterium* clone M0-Ar2-P4F09	99.6%	2
	G09	2.15%	*Uncultured Sulfitobacter sp.* clone F4C15	98.1%	2
High CO_2					
	C03	80.5%	*Uncultured Bacteroidetes bacterium* clone M0-Ar7-P2F03	99%	66
	G06	6.1%	*Pelagibacter ubique* strain HTCC1062	100%	5
	B12	3.7%	*Uncultured Psychromonas sp.* clone F1C69	99.3%	3
	F10	2.4%	*Uncultured Rhodobacteraceae bacterium* clone F4C03	99.8%	2
CTO 16S rRNA					
High CO_2					
	E12	91.4%	*Uncultured ammonia-oxidizing bacterium* clone CL1-4/E	99%	85
	D02	5.4%	*Uncultured beta proteobacterium* clone PLY-P2-82	99%	5
Bacterial *amoA*					
Ambient CO_2					
	A04	94.1%	*Uncultured ammonia-oxidizing beta proteobacterium* clone B2m-16	99%	48
High CO_2					
	D11	97.4%	*Uncultured ammonia-oxidizing beta proteobacterium* clone B2m-16	99%	38

* Only groups containing two or more sequences were included in this analysis.

** Sequences compared to the GenBank nucleotide database using the BLAST n program.

The high CO_2 betaproteobacterial ammonia oxidizer 16S rRNA gene clone library consisted almost entirely (97.4%) of sequences closely related to uncultured ammonia-oxidizing bacterium clone CL1-4/E which falls within the *Nitrosomonas oligotropha* cluster 6a (Bollmann and Laanbroek, 2001, Freitag *et al.*, 2006), a phylogenetic group that is adapted to grow at low ammonia concentrations (Norton, 2011). Ammonia concentration is likely to play an important role in determining ammonia oxidizer community structure (Webster *et al.*, 2005). Members of the *Nitrosomonas* cluster 6a are known as K-strategists possessing a low growth rate that requires low ammonia concentration for growth. Conversely R-strategists such as *Nitrosomonas europaea,* a member of the cluster 7 group, have a relatively high growth rate requiring high concentrations of ammonia which is supported by the fact that they are found in habitats with high N input and turnover (Bollmann *et al.*, 2002). Therefore, *Nitrosomonas* cluster 6a would have a distinct advantage in environments with limiting amounts of ammonia and increased competition. Ammoniacal nitrogen exists in aqueous solution as a mixture of either NH_4^+ or NH_3 and its speciation is pH dependent. In nutrient rich coastal waters a pH change of 8.1 to 7.8 would decrease the fraction of NH_3 by 50% (Raven, 1986). This may explain the presence of AOB sequences from *Nitrosomonas* cluster 6a in the high CO_2 clone library but the fact that no sequences were detected in the ambient CO_2 library suggests the ammonia concentration in this treatment was lower than its high CO_2 counterpart. This may be due to competition for inorganic nitrogen from phytoplankton and heterotrophic bacteria (Bollmann *et al.*, 2002) or inadequate library construction/primer optimization.

Competition between phytoplankton and bacteria for nutrients may influence the species composition of both communities and fundamentally alter the functioning of the microbial ecosystem by shifting the balance between phytoplankton and bacteria (Bratbak and Thingstad, 1985, Samuelsson *et al.*, 2002). The outcome of this competition may be a decrease in primary production due to heterotrophic bacteria depriving phytoplankton of valuable nutrients (Joint *et al.*, 2002). Early studies examining the interaction between phytoplankton and bacteria for shared nitrogen resources concluded that phytoplankton utilised dissolved inorganic nitrogen (DIN) such

as ammonium (NH_4^+) and nitrate (NO_3^-) to meet their nitrogen demands whereas bacterial growth was driven by dissolved organic nitrogen (DON) released into the environment (Pomeroy, 1974). To determine the role of nitrogen cycling (organic and inorganic) by phytoplankton, stable isotope tracer experiments were conducted by Bradley *et al* (2010) using water samples from Chesapeake Bay. Two methods were used to assess the uptake of ^{15}N-labeled ammonium and nitrate and dual-labelled (^{15}N and ^{13}C) urea and dissolved free amino acids (DFAA). The first method used glass fibre filters (GF/F) to isolate phytoplankton populations while the second used flow cytometric (FCM) sorting that separates cells based on specific cellular properties, such as size or pigment autofluorescence. Two methods were employed as traditional filtration overestimates N uptake by phytoplankton due to retention of heterotrophic bacteria on the filters (Lee *et al.*, 1995, Gasol and Moran, 1999). The analysis concluded that NH_4^+ is the dominant form of nitrogen used by bacteria and phytoplankton in the environment. However, phytoplankton also utilise urea and NO_3^- and to a small extent dissolved free amino acids (DFAA) whereas bacteria also utilise urea but show a higher preference towards DFAA and a lower preference for NO_3^- than that of phytoplankton (Løvdal *et al.*, 2008, Bradley *et al.*, 2010).

It is intriguing that no betaproteobacterial AOB were detected in the ambient CO_2 library using CTO primers though we can assume they were present but at low relative abundance. This can be confirmed by the fact that both the ambient and high CO_2 *amoA* clone libraries (Table 4.2) contained sequences closely related to *amoA* B2m-16 from an uncultured ammonia-oxidizing beta proteobacterium (94.1 and 97.4% respectively). A closer inspection of the sequence of clone B2m-16 at a higher phylogenetic resolution revealed that it closely related to *amoA* from *Nitrosomonas europaea* L08050 a member of the cluster 7 group (Kim *et al.*, 2008). To increase sensitivity Kim *et al* (2008) employed a nested PCR approach using 6 different primer sets for the initial amplification of different regions of the entire *amoCAB* operon. The *amoCAB* amplifications were then used as template to amplify the near full length of the *amoA* gene using primers *amoA*34f (Molina *et al.*, 2007) and *amoA*-2R (Rotthauwe *et al.*, 1997). Clone libraries were prepared from the nested amplifications and 48 colonies

from each sample were picked and sequenced. A phylogenetic tree based on the nomenclature of clusters according to Purkhold *et al* (2003) and Francis *et al* (2003) was constructed from a database of 2152 *amoA* sequences compiled from sequences published in GenBank (Figure 4.4) (Francis *et al.*, 2003, Purkhold *et al.*, 2003).

The high bootstrap value (100%) strongly supports the phylogenetic assignment of Clone B2m-16 within the cluster 7 group with over 99% of the deduced amino acid sequence identical to *Nitrosomonas europaea* (Kim *et al.*, 2008) contradicting the results of the betaproteobacterial AOB 16S rRNA gene clone library (Table 4.2).

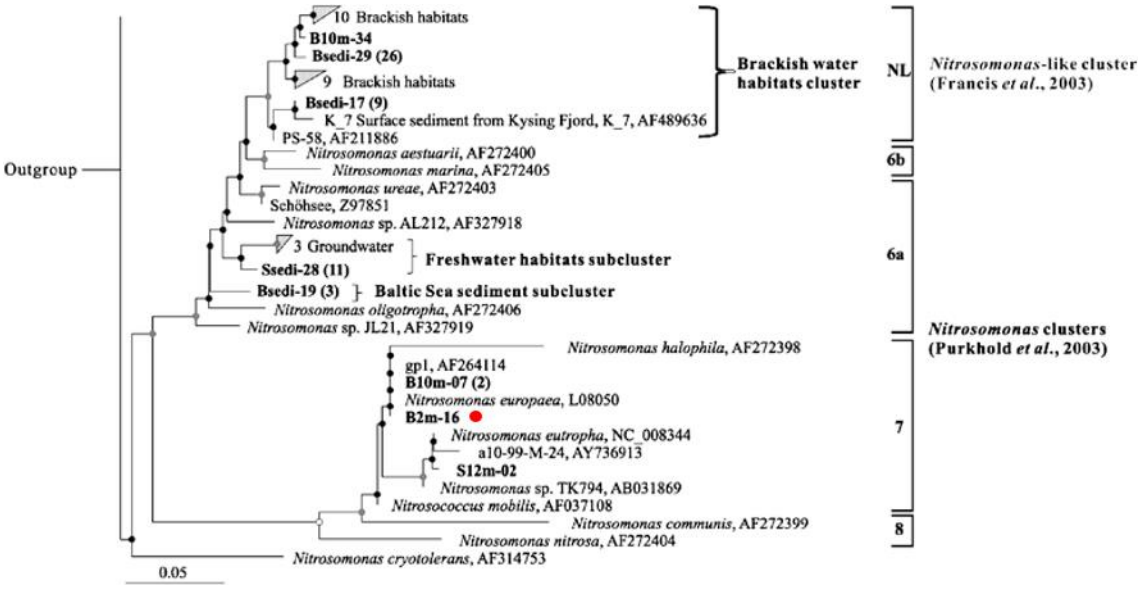

Figure 4.4 Fitch–Margoliash phylogenetic tree from Kim et al (2008) indicating the close phylogenetic relationship with clone B2m-16 and *Nitrosomonas europaea*. The tree was constructed in Arb with 248 amino acids of AmoA using PmoA from *Crenothrix polyspora* as an outgroup. Clones are illustrated in bold, with the number of identical clones in parentheses and their origin coded with three different letters: B for Baltic Sea, P for Plußsee and S for Schöhsee. Bootstrap values for ≥90 replicate trees are indicated at the nodes with three different colours: black (100%), gray (95–99%) and white (90–94%).

The difference between the two AOB clone libraries is that the CTO library was constructed using primers that targeted a structural gene (16S rRNA) while the *amoA* library targeted a functional gene (ammonia monooxygenase). The disadvantage of

using the 16S rRNA gene as a molecular marker is that it targets the phylogeny of an organism and not its physiology (Kowalchuk and Stephen, 2001, Calvo and Garcia-Gil, 2004). Comparative analysis of 16S rRNA gene and *amoA* sequences has suggested similar but not identical phylogenetic relationships between these two molecular markers (Purkhold *et al.*, 2000). This may be due to the high overall similarity of the partial 16S rRNA gene sequences from AOB making it difficult to discriminate between closely related species (Stephen *et al.*, 1996; Bothe *et al.*, 2000, Purkhold *et al.*, 2000).

A study by Junier *et al* (2008) evaluated the specificity of four PCR primers designed to specifically target the 16S rRNA gene of betaproteobacterial ammonia-oxidizers (βAMO) by comparing clone libraries. The results showed that the 16S rRNA gene primers varied in their specificity with different environmental samples, resulting in a majority of clone libraries containing non-AOB sequences (*Methylomonas*, *Variovorax*, *Hydrogenophaga*, and *Delftia*). The authors also included an analysis of AOB clusters from 24 published 16S rRNA gene clone libraries to increase the spectrum of habitats in which AOB communities were present. Interestingly, they found that sequences from *Nitrosomonas oligotropha* in cluster 6a were frequently observed in clone libraries from a variety of environments despite their low sequence similarity with the primers but sequences related to *Nitrosomonas* in cluster 7 were rarely detected (Junier *et al.*, 2008).

There are several pieces of evidence to suggest that the CTO primers are unable to detect members of the cluster 7 AOB group which were present and detected by the *amoA* primers in the clone libraries. Firstly, the 16S rRNA CTO primers have known mismatches with several of the *Nitrosomonas* strains within the *Nitrosomonas europaea* cluster (Purkhold *et al.*, 2000). Secondly, members of the *N. oligotropha* lineage are predominantly salt sensitive found in oligotrophic freshwater environments (rivers and lakes) (Koops and Pommerening-Röser, 2001), whereas the samples of this study were obtained from a saline environment. Although Raunefjorden is a tidal fjord, it has little freshwater influx and the surface salinity at the field station is rather high and constant. Salinity measurements taken during the Bergen experiment indicated that the average salinity was 31-32 practical salinity units (psu) while seawater in the north Atlantic is

usually around 35.5 psu (Crawfurd, 2010). Furthermore, microcosm perturbation experiments have shown a shift in AOB community composition from salt sensitive *N. oligotropha* to salt tolerant *N. marina* by subjecting the microcosms to basic, brackish and marine flooding media (Coci *et al.*, 2005). Thirdly, the samples were obtained from the senescent stage of a nutrient induced phytoplankton bloom when ammonia concentrations should be relatively high due to the breakdown of organic nitrogen-containing compounds, zooplankton grazing and excretion which would favour AOB communities within the group 7 cluster.

The advantage of using a functional gene marker such as *amoA* is that it makes it possible to target genes involved in specific metabolic pathways and as such has been deemed a better molecular marker to study AOB than the 16S rRNA gene (Rotthauwe *et al.*, 1997, Purkhold *et al.*, 2000). However, using a conventional marker such as the 16S rRNA gene has its advantages in that it is ubiquitous, large in size, possesses highly conserved and structural elements and does not appear to undergo extensive lateral gene transfer. In fact several environmental studies have found phylogenetic agreement between both markers (Ivanova *et al.*, 2000; Caffrev *et al.*, 2003, O'Mullan and Ward, 2005, Molina *et al.*, 2007) indicating that if done correctly the two methods can complement each other.

4.3.3 Statistical analysis of bacterial 16S rRNA gene libraries

LIBSHUFF analysis was performed to compare the bacterial 16S rRNA clone libraries (ambient and high CO_2) for homologous C_X and heterologous C_{XY} coverage using the software webLIBSHUFF version 0.96 program (Singleton *et al.*, 2001) (http://libshuff.mib.uga.edu).

Libshuff analysis indicated that differences in the community structure between the two libraries were significant (P = 0.001). In the homologous coverage curve (Figure 4.5A) of the high CO_2 library all the 16S rRNA sequences bin into just 1 group at an evolutionary distance of ~0.1, whereas the ambient CO_2 sequences (Figure 4.5B) form a single group at a higher evolutionary distance of ~0.325. The heterologous coverage

curve of the library in figure 4.5A shows that that at an evolutionary distance of ~0.075 all the sequence groups in the high CO_2 library are also found in the ambient library but because the curves are so similar the result of this comparison was not significant (P=0.747). In contrast the heterologous coverage curve in figure 4.5B (ambient versus high) indicates that the majority of sequences in the ambient CO_2 library are highly divergent from of the high CO_2 which is expressed by the higher evolutionary distance at which all sequences form a single group (~0.325). Therefore, due to the two curves in this graph being dissimilar the result of this comparison is that the two libraries are different (P = 0.001).

The reason why the two comparisons (C_{XY} and C_{YX}) did not return the same results is due to the fact that both libraries shared a large number of sequences related to *Bacteroidetes* and *Proteobacteria*. However, the ambient CO_2 library contained a greater diversity of unique sequences making it significantly different from its high CO_2 counterpart. Therefore, the p-value for the XY comparison (ambient CO_2 versus high CO_2) is likely to be significant ($p<0.05$) as Y does not fully represent X. However, the p-value of the reverse comparison YX is not likely to be significant ($p>0.05$) as X fully represents Y.

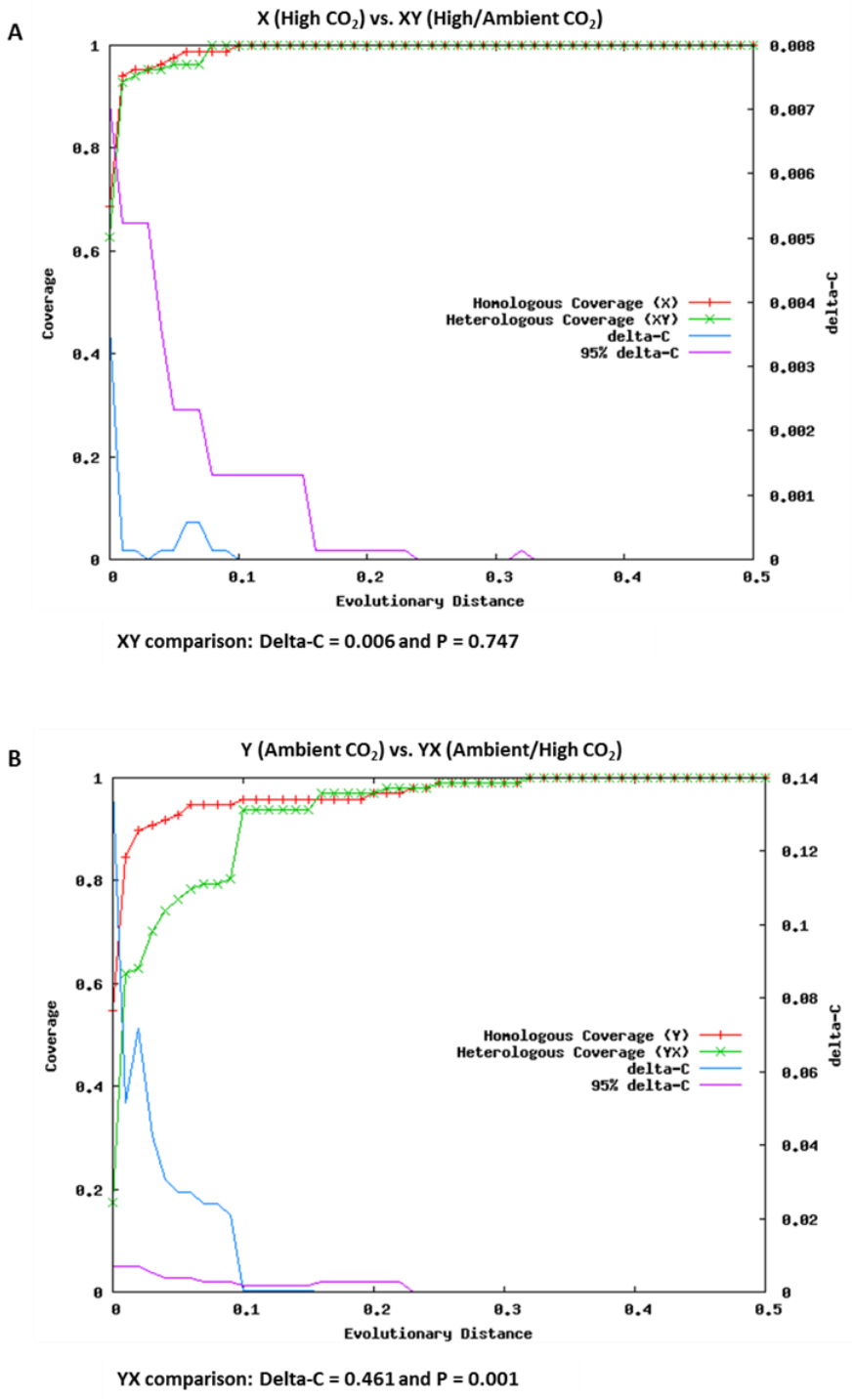

Figure 4.5 Libshuff comparison of bacterial 16S rRNA gene clones from a high CO_2 (X) and ambient CO_2 (Y) incubations. The homologous coverage (red line) shows the number of group changes throughout the range of evolutionary distances. The heterologous coverage (green line) shows the percentage of groups that the second library shares with the first over the range of evolutionary distances. Delta C (blue line) represents the difference between the homologous and heterologous coverage curves at each value of D with 95% Delta C (pink line) indicating the P-value of the random shuffling.

4.3.4 Comparative analysis of near full length bacterial 16S rRNA genes from high and ambient CO_2 clone libraries

In order to obtain near full length bacterial 16S rRNA gene sequences representative clones from both libraries (ambient and high CO_2) were sequenced using primers pDf/pDr, pEr (Lane *et al.*, 1985) and pH (Edwards *et al.*, 1989). The resulting partial sequences (four per representative sequence) were then assembled using BioEdit version 7.0.8.0 (Hall, 1999) by aligning the sequences against the 16S rRNA gene of *Escherichia coli str*. K-12 substr. MG1655. Phylogenetic analysis of near full length bacterial 16S rRNA gene sequences (~1400 bp) was conducted in MEGA 5. A Phylogenetic tree was constructed based on the neighbour-joining (NJ) method with bootstrap resampling with 1000 replicates. The tree was computed using the assembled representative sequences along with the 16S rRNA sequences of their closest relatives obtained from the RDP database.

The NJ phylogenetic tree (Figure 4.6) indicated that the majority of sequences were closely affiliated to two main families of bacteria; the *Rhodobacteraceae* within the class *Alphaproteobacteria* and the *Flavobacteriaceae* within the class *Flavobacteria*. Approximately 91% (20 sequences) of all the *Rhodobacteraceae* sequences observed were derived from the ambient CO_2 library with only 9% (2 sequences) from the high CO_2 library. Conversely, out of 127 *Flavobacteriaceae* sequences retrieved from both the high and ambient CO_2 libraries, 54.3% (69 sequences) were from the high CO_2 while 45.7% (58 sequences) were from the ambient CO_2 library.

In the *Alphaproteobacteria* branch the majority of the *Rhodobacteraceae* sequences were closely related to *Oceanicola sp.* (12 sequences) followed by *Jannaschia* sp. (4 sequences), *Loktanella* sp. (2 sequences), *Tateyamaria* sp. (2 sequences) and *Roseobacter* sp. (2 sequences). With the exception of 2 sequences (*Jannaschia* sp.), all the *Rhodobacteraceae*-like sequences observed in the tree were retrieved from the ambient CO_2 library. The remaining sequences from the *Alphaproteobacteria* branch

were observed in the high CO_2 library and were closely related to *Pelagibacter sp.* (5 sequences) within the SAR 11 clade.

All the species in the *Bacteroidetes* branch were related to the family *Flavobacteriaceae*. The majority of sequences were most closely related to *Dokdonia* sp. (110 sequences) of which 66 sequences was derived from the high CO_2 library. The remaining sequences were closely affiliated to *Psychroserpens* sp. (11 sequences), *Polaribacter* sp. (3 sequences) and *Ulvibacter* (3 sequences).

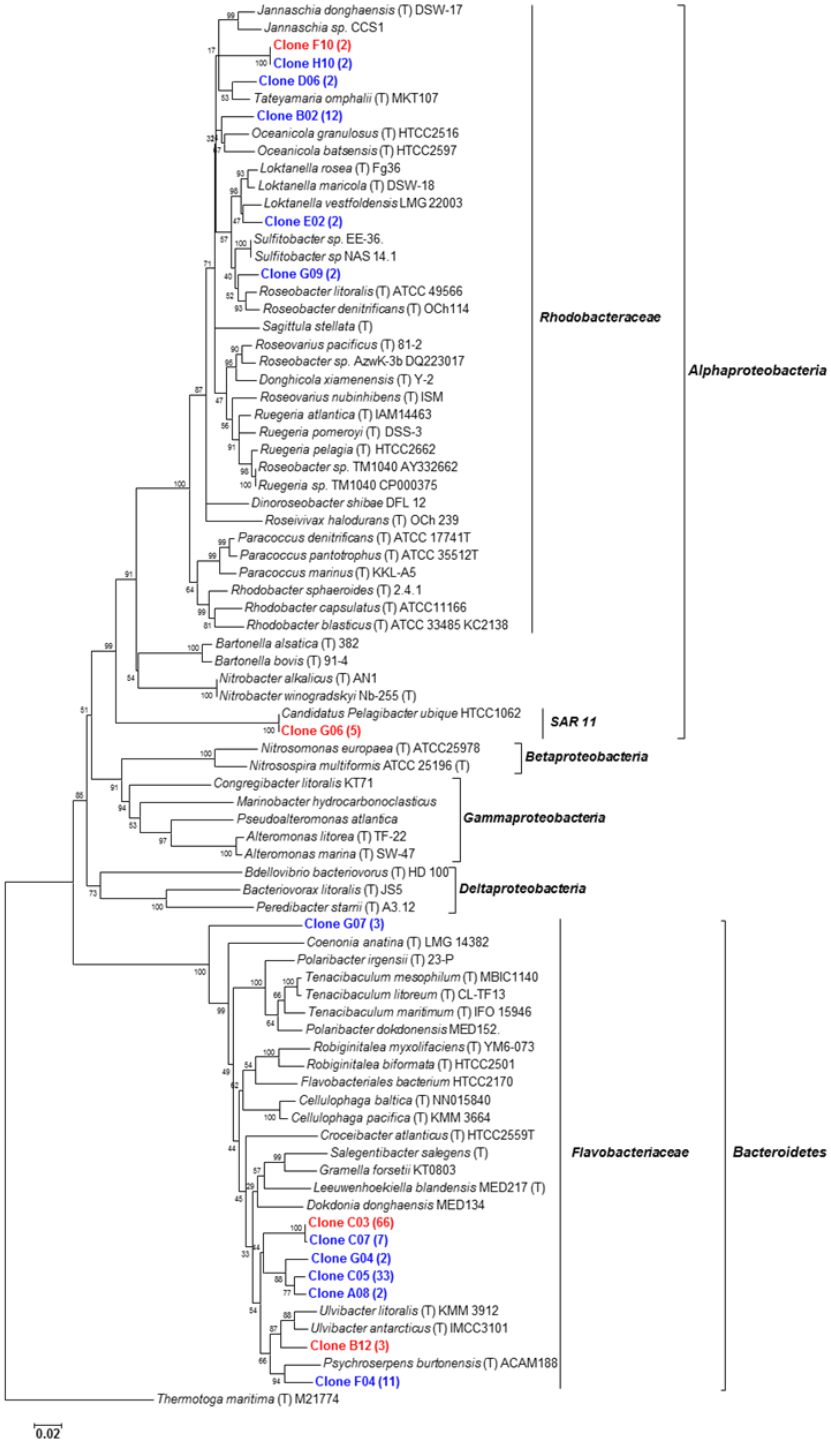

Figure 4.6 Phylogenetic relationships of representative sequences from the dark incubations and their closest relatives based on near full length 16S rRNA gene sequences. Clone sequences retrieved from the ambient CO_2 library are denoted in blue with the high CO_2 sequences in red. The number of clones associated with each representative sequence is denoted in brackets. The tree was constructed in MEGA 5 using the neighbour joining method with Bootstrap analysis with 1,000 replicates. *Thermotoga maritima* was used as an outgroup to root the tree.

4.3.5 The effect of CO_2 levels on the abundance of Rhodobacteraceae and Flavobacteriaceae

To further evaluate the effects of elevated CO_2 on bacterial community composition, 16S rRNA gene-based quantitative PCR (qPCR) was employed to enumerate the bacteria from the *Rhodobacteraceae* and *Flavobacteriaceae* that 16S rRNA gene clone library analysis had indicated were predominant in the dark incubations. This approach was also used to determine if the apparent changes in the relative abundance of these two groups observed in the clone libraries reflected differences in their absolute abundance under elevated and ambient CO_2 conditions. Primers were designed which targeted all the *Rhodobacteraceae* (RBf/RBr) and *Flavobacteriaceae* (FBf/FBr) species detected in the 16S rRNA gene clone libraries (Figure 4.6). The analysis was conducted using DNA samples (high and ambient CO_2) from day 9 incubations using duplicate samples from three different serial dilutions (100, 500 and 1000).

qPCR confirmed that the abundance of *Rhodobacteraceae*-like bacteria was lower in the high CO_2 incubations. In the ambient CO_2 treatment the abundance of 16S rRNA genes from *Rhodobacteraceae*-like bacteria was $8.85 \pm 0.9 \times 10^5$ copies/ml whereas in the high CO_2 treatment the abundance was $3.86 \pm 0.3 \times 10^5$ copies/ml representing a decrease of 56.4% in response to elevated CO_2 (Figure 4.7).

In contrast, the abundance of 16S rRNA genes from *Flavobacteriaceae*-like bacteria was $4.08 \pm 0.1 \times 10^6$ copies/ml in the ambient CO_2 treatment and $2.71 \pm 0.28 \times 10^6$ copies/ml in the high CO_2 treatment (Figure 4.7). Although this equated to a decrease of 33.6% it was considerably less than the decrease observed in *Rhodobacteraceae*. Consequently, there was no significant difference in *Flavobacteriaceae* 16s rRNA gene abundance between the two treatments (P=0.34; Two sample T test) however, a significant difference in 16S rRNA gene abundance was observed in *Rhodobacteraceae* between treatments (P=0.01; Two sample T test).

Total bacterial 16S rRNA gene abundance was 5.51 ± 0.37 x 10^6 copies/ml in the ambient CO_2 treatment which decreased to 4.00 ± 0.43 x 10^6 copies/ml in the high CO_2 treatment (-27.4%). Therefore, in the ambient and high CO_2 treatments *Flavobacteriaceae*-like sequences represented 74% and 67.7% (respectively) of the total 16S rRNA gene abundance, whereas the *Rhodobacteraceae*-like sequences represented 16.1% and 9.6% (respectively). As a result of these changes, the relative abundance of *Flavobacteriaceae*-like sequences in the bacterial 16S rRNA gene clone libraries increased from 62.3% in the ambient CO_2 library to 80.5% in the high CO_2 library (Table 4.2). Initially these results suggested an increase in *Flavobacteriaceae* numbers in response to elevated CO_2 however, it is now known that this change is due to the significant decrease in *Rhodobacteraceae*-like sequences in the high CO_2 treatment while the *Flavobacteriaceae*-like sequences remained relatively unaffected.

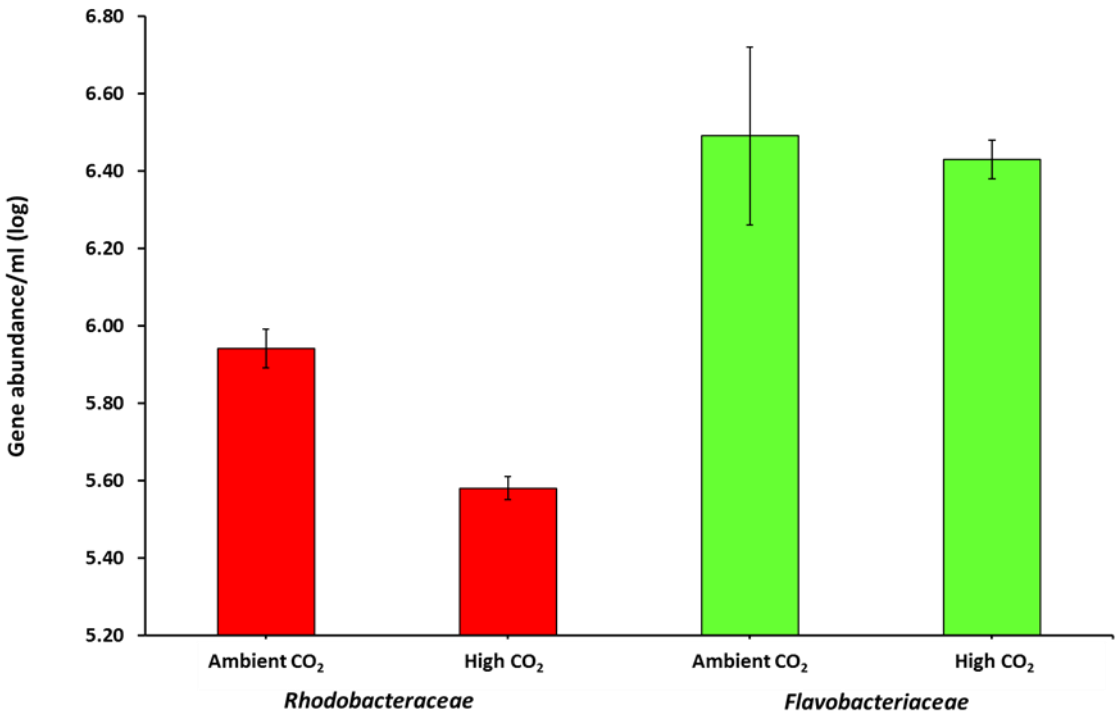

Figure 4.7 Quantitative analysis of *Rhodobacteraceae* and *Flavobacteriaceae* 16S rRNA gene abundance from ambient and high CO_2 treatments sampled on day 9 from phase 2 of the dark incubation experiment. Error bars represent the standard error of duplicate samples taken from replicate bottles.

4.4 Conclusions

The decrease in relative abundance of members of the *Rhodobacteraceae* at increased CO_2 concentrations suggests that this group is sensitive to changes in ocean pH. This was demonstrated in the bacterioplankton flow cytometry data from both the mesocosms and the dark incubation bottles (Chapter 3 section 3.3 – 3.4.4), Libshuff analysis of 16S rRNA gene clone libraries (Section 4.3.3), the phylogenetic analysis of the near full length 16S rRNA sequences (Section 4.3.4) and qPCR analysis (Section 4.3.5). There is an obvious connection between a reduction in *Rhodobacteraceae* numbers and reduced chlorophyll-*a* concentration observed in in the high CO_2 mesocosms (Chapter 3 Section 3.32). Phytoplankton are an abundant source of DMSP in the marine environment which provides a substantial source of dissolved organic carbon and sulfur (in the form of methanethiol) for marine heterotrophic bacteria. A reduction in DMSP concentration (as a consequence of reduced primary production) would therefore have consequences on bacterial production. At the peak of the phytoplankton bloom on day 8 chlorophyll-*a* concentrations in the mesocosms were ~34% higher under ambient CO_2 conditions (10.41 ± 1.14 µg/l^{-1} chlorophyll-*a*) compared to high CO_2 conditions (6.87 ± 3.33 µg/l^{-1} chlorophyll-a). Statistically, there was no significant difference between the treatments during this period (P=0.24; Mann Whitney U Test). However, a significant difference was observed (P= 0.021; Mann Whitney U Test) from day 5 to day 12 which corresponds to the period when chlorophyll-*a* concentrations were responding to the nutrient addition and the end of phase 1 of the experiment. During this period, the ambient CO_2 mesocosms had a 60% average increase in chlorophyll-a concentration compared to the high CO_2 mesocosms (Hopkins *et al.*, 2009).

A recent study by Witt *et al* (2011) investigating the impact of ocean acidification on biofilm microbial communities found a decreases in the relative abundance of *Alphaproteobacteria* (*Rhodobacteraceae)* and increases of *Cytophaga-Flavobacterium-Bacteroides* (*CFB*) at increased CO_2 concentrations. This experiment differed to the present investigation in that the biofilm microbial communities were grown on glass slides in an outdoor aquarium and no phytoplankton bloom was induced. A change in microalgae community structure was also observed with a decrease in green algae

(Chlorophyta), red algae, filamentous red algae and calcareous red algae (Rhodophyta) with rising CO_2 (Witt *et al.*, 2011).

It has been hypothesised that ocean acidification will have a negligible effect on microbial communities and biogeochemical processes other than calcification (Joint *et al.*, 2010). However, there is evidence to support the hypothesis that a decrease in primary productivity caused by elevated CO_2/reduced pH affects PAB communities according to their substrate requirement. It is already known that phytoplankton can influence bacterial communities through the different types of dissolved organic matter (DOM) produced during the various stages of a bloom (Grossart *et al.*, 2005). Future oceans will be dominated by phytoplankton species and strains that show adaptive responses to elevated CO_2 and are able to occupy the ecological niches left vacant by other less adaptive groups. If these less adaptive groups include DMSP producing phytoplankton, notably the coccolithophores and dinoflagellates (Keller *et al.*, 1989) then this would affect bacterial species such as the marine *Roseobacter* clade that are dependent on DMSP as a substrate. However, this effect may be negligible (or even beneficial) to species belonging to the CFB group as they are able to excrete exoenzymes in order to decompose high molecular weight biopolymers such as cellulose and chitin (Cottrell and Kirchman, 2000, Kirchman, 2002).

5. Increased importance of CO_2 fixation by bacterial spp. from the *Roseobacter* clade in a marine mesocosm exposed to elevated CO_2

5.1 Introduction

5.1.1 Heterotrophic CO_2 fixation

Heterotrophic CO_2 fixation was first revealed by Harland Wood (Wood and Werkman, 1935) while conducting his graduate studies in Chester Werkman's laboratory at Iowa State in the early 1930s. His research focussed on the origins of succinic acid when propionic acid bacteria were grown on glycerol in a calcium carbonate buffered system. While calculating the carbon and oxidation-reduction balances of the fermentation process Wood discovered that the amount of carbon recovered after the fermentation did not equal the amount of carbon introduced at the beginning of the experiment. In some of the bacterial strains which produced succinate the amount of carbon in the major fermentation products (propionate and succinate) was greater than the carbon supplied by the fermented glycerol (Wood and Werkman, 1935, Wood and Werkman, 1936). He hypothesised that heterotrophic CO_2 fixation could explain the carbon imbalance though he found this difficult to elucidate and so did not include the results in his thesis (Kresge *et al.*, 2005). The idea of heterotrophic CO_2 fixation was controversial; the accepted biochemical paradigm of the time was that only plants and autotrophic bacteria were able to fix CO_2. Wood *et al* (1941) persisted in their endeavours and finally elucidated the heterotrophic CO_2 fixation pathway using ^{13}C labelled sodium bicarbonate ($NaH^{13}CO_3$) which was measured with a mass spectrometer (Wood *et al.*, 1941). Later known as the Wood-Werkman reaction the pathway involves the condensation of CO_2 with the 3-carbon compound pyruvate to form a 4-carbon compound oxaloacetate (Wood *et al.*, 1941). Consequently the enzyme responsible for the direct carboxylation of pyruvate has been elucidated and the pathway is now recognized as the pyruvate carboxylase reaction (Utter and Keech, 1963). The term anaplerotic was first used in biochemistry by Sir Hans Kornberg to describe the pathways which replenish the metabolic intermediates of the TCA cycle (Kornberg, 1966). This is necessary because the intermediates of the TCA cycle are not only required for energy metabolism but are also consumed for amino acid biosynthesis (Figure 5.1). Identified in 1937 by the German biochemist Sir Hans Adolf Krebs the TCA cycle is the second step in carbohydrate catabolism, generating usable energy and essential precursors for

biosynthesis. The cycle begins with acetyl-CoA (via oxidation of pyruvate from the glycolysis pathway) which transfers its two-carbon acetyl group to the four-carbon acceptor compound oxaloacetate to form a six-carbon compound citrate. Through a series of reactions oxaloacetate is subsequently regenerated and the cycle continues. Many of the intermediates produced in the TCA cycle are precursors for important biomolecules; α-ketoglutarate can be converted into glutamate which is a precursor for the synthesis of other amino acids and purine nucleotides (Figure 5.1). Oxaloacetate can act as a substrate for gluconeogenesis or it can be transaminated to form aspartate which itself is a precursor for other amino acids and pyrimidine nucleotides. Conversely the four and five carbon intermediates of the TCA cycle which are normally produced from amino acids can accumulate in the cell and therefore have to be removed by a process known as cataplerosis. These complex interactions are strictly regulated by three mechanisms: substrate availability, product inhibition and competitive feedback inhibition.

Pyruvate carboxylase is a member of the biotin-dependent enzyme family and is regulated by acetyl-CoA which acts as an allosteric activator stimulating the cleavage of ATP and inducing a conformational change in the tetrameric structure of the enzyme. Each subunit of the tetramer contains four domains, two of which are the active binding sites for carboxylation, one an allosteric binding site and the forth acts as an anchor point (via a lysine residue) for a single biotin moiety. The biotin and lysine residues work together to act as a swinging arm in order to transport CO_2 between the two active sites. Pyruvate carboxylase uses the covalently attached biotin moiety to catalyse the two step carboxylation of pyruvate to oxaloacetate. In the first step (Figure 5.2) ATP reacts with HCO_3^- resulting in the formation of carboxyphosphate, a highly unstable molecule that rapidly dissociates to CO_2 and phosphate prior to the carboxylation of the biotin moiety. Step two involves the transfer of the newly generated carboxybiotin to the second active site where its carboxyl group is the transferred to the acceptor molecule pyruvate resulting in the formation of oxaloacetate (Jitrapakdee *et al.*, 2002)

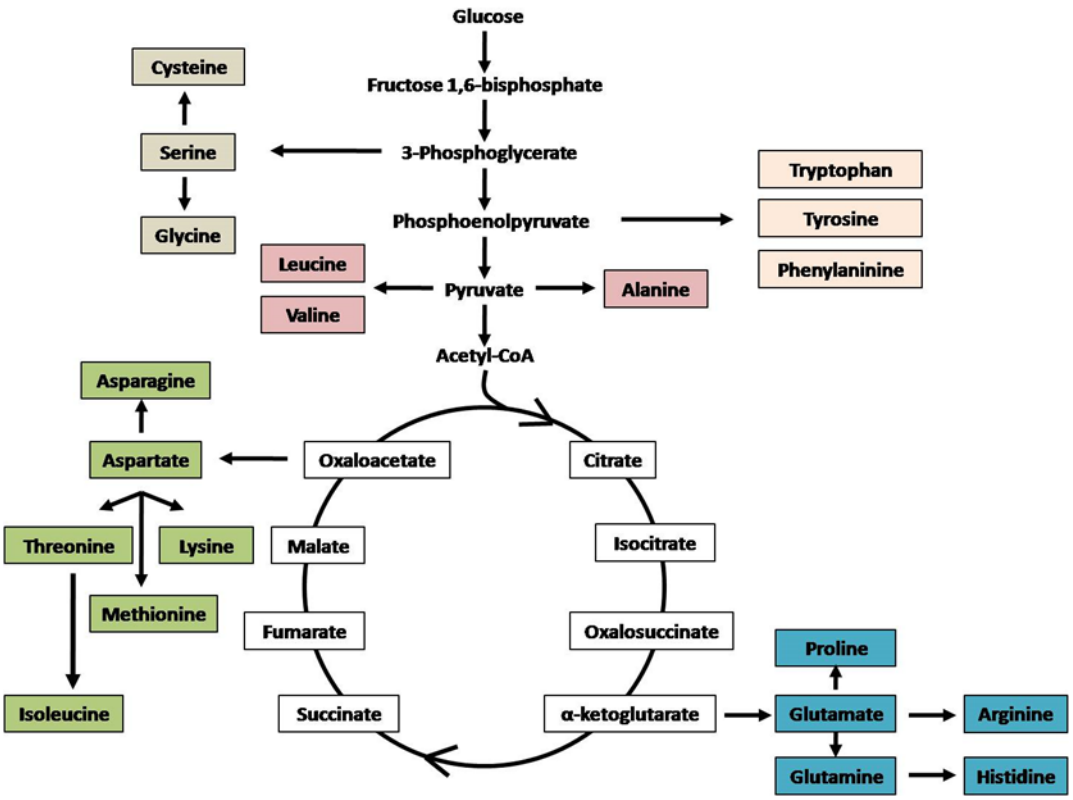

Figure 5.1 Schematic of glycolysis and the TCA cycle. The TCA cycle is the fundamental pathway in aerobic respiration which produces energy, CO_2 and H_2O from the remaining carbon (in the form of pyruvate) of glycolysis. The TCA cycle is known as an amphibolic pathway because it participates in both anabolism and catabolism with the intermediates of the TCA cycle acting as precursors for amino acid biosynthesis or in the case of catabolism the conversion of amino acids to replenish the intermediates of the cycle

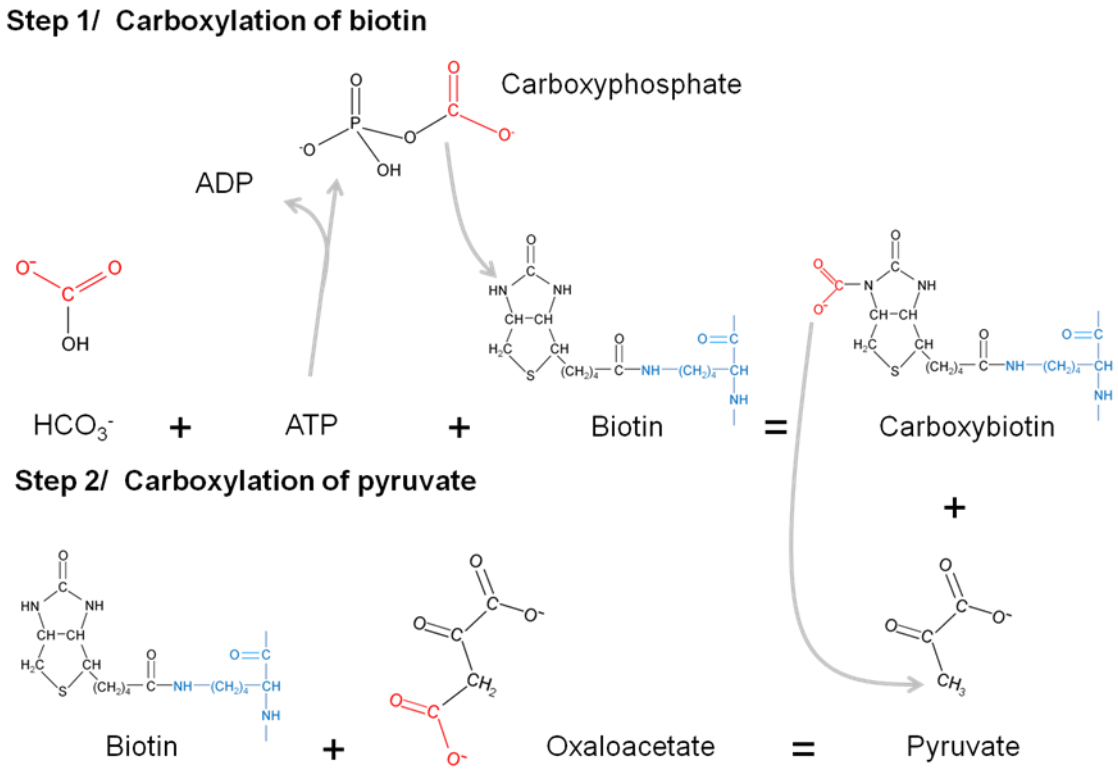

Figure 5.2 The conversion of pyruvate to oxaloacetate. Pyruvate carboxylase catalyses the anaplerotic reaction which generates oxaloacetate in a two-step process. Step 1 involves the carboxylation of biotin at one active site which is then transferred to the next active site via the lysine residue (blue). In step 2 CO_2 is transferred from the biotin to pyruvate resulting in the formation of oxaloacetate and biotin.

5.1.2 The significance of heterotrophic CO_2 fixation in the environment.

It was suggested by Romanenko (1964) that the rate of CO_2 fixation via anapleurosis could be directly coupled to microbial growth thereby providing quantitative data on total bacterial production. Using a variety of lab cultures and field samples he reported that ~6% of organic carbon in heterotrophic bacteria originates from the direct incorporation of CO_2 (Romanenko, 1964). Several investigations followed using this constant fixation ratio of 0.06 to estimate bacterial production (Kusnetsov and Romanenko, 1966; Sorokin, 1966, Kapustina, 1999) while other studies (Overbeck, 1972; Overbeck and Daley., 1973, Overbeck, 1979) found a much greater variation in CO_2 assimilation of 1-12% in both cultured and uncultured microorganisms. Using heterotrophic CO_2 fixation ratios to establish product rates can therefore be very misleading. As early as 1932 a causative link was established between CO_2 uptake in

heterotrophic bacteria and organic carbon availability in the surrounding environment (Walker, 1932). This was further supported by the work of Prescott (1965) when he confirmed that the amount of CO_2 fixed relative to total organic carbon decreased in more complex media (Prescott *et al.*, 1965). Naturally this type of medium contains all the requirements for growth such as a carbon source, water, salts, amino acids and nitrogen which is seldom seen in nature. Therefore it is highly unlikely that additional carbon (in the form of CO_2) would be required. It is now generally established that heterotrophic organisms have different CO_2 assimilation patterns under varying environmental conditions. This is further emphasised by the fact that organisms utilizing C_1 substrates such as methane, methanol, formate and carbon monoxide have been found to assimilate more CO_2 than organisms which utilize complex organic substrates (Doronia and Trotsenko, 1985). CO_2 derived carbon also varies among species due to differences in metabolic salvage pathways and growth responses (Li, 1982, Dijkhuizen and Harder, 1985). Essentially bacteria are able to respond to environmental change by recycling substrates from intermediates in degradative pathways such as methionine or nucleotides, thus saving the energy and carbon that would be required for *De Novo* synthesis. As a consequence of this variability, any estimations of bacterial production using the Romanenko technique are inaccurate as no fixed ratio actually exists.

Heterotrophic CO_2 fixation is generally considered to be a relatively minor route of inorganic CO_2 fixation. The current paradigm is that the oceans and autotrophic CO_2 fixation via photosynthesis are the main carbon sinks for the absorption of CO_2. However, the work of Overbeck (1972) has demonstrated that heterotrophic CO_2 fixation can account for 1 – 12% of assimilated carbon. At these higher levels, heterotrophic CO_2 fixation could make a considerable contribution to global carbon fixation and could play a key role in offsetting carbon emissions. The twin threat of global warming and ocean acidification has compelled scientists to study the carbon cycle and investigate the biochemistry of the organisms involved in this key process. This has been aided by recent advances in microbiology, ecology and genomics which have made it possible to sequence microbial genomes to elucidate phylogeny and the metabolic potential of an organism.

Light-independent CO_2 fixation has been demonstrated by Li and Dickie (1991) using ^{14}C labeled sodium bicarbonate on seawater sampled from the base of the euphotic zone (Li and Dickie, 1991). The results showed that the net increase in bacterial abundance approximately correlated with the measured fixation of ^{14}C in the dark incubations. Dark CO_2 assimilation under resource-limited conditions was also investigated by Alonso-Sáez (2010) using 3 month old Artic seawater cultures incubated in the dark with ^{14}C radiolabeled sodium bicarbonate (Alonso-Saez *et al.*, 2010). Bicarbonate incorporation rates correlated with rates of bacterial heterotrophic production (determined by the incorporation of [^{3}H]-leucine) with *Beta* and *Gammaproteobacteria* showing high activity in bicarbonate and leucine uptake while *Flavobacteria* only assimilated leucine. Furthermore, PCR analysis of the biotin carboxylase gene *accC* putatively involved in archaeal CO_2 fixation yielded not archaeal sequences but amplified a variety of bacterial carboxylases involved in fatty acids biosynthesis, anaplerotic pathways and leucine catabolism (Alonso-Saez *et al.*, 2010). Using single cell sorting and whole genome amplification Swan *et al* (2011) recovered complete RuBisCO operons from two single amplified genomes (SAGs) of *Deltaproteobacteria* and two *Gammaproteobacteria* obtained from the lower mesopelagic zone of two subtropical gyres (Swan *et al.*, 2011). Furthermore, using microautoradiography ^{14}C labelled bicarbonate assimilation was detected in *Deltaproteobacteria* cluster SAR324 suggesting that this group may be a major contributor in CO_2 fixation of the dark oceans. However, DeLorenzo *et al* (2012) reported a greater diversity of bacteria assimilating dissolved inorganic carbon (DIC) in waters off the Oregon and Washington coasts (DeLorenzo *et al.*, 2012). Using stable isotope probing (SIP) with ^{13}C sodium bicarbonate the authors found that *Alphaproteobacteria, Gammaproteobacteria and Bacteroidetes* dominated dark DIC assimilation in the seawater samples. Comparison of the ^{12}C and ^{13}C clone libraries found an increase of 30% to 38% in *Alphaproteobacteria* sequences and 25% to 33%, in *Bacteroidetes* sequences (^{12}C and ^{13}C respectively). Members of the SAR11 clade comprised a significant portion of *Alphaproteobacteria* assemblage as well as members of the marine *Roseobacter* clade closely related to *Roseovarius mucosus, Octadecabacter antarcticus* and *Loktanella rosea* (DeLorenzo *et al.*, 2012).

5.1.3 Metabolic strategies of the marine Roseobacter clade

One group of bacteria which are of particular relevance in CO_2 fixation is the marine *Roseobacter* clade. Their physiological diversity and metabolic versatility has enabled them to occupy a range of habitats from polar ice to deep ocean sediments though the majority of them are marine organisms (pelagic and coastal) accounting for ~10% of all the bacteria in the Arctic Ocean (Malmstrom *et al.*, 2007) and ~20% in the southern ocean (Selje *et al.*, 2004). The *Roseobacter* clade falls within the α-3 subclass of *Proteobacteria* with members sharing >89% identity of the 16S rRNA gene (Buchan *et al.*, 2005). More than 38 genera affiliated with the *Roseobacter* clade have been described (Brinkhoff *et al.*, 2008) including *Roseobacter, Roseovarius, Ruegeria, Sulfitobacter, Silicibacter, Jannaschia, Loktanella* and *Oceanicola*.

A strategy used by several species of marine *Roseobacter* to supplement energy is aerobic anoxygenic phototrophy (AAnP). The literal interpretation of this term implies photosynthesis in the presence of oxygen without the generation of oxygen. The term is slightly misleading because no light driven synthesis of organic carbon is carried out and the organism still requires organic matter as a source of carbon (Wagner-Dobler and Biebl, 2006, Moran *et al.*, 2007). These organisms share common features: the presence of bacteriochlorophyll, light-harvesting complexes, an abundance of carotenoids, and the inability to grow photosynthetically under anaerobic conditions (Yurkov and Beatty, 1998). Previous studies have reported CO_2 fixation in several AAnPs though the amount of CO_2 assimilated was deemed insufficient to maintain autotrophic growth (Shiba, 1984, Kishimoto *et al.*, 1995). Recent studies investigating AAnPs from the marine *Roseobacter* clade have established compelling evidence to suggest that this particular group of bacteria is able to fix CO_2 via anaplerotic reactions using photoheterotrophic metabolism (Kolber *et al.*, 2001; Moran and Miller, 2007, Swingley *et al.*, 2007, Tang *et al.*, 2009). Additionally several species of AAnPs such as *Jannaschia* sp. CCS1, *Loktanella vestfoldensis* SKA53 and *Roseobacter litoralis* are able to oxidize CO to CO_2 to further supplement energy for heterotrophic growth.

A greater variety of metabolic strategies are available to *Roseobacter denitrificans* OCh114. Typical of all AAnPs they are able to grow photoheterotrophically in the presence of oxygen and light. However they also grow anaerobically in the dark using nitrite and trimethylamine *N*-oxide as an electron acceptor (Yurkov and Beatty, 1998, Swingley *et al.*, 2007). CO oxidation has not been observed in this species in culture; however it does possess the necessary *cox* genes to mediate CO oxidation though the circumstances in which this occurs are still undetermined. Several species of *Roseobacter* are known to be lithoheterotrophic, capable of utilizing the oxidation of inorganic compounds to supplement heterotrophic energy generation (Moran and Miller, 2007). This has been proven experimentally when enhanced biomass (45%) was observed in cultures of *Silicibacter pomeroyi DSS-3* grown on acetate and amended with 10 mM thiosulfate relative to cultures receiving no thiosulfate (Moran *et al.*, 2004). Moreover, increased dark anaplerotic CO_2 fixation of between 20 – 200% was observed in members of the alpha-3 subgroup of the *Roseobacter* cluster that oxidize thiosulfate completely to sulfate (Sorokin, 2003). One of the strains investigated (ChLG 1) possessed high pyruvate carboxylase activity and the addition of pyruvate significantly stimulated CO_2 assimilation.

The origin of CO_2 fixation in this group of bacteria still remains unanswered. It has been proposed that the photosynthetic genes were obtained by horizontal gene transfer (Nagashima *et al.*, 1997) or that AAnPs diverged from a purple photosynthetic bacterial ancestor by becoming dependent on organic compounds when the oxygen level in the Earth's atmosphere became elevated (Beatty, 2002). However, what is becoming evident is the ecological significance this group plays in the cycling of both organic and inorganic carbon.

5.1.4 Metabolic pathways of CO_2 fixation in Roseobacter denitrificans OCh 114

New insights into the lifestyle and physiology of AAnPs were gained by sequencing the genome of *Roseobacter denitrificans* OCh114 (Swingley *et al.*, 2007). Using phylogenetic analysis the researchers suggested that due to the presence of RuBisCO in related *Alphaproteobacteria*, ancestral AAnPs may have once contained

Calvin cycle enzymes but due to their ever increasing dependence on organic carbon compounds for growth their requirement for CO_2 diminished (Figure 5.3). This hypothesis is however speculative based solely on the presence of RuBisCO in lineages that root more deeply in phylogenetic trees than marine *Roseobacters* and therefore does not take into account the evolutionary origins of RuBisCO or the possibility of lateral gene transfer (Ashida *et al.*, 2005).

Swingley *et al* (2007) proposed that *R. denitrificans* fixes CO_2 via 3 key enzymes, pyruvate carboxylase, phosphoenolpyruvate (PEP) carboxylase and pyruvate-orthophosphate dikinase. The carboxylases catalyse the addition of CO_2 (via HCO_3^-) to either pyruvate (pyruvate carboxylase) or PEP (PEP carboxylase) producing oxaloacetate. Pyruvate-orthophosphate dikinase is not directly responsible for the fixation of CO_2; it catalyses the reversible phosphorylation of pyruvate to PEP. In the *Roseobacter* group the enzymes pyruvate carboxylase and pyruvate-orthophosphate dikinase form monophyletic clusters which are distinct from those from closely related species (Swingley *et al.*, 2007). It was proposed by the reseachers that this sequence divergence combined with photoheterotrophic energy metabolism could enhance CO_2 fixation over and above that of normal anaplerotic reactions. In essence AAnPs lead a mixotrophic rather than a photoheterotrophic lifestyle capable of deriving metabolic energy and carbon from various different sources.

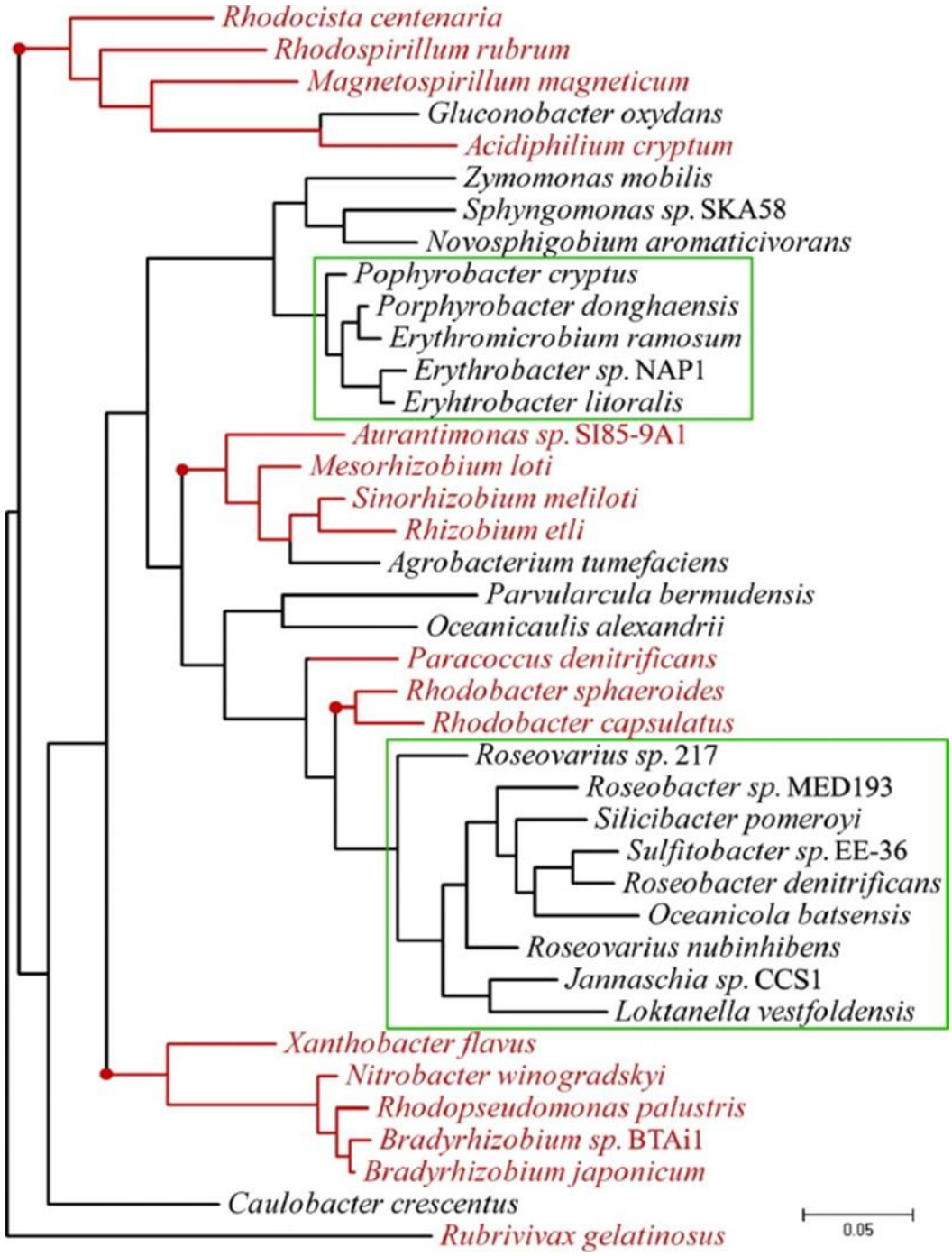

Figure 5.3 16S rRNA phylogenetic tree taken from Swingley et al (2007). The tree indicates the presence of RuBisCO within the Proteobacteria (red text), with putative RuBisCO-containing nodes highlighted with red dots. It is speculated that the widespread presence of RuBisCO in the tree suggests that the ancestral species of *Rhodobacteraceae* contained this enzyme which was subsequently lost by the AAnPs (green text) due to their ever increasing dependence on organic carbon. The tree was constructed using the maximum likelihood method.

As well as PEP carboxylase, EC 4.1.1.31(*ppc*) and pyruvate carboxylase, EC 6.4.1.1 (*pyc*) two other enzymes are also known to assimilate CO_2 via anaplerotic reactions. Phosphoenolpyruvate (PEP) carboxykinase, EC 4.1.1.49 (*pckA*) catalyses the reversible reaction ATP + oxaloacetate (OAA) = ADP + phosphoenolpyruvate + CO_2, while malic enzyme EC 1.1.1.40 (*tme*) catalyses the reversible reaction (S)-malate + NADP+ = pyruvate + CO_2 + NADPH (Figure 5.4). All four genes are present in the genome of *R. denitrificans* which coupled to photoheterotrophic energy metabolism could explain the increased CO_2 fixation observed in several AAnP studies (Shiba, 1984; Yurkov, 1990, Kishimoto *et al.*, 1995, Yurkov and Beatty, 1998, Kolber *et al.*, 2001, Swingley *et al.*, 2007, Tang *et al.*, 2009).

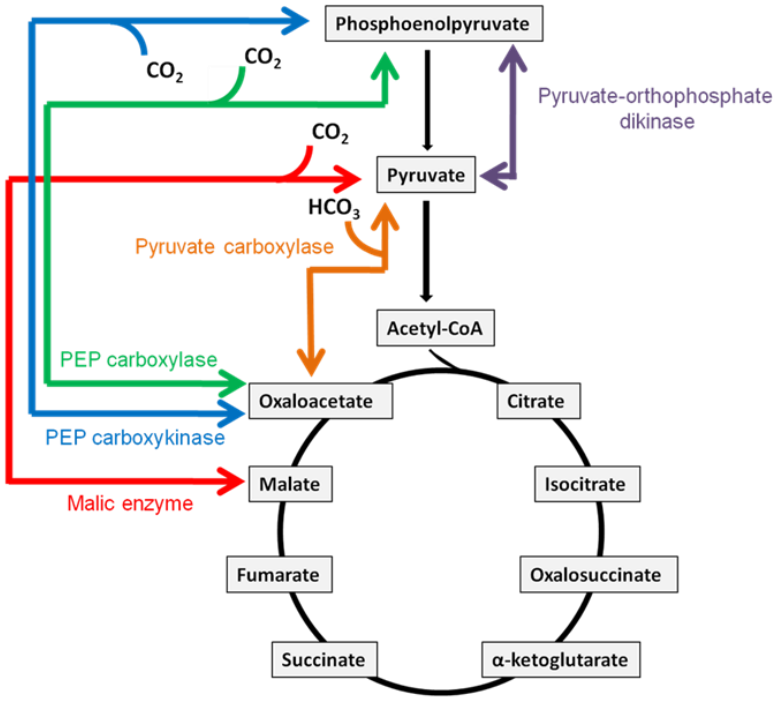

Figure 5.4 Major anaplerotic reactions known to assimilate CO_2 in order to replenish the intermediates of the TCA cycle.

The objective of this study was to investigate the effects of elevated CO_2 on microorganisms capable of fixing inorganic carbon in the dark. The working hypothesis was that we would observe effects most particularly among chemoautotrophic bacteria but effects on heterotrophic CO_2 fixation might also be apparent. Mesocosm CO_2 perturbation experiments were set up to simulate the conditions of a future high CO_2 world predicted in the "business as usual "scenario by the Intergovernmental Panel on Climate Change (IPCC, 2001). Comparison of marine microbial communities responsible for dark CO_2 fixation under ambient and high CO_2 conditions was achieved by stable isotope probing (SIP) with ^{13}C-$NaHCO_3$ incubations.

5.2 Methods

To identify putative chemoautotrophic bacteria Stable Isotope Probing (SIP) using ^{13}C-labelled bicarbonate as a substrate was employed. Mesocosms in a Norwegian fjord, designed to simulate the predicted high CO_2 world of 2100 based on current emissions (~ pH 7.8/pCO_2 750 ppm) were sub-sampled into duplicate 4 L dark bottles containing the labelled bicarbonate and incubated *in situ* in the fjord for 5 days. 1L samples of water were collected from the dark incubations on days 1, 2, 3, 5, (phase 1) and 8, 9, 10, 12 (phase 2), pre-filtered through a 5 µm polycarbonate filter and then a 0.2 µm sterivex filter. DNA was extracted from each sterivex filter using a phenol/chloroform/isoamyl alcohol method (Maniatis *et al.*, 1982) and the ^{12}C and ^{13}C DNA fractions resolved via isopycnic CsCl density gradient centrifugation. To act as a control a second set of ambient CO_2 mesocosms was established (~pH 8.1/pCO_2 380 ppm). Preparation of dark bottle incubations, incubation time, sampling regimes and extraction methods were identical to those of the high CO_2 treatments (see chapter 2 for full methodological details).

All the steps taken in the SIP procedure were fully optimised prior to the analysis of mesocosm samples. Using ^{13}C DNA from a preliminary test experiment, centrifuge speed, duration and gradient densities were calibrated to obtain optimal separation of ^{12}C and ^{13}C DNA. Control tubes containing ethidium bromide and ^{13}C/^{12}C DNA were included in all centrifuge runs to provide visual confirmation of the success of the

isopycnic separation (Figure 5.5). Preliminary investigations to deduce the optimal volume of fractions to collect indicated that fraction volumes of 400 µl typically reported in the literature (Lueders *et al.*, 2004; Singleton *et al.*, 2005, Neufeld, 2008) were too large to sufficiently determine the boundary between ^{13}C and ^{12}C DNA. This unresolved boundary resulted in intermediate fractions containing both ^{13}C and ^{12}C DNA. This was resolved by collecting smaller fractions of 200 µl which improved the definition between the ^{13}C and ^{12}C DNA visualized on an agarose gel (Figure 5.6). The SIP experiment (fractionation) was conducted in triplicate using samples taken on day 10 of the dark incubation experiment from both the high and ambient CO_2 treatments incubated with ^{13}C sodium bicarbonate.

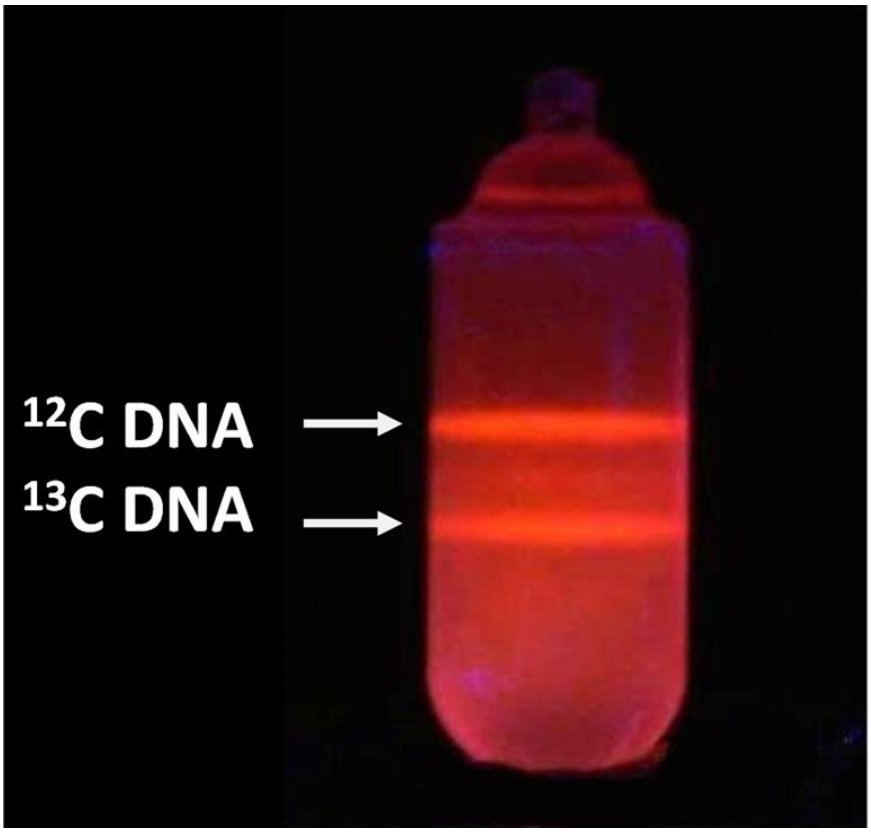

Figure 5.5 Control tube used in every centrifugation run for the isopycnic separation of the heavy (^{13}C) and light (^{12}C) DNA fractions. Tubes were constructed by culturing E. coli K12 on ^{13}C and ^{12}C glucose, extracting the DNA and combining it in equal amounts. Ethidium bromide was then added to the caesium chloride gradient for visualization purposes only.

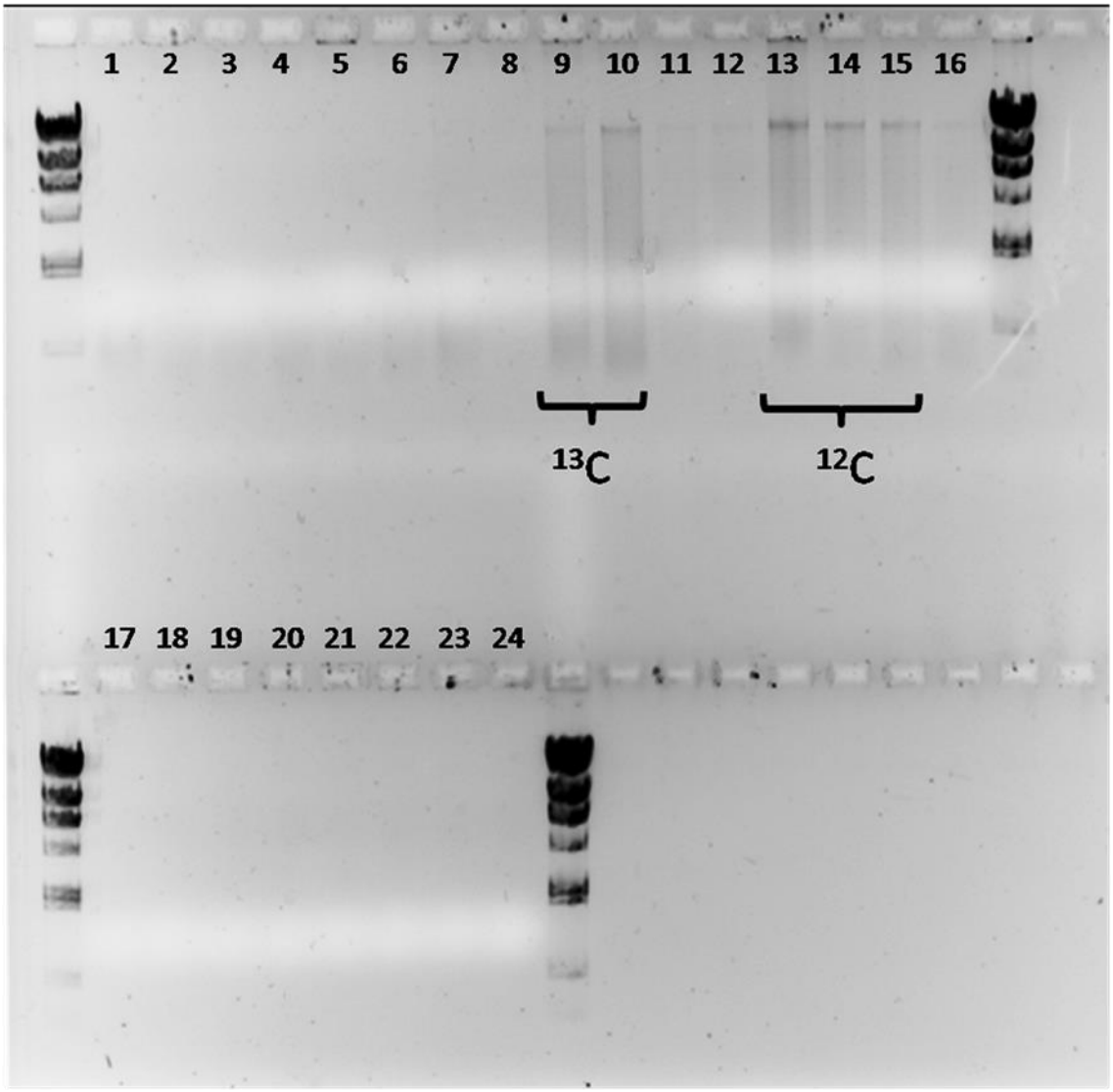

Figure 5.6 Fractionation of SIP tubes. Each tube was fractionated into 28 x 200 µl aliquots with the first and last two aliquots were discarded. The remainder was visualized by running 5 µl of each aliquot on a 0.7% agarose gel to establish which aliquots contain the ^{13}C and ^{12}C fractions.

Due to the low yields of DNA obtained after the isopycnic separation multiple displacement amplification (MDA) was employed to generate microgram quantities of DNA from an initial starting quantity of less than 10 ng. This method has proven to be highly accurate in amplifying DNA which is almost identical to the original sample (Yvette *et al.*, 2007, Giardina *et al.*, 2009) and generates the least bias compared to other whole genome amplification methods (Pinard *et al.*, 2006). The MDA was repeated numerous times and the products pooled in order to ensure that the amplified DNA was representative of the original DNA and to obtain a sufficient quantity of high molecular

weight DNA suitable for further analysis. The comparability of MDA amplified DNA and the original template DNA was confirmed by comparison of bacterial 16S rRNA gene DGGE profiles before and after MDA amplification.

The composition of bacterial communities represented in the ^{13}C and ^{12}C DNA fractions from replicate incubations was analysed by denaturing gradient gel electrophoresis (DGGE) of PCR amplified 16S rRNA genes and near full length 16S rRNA gene clone libraries were constructed from each representative sample. 16S rRNA gene clones were sequenced and compared to the GenBank database to identify the most closely related sequences. The evolutionary relationship between the bacterial species identified was inferred from a phylogenetic tree constructed in MEGA 4 (Tamura *et al.*, 2007).

The metabolic potential of bacterial communities represented in the ^{13}C and ^{12}C DNA fractions was established by creating four metagenomic libraries consisting only of species within the *Rhodobacteraceae* and *Flavobacteriaceae*. The relevant species were subtracted (*in silico*) from two metagenomic libraries (total DNA, not SIP) of the ambient and high CO_2 dark incubations. The sequence data from the four subsets (*Rhodobacteraceae*, ambient and high CO_2, *Flavobacteriaceae*, ambient and high CO_2) was uploaded to MG-RAST (Metagenomics Rapid Annotation Server) which annotates DNA sequences and provides phylogenetic and functional classification of samples (Meyer *et al.*, 2008). The datasets were also uploaded into KAAS (KEGG Automatic Annotation Server) (http://www.genome.jp/tools/kaas/) which identifies genes by BLAST comparison against the manually curated KEGG database (Kyoto Encyclopaedia of Genes and Genomes) and maps them onto metabolic pathways (Moriya *et al.*, 2007). Sequences identified by KAAS as partial fragments of anaplerotic genes were then obtained and their identity verified by comparing them against the non-redundant (nr) protein database using the BLASTX program. Statistical analysis of partial anaplerotic gene fragments was conducted in the STAMP (Statistical Analysis of Metagenomic Profiles) software package using the metabolic profiles created by MG-RAST as input data.

To access the similarity of pyruvate carboxylase amino acid sequences of different bacterial species, pairwise alignments were conducted using the BLASTP program of the NCBI. Full length pyruvate carboxylase amino acid (aa) sequences from *Flavobacteriaceae* and *Rhodobacteraceae* species were downloaded from GenBank http://www.ncbi.nlm.nih.gov/genbank/ and compared against the pyruvate carboxylase aa sequence of *Roseobacter denitrificans* OCH114. Sequences were aligned in the software program MUSCLE (multiple sequence comparison by log-expectation) (Edgar, 2004) and a phylogenetic tree from the amino acid sequences was generated in ARB (Ludwig *et al.*, 2004) using a Phylip maximum-likelihood method (Phylip PROML), including bootstrap support of 500 replicates. Pyruvate carboxylase aa sequences identified from the metagenomes were added to the tree by parsimony methods.

For clarification and to diminish any form of ambiguity the results presented in this study are predominantly from the analysis of the DNA retrieved from the ^{13}C and ^{12}C CsCl fractions obtained via the isopycnic separation of samples taken on day 10 from the ^{13}C DNA dark incubation bottles (ambient and high CO_2 treatments).

5.3 Results and discussion

5.3.1 DGGE analysis of SIP fractions

Nested PCR with primers pA/pH and primers2/3 (Edwards *et al.*, 1989) was used to amplify bacterial 16S rRNA gene fragments from all the SIP fractions and the community composition was visualised using DGGE analysis. A high degree of similarity was observed between the triplicate samples (SIP 1, 2, 3) which showed distinct profiles for the high and ambient CO_2 treatments (Figure 5.7). In order to explore the similarities in bacterial community structure a cluster analysis was performed using the Pearson product moment correlation coefficient to compute the similarity matrix and UPGMA (unweighted pair group method with arithmetic averages) to generate the dendrogram. The Pearson correlation was used in the DGGE analysis as it takes into account the relative intensity of each band by comparing the densitometric curves rather than the banding patterns themselves (Bernhard *et al.*, 1993). It has the advantage of being insensitive to pattern intensity and relative differences in background

while at the same time being sensitive to the intensity of individual bands. The slight disadvantage is that it never indicates a perfect match, even between profiles which are visually indistinguishable. The analysis clearly indicated a difference in the community structure associated with elevated CO_2 resulting in a defined clustering of the high and ambient CO_2 treatments. However no such clustering was observed between the $^{13}C/^{12}C$ fractions leading to the conclusion that the ^{13}C treatment had little effect on community composition (Figure 5.8).

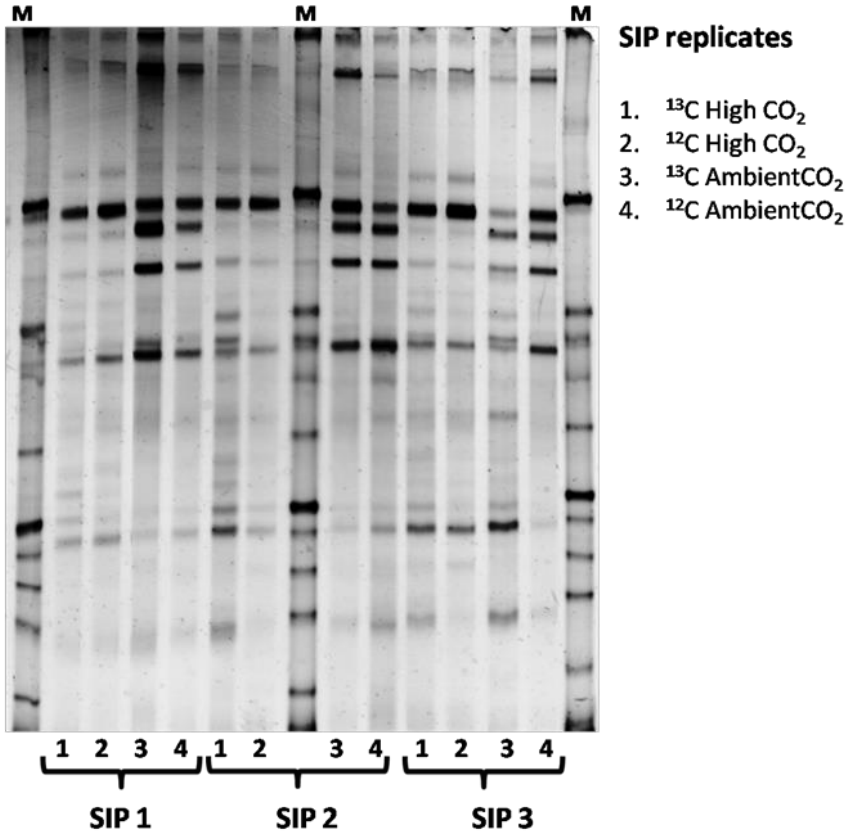

Figure 5.7 DGGE analysis of ^{12}C and ^{13}C DNA fractions obtained from day 10 of the ^{13}C dark incubations (high and ambient CO_2 treatments). Fractionation and whole genome amplification was performed in triplicate denoted as SIP 1, 2 and 3.

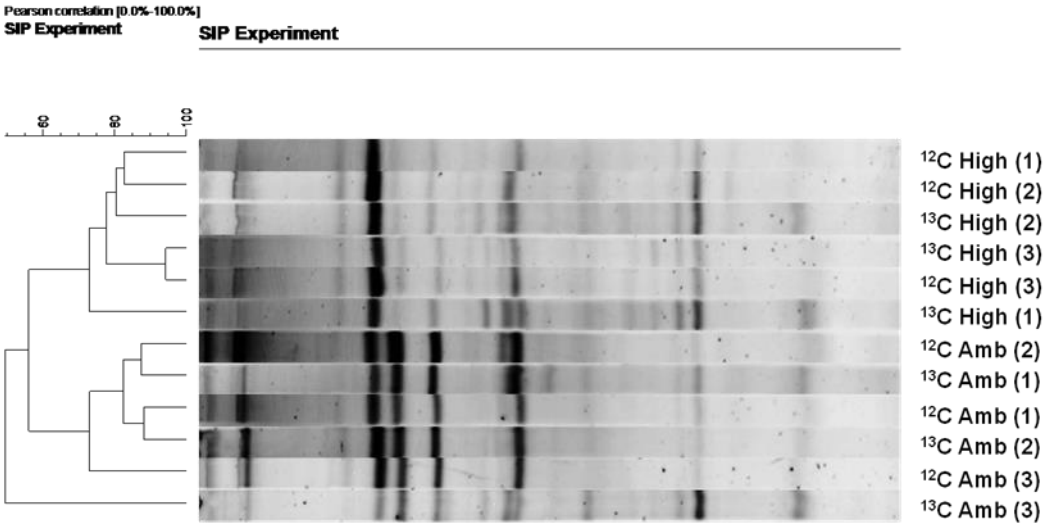

Figure 5.8 Cluster analyses of DGGE profiles from triplicate SIP experiments with the experiment number denoted in brackets. The community profiles and resulting dendrogram indicate a defined clustering due to their specific treatment (high/ambient CO_2) rather than incubation with labelled bicarbonate. The cluster analysis was generated using Pearson's correlation and the unweighted pair-group method with arithmetic averages.

To statistically test whether there were significant differences between the profiles from different treatments ANOSIM (Analysis of similarities) was performed using the software package PRIMER 6 (Clarke, 1993). This method uses the Bray-Curtis measure of similarity to test whether there is a significant difference between 2 or more groups of samples. The test generates a value of R (based on the ranks of the dissimilarities) and a P value which is given as a percentage. The R value lies between -1 and +1, with a value of zero representing the null hypothesis that the samples are not significantly different. Three ANOSIM tests were conducted using the similarity matrix calculated from the DGGE profiles. As SIPs 1, 2 and 3 were from triplicate fractionation and amplification experiments the first ANOSIM test was to determine reproducibility of the 3 experiments. The test revealed an R value of – 0.013 and a P value of 0.44 indicating that there were no significant differences between the triplicate fractionation experiments (Figure 5.7).

The second ANOSIM test was to investigate if there was a significant difference in the DGGE profiles between the high and ambient CO_2 treatments. In this instance the test revealed an R value of 0.783 and a P value of 0.002 indicating that the similarities between the samples was greater within groups than between groups therefore rejecting the null hypothesis and indicating a significant difference between the high and ambient CO_2 treatments.

Finally, an ANOSIM test was performed to investigate if there was a significant difference in the DGGE profiles between the ^{13}C and the ^{12}C sodium bicarbonate incubations. In this instance the profiles were more similar between the groups than within the groups with an R value of -0.107 and a P value of 0.816 concluding that there were no significant differences between the ^{13}C and ^{12}C treatments.

5.3.2 Characterisation of dominant bacteria from SIP fractions

The aim of this study was to investigate the response of aquatic bacterial populations to elevated CO_2 and reduced pH. One group of bacteria which may be particularly susceptible to the effects of elevated CO_2 are the chemoautotrophic ammonia-oxidising bacteria (AOB). These organisms are responsible for the rate-limiting step of nitrification by utilizing the conversion of ammonia (NH_3) to nitrite (NO_2^-) as their sole energy source and using this energy to fix CO_2. Experimental evidence has revealed that a reduction in ocean pH will result in a decrease in the amount of available ammonia thus reducing nitrification (Huesemann *et al.*, 2002). This is due to the fact that the ratio of ammonia (NH_3) to ammonium (NH_4^+) is significantly reduced with decreasing pH favouring the production of ammonium over that of ammonia. The ammonium ion cannot be utilised by AOBs as it is unable to cross the cell membrane via simple diffusion due to its positive charge. At pH 8.1, ~4% of the ammonia is present as $NH_{3\,(Aq)}$ but at pH 7.8 the proportion of $NH_{3\,(Aq)}$ is reduced by ~50% with complete inhibition of nitrification at pH 6.0 (Raven, 1986, Huesemann *et al.*, 2002).

Based on the reproducibility of replicate DGGE profiles, (Figure 5.7 and 5.8), a single 16S rRNA gene clone library was considered representative of the DGGE profiles

from each treatment. The similarity of DGGE profiles within each treatment was 73.1 ± 11.9% as opposed to between treatments where the average similarity was significantly lower (57.6 ± 8.3 %; P = < 0.01; Mann Whitney U Test). Thus four 16S rRNA gene clone libraries (^{13}C high CO_2, ^{12}C high CO_2, ^{13}C ambient CO_2, and ^{12}C ambient CO_2) were prepared from the pooled triplicate fractions which were then sequenced and the 16S rRNA sequences recovered were compared to the GenBank database using the BLAST program (Altschul *et al.*, 1990). All the sequences recovered were between 96 and 99 % identical to previously identified 16S rRNA sequences. No sequences from known chemoautotrophic bacteria were identified during the analysis, with the majority of sequences being classified in the family *Flavobacteriaceae* and *Rhodobacteraceae* (Table 5.1 & 5.2).

It was anticipated that the DGGE profiles generated from ^{13}C bicarbonate labelled DNA, would represented 16S rRNA genes from chemoautotrophic bacteria but in fact only sequences from heterotrophic bacteria were recovered. The data suggest that inorganic carbon uptake in this system was dominated by heterotrophic CO_2 fixation rather than autotrophic CO_2 fixation. This situation may have been promoted by the conditions under which the experiment was conducted. The experiment was designed to stimulate a phytoplankton bloom which influences both the structure and abundance of the bacterioplankton community by the release of DOM (dissolved organic matter) (Jensen, 1983). Consequently when the mesocosms were sub sampled into dark incubation bottles photosynthesis was inhibited and the phytoplankton released a readily utilizable carbon and energy source resulting in the enrichment of heterotrophic bacterial populations. In effect the experiment positively selected for microorganisms such as *Roseobacter* (*Alphaproteobacteria*) and *Flavobacteria* (*Bacteroidetes*) which frequently dominate dimethylsulphoniopropionate (DMSP) rich algal blooms (Pinhassi *et al.*, 2005; Garces *et al.*, 2007, Allgaier *et al.*, 2008) and as a consequence chemoautotrophic bacteria represented only a minor fraction of the total bacterial consortium. The relative low abundance of chemoautotrophic bacteria made them virtually undetectable using stable isotope probing as their DNA would have been totally overwhelmed by the labelled DNA derived from heterotrophic CO_2 fixation. As no chemoautotrophic bacteria were detected in the SIP analysis, the SIP DGGE profiles bore a high degree of

similarity to the DGGE profiles obtained from total genomic DNA extracted from the dark incubated bottles that were not subject to SIP analysis and density gradient fractionation (Chapter 4 section 4.3.1-4.3.2).

Table 5.1 Phylogenetic assignment of 16S rRNA gene clone libraries prepared from the ^{12}C CsCl fractions of the SIP experiment.

SIP fraction	*Representative sequence	Clone frequency	**Organism ID/nearest neighbour in NCBI	Identity	No of sequences
^{12}C High CO_2					
	H02	79.2%	Uncultured Bacteroidetes bacterium clone M0-Ar7-P2F03	99.0%	76
	E11	4.2%	Uncultured Flavobacteria bacterium clone MS056-2A	99.0%	4
	F12	2.1%	Uncultured Flavobacteria bacterium clone MS024-1F	99.0%	2
^{12}C Ambient CO_2					
	B07	40.6%	Uncultured Bacteroidetes bacterium clone M0-Ar7-P2F03	99.0%	39
	B03	18.8%	Uncultured Flavobacteria bacterium clone MS024-3C	99.0%	18
	D12	14.6%	Uncultured Bacteroidetes bacterium clone NABOS_FLbact44	99.0%	14
	B06	4.2%	Uncultured alpha proteobacterium clone M0-Ar2-P4F09	99.0%	4
	F02	3.1%	Uncultured Flavobacteria bacterium clone MS056-2A	98.0%	3
	C11	2.1%	Uncultured Flavobacteria bacterium clone MS024-3C	96.0%	2
	D01	2.1%	Uncultured Flavobacteria bacterium clone MS024-3C	99.0%	2

* Only groups containing two or more sequences were included in this analysis

** Sequences compared to Genbank nucleotide nr/nt database using the BLASTn program

Table 5.2 Phylogenetic assignment of 16S rRNA gene clone libraries prepared from the ^{13}C CsCl fractions of the SIP experiment.

SIP fraction	*Representative sequence	Clone frequency	**Organism ID/nearest neighbour in NCBI	Identity	No of sequences
^{13}C High CO_2					
	G05	19.7%	Uncultured alpha proteobacterium clone M0-Ar2-P4F09	99.1%	19
	D11	16.7%	Uncultured Bacteroidetes bacterium clone M0-Ar7-P2F03	99.0%	16
	B03	15.6%	Uncultured Rhodobacteraceae bacterium	99.0%	15
	H12	8.3%	*Sulfitobacter donghicola* strain DSW-25	99.6%	8
	C09	4.2%	Marine gamma proteobacterium HTCC2188	99.7%	4
	F07	3.1%	Uncultured gamma proteobacterium clone NABOS_SSPbact4	98.0%	3
	C10	2.1%	*Sulfitobacter* sp. NF1-26	99.5%	2
	G02	2.1%	Uncultured Flavobacteria bacterium clone MS056-2A	99.0%	2
^{13}C Ambient CO_2					
	H06	38.5%	Rhodobacteraceae bacterium IMCC1923	99.7%	37
	H02	19.8%	Uncultured alpha proteobacterium clone M0-Ar2-P4F09	99.0%	19
	G04	4.2%	Uncultured Bacteroidetes bacterium clone M0-Ar7-P2F03	99.0%	4
	D09	4.2%	Uncultured Flavobacteria bacterium clone MS024-3C	99.0%	4
	E01	3.1%	*Sulfitobacter donghicola* strain DSW-25	99.7%	3

* Only groups containing two or more sequences were included in this analysis

** Sequences compared to Genbank nucleotide nr/nt database using the BLASTn program

Analysis of 16S rRNA gene clone libraries obtained from total DNA from ^{12}C dark incubation bottles (Chapter 4, section 4.3.2) revealed that seawater from the ambient CO_2 treatment was dominated by members of the Flavobacteriaceae within the *Bacteroidete*s (62.4% of sequences; n =96) and the *Rhodobacteraceae* within the *Alphaproteobacteria* (21.5%; n =96), which was comparable with the known relative abundance of the marine *Roseobacter* clade in coastal waters of between 10– 25% (Beja *et al.*, 2002; Buchan *et al.*, 2005, Wagner-Dobler and Biebl, 2006, Brinkhoff *et al.*, 2008). By contrast, representation of the *Rhodobacteraceae* was substantially reduced in the high CO_2 treatment (2.4% of sequences; n =96).

As anticipated, the ^{12}C 16S rRNA gene clone SIP libraries were similar in composition to those of the total DNA libraries (Chapter 4, section 4.3.2) with members of the *Flavobacteriaceae* family dominating both the ^{12}C ambient and ^{12}C high CO_2 SIP libraries (79.2 and 85.5% respectively, n =96) (Table 5.1). The ^{12}C ambient CO_2 SIP library also contained a higher frequency of *Rhodobacteraceae* sequences (4.2%, n=96) compared to the ^{12}C high CO_2 SIP library (0%, n=96) consistent with previous results. Surprisingly, the ^{13}C 16S rRNA gene clone SIP libraries were dominated by *Rhodobacteraceae* both in the ^{13}C ambient and ^{13}C high CO_2 treatments with 61.4% and 45.7% of sequences respectively (n =96), suggesting that this particular group may play an important role in the assimilation of inorganic carbon (Table 5.2). By contrast, sequences from *Flavobacteriaceae* represented 8.4% of the clones in the ^{13}C ambient CO_2 SIP library and 18.8% in the ^{13}C high CO_2 SIP library. Representatives of the *Gammaproteobacteria* were also observed in the ^{13}C high CO_2 SIP library (7.3% of sequences, n =96).

5.3.3 Phylogenetic analysis of 16S rRNA sequences recovered from total SIP fractions

Prior to phylogenetic analysis, sequences from the SIP clone libraries were screened for chimeras using Mallard (Ashelford *et al.*, 2006). One chimeric sequence was identified during this analysis and therefore eliminated from further analyses. The sequences from each library were then grouped and dereplicated using the FastGroupII program (Yu *et al.*, 2006) and a representative sequence from each defined bacterial

group was used to produce a 16S rRNA phylogenetic tree. The phylogenetic analysis revealed that out of the 136 sequences obtained from the ^{13}C SIP fractions, 81% (110 sequences) were attributed to the phylum *Proteobacteria* and 19% (26 sequences) to *Flavobacteria* within the phylum *Bacteroidetes* (Figure 5.9). Whereas 164 sequences were obtained from the ^{12}C SIP fractions of which 2.5% (4 sequences) were assigned to the *Proteobacteria* and 97.5% (160 sequences) were assigned to *Flavobacteria*. Furthermore, out of the total number of sequences assigned to the *Proteobacteria* (both $^{13}C/^{12}C$) 96.5% (110 sequences) were from the ^{13}C fractions whereas only 14% (26 sequences) of the *Flavobacteria* sequences were derived from the ^{13}C fractions (Figure 5.9).

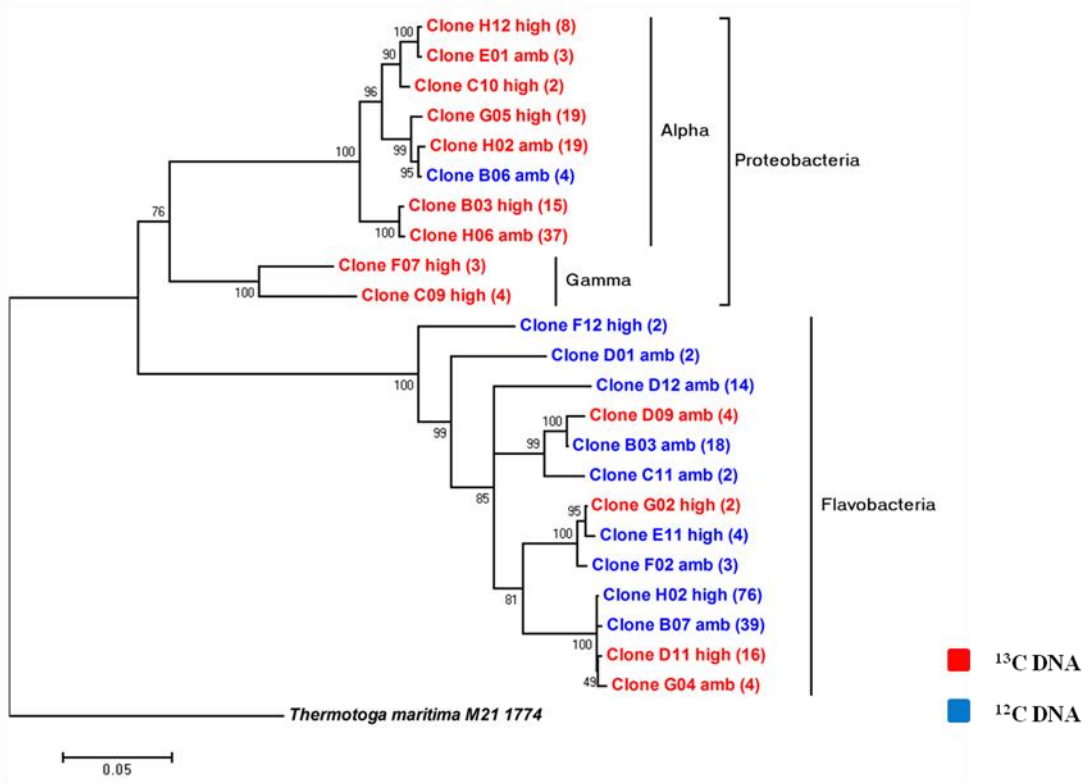

Figure 5.9 Phylogenetic association of 16S rRNA sequences recovered from different SIP fractions recovered from the ambient and high CO_2 dark incubations. Sequences from ^{13}C SIP fractions are denoted by red text with sequences from the ^{12}C SIP fractions in blue. The number of reads assigned to each group is given in brackets. The analysis was conducted in MEGA4 using the Neighbour –joining method together with a bootstrap value inferred from a 1000 replicates. *Thermotoga maritima* M21774 was used as an outgroup to root the tree.

To determine if there was a significant association between bacterial phyla (*Proteobacteria*, *Bacteroidetes*) and different DNA fractions (^{13}C and ^{12}C) a Fisher's exact test was performed. This test is used to establish if there are non-random associations between two categorical variables. In this instance the null hypothesis (no association between the DNA fraction and the phyla observed) was rejected ($P = < 0.01$) indicating that there was a significant relationship between bacterial phylum and carbon isotope label. These results strongly implicate the *Proteobacteria* in heterotrophic CO_2 fixation due to the fact that the composition of 16S rRNA gene clone libraries from ^{13}C DNA SIP fractions was strongly skewed towards this group. It is uncertain why this significant difference was not observed in the DGGE analysis though the possibility of bias in primers 2 and 3 while amplifying the variable V3 region the16S rRNA gene was considered as this primer set was not used in the construction of the clone libraries.

To ascertain if this primer set favoured either *Rhodobacteraceae* or *Flavobacteriaceae* the oligonucleotide sequences were input into the probe match facility of the Ribosomal Database Project (RDP). The results revealed this primer set targeted 25,453 out of a possible 31,039 *Flavobacteriaceae* and 16,032 out of a possible 21,481 *Rhodobacteraceae* 16S rRNA sequences. Though it is clear that these primers target a slightly lower proportion of *Rhodobacteraceae* sequences the numbers alone are meaningless unless we know which species they do not target. Therefore the full length 16S rRNA *Rhodobacteraceae* sequences identified from the 16S rRNA clone libraries were downloaded from the RDP database to confirm that each sequence contained both binding sites. The analysis revealed that all sequences identified contained both binding sites for primers 2 and 3 and consequently no bias of this nature could have been observed in the DGGE gels.

5.3.4 Phylogenetic analysis of 16S rRNA sequences recovered from ^{13}C DNA

A more detailed phylogenetic analysis was conducted to assign the sequences at higher phylogenetic resolution (Figure 5.10). The tree included the 16S rRNA sequences from representative members of the *Proteobacteria* and *Bacteroidetes* obtained from the Ribosomal Database Project (RDP) (Cole *et al.*, 2009). The analysis established that the

majority of sequences retrieved from the ^{13}C ambient CO_2 SIP library were affiliated to *Rhodobacteraceae* with the most abundant group being most closely related to *Oceanicola granulosus* (37 sequences) followed by sequences closely related to *R. denitrificans/R. litoralis* (22 sequences). The *Rhodobacteraceae* also dominated the ^{13}C high CO_2 SIP library (though to a lesser extent) with sequences closely related to R. denitrificans/R. litoralis (29 sequences) being the most abundant followed by *O. granulosus* (15 sequences). Seven sequences from the ^{13}C High CO_2 SIP clone library were affiliated to the class *Gammaproteobacteria*. These were most closely related to the recently identified aerobic anoxygenic phototrophic (AAnP) bacteria *Congregibacter litoralis* (Spring *et al.*, 2009). In fact, sequences closely related to known AAnPs represented 30.2% of the total ^{13}C SIP reads of which 36 sequences were from the ^{13}C high CO_2 SIP library and 22 sequences were from the ^{13}C ambient CO_2 SIP library. In contrast, sequences closely related to known AAnPs only represented (2.1%, 4 sequences) of the total ^{12}C sequences, all of which were from the ambient CO_2 SIP library.

Sequences from the *Flavobacteriaceae* in the phylum *Bacteroidetes* were also recovered from the ^{13}C fractions that showed a weak affiliation to *Dokdonia donghaensis*, (24 sequences). Although quite distinct from *Dokdonia*, the majority of all the *Flavobacteriaceae*-like sequences (both ^{13}C and ^{12}C) were in two main clades, designated as *Dokdonia* clade A and clade B (Figure 5.10). In the ^{13}C high CO_2 SIP library 16 sequences were associated to *Dokdonia* clade B while in the ^{13}C ambient CO_2 SIP library 4 sequences were assigned to *Dokdonia* clade B and 4 sequences assigned to *Dokdonia* clade A. The only other *Flavobacteriaceae* sequences recovered from the ^{13}C SIP fractions were from the high CO_2 SIP library which were affiliated to *Ulvibacter litoralis* (2 sequences).

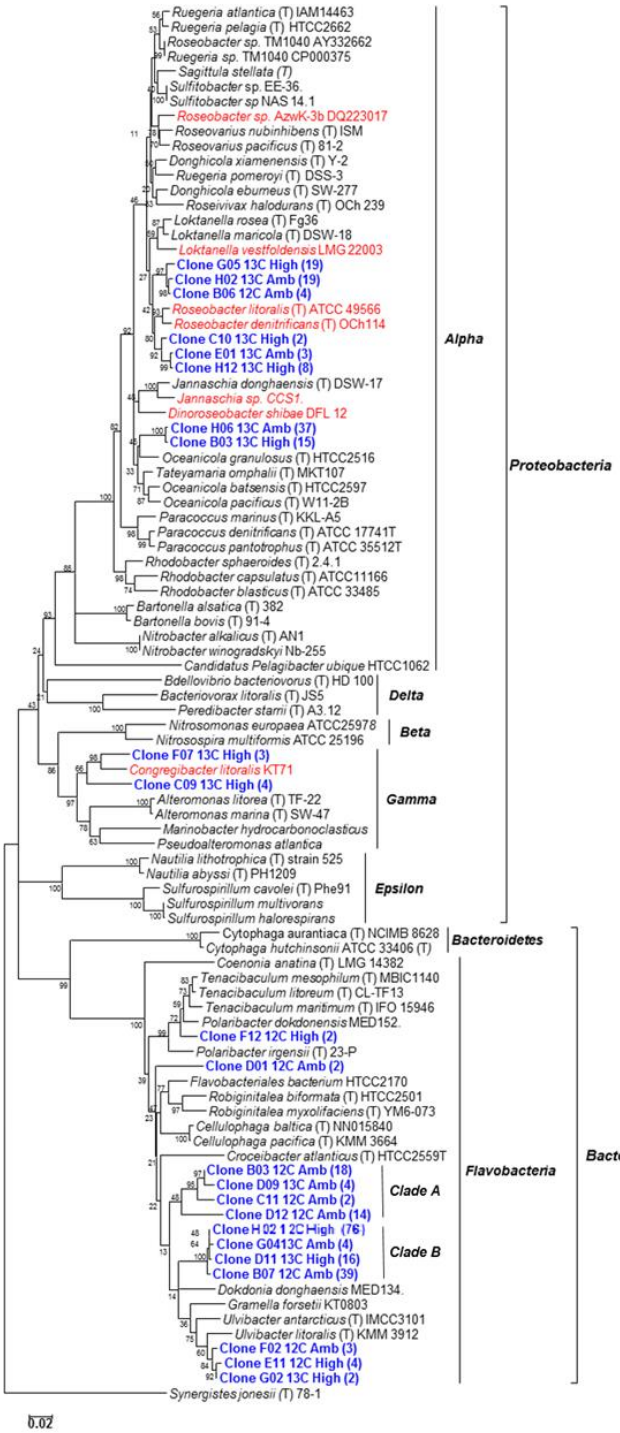

Figure 5.10 Neighbour-joining tree based on partial 16S rRNA gene sequences obtained from SIP clone libraries and full length 16S rRNA sequences from the RDP database. Each sequence (denoted in blue) is representative of a particular group with all groups representing two or more sequences. The total number of reads assigned to each group is indicated in brackets. Aerobic Anoxygenic Phototrophs (AAnPs) are denoted in red. The tree was constructed in MEGA4 with bootstrap value inferred from 1000 replicates with evolutionary distances computed using the Maximum Composite Likelihood method.

5.3.5 Phylogenetic analysis of 16S rRNA sequences recovered from ^{12}C DNA

Libraries from the ^{12}C DNA SIP fractions were dominated by sequences from the *Flavobacteriaceae* which accounted for 85% of the sequences in the high CO_2 and 81% in the ambient CO_2 library. The ambient CO_2 library comprised sequences related to *Dokdonia* clade B (39 sequences) and *Dokdonia* clade A (34 sequences) followed by *U. litoralis*, (3 sequences) and *Flavobacteriales* HTCC2170 (2 sequences). The *Rhodobacteraceae* were represented by only 1 sequence type in this library which was most closely related to the AAnP *R. denitrificans*/*R. litoralis* (4 sequences). In the ^{12}C high CO_2 SIP library, no sequences were observed in *Dokdonia* clade A but 76 sequences closely associated to *Dokdonia* clade B. The remaining sequences in this library were related to *U. litoralis* (4 sequences) and *Polaribacter donghaensis* (2 sequences). No sequences related to the *Rhodobacteraceae* were detected in the ^{12}C high CO_2 library.

It is unclear why the frequency of sequences related to clade B were greater in the ^{12}C high CO_2 SIP library than its ambient counterpart though a similar pattern was observed in the ^{13}C SIP libraries. In this instance four sequences were assigned to *Dokdonia* clade B from the ^{13}C ambient CO_2 SIP library whereas 16 sequences were assigned from the^{13}C high CO_2 SIP library. Although these apparent differences may be attributed to the small sample size rather than a treatment effect, there does seem to be a tentative relationship between *Flavobacteria* observed in clade B and their ability to tolerate elevated CO_2/reduced pH.

5.3.6 Factors potentially relevant to the dominance of Flavobacteriaceae in ^{12}C SIP fractions

Analysis of the genomes of members of the *Flavobacteriaceae* identified in the 16S rRNA gene clone libraries (section 5.3.4 and 5.3.5) revealed the presence of proteorhodopsin genes in both *D. donghaensis* and *P. dokdonensis/irgensii. Proteorhodopsin is a* retinal containing membrane protein that functions as a light-driven proton pump to generate energy. The absorption of light causes a conformational change which transports a proton across the membrane resulting in electrochemical membrane

potential that drives ATP synthesis (DeLong and Béjà, 2010). Growth experiments conducted in natural and artificial seawater have established an increase in cell yield of *D. donghaensis* when exposed to the light in comparison to the dark (Gomez-Consarnau *et al*., 2007). The authors speculated that the advantages of proteorhodopsin might be more pronounced when bacterial growth was limited by organic matter.

The research was furthered several years later this time using a member of the *Gammaproteobacteria Vibrio* sp. AND4 which is believed to have obtained proteorhodopsin via lateral gene transfer (Gómez-Consarnau *et al.*, 2010). It was demonstrated that proteorhodopsin improved the survival of bacteria during periods of starvation when after day 10 of the experiment bacterial cell numbers were 2.5 times higher in the light compared to the dark. Due to the fact that the strain was amenable to genetic manipulation an AND4 knockout mutant was created with the function of the proteorhodopsin gene removed (AND4 Δ*prd*). In starvation experiments the *Δprd* strain showed no differences in bacterial cell numbers in either the light or dark. However, when the function of the gene was restored via the expression of the gene on a plasmid it regained its wild type phenotype and on starvation maintained higher cell numbers in the light. These results strongly suggest that photoheterotrophy via proteorhodopsins is advantageous to bacteria in a competitive environment as it permits growth even when the concentration of organic matter is declining or is extremely scarce.

This could in part explain the increase in the number of sequences related to *D. donghaensis* in the high CO_2 libraries. Bacterial production in the ocean is regulated by the release of DOM from phytoplankton and by the sloppy feeding of zooplankton (Azam *et al.*, 1983, Fuhrman, 1992). It has been demonstrated during this investigation that elevated CO_2 had a detrimental effect on some phytoplankton species (Chapter 3 section 3.4) reducing the concentration of DOM. The environment was therefore suitable for the proliferation of *D. donghaensis* but for one exception, the bottles were dark and therefore little or no sunlight should have been able to penetrate the container to facilitate phototrophy. In essence the presence of a proteorhodopsin gene should have had no selective advantage in *D. donghaensis* as the resulting enzyme could not have been activated.

5.3.7 Substrate incorporation of heterotrophic bacterioplankton

It was anticipated that members of the *Flavobacteriaceae* would be dominant in the experimental mesocosms following the phytoplankton bloom. *Flavobacteriaceae* like the *Rhodobacteraceae* are heterotrophic and depend on organic compounds for carbon and for most of their energy. However, *Rhodobacteraceae* are specialised to process low molecular weight DOM (Moran *et al.*, 2003, Alonso *et al.*, 2007) while *Bacteroidetes* utilize high molecular weight DOM (Kirchman, 2004, Teira *et al.*, 2008) which is likely to be in abundance after the collaspe of algal blooms due to increased relase of organic exudates. *Bacteroidetes* related species (formerly known as the *Cytophaga-Flavobacteria-Bacteroidetes* (CFB) phylum) include major taxa of marine bacterioplankton which are known to increase in abundance during the decay of algal blooms (Pinhassi *et al.*, 2004, Fandino *et al.*, 2005). They have clear adaptations to the degradation of high molecular weight organic matter including a suite of genes encoding hydrolytic enzymes and a predicted preference for polymeric carbon sources (Bauer *et al.*, 2006, González *et al.*, 2008). Both *Flavobacteriaceae* and *Rhodobacteraceae* seem to be well adapted to respond rapidly to the various phases of phytoplankton development during a bloom though each occupies a particular niche with respect to their lifestyle and preferred carbon sources. Generally *Flavobacteriaceae* can utilize cellulose and chitin whereas *Rhodobacteraceae* are actively involved in sulfur cycling utilizing DMSP both as a carbon and sulfur source. This was demonstrated by Cottrell and Kirchman (2000) when they examined the uptake of DOM by microbial assemblages from the Delaware Bay estuary. Using a technique known as MICRO-FISH (Lee *et al.*, 1999) they were able to show that bacteria belonging to the *Cytophaga-Flavobacter* cluster were the most abundant microbes utilizing chitin and protein (high molecular weight) whereas the *Alphaproteobacteria* were the largest fraction utilizing low molecular weight amino acids (Cottrell and Kirchman, 2000). A recent study into bacterioplankton community composition has indicated that *Bacteroidetes* comprised up to 63% of the prokaryotic community at the senescent stage of a phytoplankton bloom (Teira *et al.*, 2008). The conditions in the system studied by Teira et al. (2008) would have been similar to those in the dark incubation bottles as phytoplankton decay would

have commenced almost immediately after the water samples were added to the dark incubation bottles.

It is therefore proposed that *Flavobacteriaceae* had a selective advantage in the dark incubation bottles as the absence of light would hasten phytoplankton senescence and decay. Bacterial succession due to algal derived decomposition has been observed in the North Sea in which the relative abundances of specific *Flavobacteria* were found to peak after a phytoplankton bloom while the *Roseobacter* clade remained relatively constant (Teeling *et al.*, 2012). However, heterotrophic *Flavobacteriaceae* have not been known to fix CO_2 despite *Dokdonia* sp. MED134 containing an unexpected number of enzymes involved in anaplerotic metabolism (González *et al.*, 2011). This may account for their dominance in the ^{12}C SIP libraries whereas, a CO_2 assimilation pathway has been proposed for the alphaproteobacterium *Roseobacter denitrificans* (Swingley *et al.*, 2007).

5.3.8 Dominance of Rhodobacteraceae in ^{13}C SIP fractions

A close correlation has been established between the abundance of *Roseobacter*-related species and dissolved DMSP (DMSPd) turnover in the ocean (Zubkov *et al.*, 2001). During the course of this investigation it was observed that elevated CO_2/reduced pH had a detrimental effect in some phytoplankton species resulting in lower DMSP concentration and a decrease in *Rhodobacteraceae* numbers (Chapter 3 section 3.3-3.4, Chapter 4 section 4.3) (Hopkins *et al.*, 2009). DMSPd can fulfil up to 95% of the reduced sulfur demand and 15% of the carbon demand in bacterioplankton communities and as a consequence *Roseobacter* species have evolved to efficiently turnover DMSPd at a rate of 4 – 6 times per day (Zubkov *et al.*, 2001). In the incubations such a rapid turnover would quickly deplete DMSP in comparison to the higher molecular weight DOM utilized by the *Flavobacteriaceae* and as a consequence *Rhodobacteraceae* species would have to switch to alternate carbon sources.

The abundance of sequences from *Rhodobacteraceae* in both the high and ambient ^{13}C SIP libraries (45 and 61% respectively) provides compelling evidence that

they are able to assimilate inorganic carbon. How and why this mechanism has evolved remains to be answered but there is now persuasive experimental evidence coupled with the release of new bacterial genomes that strongly suggests this unique group of bacteria are able to fix inorganic carbon to a greater extent than previously thought.

5.3.9 Anaplerotic enzymes from Rhodobacteraceae identified by metagenome analysis

As previously stated, no metagenomic analysis was conducted on the actual SIP fractions of the dark incubation experiment. However, a subset of the total DNA metagenomes (ambient/high CO_2) comprising only those sequences assigned to the *Rhodobacteraceae* was constructed *in silico* using MG-RAST (Meyer *et al.*, 2008). The *Rhodobacteraceae* metagenome from the ambient CO_2 incubations comprised 3,114 sequences with an average read length of 245 bp, whereas the *Rhodobacteraceae* metagenome from the high CO_2 incubations comprised 1,102 sequences also with an average read length of 245 bp. The sequences from both datasets were uploaded to the KEGG Automatic Annotation Server (KAAS) to provide functional annotation of genes by BLAST comparisons against the manually curated KEGG gene database (Moriya *et al.*, 2007). Both datasets contained partial sequences homologous to genes associated with anaplerotic CO_2 assimilation (Table 5.3). The *Rhodobacteraceae* dataset from the ambient CO_2 incubations contained 14 anaplerotic sequences; 6 sequences encoding pyruvate carboxylase, (EC 6.4.1.1) 5 sequences for malic enzyme, (EC 1.1.1.40) 2 sequences for PEP carboxykinase, (EC4.1.1.49) and 1 sequence for PEP carboxylase (EC 4.1.1.31). The *Rhodobacteraceae* dataset from the high CO_2 incubations contained 5 anaplerotic sequences; 2 sequences encoding for malic enzyme, (EC 1.1.1.40) 2 sequences for pyruvate carboxylase (EC 6.4.1.1) and 1 PEP carboxylase sequence (EC 4.1.1.31). To validate these assignments the sequences from both datasets were compared against the GenBank database using BLASTX. The results were in complete agreement with the KAAS assignments with percent identities ranging from 63 – 100% (Appendix 1, alignments). The percentage of anaplerotic sequences from the *Rhodobacteraceae* high and ambient CO_2 treatments was exactly the same at 0.45% and despite the low sample size (0.76 Mb ambient CO_2, 0.27 Mb high CO_2) all four anaplerotic genes were represented.

5.3.10 Anaplerotic enzymes from Flavobacteriaceae identified by metagenome analysis.

A similar analysis was conducted on *Flavobacteriaceae* datasets which were also obtained from the total DNA metagenomes using MG-RAST. The ambient *Flavobacteriaceae* dataset contained 1,961 sequences with an average read length of 260 bp and a total sequence length of 0.51Mb, while the high CO_2 dataset contained 7,281 sequences with an average read length of 257 bp and a total sequence length of 1.9 Mb. Both datasets were annotated using KAAS and the resulting assignments verified via BLAST analysis against the GenBank database (Appendix 1). Only 2 anaplerotic gene sequences were observed in the ambient *Flavobacteriaceae* dataset, (Table 5.3) malic enzyme (EC1.1.1.40) and PEP carboxylase (EC 4.1.1.31). The high *Flavobacteriaceae* dataset contained 10 sequences; 3 malic enzyme, (EC 1.1.1.40) 3 PEP carboxykinase, (EC 4.1.1.49) 3 pyruvate carboxylase (EC 6.4.1.1) and 1 PEP carboxylase sequence (EC 4.1.1.31). Similar to the *Rhodobacteraceae* datasets, the percentage of anaplerotic sequences from each treatment was highly similar, accounting for 0.1% of the sequences in the ambient CO_2 metagenome and 0.14% of the sequences in the high CO_2 metagenome.

Table 5.3 Phylogenetic assignments obtained from MG-RAST of anaplerotic enzymes observed in the *Rhodobacteraceae* and *Flavobacteriaceae* subsets of the total DNA metagenomes.

Metagenome subset	Alignment Length (aa)	Identity	*Functional Role Assignment	Organism
Rhodobacteraceae **ambient CO_2**				
	78	82%	Malic enzyme (EC 1.1.1.40)	*Oceanibulbus indolifex* HEL-45
	60	83%	Malic enzyme (EC 1.1.1.40)	*Roseobacter* sp. SK209-2-6
	57	81%	Malic enzyme (EC 1.1.1.40)	*Ruegeria pomeroyi* DSS-3
	50	82%	Malic enzyme (EC 1.1.1.40)	*Silicibacter* sp. TrichCH4B
	86	87%	Malic enzyme (EC 1.1.1.40)	*Silicibacter* sp. TrichCH4B
	85	76%	PEP carboxykinase (EC 4.1.1.49)	*Roseobacter* sp. MED193
	53	79%	PEP carboxykinase (EC 4.1.1.49)	*Roseobacter* sp. SK209-2-6
	83	59%	Pyruvate carboxylase (EC 6.4.1.1)	*Roseobacter denitrificans* OCh 114
	82	85%	Pyruvate carboxylase (EC 6.4.1.1)	*Roseobacter* sp. AzwK-3b
	73	96%	Pyruvate carboxylase (EC 6.4.1.1)	*Roseobacter* sp. GAI101
	80	91%	Pyruvate carboxylase (EC 6.4.1.1)	*Roseovarius* sp. TM1035
	85	94%	Pyruvate carboxylase (EC 6.4.1.1)	*Rhodobacteraceae* bacterium KLH11
	83	89%	Pyruvate carboxylase (EC 6.4.1.1)	*Loktanella vestfoldensis* SKA53
	80	63%	PEP carboxylase EC 4.1.1.31)	*Rhodobacterales* bacterium Y4I
Rhodobacteraceae **high CO_2**				
	85	89%	Malic enzyme (EC 1.1.1.40)	*Ruegeria* sp. TM1040
	71	90%	Malic enzyme (EC 1.1.1.40)	*Paracoccus* sp. N5
	74	95%	Pyruvate carboxylase (EC 6.4.1.1	*Rhodobacter sphaeroides* ATCC 17025
	89	100%	Pyruvate carboxylase (EC 6.4.1.1)	*Rhodobacterales* bacterium HTCC2255
	72	78%	PEP carboxylase EC 4.1.1.31)	*Rhodobacterales* bacterium HTCC2083
Flavobacteriaceae **ambient CO_2**				
	84	99%	Malate dehydrogenase EC 1.1.1.40	*Flavobacteria* bacterium MS024-3C
	81	72%	PEP carboxylase (EC4.1.1.31)	*Flavobacteriales* bacterium ALC-1
Flavobacteriaceae **high CO_2**				
	62	97%	Malate dehydrogenase EC 1.1.1.40	*Flavobacterium* psychrophilum
	82	79%	Malate dehydrogenase EC 1.1.1.40	*Flavobacteria* bacterium MS024-3C
	77	79%	Malate dehydrogenase EC 1.1.1.40	*Flavobacteria* bacterium MS024-3C
	92	85%	PEP carboxykinase (EC 4.1.1.49)	*Croceibacter atlanticus* HTCC2559
	87	76%	PEP carboxykinase (EC 4.1.1.49)	*Dokdonia donghaensis* MED134
	84	94%	PEP carboxykinase (EC 4.1.1.49)	*Maribacter* sp. HTCC2170
	89	83%	Pyruvate carboxylase (EC 6.4.1.1)	*Dokdonia donghaensis* MED134
	89	83%	Pyruvate carboxylase (EC 6.4.1.1)	*Dokdonia donghaensis* MED134
	100	82%	Pyruvate carboxylase (EC 6.4.1.1)	*Flavobacteriales bacterium* ALC-1
	98	85%	PEP carboxylase (EC 4.1.1.31)	*Polaribacter irgensii* 23-P

* Sequences compared to the GenBank database using BLASTX program

5.3.11 Analysis of anaplerotic enzymes

A cursory examination of the metagenomic subsets revealed that the majority of anaplerotic gene sequences were derived from members of the marine *Roseobacter* clade of *Rhodobacteraceae*. The total size of the *Rhodobacteraceae* datasets in base pairs (ambient and high CO_2) equalled ~1 Mb in which a total of 19 partial anaplerotic gene sequences were observed. In contrast, the *Flavobacteriaceae* datasets contained 2.4 Mb

of sequence data in which 12 partial anaplerotic gene sequences were observed. This equates to an anaplerotic gene sequence every 0.05 Mb in the *Rhodobacteraceae* dataset and approximately every 0. 2 Mb in the *Flavobacteriaceae* dataset. The reproducibility of the relative percentages of anaplerotic sequences in both treatments strongly suggests that the *Rhodobacteraceae* consortium has at least the potential to assimilate more inorganic carbon due to the increased number of anaplerotic enzymes observed in the datasets. Statistically, no significant difference was observed in the number of anaplerotic sequences assigned to the *Rhodobacteraceae* and *Flavobacteriaceae* subsets of the metagenomes (P=0.287; G-test) (Figure 5.11A). However, taken individually a significant difference was observed in the number of pyruvate carboxylase sequences assigned to each dataset (P=0.01; G-test) with malic enzyme sequences showing a slight difference (P=0.052; G-test) at the 95% confidence level (Figure 5.11B).

It is also worth emphasising that the metagenomes are libraries consisting of thousands of DNA sequences and while they can provide information regarding the genomic potential of a microbial community they cannot provide information as to how the potential changes in response to environmental forces. Therefore this analysis cannot reveal if the expression of anaplerotic genes alters in response to the decrease in pH.

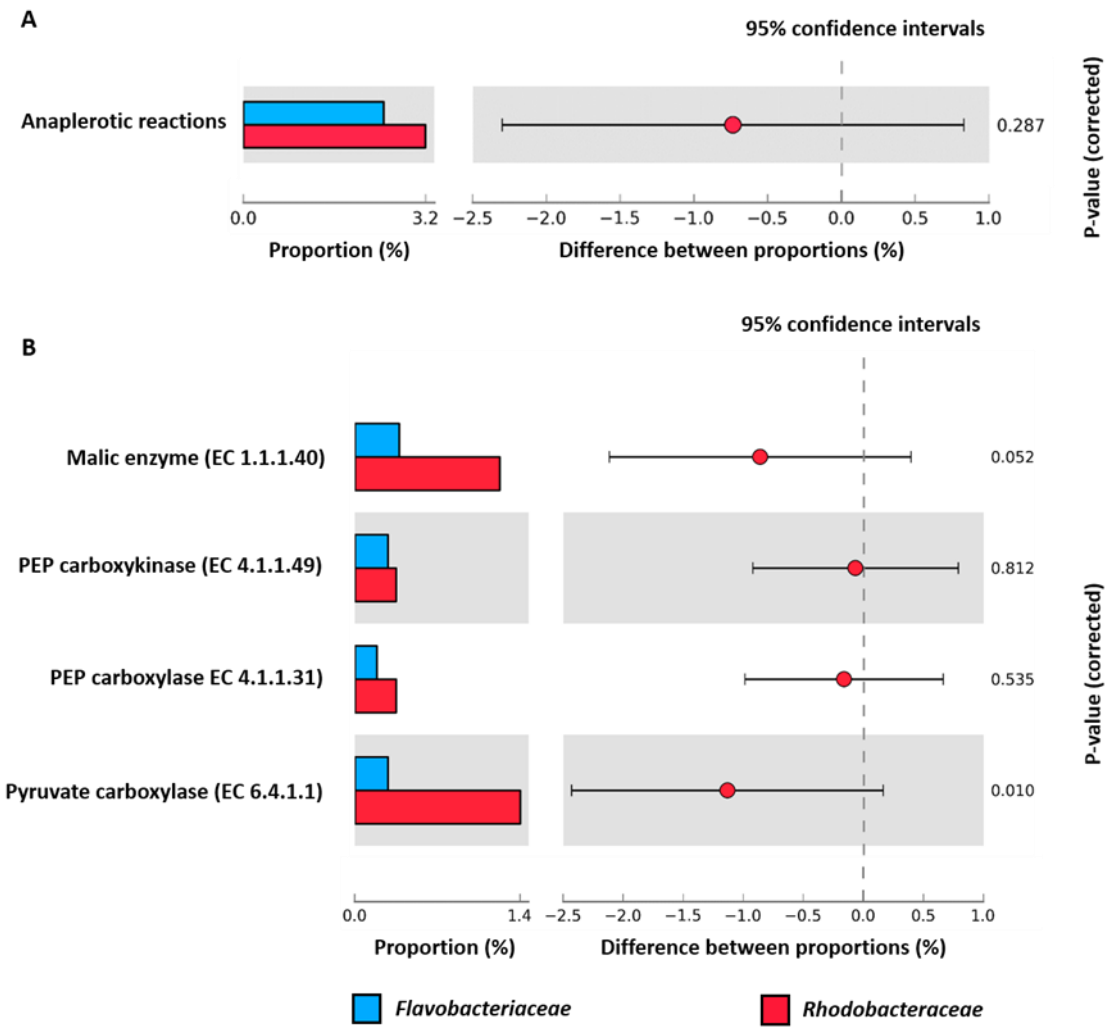

Figure 5.11 G-test conducted in STAMP showing the overrepresentation of anaplerotic sequences (A) and the overrepresentation of individual anaplerotic enzymes (B) in two metagenomic datasets.

5.3.12 Analysis of pyruvate carboxylase sequences

Comparative analysis of pyruvate carboxylase aa sequences revealed a distinct difference between the two groups of sequences. On average, the *Flavobacteriaceae* aa sequences were 49% identical to *R. denitrificans*, whereas the *Rhodobacteraceae* aa sequences were 82% identical.

Phylogenetic analysis revealed a grouping of the pyruvate carboxylases in the *Rhodobacteraceae* sequences which was distinct from that of the *Flavobacteriaceae*, thereby partly supporting the statement of Swingley *et al* (2007) that marine *Roseobacter*

pyruvate carboxylases form monophyletic clusters which are distinct from those from closely related species (Swingley *et al.*, 2007). Furthermore, phylogenetic analysis of pyruvate carboxylase sequences retrieved from the ambient and high CO_2 metagenomes placed the sequences in the correct phylogeny (3 sequences *Flavobactriaceae* and 7 sequences *Rhodobacteraceae*) despite their short sequence length.

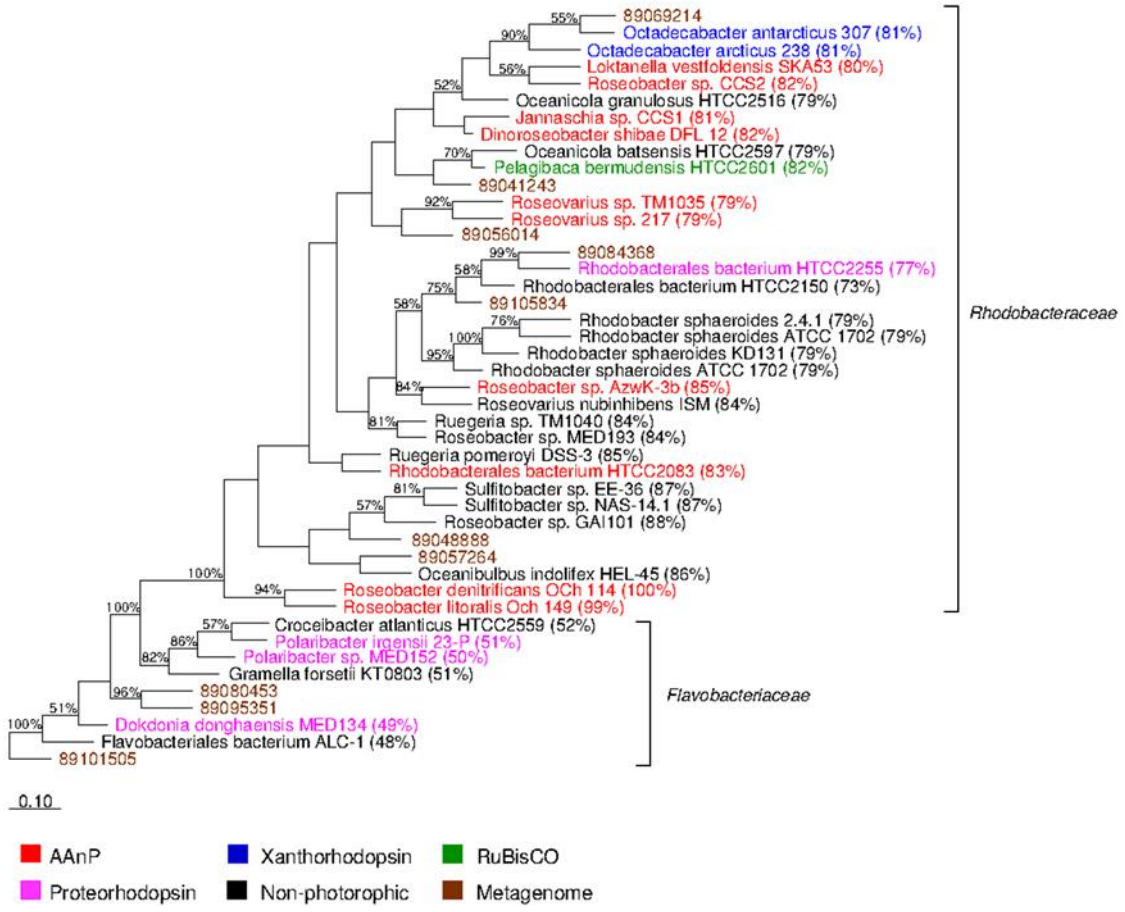

Figure 5.12 Phylogenetic analysis of pyruvate carboxylase amino acid sequences from phototrophic and non-phototrophic members of the *Flavobacteriaceae* and *Rhodobacteraceae*. Each sequence was compared against Roseobacter denitrificans OCH 114 pyruvate carboxylase with the resulting percentage identity next to each sequence in brackets. The tree is colour coded showing the photosynthetic pigment or the presence of RuBisCO used in photosynthesis along with pyruvate carboxylase sequences retrieved from the metagenomes. The evolutionary history was inferred by the Phylip maximum-likelihood method (Phylip PROML) and the tree is drawn to scale with branch lengths measured in the number of substitutions per site. Evolutionary analysis was conducted in ARB and the bootstrap consensus tree was inferred from 500 replicates.

5.3.13 Genome mapping of the metagenome subsets

The phylogenetic profiles of the datasets determined by MG-RAST revealed that the majority of the sequences from the *Rhodobacteraceae* datasets were assigned to *R. denitrificans* OCh 114 (473 sequences ambient, 209 sequences high) whereas the majority of the sequences from the *Flavobacteriaceae* datasets were assigned to *Dokdonia donghaensis* MED134 (202 sequences ambient CO_2, 1,324 sequences high CO_2). Recruitment plots to determine the overall sequence coverage were constructed which mapped the phylogenetic assigned sequences from the datasets on to its affiliated genome. Only the datasets that contained the highest number of anaplerotic sequences from each bacterial family were used in this analysis resulting in 473 sequences being mapped onto the *R. denitrificans* genome and 1,324 sequences being mapped onto the *D. donghaensis* genome. The results revealed that the coverage of *R. denitrificans* OCh 114 was 0.008X (Figure 5.13) while the coverage of *D. donghaensis* MED134 was 0.029X (Figure 5.14).

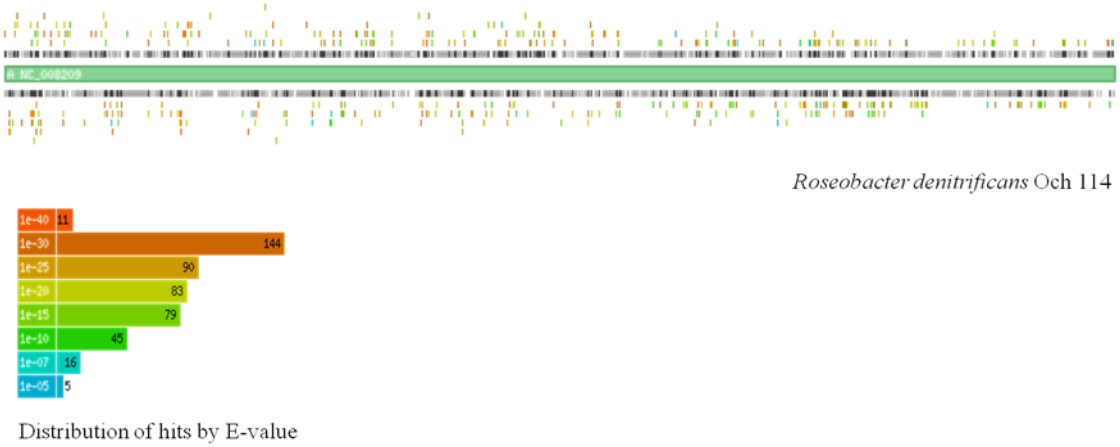

Figure 5.13 Recruitment Plot from *Rhodobacteraceae* ambient CO_2 dataset with the sequences mapped on to the *Roseobacter denitrificans* OCh 114 genome. 473 sequences map to 386 of 4,032 features from the *Roseobacter denitrificans* OCh 114 genome. The total base pair length of all sequences mapping to this genome in *Rhodobacteraceae* ambient CO_2 dataset is 34,462 bp, resulting in approximately 0.008X coverage. The reference genome *Roseobacter denitrificans* OCh 114 contains 1 contig(s) and is 4.1 Mb.

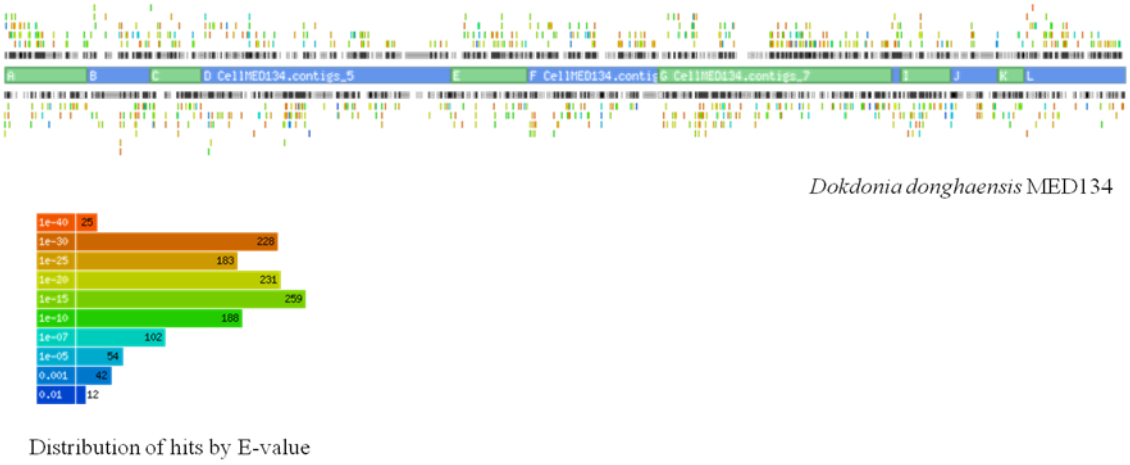

Figure 5.14 Recruitment Plot from *Flavobacteriaceae* high CO_2 dataset with the sequences mapped on to the *Dokdonia donghaensis* MED134 genome. 1,324 sequences map to 652 of the 3,026 features from the *Dokdonia donghaensis*. MED134 genome. The total base pair length of all sequences mapping to this genome in *Flavobacteriaceae* high CO_2 dataset is 94,914 bp, resulting in approximately 0.029X coverage. The reference genome *Dokdonia donghaensis* MED134 contains 17 contigs and is 3.3 Mb.

5.4 Photoheterotrophy in the dark incubation bottles

Examination of genome sequences from species most closely related to those identified in the 16S rRNA sequence analysis (Figure 5.10) revealed that they possessed genes for phototrophy (Table 5.4). Photoheterotrophy may provide a selective advantage over a strictly heterotrophic lifestyle in that less organic carbon would be oxidised to yield energy if it was supplemented by energy harvested by light. It has been speculated by Zubkov (2009) that as well as being used for photophosphorylation, (ATP production) sunlight may also be used to power flagella or import molecules into the cell (Zubkov, 2009). This has been proven by Walter *et al* (2007) when they demonstrated that light driven proton pumping via proteorhodopsin can sufficiently supplement the energy requirement to power cell motility (Walter *et al.*, 2007).

The fact that there were more sequences associated with phototrophy in the high CO_2 incubations seems to suggest that this attribute may have a selective advantage in elevated CO_2 conditions. Analysis of datasets from the ambient and high CO_2 treatments containing only *Rhodobacteraceae* and *Flavobacteriaceae* species revealed that there

was no significant difference (P=1.00; G-test) in the number of sequences assigned to photosynthesis between the ambient and high CO_2 treatments (Figure 5.15A). However, the method of phototrophy differed between the treatments which is indicative of changes in bacterial species composition (Figure 5.15B). The ambient CO_2 dataset contained significantly more sequences attributed to type II photosynthetic reaction centre (P=0.005; G-test) which is part of the photosynthetic apparatus of AAnPs (Yurkov and Csotonyi, 2008, Yutin *et al.*, 2009). In contrast, the high CO_2 dataset contained significantly more sequences attributed to proteorhodopsin, (P=0.02; G-test) a retinal based photoreceptor in which light stimulated growth has been observed in the flavobacterium *Dokdonia donghaensis* MED134 (Gomez-Consarnau *et al.*, 2007). In this instance, the change in metabolic strategy from chlorophyll to non–chlorophyll-based phototrophy is indicative of a decrease in *Rhodobacteraceae* numbers in the high CO_2 treatment that has been observed throughout this study.

Table 5.4 Phylogenetic assignments of SIP sequences indicating organisms which possess phototrophic metabolism.

Library	Nearest neighbour in phylogenetic tree	Phototrophy	Number of sequences
^{13}C High CO_2			
	Roseobacter denitrificans sp. OCh114	Bacteriochlorophyll-a	29
	Dokdonia donghaensis MED134 (clade B)	Proteorhodopsin	16
	Oceanicola granulosus HTCC2516	None	15
	Congregibacter litoralis KT71	Bacteriochlorophyll-a	7
	Ulvibacter litoralis	None	2
^{13}C Ambient CO_2			
	Oceanicola granulosus HTCC2516	None	37
	Roseobacter denitrificans sp. OCh114	Bacteriochlorophyll-a	22
	Dokdonia donghaensis MED134 (clade A)	Proteorhodopsin	4
	Dokdonia donghaensis MED134 (clade B)	Proteorhodopsin	4
^{12}C High CO_2			
	Dokdonia donghaensis MED134 (clade B)	Proteorhodopsin	76
	Roseobacter denitrificans sp. OCh114	Bacteriochlorophyll-a	4
	Ulvibacter litoralis	None	4
	Polaribacter irgensii 23-P	Proteorhodopsin	2
^{12}C Ambient CO_2			
	Dokdonia donghaensis MED134 (clade A)	Proteorhodopsin	39
	Dokdonia donghaensis MED134 (clade B)	Proteorhodopsin	34
	Ulvibacter litoralis	None	3
	Flavobacteriales bacterium HTCC2170	None	2

* Only groups containing two or more sequences were included in this analysis

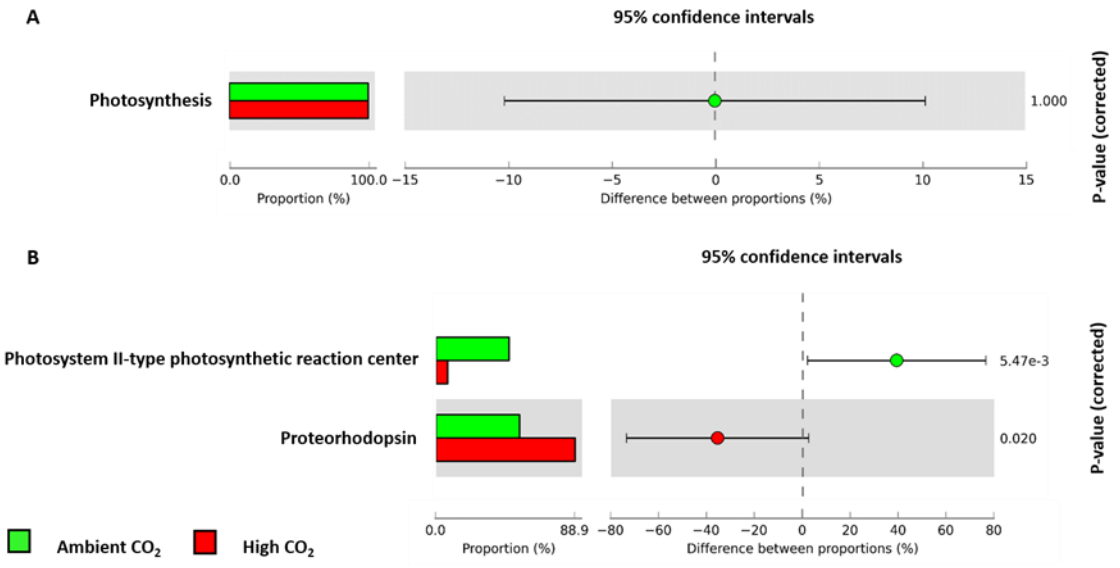

Figure 5.15 G-test conducted in STAMP showing the proportion of sequences attributed to photosynthesis in the ambient and high CO_2 datasets consisting of Flavobacteriaceae and Rhodobacteraceae species (A). Proportion of sequences attributed to methods of light generated phototrophy in the ambient and high CO_2 datasets (B).

Further tests were conducted to determine if light was able to permeate the dark incubation bottles in order to facilitate phototrophy. Although the bottles themselves were completely opaque the screw caps were translucent allowing some light to pass through (Figure 5.16A). This was demonstrated by placing a small pen-light torch in the bottle in a darkened room (Figure 5.16B). The beam of the torch was clearly visible emanating from the translucent cap (though not the main body of the bottle) proving that it was possible for a small amount of sunlight to enter the bottles. For the duration of the incubation period (5 days) the bottles were left in the fjord attached to a tether line (Figure 5.16C). AAnPs are abundant in the euphotic zone of the ocean where there is sufficient light for photosynthesis but decline rapidly below the 1% light depth. The fact that the light of the torch was barely visible through the cap strongly suggests that the meagre light entering the bottles during the incubation period would be insufficient for photoheterotrophy and therefore any CO_2 fixed is unlikely to be attributed to this process.

Figure 5.16 Examination of 4 L dark incubation bottle indicating the translucent screw top (A). Bottle placed in complete darkness with a small torch suspended inside (B). Bottles incubating in the fjord with the caps exposed to the sunlight (C).

5.5 Caveats in interpreting DNA SIP data

DNA-SIP has its limitations in that it can be difficult to interpret results due to the variation of genome G+C content in complex communities. DNA samples can vary in buoyant density by as much as 0.05 g/ml^{-1} due to variation in mol %G+C, explaining why smears are observed across the entire CsCl gradient in some SIP experiments (Buckley *et al.*, 2007). Fully ^{13}C-labeled DNA increases in buoyant density by 0.036 g/ml^{-1} relative to unlabeled DNA (Birnie and Rickwood, 1978). Thus the challenge is to determine whether microorganisms detected in the heavy DNA fraction are actively involved in the utilization of the added ^{13}C labelled substrate or whether they are detected simply because they have genomes with a high mol% G+C with similar buoyant densities to ^{13}C-labelled DNA from organisms with a lower mol% G+C in their genomes.

Unfortunately, the buoyant densities of the CsCl fractions were not determined in this investigation. However, it is possible to estimate them from another SIP experiment which used comparable methods to this study (Lueders *et al.*, 2004). Both experiments used the same type and size of ultracentrifugation tube and a similar protocol was followed in order to prepare the CsCl gradients to an average density of 1.725 g/ml. The only exceptions were the type of rotor used and the manner in which the tubes were fractionated. The experiment of Lueders *et al* (2004) revealed the density range of the CsCl gradient in the ultracentrifuge tube was 1.68 – 1.78 g/ml^{-1} with the buoyant densities of the ^{12}C DNA in CsCl gradient ranging from 1.69 - 1.72 g/ml^{-1}. Fully ^{13}C

labelled DNA from *Methylobacterium extorquens* grown on ^{13}C methanol had a buoyant density of 1.757 g/ml^{-1} which was an increase of ~0.04 g/ml^{-1} compared to the buoyant density of *Methylobacterium extorquens* grown on ^{12}C methanol.

The CsCl gradient density range (1.68 – 1.78 g/ml^{-1}) derived from Lueders *et* al (2004) was used to estimate the buoyant densities of the 28 fractions recovered from the SIP tube. Only 24 of these fractions were subject to analysis, the first and last two fractions were discarded as these densities were reasoned to contain no DNA. The first 16 fractions were then plotted on a graph in order to determine if the buoyant density of the ^{13}C fractions dominated by DNA from the *Rhodobacteraceae* were a consequence of high genome G+C content or due to the incorporation of the ^{13}C labelled substrate (Figure 5.17).

The results show the buoyant density of ^{12}C DNA in CsCl (lanes 13, 14 and 15) ranged from 1.72 – 1.727 g/ml^{-1} (average 1.723 g/ml^{-1}) slightly higher than the values of Lueders *et al* (2004) though densities ranging from 1.70 – 1.725 have been reported (Carter *et al.*, 1983). In comparison, the buoyant density in CsCl of the ^{13}C labelled DNA (lanes 9 and 10) ranged from 1.738 – 1.741 g/ml^{-1} (average 1.739 g/ml^{-1}) which was anticipated to be lower than the fully ^{13}C labelled DNA from *Methylobacterium extorquens*. Additionally, the high genome G+C content (66%) of *Methylobacterium extorquens* would increase the buoyant density further in contrast to the average genome G+C content (49%) observed in the *Rhodobacteraceae* metagenome (Chapter 6 section 3.2).

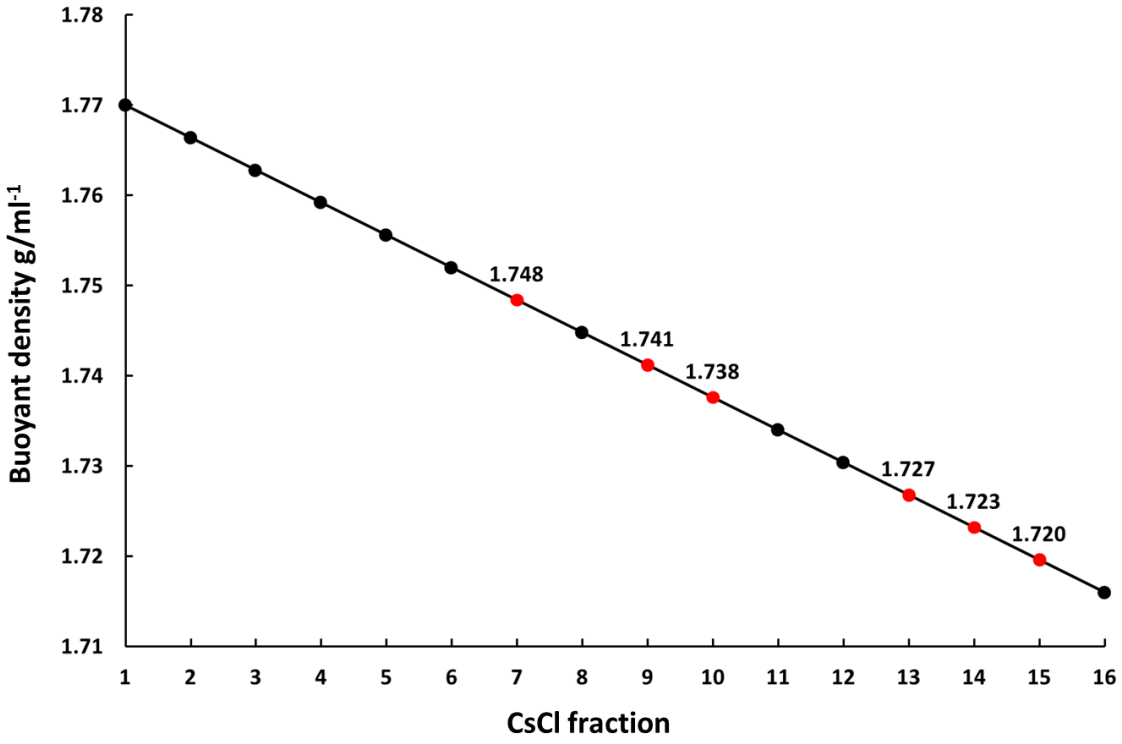

Figure 5.17 Estimated buoyant density of DNA in a CsCl gradient inferred from the data of Lueders *et* al (2004). Fractions from the SIP experiment are depicted by the red circles with fractions 13, 14 and 15 representing the ^{12}C fractions and lanes 9 and 10 representing the ^{13}C fractions containing members of the *Rhodobacteraceae.* Lane 7 represents the buoyant density of the genome of *Nitrosomonas europaea* ATCC 19718 with 50.7% G+C content and full ^{13}C substrate incorporation.

Under constant conditions (25°C in caesium chloride at neutral pH) the buoyant density of DNA as a function of its G+C content is given by the following: (equation 5.1)

$$\%\mathrm{G+C\ content} = \frac{\mathrm{Buoyant\ density\ (g/ml^{-1})} - 1.66}{0.098}\ x\ 100$$

[5.1]

From this equation the buoyant density of the *Rhodobacteraceae* metagenome with zero percent ^{13}C labelled incorporation was calculated as 1.708 g/ml^{-1}. This was based on the actual mol% G+C of reads in the metagenome data assigned to the *Rhodobacteraceae*. *Roseobacter denitrificans* is representative of the *Rhodobacteraceae* identified in the metagenome obtained in this study and it has been

suggest that this organism obtains 15% of its cellular carbon from inorganic carbon (Swingley *et al.*, 2007, Tang *et al.*, 2009). Incorporation of 15% of cellular carbon from ^{13}C labelled bicarbonate would increase the buoyant density of the *Rhodobacteraceae* DNA from the metagenome to 1.713 g/ml^{-1}. However, the approximate buoyant density of the ^{13}C labelled DNA observed in lanes 9 and 10 is 1.739 g/ml^{-1} suggesting that the *Rhodobacteraceae* had actually assimilated ~86% of the ^{13}C labelled substrate. Even if the degree of ^{13}C incorporation is not that high in reality, this suggests at the very least, that the *Rhodobacteraceae* DNA recovered in the heavy fraction was not purely a consequence of fortuitous recovery of unlabelled high mol% G+C DNA in the heavy DNA fraction.

To support these findings the buoyant density of a chemolithoautotroph, *Nitrosomonas europaea* ATCC 19718, which would be expected to obtain the vast majority of its carbon from inorganic carbon, was calculated with fully ^{13}C labelled DNA. This was done to ascertain the relative positons of DNA representing ^{12}C and ^{13}C *Rhodobacteraceae* DNA and ^{13}C from a chemolithoautotroph (*Nitrosomonas europaea*). Fully labelled DNA from *Nitrosomonas europaea* ATCC 19718 was calculated to have a buoyant density of 1.746 g/ml^{-1} which is similar to the buoyant density of the fraction in lane 7 of 1.748 g/ml^{-1} (Figure 5.17). An inspection of the agarose gel in which these fractions were visualised reveals the possible presence of DNA in lane 7 which could represent the "missing" autotrophic fraction (Figure 5.18). Preliminary PCR analysis (using bacterial 16S rRNA gene primers) previously conducted on this fraction was negative, thereby supporting the absence of DNA at that time. However, it now seems highly likely that this fraction may have contained chemoautotrophic DNA, albeit in extremely low concentrations.

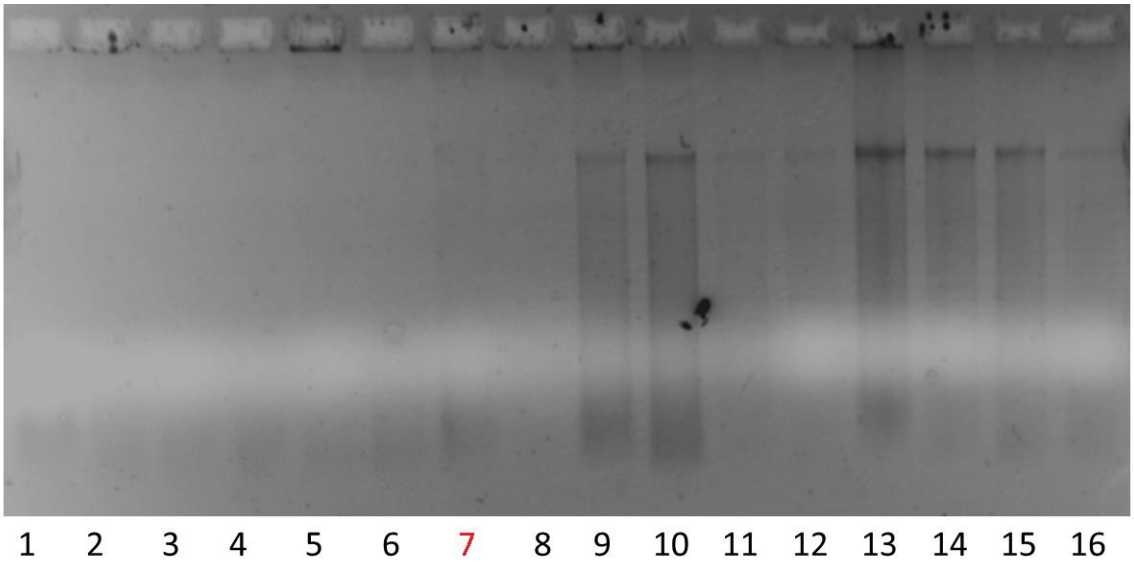

Figure 5.18 DNA SIP fractions viewed by running 5 µl of each aliquot on a 0.7% agarose gel. In this instance the contrast has been manipulated in order to visualize the probable ^{13}C heavy fraction in lane 7 (denoted in red) which may contain the DNA from chemoautotrophic bacteria.

The analysis presented here thus suggests that the presence of *Rhodobacteraceae* DNA in the heavy DNA fractions is not a mere consequence of a high genome mol% G+C but rather is a direct result of the assimilation of ^{13}C bicarbonate in excess of what has previously been reported (Swingley *et al.*, 2007, Tang *et al.*, 2009). Naturally, this is an imperfect estimate and the 86% ^{13}C incorporation for the *Rhodobacteraceae* fraction is likely to be excessive. However, it does suggest that heterotrophic CO_2 fixation by members of the *Rhodobacteraceae* is more substantial than the current accepted paradigm.

5.6 Conclusions

In this study I have shown that heterotrophic CO_2 fixation can occur in the absence of light and therefore phototrophy plays little or no part in this process. Anaplerotic reactions are important in the central metabolism of heterotrophic organisms as they are closely linked to biosynthesis and growth via the regeneration of

oxaloacetate, the acceptor molecule of the TCA cycle. It has been demonstrated that members of the marine *Roseobacter* clade use a mixotrophic carbon metabolism (Moran and Miller, 2007; Swingley *et al.*, 2007, Tang *et al.*, 2009). Similar ocean acidification experiments have found changes in bacterial and phytoplankton taxonomic composition in response to elevated CO_2. Allgaier *et al* (2008) showed changes in free-living bacterioplankton community structure but not in particle associated communities, suggesting that the effects of elevated CO_2 concentrations varied between species. Mesocosm studies near Svalbard reported a shift in community composition of phytoplankton from larger to smaller species (pico and nanoplankton) in response to elevated CO_2 (Brussaard *et al.*, 2013). The authors speculate that the shift to smaller phytoplankton species in response to elevated CO_2 would have direct consequences on the microbial food web and biogeochemical cycles. Increased temperature and pCO_2 have also been shown to stimulate the grazing rates of microzooplankton which are key players in phytoplankton mortality in the ocean (Calbet and Landry, 2004, Sherr and Sherr, 2007). A study by Rose *et al* (2009) demonstrated a significant effect in response to rising CO_2 on microzooplankton abundance and grazing rates which led to the development of phytoplankton assemblages which were unpalatable to microzooplanton due to their morphology (Rose *et al.*, 2009). Furthermore, a significant correlation between DMS concentration and the abundance of microzooplankton has been observed in a mesocosm perturbation experiment with increased CO_2 and temperature (Kim *et al.*, 2010).

The bacteria studied in this investigation were from a nutrient replete phytoplankton bloom. These large seasonal blooms terminate in an abrupt crash brought about by a decrease in nutrients, predation by zooplankton or viral lysis. It is envisaged that the low molecular weight carbon (including DMSP) was severely depleted in both treatments as no nutrients were added during the incubation period and the exclusion of light prohibited phototrophy. Such an environment would be unfavourable for cellular growth in some organisms as there would be insufficient carbon to replenish the intermediates of the TCA cycle. It is hypothesised that *Rhodobacteraceae* overcome this carbon deficit by supplementing organic carbon with inorganic carbon via anaplerosis in order to sustain growth until an alternative organic carbon source was available. This

adaptive response was substantiated by the dominance of *Rhodobacteraceae* in the ^{13}C SIP fractions of 16S rRNA SIP clone libraries accounting for 46% in the high CO_2 library and 61% in the ambient CO_2 library. It is proposed that the lower representation of *Rhodobacteraceae* in the high CO_2 treatments (both ^{13}C and ^{12}C) were a direct consequence of elevated CO_2 reducing primary productivity (Chapter 3 section 3.3.2) possibly due to the potential effect on calcification (Riebesell *et al.*, 2000; Engel *et al.*, 2005, Iglesias-Rodriguez *et al.*, 2008). A decrease in the relative abundance of marine *Roseobacter* species and an increase in relative abundance of *Flavobacteriaceae* were observed in natural biofilms from the Great Barrier Reef (Witt *et al.*, 2011). Terminal restriction fragment length polymorphism (T-RFLP) of bacterial biofilm communities revealed that the average relative abundance of *Roseobacter* and *Silicibacter* T-RFs decreased with rising CO_2 while the *Tenacibaculum (Flavobacteriaceae)* T-RF increased in elevated CO_2 treatments (P=0.0009; ANOVA).

As CO_2 assimilation rates were not measured in the study we can only examine the literature and make assumptions regarding the results obtained. Although, Overbeck (1979) discovered a variation in anaplerotic heterotrophic CO_2 fixation of 1-12% others studies have estimated it around 10% (Perez and Matin, 1982, Sonntag *et al.*, 1995). However, the recent work of Tang *et al* (2009) has postulated that *Roseobacter denitrificans* OCh114 can fix up to 15% CO_2 through its anaplerotic enzymes supporting the proposal by Swingley *et al* (2007). A recent study investigating the effects of elevated CO_2 on two bacterial groups (*Rhodobacteraceae* and *Flavobacteriaceae*) found that anaplerotic CO_2 fixation rates (both dissolved and particulate) were higher in *Roseobacter* than in *Cytophaga* (Teira *et al.*, 2012). Although there was no significant difference in anaplerotic CO_2 fixation between the treatments, (high versus ambient CO_2) the daily cellular rates of CO_2 fixation in the ambient CO_2 treatment was 1.2 fg C $cell^{-1}$ d^{-1} for *Roseobacter* and 0.43 fg C $cell^{-1}$ d^{-1} in *Cytophaga*. This ~3-fold increase in CO_2 assimilation rate by *Roseobacter* explains their presence in the ^{13}C SIP fractions results of this study as both bacterial groups dominated the dark CO_2 incubations.

Tang *et al* (2009) reported that *R. denitrificans* uses anaplerotic pathways to fix 10–15% of protein carbon from CO_2. If this assumption is correct then the marine

*Roseobacte*r clade must make a significant contribution to the global carbon cycle by not only producing CO_2 via respiration but by also absorbing it via anaplerosis. Therefore the important question may not be the rate of CO_2 assimilation but rather the circumstances in which CO_2 is assimilated.

There is now strong evidence to suggest that CO_2 assimilation may play an essential role in heterotrophic growth and is an important contributor to cell biomass. This may be especially significant in the era of climate change which is driven by the accumulation of greenhouse gases causing a rapid change in temperature and ocean pH. Therefore a greater understanding of the relationship between diversity and functional capabilities is urgently required as a reduction in any key bacterial group could have devastating consequences on ocean productivity and biogeochemical cycles.

6. Metagenomic assessment of the effect of ocean acidification on marine bacterioplankton

6.1 Introduction

The "great plate-count anomaly" was a term used by Staley and Konopka (1985) to describe the discrepancy between the plate counts of bacteria from soil, river and ocean samples and those obtained via microscopic enumeration. Significantly higher numbers (by several magnitudes) were observed via microscopy compared to viable cell counts on agar plates leading microbial ecologists to conclude that less than 1% of viable bacteria were culturable (Staley and Konopka, 1985). This is especially true of marine bacteria which grow as consortia in the ocean and rely on other bacteria for essential nutrients and substrates that are difficult to replicate in the laboratory (Joint *et al.*, 2010). Unfortunately, organisms isolated in pure culture may not represent the numerically dominant and/or functionally significant species of that environment but rather species which are able to grow rapidly in rich media. Therefore from a purely ecological perspective the vast majority of isolates from environmental samples represent nothing more than microbial weeds (Hugenholtz, 2002) and may not be indicative of the natural population.

Microbial ecologists realized that microbial communities consisted of hundreds if not thousands of species interacting with each other on varying levels. To fully characterise this diversity a new culture independent method was devised based on the comparative analysis of ribosomal RNA sequences to deduce evolutionary relationships. This technique resulted in several influential studies revealing numerous microbial species for which no cultivated representatives were known (Stahl *et al.*, 1984; Pace *et al.*, 1985, Ward *et al.*, 1990). Although this technique greatly advanced microbial ecology and provided the basis of what is now known as molecular microbial ecology it is still primarily a phylogenetic technique allowing the assessment of diversity only (Head *et al.*, 1998). Microbial ecology studies the interaction of microorganisms in the environment by answering two fundamental questions; "what microorganisms are out there?" and "what are they doing?" In order to answer these questions the disciplines of molecular biology, genomics, computational biology and the latest advances in sequencing technology converged to create a new discipline known as metagenomics.

The term "metagenomics" was coined by while investigating the chemical diversity of soil microflora (Handelsman *et al.*, 1998) though similar techniques were used previously with landmark successes (Schmidt *et al.*, 1991; Healy *et al.*, 1995, Stein *et al.*, 1996). Metagenomics is employed as a means of systematically investigating, classifying and manipulating the genetic material isolated from environmental samples (Tripathi *et al.*, 2007). The basic techniques are similar to genomics of clonal cultures except in this instance the genomic material does not come from a single organism but from a community of microorganisms. After isolating the DNA (the metagenome) it is then cloned in large fragments into a suitable vector and transformed in to a host bacterium thereby creating a metagenomic library. These libraries may then be screened using a phylogenetic anchor such as the 16S rRNA gene, another chosen gene or by the heterologous expression of gene products. However, the development of massively parallel sequencing platforms such as Roche 454, illumina and ABI SOLiD permitted the whole genome shotgun (WGS) sequencing of entire clone libraries allowing phylogenetic and metabolic characterization as well as reconstructing almost entire genomes (Chen and Pachter, 2005). This global analysis of community composition permitted researchers to conduct landmark shotgun sequencing projects in various habitats such as acid mine biofilms (Tyson *et al.*, 2004) Sargasso Sea (Venter, 2004) whale fall carcasses (Tringe *et al.*, 2005) and probably the most ambitious project to date, the human microbiome project (HMP) which is attempting to characterize the collective genomes of our microbial symbionts (the microbiome) and their influence on disease (http://commonfund.nih.gov/hmp/overview). Launched in 2008 this two phase initiative employs 16S rRNA gene sequencing using the Roche 454 titanium platform to identify the microbiome community structure from various body sites followed by WGS sequencing using the Illumina GAIIx platform (Peterson *et al.*, 2009). At the end of phase 1 of the project, (2008 – 2012) 5,177 taxonomically characterized communities had been identified from 5,298 samples using 16S rRNA sequencing while 800 reference bacterial genomes had been fully sequenced and deposited in the National Center for Biotechnology Information (NCBI) and the Data Analysis and Coordination Center (DACC) (Human Microbiome Project Consortuim, 2012).

Meta-analysis is an analytical technique that uses statistical methods to combine the results of multiple studies in order to identify the underlying patterns of biological responses in measured experimental effects (Gurevitch and Hedges, 1999). Meta-analysis summarizes the results of each experiment with an estimate of the magnitude (effect size) of the response to the manipulation (Osenberg *et al.*, 1999). There have been several meta-analysis studies in recent years assessing the biological effects of ocean acidification and global ocean warming (Dupont *et al.*, 2010; Hendriks *et al.*, 2010, Kroeker *et al.*, 2010, Harvey *et al.*, 2013, Kroeker *et al.*, 2013, Wittmann and Pörtner, 2013) of which only two (Hendriks *et al.*, 2010, Harvey *et al.*, 2013) included single cell organisms (cyanobacteria) in their studies. Each meta-analysis was conducted using data from multiple published studies (23 – 228 studies) in order to assess the effects of either ocean acidification or ocean acidification plus warming. Different taxonomic marine groups were included in each analyses consisting primarily of calcifying organisms (calcifying algae, corals, coccolithophores, molluscs, echinoderms and crustaceans) and non-calcifying organisms (fish, fleshy algae and seagrasses). The biological effects of ocean acidification and /or warming were based on the effect size of several response variables: survival; calcification; growth; photosynthesis; development; abundance and metabolism. The study of Dupont *et al* (2010) differered signifcantly in that only echinoderms (brittlestars, seastars, sea urchins and sea cucumbers) were investigated in order to assess the impact of ocean acidification during all life-cycle stages (Dupont *et al.*, 2010).

The analysis conducted by Hendriks *et al* (2010) concluded that the effects of ocean acidification are likely to be minor and most biological processes would not be affected (Hendriks *et al.*, 2010). However, the review was criticized for not combiniing the results of several studies in to an overall mean effect which is standard practise in any quantitave study (Kroeker *et al.*, 2010). In contrast, the meta-analysis of Harvey *et al* (2013) revealed significant negative effects on calcification, reproduction and survival with a significant positive effect on photosynthesis when the twin stresses of warming and acidification were combined (Harvey *et al.*, 2013).

The majority of meta-analysis studies have found negative effects on survival, calcification, growth and reproduction though the degree of response varied among taxonomic groups. Calcification was the process most sensitive to ocean acidification with a reduction in calcification of 22–39% in corals, coccolithophores and molluscs (Kroeker *et al.*, 2013) and reduced calcification rates of between 9-51% of all functional groups studied (Hendriks *et al.*, 2010).

In previous chapters, the microbial diversity of two seawater samples obtained from a mesocosm perturbation experiment were assessed. Bacterial communities were characterized using denaturing gradient gel electrophoresis (DGGE) analysis of PCR-amplified 16S rRNA gene fragments. This demonstrated systematic differences between the bacterioplankton communities in high and ambient CO_2 treatments (Chapter 4 section 4.3.2). The DGGE profiles from replicate bottles were reproducible and single samples from the high CO_2 and ambient CO_2 treatments were used for more detailed analysis of the bacterial communities using 16S rRNA gene clone libraries. Analysis of 16S rRNA gene clone libraries demonstrated that the bacterioplankton communities in the ambient CO_2 treatment were dominated by members of the *Flavobacteriaceae* within the *Bacteroidetes* (62.4% of clones, n =96) and the *Rhodobacteraceae* within the *Alphaproteobacteria* (21.5% of clones, n =96). By contrast, representation of the *Rhodobacteraceae* was substantially lower in the communities from the high CO_2 treatment (2.4% of clones, n =96).

In marine surface waters, *Rhodobacteraceae* of the marine *Roseobacter* clade have been observed to be the dominant bacterial species in marine algae blooms that produce large amounts of the sulfur metabolite DMSP (González *et al.*, 2000, Zubkov *et al.*, 2001). Marine *Roseobacter* spp. are important in controlling the sulfur flux of the oceans as they are predominantly responsible for the degradation of DMSP and its catabolites (González *et al.*, 1999). Approximately, 90% of DMSP is degraded via the demethylation pathway which generates methanethiol that can be used as a carbon and sulfur source for microbial communities (Kiene and Linn, 2000, Kiene *et al.*, 2000). The alternate pathway is the cleavage of DMSP via lyase enzymes which results in the

production of dimethylsulfide (DMS), a climatically active gas responsible for the formation of aerosol particles that can impact the global climate (Charlson *et al.*, 1987, Simó, 2001).

In this current investigation we used a metagenomic approach to assess the microbial diversity and metabolic potential of the ambient and high CO_2 samples. Metagenomic libraries were created via random shotgun sequencing of total DNA isolated from each sample which was then interrogated using software packages for metagenome analysis to produce gene profiles of each community.

6.2 Methods

Based on the results of the molecular analysis presented in chapter 4 (Sections 4.3.1 and 4.3.2) samples taken on day 8 (21st May) of the dark incubation experiment were chosen for metagenomic analysis. The samples were subjected to whole genome amplification via Multiple Displacement Amplification (MDA) (Dean *et al.*, 2002) in order to obtain the required 8 µg of DNA (per sample) for pyrosequencing (Ronaghi *et al.*, 1998). This method has proven highly successful during the course of this study producing DNA that gave highly similar DGGE profiles to that of the starting DNA (Sections 4.32 and 5.32). Sequencing of the libraries was conducted by the Advanced Genomic Facility, University of Liverpool on 2 x one-eighth of a picotiter plate using a Roche 454 GS FLX sequencer (Branford, CT, USA). The resulting sequence data were compiled into two large BLAST files (BLAST-in) that were compared to the GenBank database using the BLASTX program (Altschul *et al.*, 1990). Results were retrieved in BLAST-out files which contained the top hits for each sequence.

Analysis of the metagenomes was performed using MG-RAST server which annotates metagenomes without the need of sequence assembly or phylogenetic markers (Meyer *et al.*, 2008). As a comparison to MG-RAST a second analysis was undertaken using MEGAN (Huson *et al.*, 2007) which requires the BLAST-out files for the subsequent analysis of metagenomic data.

Statistical analysis of the metagenomes was performed using the software package STAMP (Statistical Analysis of Metagenomic Profiles) using the functional and taxonomic profiles produced by MG-RAST (Parks and Beiko, 2010). STAMP provides a graphical environment for performing comparative analysis of metagenomic profiles which can be interactively explored through high quality plots. The program implements several statistical hypothesis tests such as Fisher's exact test, Chi-square test and G-test as well as the non-parametric bootstrap test. Effect size, P-value and confidence levels may also be calculated as well as a mechanism for filtering datasets according to their profile level, effect size or a threshold P-value.

6.3 Results and discussion

The metagenome library from the ambient CO_2 treatment contained 34,339 sequences with a mean sequence length of 221 ±65 bp and a mean mol% G+C of 45 ± 8 %. In contrast, the metagenome library from the high CO_2 treatment contained 37,595 sequences with a mean sequence length of 204 ± 76 bp and a mean mol% G+C of 35 ± 8 %. The MG-RAST analysis was conducted using the M5NR/Subsystems annotation databases (Overbeek *et al.*, 2005) using a minimal alignment length cut off of 15 (aa or bp), minimal identity cut off of 60% and a maximum e-value cut off of 1E-5. The MEGAN analysis was conducted by comparing the metagenome sequences against the NCBI's Nr/Nt database and assigns input reads to the lowest common ancestor (LCA) of BLAST hits.

6.3.1 Rarefaction analysis

Rarefaction is a technique to compare species richness from samples of different sizes and as such provides a framework for quantifying expected species richness as a function of sampling effort (Gotelli and Colwell, 2001). The resulting rarefaction curve plots the number of taxa as a function of the number of individuals sampled (in the case of metagenome data individual sequence reads). A steep slope indicates that a large fraction of the microbial diversity remains to be discovered while a flatter curve indicates

that sampling has been sufficient to recover sequences from the most prevalent taxa in the sample and any further sampling is likely to yield only few additional new taxa. The rarefaction analysis conducted in MG-RAST indicated that the high CO_2 metagenome had a slightly lower diversity compared to its ambient CO_2 counterpart (Figure 6.1). This was supported by the alpha diversity results which calculated the number of distinct species in each treatment. In this instance, the alpha diversity for the ambient CO_2 treatment was estimated at 329.8 species which was reduced in the high CO_2 treatment to 134.8 species. Furthermore, the results indicated that despite the fact that the metagenome libraries were relatively small, the predominant taxa present were likely captured by the metagenome analysis. Of course this does not represent a comprehensive sampling of their individual genomes only that the reads obtained were consistently assigned to a modest number of taxa.

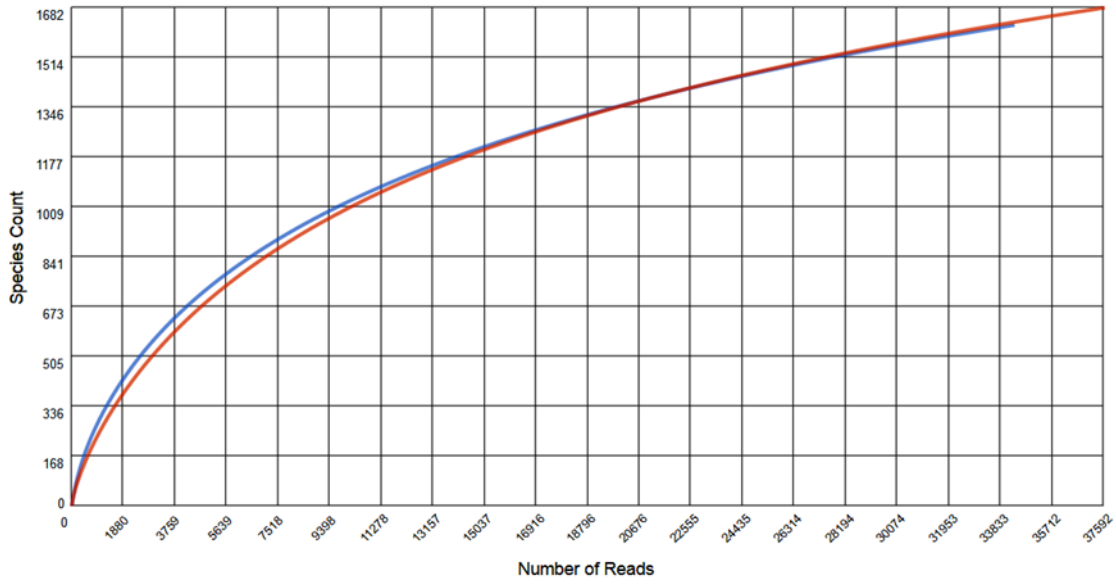

Figure 6.1 Rarefaction curves for the ambient CO_2 metagenome (blue line) and the high CO_2 metagenome (red line). The analysis was conducted in MG-RAST using the M5NR database and a minimum alignment length of 15 bp.

6.3.2 Phylogenetic assignment of ambient CO_2 and high CO_2 metagenomes

1,402 reads from the high CO_2 metagenome failed quality control (QC) of which 1,131 reads were removed as a result of dereplication. Of the remaining 36,163 reads,

10.8% (3,900 reads) were assigned as no hits (no matches in the M5NR database) and 0.17% (61 reads) were unclassified. In the ambient CO_2 metagenome 3,422 reads failed QC of which 2,464 were due to dereplication. 18% (5,135 reads) of the remaining 28,453 reads were assigned as having no hits while 0.4% (110 reads) were unassigned due to having a bit score less than 35. The majority of the remaining reads from both datasets were assigned to the domain bacteria accounting for 87.1% (31,520 reads) in the high CO_2 metagenome and 75.4% (21,454 reads) in the ambient CO_2 metagenome (Figure 6.2).

In contrast, the MEGAN analysis revealed that 13,809 reads (42.2%) of the ambient CO_2 metagenome and 12,900 reads (34.3%) of the high CO_2 metagenome where assigned as having no BLAST hits with 46 reads from each dataset being unassigned (Figure 6.3). As with the MG-RAST analysis the majority of the remaining reads from both datasets were assigned to the domain bacteria. In the high CO_2 metagenome 94.4% (21,782 reads) were assigned to this domain while the ambient CO_2 metagenome had 86.9% (16,226 reads).

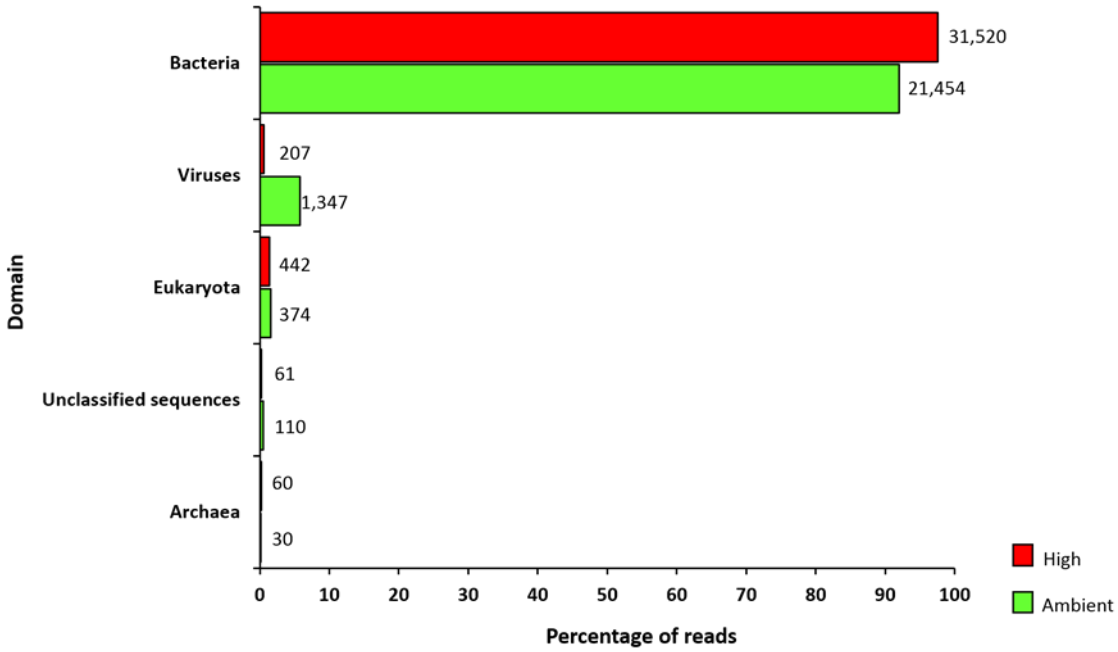

Figure 6.2 Domain distribution of reads from ambient and high CO_2 metagenomes obtained from the MG-RAST analysis. The percentages were calculated from both datasets after the removal of reads which failed QC and those assigned as having no hits. The numbers next to each bar on the graph represent the actual number of reads assigned.

At the bacterial phylum level, both MG-RAST and MEGAN assigned the majority of reads from both treatments to *Bacteroidetes* and *Proteobacteria*. In MG-RAST, the high CO_2 treatment was dominated by *Bacteroidetes* with 73.3% (23, 115 reads) followed by *Proteobacteria* with 22.4% (7,059 reads) (Figure 6.4). A reversal of dominant phyla was observed in the ambient CO_2 metagenome with the highest number of reads associated to *Proteobacteria* with 65.2% (13,993 reads) followed by *Bacteroidetes* 24.5% (5,254 reads). Similar results were obtained in the MEGAN analysis (Figure 6.5) with the phyla from high CO_2 metagenome consisting predominantly of 66.9% (14,567 reads) *Bacteroidetes* and 21.3% (4,650 reads) *Proteobacteria*. In contrast, the dominant phyla in the ambient CO_2 metagenome was *Proteobacteria* with 60.8% (9,867 reads) followed by *Bacteroidetes* with 20.6% (3,346 reads).

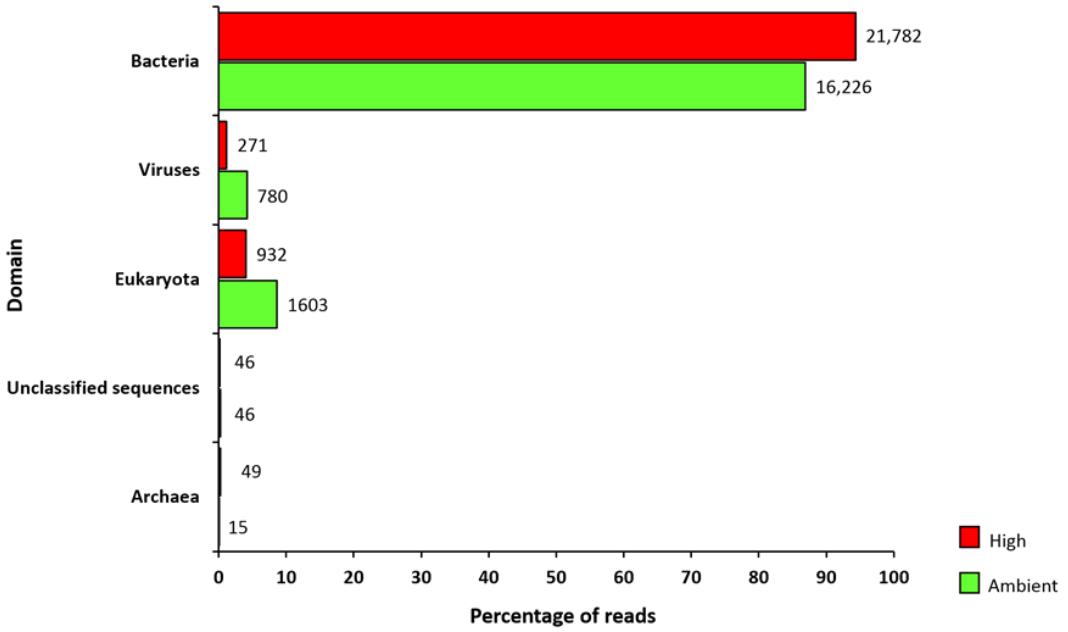

Figure 6.3 Domain distribution of reads from ambient and high CO_2 metagenomes generated in MEGAN version 4.62.1 using LCA parameters of minimum support 5, minimum score 35 and a top percent score of 10. The percentages were calculated for both datasets after the removal of reads classed as having no hits. Actual read numbers shown beside each bar on the graph.

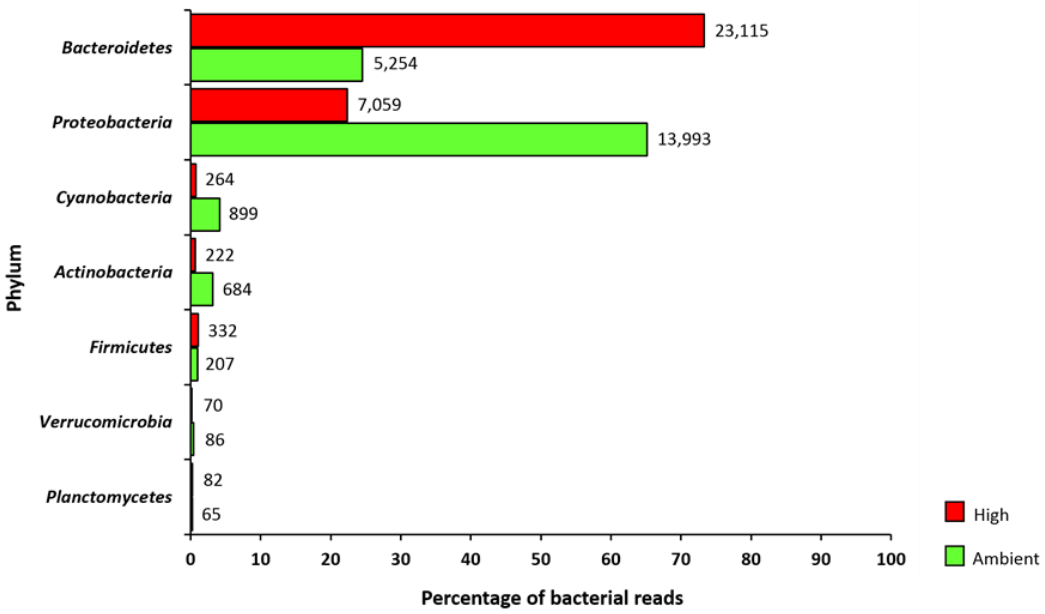

Figure 6.4 Bacterial phylum distribution of reads from ambient and high CO_2 metagenomes generated by MG-RAST. Percentages were calculated from the total number of bacterial reads assigned to each metagenome (high CO_2 = 31,520 reads, ambient CO_2 = 21,454 reads). The actual reads assigned are shown next to each bar on the graph.

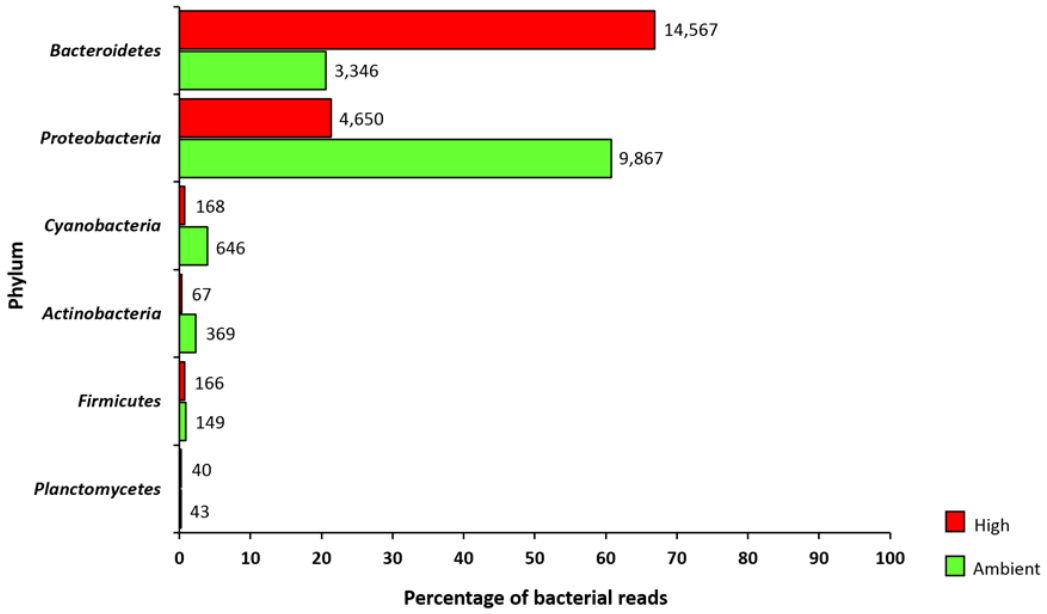

Figure 6.5 Bacterial phylum distribution of reads from ambient and high CO_2 metagenomes generated by MEGAN. Percentages were calculated from the total number of bacterial reads assigned to each metagenome (high CO_2 = 21,782 reads, ambient CO_2 = 16,226 reads). The actual number of reads assigned are shown next to each bar on the graph.

The results from both MG-RAST and MEGAN suggested that elevated CO_2 (which is accompanied by a reduction in pH) has a detrimental effect on *Proteobacteria* while *Bacteroidetes* fare better. This was supported by qPCR data of the ambient and high CO_2 samples in which a decrease of 56.4% in 16S rRNA gene abundance was observed in *Rhodobacteraceae* in response to elevated CO_2 (Chapter 4 section 4.3.5). To ascertain which particular groups of these phyla are susceptible to a reduction in seawater pH the metagenome datasets were analysed at a higher phylogenetic resolution. At the family level, both MG-RAST and MEGAN indicated that in comparison to the ambient CO_2 metagenome, the high CO_2 metagenome had fewer reads assigned to the *Rhodobacteraceae* and a greater number of reads assigned to the *Flavobacteriaceae* and to lesser extent the *Bacteroidaceae* and *Cytophagaceae*. These results are supported by the initial analysis of the metagenomes which saw a decrease in the mean mol% G+C content from 45 ± 8 % in the ambient CO_2 treatment to 35 ± 8 % in the high CO_2 treatment. This shift in G+C content is indicative of a change in species composition

which is consistent with the predominance of the *Rhodobacteraceae* in the ambient CO_2 metagenome which are known to have a high mol %G+C content (Temperton, 2009).

Although the general trends are similar regarding community composition in both the 16S rRNA gene clone library data and the metagenome data there are slight differences which may be attributed to the method of library construction. The 16S rRNA gene clone libraries defined the community composition based on the PCR amplification of the 16S rRNA gene. However, amplicon products may be subjected to biases due to the intrinsic differences in the amplification efficiency of templates (Polz and Cavanaugh, 1998) or unequal amplification caused by the self-annealing of the most abundant templates (Suzuki and Giovannoni, 1996). Furthermore, PCR amplification of the 16S rRNA gene discriminates between species with large genome sizes and a small number of *rrn* operons against species with small genome sizes and a large number of *rrn* operons (Stackebrandt *et al.*, 1999). As a consequence, the variation in the relative abundance of distinct taxa in a clone library can be attributed both to variation in the relative abundance of different organisms and to variation in the 16S rRNA copy number of those organisms (Kembel *et al.*, 2012). Based on the results of the rrnDB, a database in Michigan state university which documents the variation of RNA operons in bacterial and archaea, (Klappenbach *et al.*, 2001, Lee *et al.*, 2009) *Flavobacteriaceae* have on average 3 copies of the 16S rRNA gene per genome while the *Rhodobacteraceae* have 3.14 copies per genome. Therefore, both groups should be equally represented in the clone libraries due to the similarity of 16S rRNA copy number.

In the metagenomic libraries, the collective genetic material is utilized to uncover phylogeny and microbial functions present in the environmental sample. However, in order to have a sufficient amount of DNA for 454 sequencing (~8 µg) the samples were subjected to Whole Genome Amplification (WGA) using Multiple Displacement Amplification (MDA) (Dean *et al.*, 2001, Dean *et al.*, 2002). It is known that random amplification bias can occur using MDA with sequences that are over represented in one reaction being underrepresented in another (Raghunathan *et al.*, 2005; Zhang *et al.*, 2006, Lasken, 2012). However, in this study the two metagenomic libraries were each

constructed from 5 separate reactions which were then pooled prior to sequencing. MDA is also reported to show bias towards DNA templates with high G+C content preferentially amplifying low or intermediate G+C regions. Several studies have reported significantly less amplification of species with a high GC content due to the stability of G+C rich templates (Pinard *et al.*, 2006; Yilmaz *et al.*, 2010, Direito *et al.*, 2014). To ascertain the average G+C content of the *Rhodobacteraceae* and *Flavobacteriaceae* in the ambient and high CO_2 metagenomes, two subset metagenomes were created in MG-RAST that contained only these two bacterial families. The analysis revealed that the *Rhodobacteraceae* metagenome (ambient and high CO_2) had an average G+C content of 49±6%, while the *Flavobacteriaceae* (ambient and high CO_2) had an average G+C content of 35±4% (Figure 6.6). Members of the marine *Roseobacter* are known to possess a high G+C content such as *Roseobacter denitrificans*, (58.9%) *Sulfitobacter pomeroyi* DSS-3, (64.0%) *Silicibacter* TM1040 (60.0%) and *Jannaschia* CCS1 (62.2%) (Moran *et al.*, 2007; Swingley *et al.*, 2007, Temperton *et al.*, 2009). In contrast, species belonging to the *Flavobacteriaceae* have a lower G+C content such as *Dokdonia donghaensis* MED134, (38.2%) *Croceibacter atlanticus* HTCC2559, (33.9%) *Gramella forsetii* KT0803 (36.6%) and *Polaribacter irgensii* 23-P (31%) (Gosink *et al.*, 1998, Chaudhuri *et al.*, 2008). This would suggest that the results of the metagenomic analysis should be treated cautiously as members of the *Rhodobacteraceae* may be underrepresented in the metagenomic libraries skewing relative abundances.

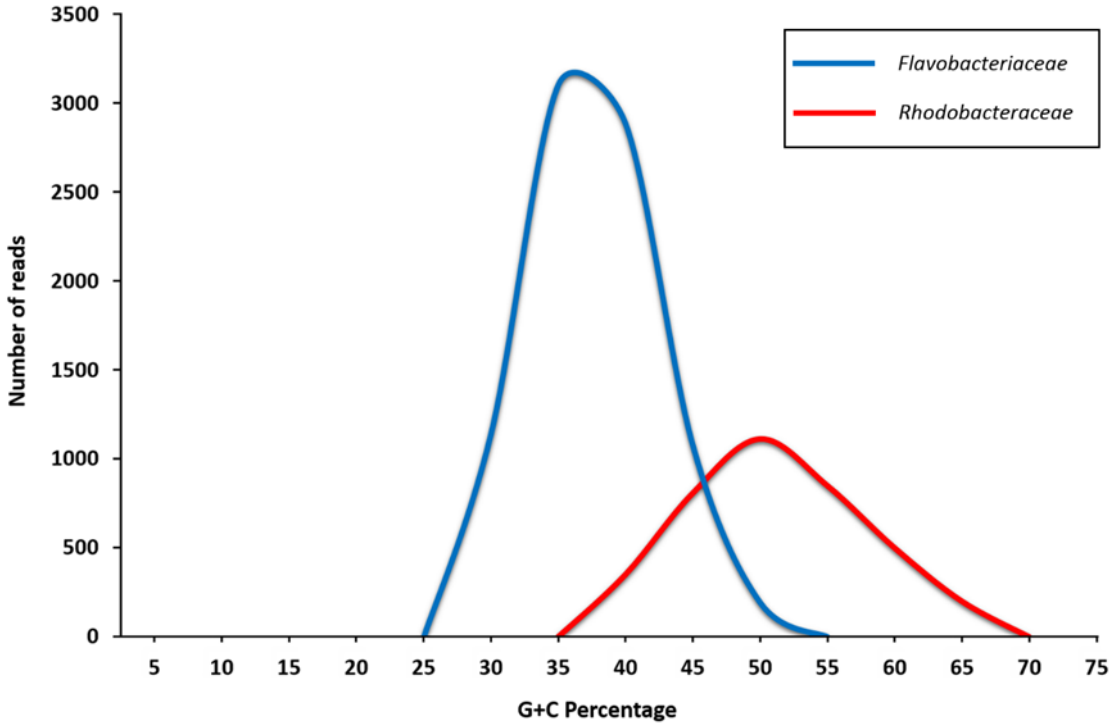

Figure 6.6 Histogram showing the G+C distribution (%) of reads assigned to *Rhodobacteraceae* and *Flavobacteriaceae* retrieved from the ambient and high CO_2 metagenomes. Each position represents the number of sequences within a G+C percentage range.

At the family level, the MG-RAST analysis revealed a decrease in the percentage of reads assigned to the *Rhodobacteraceae* in the high CO_2 metagenome. In this instance, the ambient CO_2 metagenome was assigned 34.7% (7,443 reads) in contrast to 8.8% (2,767 reads) assigned to the high CO_2 metagenome (Figure 6.7). However, the percentage of reads assigned to the *Flavobacteriaceae* increased from 17.7% (3,808 reads) in the ambient CO_2 metagenome to 58.7% (18,498 reads) in the high CO_2 metagenome. MG-RAST analysis also revealed a decrease in the percentage of reads assigned to the *Pseudomonadaceae* with 3.4% (544 reads) assigned to the ambient CO_2 metagenome whereas 0.8% (173 reads) were assigned to the high CO_2 metagenome (Figure 6.7).

A similar response to elevated CO_2 was observed in the MEGAN analysis with the percentage of reads assigned to the *Rhodobacteraceae* decreasing in the high CO_2

metagenome to 4.6% (998 reads) whereas the percentage of reads assigned to the ambient CO_2 metagenome was 16.4% (2,664 reads) (Figure 6.8). Conversely, the percentage of reads associated with *Flavobacteriaceae* was higher in the high CO_2 metagenome accounting for 11% (2,405 reads) in comparison to 3.6% (588 reads) observed in the ambient CO_2 metagenome (Figure 6.8). A decrease in reads associated with the *Pseudomonadaceae* was also observed in this analysis with 45 reads in the ambient CO_2 metagenome and 29 reads in the high CO_2 metagenome (Figure 6.8).

Although the metagenome data suggest that overall, elevated CO_2 had a negative effect on *Proteobacteria,* there is one group which seems to do better in a reduced pH environment. *Candidatus Pelagibacter* is a member of the SAR11 clade of *Alphaproteobacteria*, which is widely accepted as the most abundant group of heterotrophic bacteria in the oceans, accounting for 26% of all ribosomal RNA genes that have been identified in seawater (Rappe *et al.*, 2002). Evolution has streamlined its genome so that only the most fundamental cellular systems are present in order to replicate under limiting nutrient resources as efficiently as possible (Giovannoni *et al.*, 2005). MEGAN analysis revealed that all the reads associated to the SAR11 clade were assigned to *C. Pelagibacter* with 2.5% (549 reads) of the high CO_2 metagenome and 0.07% (11 reads) assigned to the ambient CO_2 metagenome (Figure 6.8). This was substantiated by 16S rRNA gene clone library data (Chapter 4, section 4.32) where *C. Pelagibacter* was found in the high CO_2 treatment only (5 clones). MG-RAST analysis corroborates the higher relative abundance of *C. Pelagibacter* in the high CO_2 metagenome. In this instance, 0.4% (83 reads) were assigned *C. Pelagibacter* from the ambient CO_2 metagenome whereas 1.5% (462 reads) were assigned to this genus from the high CO_2 metagenome.

To determine if there was a significant difference in the number of *C. Pelagibacter* reads assigned to the metagenomes, a G-test was conducted using STAMP (Statistical Analysis of Metagenomic Profiles) an open-source software package for analysing metagenomic profiles (Parks and Beiko, 2010). Using the profiles generated by MG-RAST, the results revealed a significant difference in the proportion of *C.*

Pelagibacter reads assigned to the metagenomes from the high CO_2 treatment (P= < 0.05). A significant difference was also observed between the metagenomes in some genera of the marine *Roseobacter* clade indicating that there were proportionally more reads associated to the ambient CO_2 metagenome; *Roseobacter*, *Ruegeria* and *Sulfitobacter* (P= < 0.05) at the 95% confidence level (Figure 6.9).

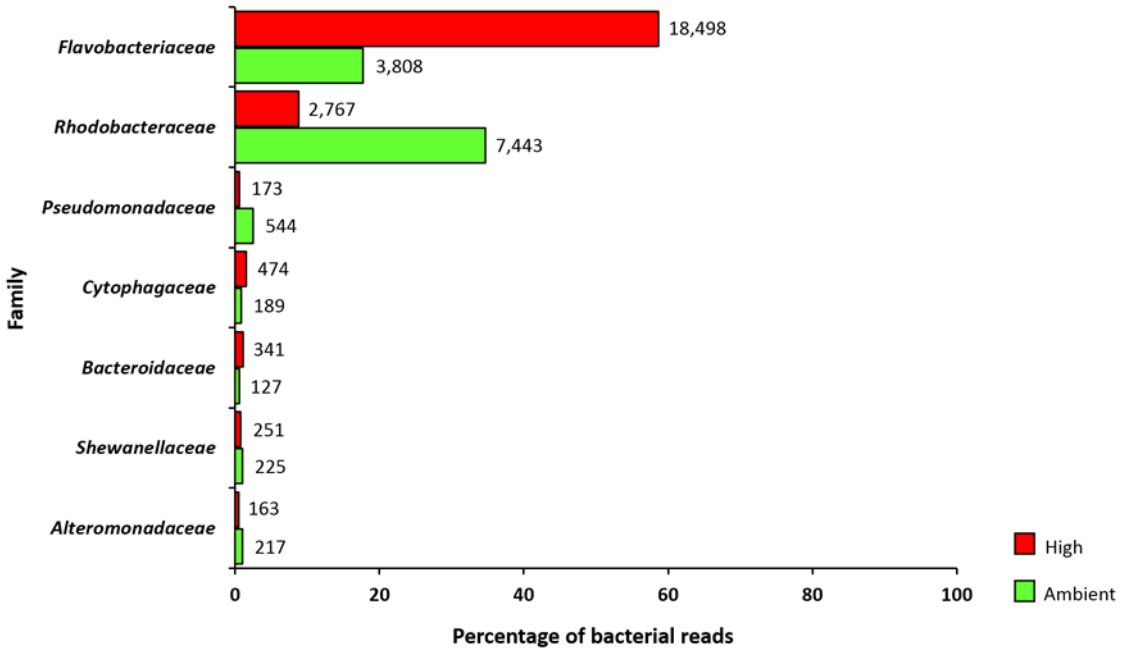

Figure 6.7 Family distribution of bacterial reads from ambient and high CO_2 metagenomes. Percentages were calculated from the total number of bacterial reads assigned to each metagenome by MG-RAST with the number of reads assigned to each family depicted next to the bar on the graph.

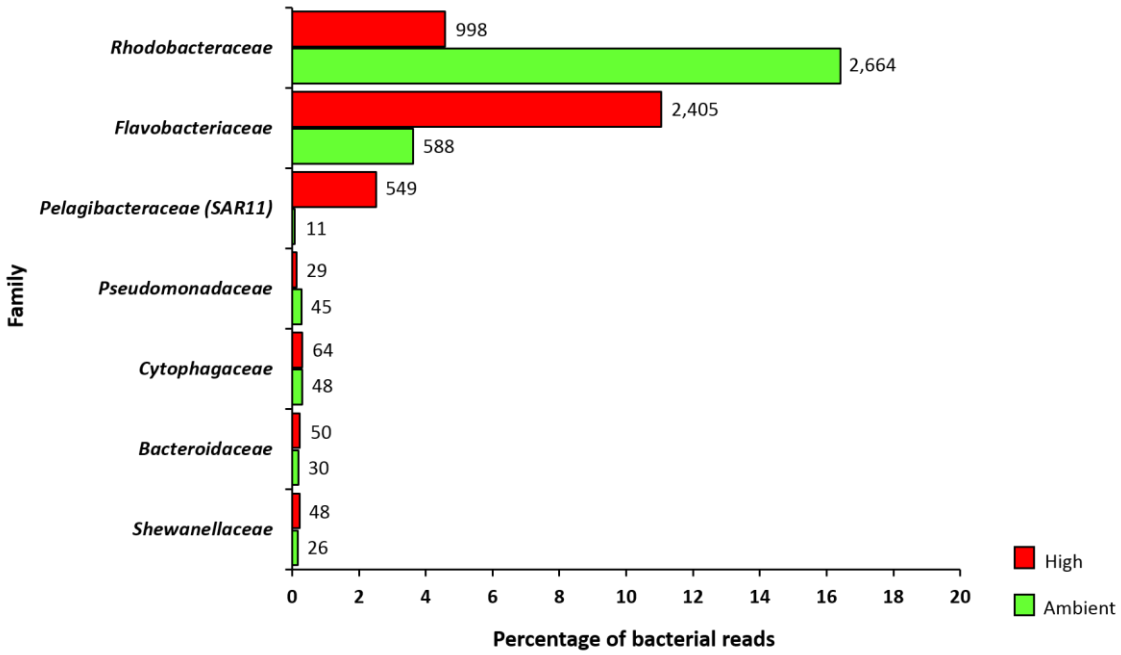

Figure 6.8 MEGAN analyses showing the family distribution in percent obtained from the total number bacterial reads assigned to each ambient and high CO_2 metagenome. Actual number of reads assigned to each family is depicted next to the bar on the graph.

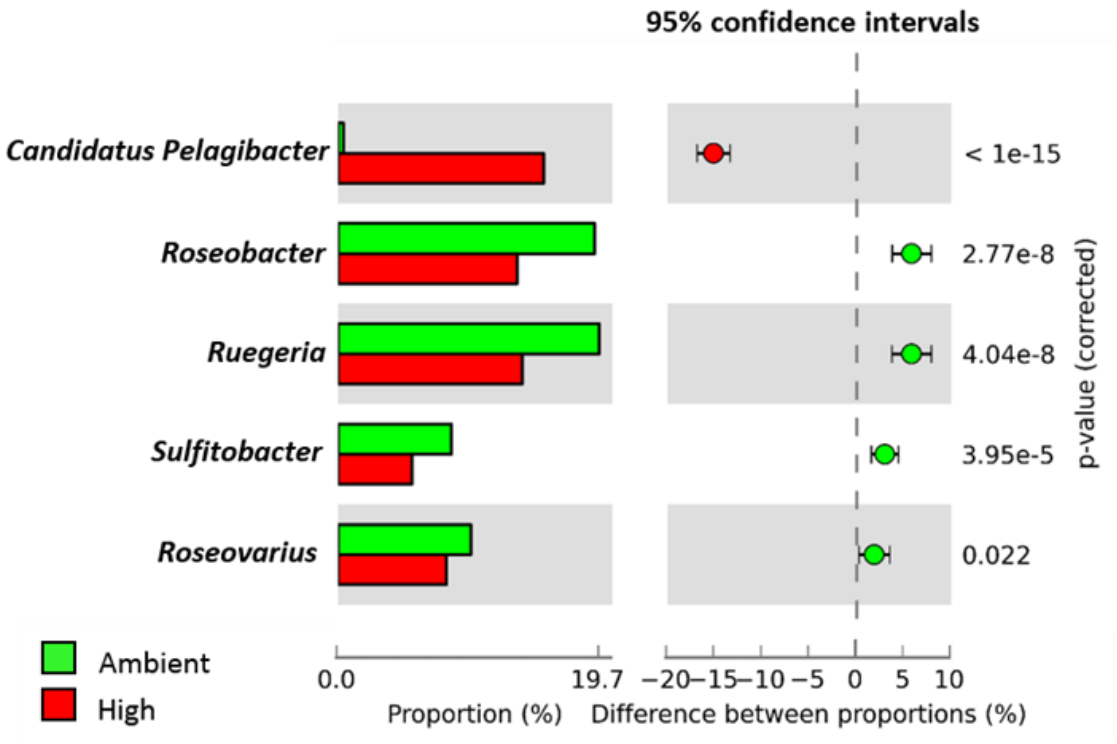

Figure 6.9 Extended error plot for 5 genera within the *Alphaproteobacteria* identified by MG-RAST from the ambient and high CO_2 metagenomes. The plot illustrates the proportion of sequences assigned to each genus and the differences between the proportions as well as the confidence interval and corrected p-value. The genera are ordered according to their corrected p-values with the ambient CO_2 metagenome represented in green and the high CO_2 metagenome represented in red. From this analysis we can be 95% confident that the difference in proportions of *Candidatus Pelagibacter* is between 13% and 18%. The analysis was conducted in STAMP using a two-sided G-test with a 95% confidence level.

Both the MG-RAST and MEGAN analyses had indicated that elevated CO_2 had a negative effect on *Rhodobacteraceae* with the percentage of reads assigned to this group reduced in the high CO_2 metagenome, 34.7% to 8.8% (MG-RAST), 16.4% to 4.6% (MEGAN). In order to determine the possible consequences this may have on ocean productivity and biogeochemical processes the read assignment were investigated at species level.

Higher resolution analysis indicated that the majority of *Rhodobacteraceae* reads recovered were from members of the marine *Roseobacter* clade particularly species from the genera *Roseobacter*, *Ruegeria*, *Sulfitobacter*, *Loktanella* and *Roseovarius* (Figure 6.10). According to the MG-RAST analysis, *Roseobacter denitrificans* dominated the *Rhodobacteraceae* in both treatments. In the ambient CO_2 metagenome *R. denitrificans* accounted for 4.9% (1,056 reads) of the total number of bacterial reads while in the high CO_2 metagenome this percentage was 1.3% (412 reads). Similar percentage decreases were also observed in the high CO_2 metagenome in nearly all the marine *Roseobacter* species identified by MG-RAST such as: *Ruegeria pomeroyi* (3.8% to 1%), *Jannaschia sp. CCS1* (1.6% to 0.4%), *Roseovarius sp*. 217 (1.1% to 0.2%), *Sulfitobacter* sp. NAS 14.1 (1% to 0.2%), *Loktanella vestfoldensis* (1% to 0.2%) and *Sulfitobacter* sp. EE-36 (0.9% to 0.2%) (Figure 6.10).

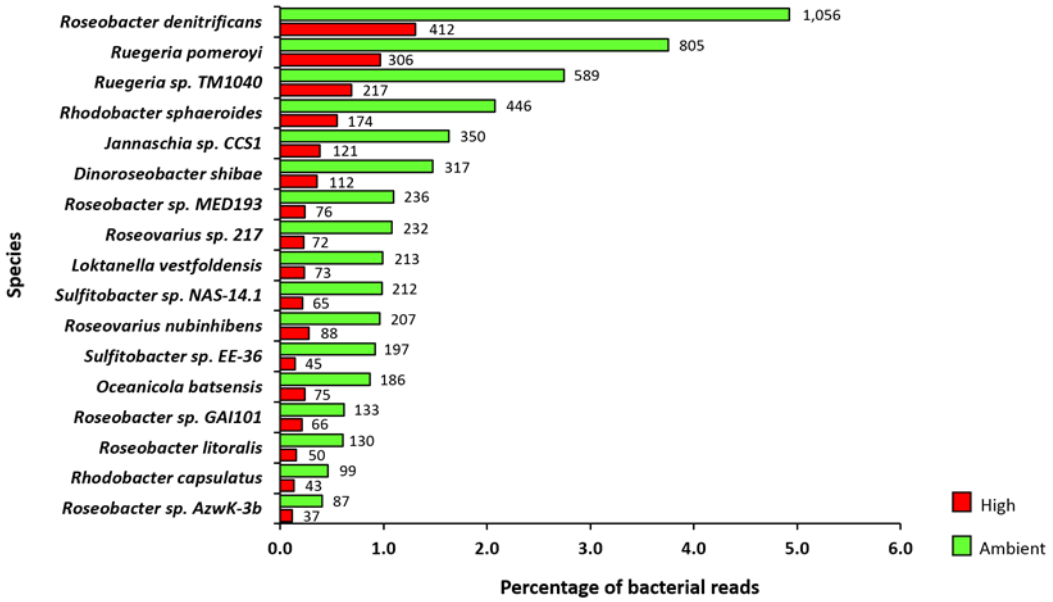

Figure 6.10 Species distribution of the percentage of reads assigned to *Rhodobacteraceae* from ambient and high CO_2 metagenomes. The percentages are calculated from the total number of bacterial reads assigned to each metagenome by MG-RAST. The actual number of reads assigned to each species is shown next to each bar on the graph.

A Similar decline in the number of marine *Roseobacter* reads was observed in the MEGAN analysis with *Roseobacter* being the dominant species of the *Rhodobacteraceae* except in this instance the majority of the reads were more closely associated to *Roseobacter sp*. AzwK-3b with 2.4% (63 reads) in the ambient CO_2 metagenome and 2.2% (22 reads) in the high CO_2 metagenome.

To determine if there was a significant difference in the proportion of *Rhodobacteraceae* species assigned to the ambient and high CO_2 metagenomes a G-test was conducted using STAMP (Parks and Beiko, 2010). The results revealed that despite the ambient CO_2 metagenome having a higher number of reads attributed to species within the *Rhodobacteraceae* most of the differences were not statistically significant (Figure 6.11). In fact, only three species were significantly more numerous (proportionally) in the ambient CO_2 metagenome, *Rhodobacteraceae bacterium* HTCC2083 (P= 0.012), *Citreicella sp*. SE45 (P=0.030) and *Rhodobacteraceae bacterium* HTCC2150 (P=0.032). *Sulfitobacter sp. EE-36* was slightly over the significance level of 0.05 with P=0.054. Conversely, two *Rhodobacteraceae* species were determined to be proportionally more numerous in the high CO_2 metagenome, *Paracoccus denitrificans* (P=0.015) and *Roseobacter sp.* GAI101 (P=0.042).

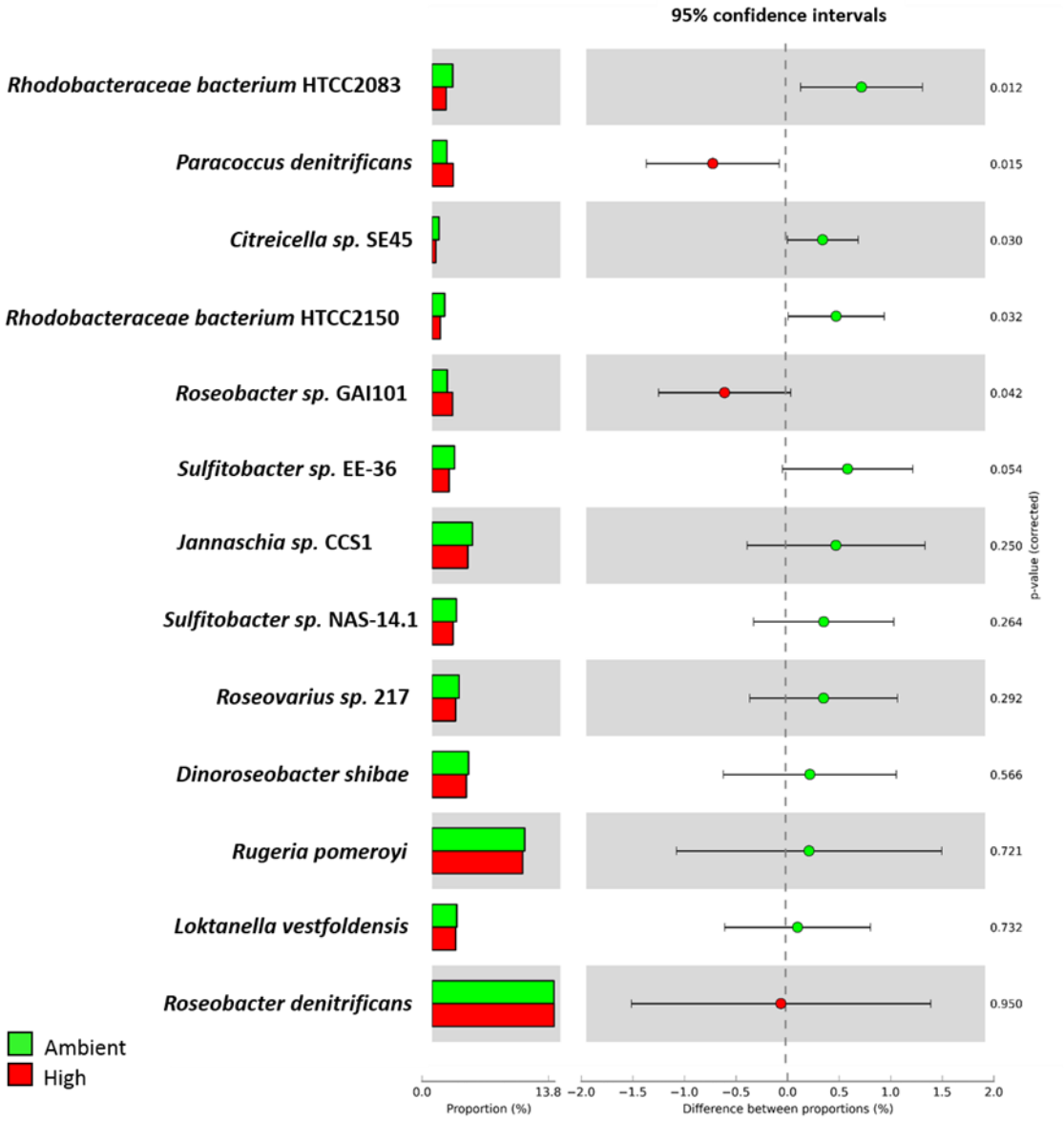

Figure 6.11 Statistical analysis of *Rhodobacteraceae* species identified in MG-RAST from the ambient and high CO_2 metagenomes. Species overrepresented in either the ambient CO_2 treatment (Green) or high CO_2 treatment (Red) are represented as having a positive difference between proportions. The analysis was conducted in STAMP using a G-test with a 95% confidence level.

Defining bacterial taxonomy at a species level is extremely difficult using these datasets due to the small size of the metagenomic libraries and the average read lengths of the sequences (high CO_2 metagenome 205 ± 75 bp, ambient CO_2 metagenome 237 ± 45 bp). Furthermore, currently accepted prokaryote taxonomy is based on Bergey's

Manual of Systematic Bacteriology (Bergey's Manual Trust, 2001) and the Taxonomic Outline of Bacteria and Archaea (TOBA) (Garrity *et al.*, 2007), both of which are based on 16S rRNA gene phylogeny complemented by one or more other genes and morphological characteristics (Sun *et al.*, 2010). As a consequence of library size (number of reads), both metagenomes contained only a few partial 16S rRNA genes (high CO_2 metagenome 18 reads, ambient CO_2 metagenome 15 reads) and therefore species identification is based primarily on protein similarity against the M5NR database.

However, the statistical analysis on the genus and family level (and to some degree species) does support the qPCR analysis of the high and ambient CO_2 treatments (Chapter 4, section 4.3.5) which showed a decrease in the abundance of 16S rRNA genes from *Rhodobacteraceae*-like bacteria from $8.85 \pm 0.9 \times 10^5$ copies/ml (ambient CO_2 treatment) to $3.86 \pm 0.3 \times 10^5$ copies/ml (high CO_2 treatment).

There is now strong evidence to support the hypothesis that elevated CO_2 decreases the abundance of *Rhodobacteraceae*-like bacteria. This decrease may not necessarily be a consequence of elevated CO_2 acting directly on the *Rhodobacteraceae* reducing abundance, but rather the consequence of elevated CO_2 having a detrimental effect on phytoplankton abundance thereby reducing primary production and/or the type of DOM produced (Chapter 3 section 3.4). This is further supported by the chlorophyll-a data (Chapter 3 section 3.31) which showed that at the peak of the bloom chlorophyll-a concentration was ~34% higher in the ambient CO_2 treatment (10.41 ± 1.14 µg/l^{-1}) compared to the high CO_2 treatment (6.87 ± 3.33 µg/l^{-1}).

6.3.3 Analysis of metabolic assignments of reads from ambient CO_2 and high CO_2 metagenomes

Analysis of functional assignments in MG-RAST revealed a reduction in the number of reads assigned to key metabolic functions in the high CO_2 treatment (Figure 6.12). All analyses of the bacterioplankton communities (16S rRNA gene clone libraries, DGGE analysis, DNA SIP analysis, qPCR and metagenome analysis) in high and

ambient CO_2 treatments indicated that there was a detrimental effect of ocean acidification on organisms from the marine *Roseobacter* clade. To determine if the decrease in metabolic functions was attributed to a reduction of marine *Roseobacter* clade the genome characteristics of this group was examined.

The marine *Roseobacter* clade is a diverse group of bacteria and members of this group have been characterised as ecological generalists (Moran *et al.*, 2007) as they possess multiple pathways for acquiring carbon and energy including carbon monoxide/hydrogen sulfide oxidation (King, 2003; Moran *et al.*, 2004, Cunliffe, 2011) and anaplerotic CO_2 fixation (Sorokin *et al.*, 2003; Moran *et al.*, 2004, Swingley *et al.*, 2007). Furthermore, they play an important role in several biogeochemical processes such as the degradation of algal derived dimethylsulfoniopropionate (DMSP) (González *et al.*, 1999; Yoch, 2002, Moran *et al.*, 2012), aerobic anoxygenic photosynthesis (Yurkov and Beatty, 1998; Beja *et al.*, 2002, Allgaier *et al.*, 2003) and in the oxidation and cycling of manganese (Mn) (Hansel and Francis, 2006, Learman *et al.*, 2011). Five C1 utilization pathways have been identified in *Roseobacter* genomes (serine cycle, methanol oxidation, trimethylamine oxidation, formaldehyde oxidation and formate oxidation) as well as six identified aromatic degradation pathways (b-ketoadipate, gentisate, benzoate, phenylacetic acid, homoprotocatechuate and homogenisate) (Newton *et al.*, 2010).

Members of the marine *Roseobacter* clade typically inhabit nutrient replete planktonic aggregates where components of eukaryotic cytosols (polyamines, taurine, phosphoesters, phosphonates, glyoxylate, allophanate, acetate, glycine betaine, branched-chain amino acids, organic acids and DMSP) may become available through exudation, diffusion driven loss or viral lysis and grazing (Moran *et al.*, 2007). Organic nitrogen and ammonium are the primary sources of nitrogen which is in keeping with their vertical distribution (surface waters) and their close association with nitrogen rich planktonic cells (Moran *et al.*, 2007).

Given the significant effects seen on the marine *Roseobacter* group and their important role in the processes outlined above, functional analysis of the metagenomes focussed on key genes relevant to DMSP metabolism (DMSP demethylase), ammonium transporters, CO dehydrogenase and photoreaction centre subunits.

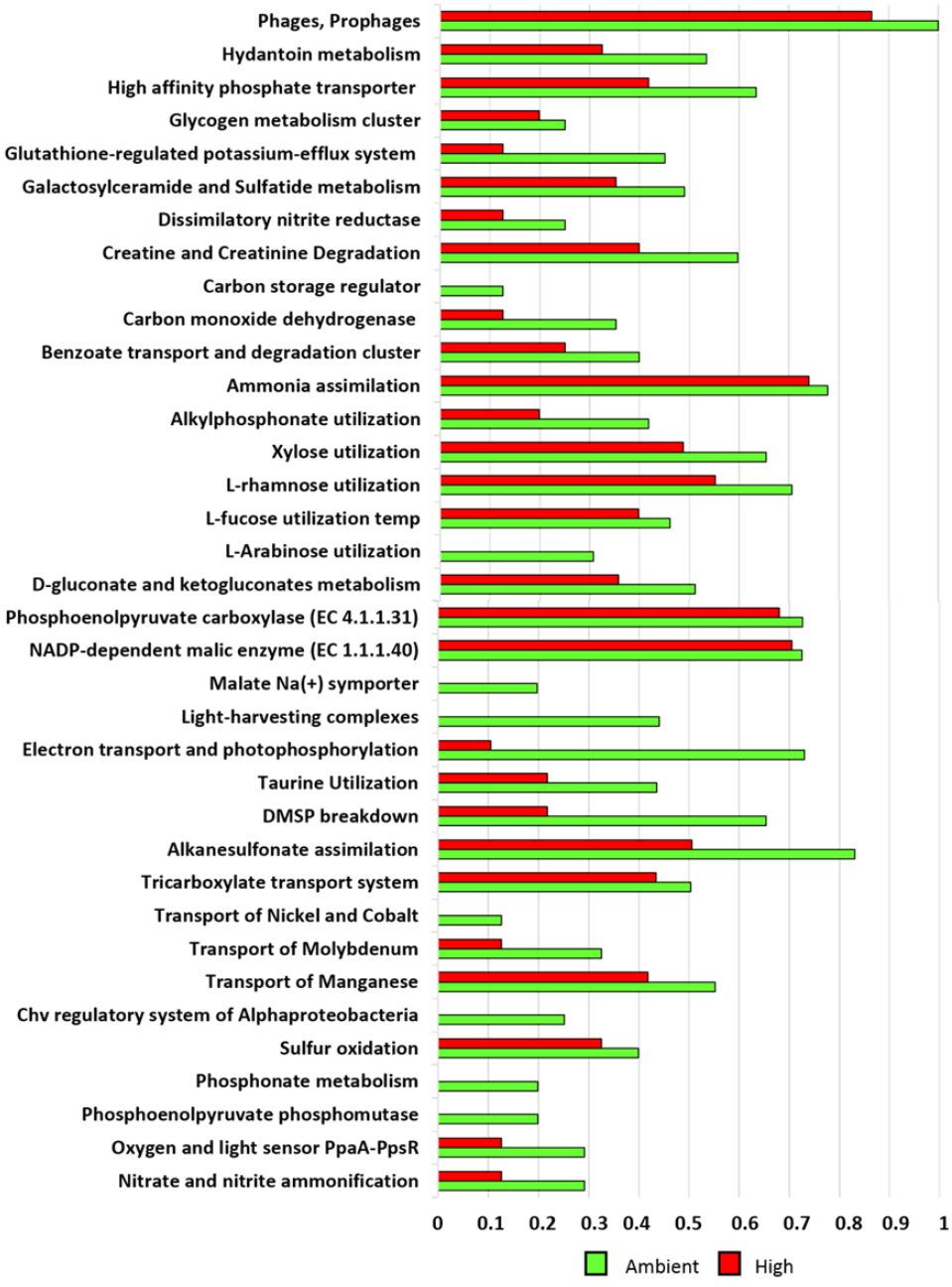

Figure 6.12 Functional analysis of ambient and high CO_2 metagenomic libraries illustrating the decrease in the number of reads assigned to specific metabolic functions. The data have been normalised using a scale of 0 – 1 in order to allow for comparison of different sized datasets.

6.3.3.1 DMSP Demethylase

The phylogenetic analysis indicated that the majority of *Rhodobacteraceae* sequences were recovered from members of the marine *Roseobacter* clade which play an important role in the marine sulfur cycle and are abundant in dimethylsulfoniopropionate (DMSP) rich algal blooms. It has been proposed that this bacterial group dominate the demethylation pathway in phytoplankton blooms in coastal regions, where DMSP concentrations are high (Howard *et al.*, 2006).

The enzymes which catalyze the demethylation/demethiolation of DMSP to methanethiol (MeSH) are DMSP demethylase (*DmdA*), MMPA-CoA ligase (*DmdB*), MMPA-CoA dehydrogenase (*DmdC*), and methylthioacryloyl-CoA hydratase (*DmdD*). The initial step in the demethylation pathway is the removal of a methyl group from DMSP to form methylmercaptopropionate (MMPA) (Figure 6.13). MMPA is then further processed through a demethiolation pathway requiring three coenzyme A (CoA)–mediated reactions (Reisch *et al.*, 2011). The pathway results in the generation of MeSH, acetaldehyde, CO_2 and a CoA. MeSH, is a source of cellular sulfur for marine bacteria where it is incorporated into sulfur-containing amino acids or may be oxidized via MeSH-oxidase resulting in the formation of formaldehyde, hydrogen sulfide and hydrogen peroxide (Reisch *et al.*, 2011). It has been estimated that the *dmdA* gene (which is currently only known to occur in marine bacteria) is particularly abundant with approximately 27% of cells in ocean surface waters possessing the gene (Moran *et al.*, 2012).

The gene *dmdA* was originally annotated as a glycine cleavage T-protein (GcvT) due to the high degree of sequence similarity and the requirement for the cofactor tetrahydrofolate (THF) used to accept the methyl group (Reisch *et al.*, 2011). In *dmdA* the transfer of the *S*-methyl group from DMSP form 5-methyl-THF and MMPA while other enzymes in the GcvT family result in the production of 5,10 methylene-THF (Schubert *et al.*, 2003, Schuller *et al.*, 2012).

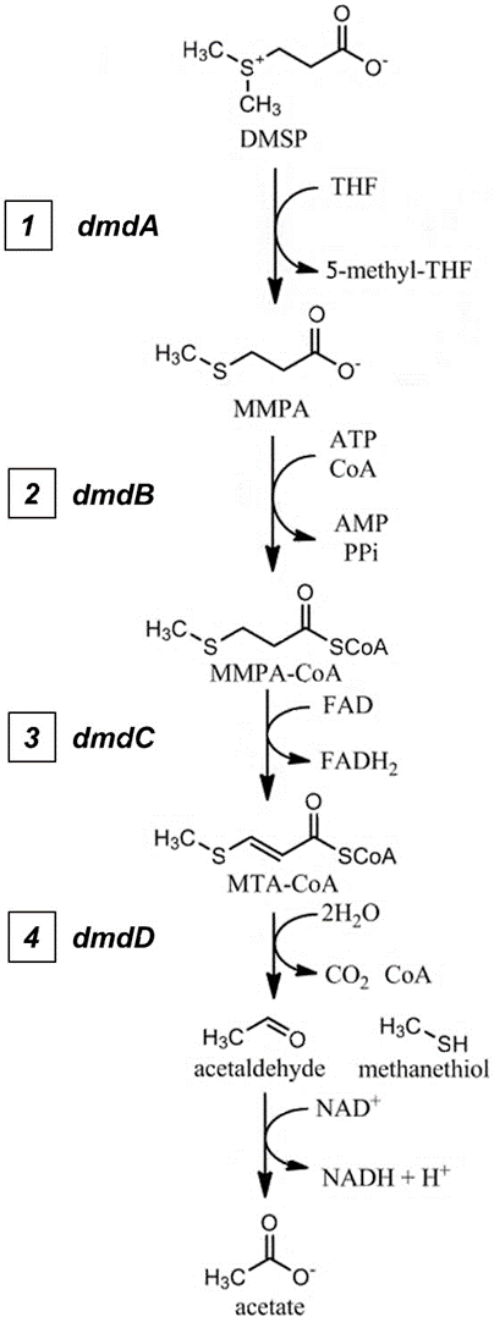

Figure 6.13 Diagram adapted from Reisch et al (2011) illustrating the demethylation/demethiolation pathway of DMSP degradation with the name of the gene involved in each step of the pathway. The first step is the removal of a methyl group from DMSP to form methylmercaptopropionate (MMPA) (1). MMPA is then converted to MMPA-CoA via MMPA-CoA ligase (2). This is then dehydrogenated forming an enoyl-CoA intermediate, methylthioacrylyl (MTA-CoA) (3). MTA-CoA is hydrated by MTA-CoA hydratase to release the product methane thiol (MeSH) as well as CoA, CO_2 and acetaldehyde (4). Acetaldehyde dehydrogenase then oxidizes acetaldehyde to acetate.

The assignment of pyrosequencing reads to metabolic subsystems in MG-RAST indicated that 2 reads in the high CO_2 metagenome were assigned to DMSP breakdown whereas 9 reads were assigned to the ambient CO_2 metagenome. Of the 11 reads recovered, 8 were partial fragments of the *dmdA* gene, 2 were assigned as aminotransferase involved in DMSP breakdown and 1 was identified as partial fragment of the DMSP demethylase transcriptional regulator (Table 6.1).

No sequences were detected from the demethiolation pathway (*dmdB*, *dmdC* and *dmdD*) in either of the metagenomes. Marine metagenomic studies have revealed that the DMSP demethylase gene (*dmdA*) is taxonomically diverse and is present in >50% of bacterioplankton species (Howard *et al.*, 2008). Similar to *dmdA*, the genes which encode *dmdB* and *dmdC* are also abundant in metagenomic datasets. However they belong to gene families with many different functions and therefore can easily be misidentified (Reisch *et al.*, 2011). In contrast, the *dmdD* gene is rare compared to the other genes in the DMSP degradation pathway being present in only 0.1% of the cells in the Global Ocean Sampling (GOS) metagenomic dataset while *dmdB* and *dmdC* genes were present in 61% of the cells (Reisch *et al.*, 2011, Moran *et al.*, 2012).

Table 6.1 MG-RAST metabolic analysis of ambient and high CO_2 metagenomes depicting reads associated to DMSP breakdown.[1]

Metagenome	Level 1	Level 2	Level 3	Function	Avg eValue	Avg % ident	Avg align len	Hits
Ambient CO_2	Sulfur Metabolism	Organic sulfur assimilation	DMSP breakdown	Aminotransferase involved in DMSP breakdown	-27	88.89	63	2
Ambient CO_2	Sulfur Metabolism	Organic sulfur assimilation	DMSP breakdown	DMSP demethylase EC 2.1.2.10	-18.38	75.04	55.75	7
High CO_2	Sulfur Metabolism	Organic sulfur assimilation	DMSP breakdown	DMSP demethylase EC 2.1.2.10	-24	68	74.5	1
High CO_2	Sulfur Metabolism	Organic sulfur assimilation	DMSP breakdown	DMSP demthylase transcriptional regulator	-26	81.33	75	1

All the reads identified in the MG-RAST analysis had their sequence assignments verified by comparing them against the GenBank protein nr database using BLASTX. The results revealed that the reads were between 60 – 95% identical on a protein level to known genes associated with DMSP breakdown (Table 6.2) with the majority of reads (6 out of 11) being highly similar to dimethyl sulfoniopropionate demethylase (Figure 6.14 and Appendix 1). Furthermore, 73% (8 reads) had a high similarity to proteins closely associated to the marine *Roseobacter* clade. At a higher phylogenetic level they had a high degree of similarity to species within the genera *Ruegeria* (4 reads), *Roseobacter* (1 read), *Thalassobacter* (1 read), *Loktanella* (1 read) and *Octadecabacter* (1 read). The remaining 3 reads were closely associated to *Candidatus Pelagibacter*, two of which were derived from the high CO_2 metagenome (Table 6.2).

Statistical analysis of the reads using a G-test in the STAMP software package revealed a significant difference in the number of reads assigned to genes involved in DMSP degradation between the libraries (P=0.037) suggesting the ambient CO_2 metagenome had a greater metabolic potential for the utilization of DMSP than its high CO_2 counterpart. Interestingly, no reads were recovered from either metagenome from

[1] Reads were annotated using the MG-RAST subsystems database with the following parameter; maximum e-value cutoff 1e-5, minimal % cutoff 60% and minimal alignment length cutoff 15.

the alternate DMSP degradation pathway which results in the production of DMS. However, this was not entirely unexpected as the genes involved in the DMSP lyase pathway (*dddD*, *dddL*, *dddP*, *dddQ*, *dddW*, and *dddY*) are up to two orders of magnitude less abundant in the ocean than the bacterial DMSP demethylation genes (Todd *et al.*, 2009; Reisch *et al.*, 2011, Todd *et al.*, 2011, Moran *et al.*, 2012). This is consistent with the fact that DSMP is mostly catabolized via the demethylation pathway (*dmdA*) due to the abundance of *Roseobacter* and SAR11 clade bacteria (Curson *et al.*, 2011).

Table 6.2 Results of similarity analysis showing the top hit for each of the 11 reads associated to DMSP breakdown identified by MG-RAST.[2]

Description	Max score	Total score	Query cover	E value	Ident	Accession	Align start	Align end	Library
Dimethyl sulfoniopropionate demethylase [*Candidatus Pelagibacter sp*. HTCC7211]	95.1	95.1	68%	1.00E-21	76%	WP_008546106.1	7	60	Ambient
Dimethyl sulfoniopropionate demethylase [*Ruegeria lacuscaerulensis*]	154	154	84%	3.00E-43	91%	WP_005983312.1	183	258	Ambient
Dimethyl sulfoniopropionate demethylase [*Ruegeria sp.* TW15]	68.6	68.6	53%	7.00E-12	70%	WP_010439960.1	218	263	Ambient
Dimethyl sulfoniopropionate demethylase [*Ruegeria sp. TM1040*]	35	65.5	97%	0.004	89%	YP_613439.1	366	383	Ambient
Dimethyl sulfoniopropionate demethylase [*Candidatus Pelagibacter sp*. HTCC7211]	113	113	99%	3.00E-28	65%	WP_008546106.1	62	139	Ambient
Dimethyl sulfoniopropionate demethylase [*Candidatus Pelagibacter ubique*]	97.1	97.1	90%	2.00E-22	60%	WP_006997663.1	65	134	High
Aminomethyltransferase GcvT [*Octadecabacter arcticus* 238	180	180	99%	5.00E-53	89%	YP_007698959.1	17	103	Ambient
Aminotransferase [*Roseobacter denitrificans* OCh 114]	123	123	96%	7.00E-32	90%	YP_682561.1	173	235	Ambient
Aminotransferase [*Ruegeria pomeroyi* DSS-3]	134	134	82%	1.00E-35	89%	YP_167151.1	1	71	Ambient
Glycine cleavage system protein T [*Loktanella vestfoldensis SKA53*]	158	158	99%	6.00E-45	95%	WP_007205555.1	70	147	Ambient
DMSP demethylase transcriptional regulator [*Thalassobacter arenae*]	125	125	92%	1.00E-33	79%	WP_021100141.1	7	83	High

[2] Reads were aligned in the NCBI using BLASTX (protein search against a translated nucleotide query) against the non-redundant protein database.

dimethyl sulfoniopropionate demethylase [Ruegeria lacuscaerulensis]

Sequence ID: ref|WP_005983312.1| **Length:** 367 **Number of Matches:** 1

Range 1: 183 to 258 GenPept Graphics ▼ Next Match ▲ Previous Match

Score	Expect	Method	Identities	Positives	Gaps	Frame
154 bits(388)	3e-43	Composition-based stats.	69/76(91%)	72/76(94%)	0/76(0%)	-1

```
Query  230  FKADEMAIARSGYSKQGGFEIYVEGSDIGMPLWNALFAAGEDLNVRAGCPNLIERIEGGL  51
            F+  ++AIARSGYSKQGGFEIYVEGSDIGMPLWNALFAAG DL VRAGCPNLIERIEGGL
Sbjct  183  FEGRDLAIARSGYSKQGGFEIYVEGSDIGMPLWNALFAAGGDLQVRAGCPNLIERIEGGL  242

Query  50   LSYGNDMTDDNTPHEC  3
            LSYGNDMTDDNTPHEC
Sbjct  243  LSYGNDMTDDNTPHEC  258
```

Figure 6.14 Sequence alignment of a read identified by MG-RAST as being associated to DMSP breakdown. The analysis was conducted using BLASTX against the non-redundant protein database.

6.3.3.2 Ammonium transporters

Further differences in the metabolic potential between the metagenomes were observed in MG-RAST using subsystems assignments. In the ambient CO_2 treatment 11 reads were assigned as ammonium transporters while none was found in the high CO_2 treatment. To corroborate the assignments the reads were compared against the GenBank database using the BLASTX program. The analysis confirmed the MG-RAST assignments with a percentage identity of 71 – 98% on a protein level (Table 6.3) all of which were classified as ammonia transporters (Figure 6.15 and Appendix 1). The majority of the reads were assigned to members of the marine *Roseobacter* clade with *Phaeobacter gallaeciensis* (2 reads), *Roseobacter sp.* MED193 (1 read), *Roseovarius nubinhibens* (1 read) and *Rhodobacteraceae bacterium* HTCC2083 (1 read). *Phaeobacter gallaeciensis* is known to be an effective colonizer of biotic and abiotic marine surfaces able to produce the antibacterial compound tropodithietic acid (TDA) which gives them a competitive advantage over other species when colonizing phytoplankton hosts (Geng *et al.*, 2008, Thole *et al.*, 2012).

Three of the reads were assigned to the oligotrophic marine *Gammaproteobacteria* (OMG) group (Cho and Giovannoni, 2004). Two of these reads were highly similar to sequences from marine *gammaproteobacterium* HTCC2080 in the OM60/NOR5 clade. Organisms from this clade are ubiquitous throughout the euphotic

zone and can comprise up to 11% of the total bacterial population (Pernthaler and Pernthaler, 2005, Yan *et al.*, 2009). Furthermore, the OM60/NOR5 clade has been shown to contain aerobic, anoxygenic, phototrophic bacteria (AAnPs) with predicted phototrophy genes in the HTCC2080 genome (Cho *et al.*, 2007, Thrash *et al.*, 2010). The remaining read assigned to the OMG group was most similar to gammaproteobacterium HTCC2207 from the SAR92 clade which utilizes proteorhodopsin as a method of light-driven energy generation. This bacterium is highly motile and contains several genes involved in complex carbohydrate degradation via cell aggregation and direct binding to cellulose and xylan (Fraiberg *et al.*, 2010, Gifford *et al.*, 2013).

The remaining 3 reads were closely associated to *Flavobacteria* (2 reads) and *Cytophaga* (1 read) within the phylum *Bacteroidetes*. This group of bacteria are frequently observed attached to phytoplankton aggregates and are known to degrade and consume high molecular weight organic matter (DeLong *et al.*, 1993).

A G-test of the reads assigned as ammonium transporters was conducted showing that the representation of reads assigned as ammonium transporters was significantly greater in the metagenome from the ambient CO_2 treatments ($P=<0.05$).

Table 6.3 Results of similarity analysis showing the top hit for each of the 11 reads assigned as ammonia transporters identified by MG-RAST.[3]

Description	Max score	Total score	Query cover	E value	Ident	Accession	Align start	Align end	Library
Ammonium transporter [Marine gamma proteobacterium HTCC2080]	139	139	98%	2.00E-37	98%	WP_007235465.1	257	341	Ambient
Ammonium transporter [Phaeobacter gallaeciensis DSM 17395]	96.7	96.7	100%	9.00E-22	87%	YP_006574316.1	64	149	Ambient
Ammonium transporter [Rhodobacteraceae bacterium HTCC2083]	86.3	86.3	55%	4.00E-18	91%	WP_009828878.1	395	440	Ambient
Ammonium transporter [Phaeobacter gallaeciensis]	55.5	90.5	98%	2.00E-10	71%	WP_019296213.1	322	387	Ambient
Ammonium transporter [Roseobacter sp. MED193]	133	133	99%	6.00E-35	94%	WP_009810666.1	231	317	Ambient
Ammonium transporter [Roseovarius nubinhibens]	135	135	95%	4.00E-36	94%	WP_009813814.1	136	204	Ambient
Ammonium transporter [Owenweeksia hongkongensis DSM 17368]	77	141	98%	2.00E-25	71%	YP_004990125.1	299	347	Ambient
Ammonium transporter [Marine gamma proteobacterium HTCC2080]	86.3	86.3	86%	4.00E-18	87%	WP_007235465.	1	71	Ambient
Ammonium transporter [Croceibacter atlanticus HTCC2559]	73.9	73.9	68%	7.00E-14	73%	YP_003716094.1	332	376	Ambient
Ammonium transporter [Marine gamma proteobacterium HTCC2207]	123	123	95%	1.00E-31	94%	WP_007233085.1	145	221	Ambient
Ammonium transporter [Cytophaga aurantiaca]	84.3	84.3	98%	5.00E-18	84%	WP_018341692.1	70	119	Ambient

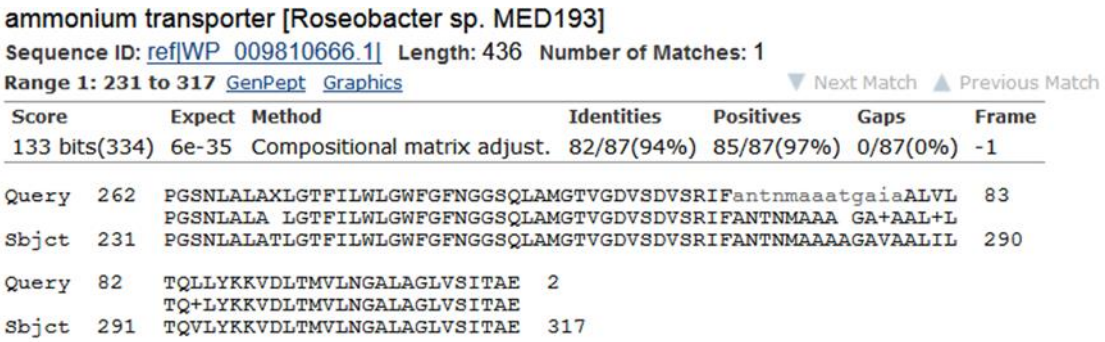

Figure 6.15 Sequence alignment of a read identified as an ammonium transporter by MG-RAST. The analysis was conducted in the NCBI using BLASTX against the non-redundant protein database.

[3] Reads were aligned in the NCBI using BLASTX (protein search against a translated nucleotide query) against the non-redundant protein database.

6.3.3.3 Carbon monoxide dehydrogenase

Due to photodegradation of organic matter the surface waters of the oceans are saturated with carbon monoxide (CO) which can be utilized by CO metabolizing marine organisms (Tolli *et al.*, 2006). It has been revealed that microbial CO oxidation rates can be an order of magnitude greater in coastal waters (0.01 to 0.11 h^{-1}) than those measured in oligotrophic environments (0.01 to 0.02 h^{-1}) suggesting that the key players in this process are microbial communities which inhabit the nutrient rich waters of the continental shelf (Tolli, 2003, Tolli, 2005). The vast majority of bacteria in the marine *Roseobacter* clade are able to oxidize CO to CO_2 via the gene carbon monoxide dehydrogenase and as such are considered to be important players in marine CO cycling (Tolli *et al.*, 2006, Cunliffe, 2011). Although they are not able to assimilate the carbon dioxide produced directly into biomass they can add it to pyruvate, aspartate or glutamate via a series of reactions to produce oxaloacetate for anaplerosis (Chapter 5, section 5.3.11). These organisms are therefore classified as chemolithoheterotrophs that use CO as an additional energy source.

Thirteen reads were assigned as carbon monoxide dehydrogenases by MG-RAST which were verified by BLAST analysis. The read assignments had a sequence identity of 64 – 99% on a protein level (Table 6.4) with 12 reads classified as either CO dehydrogenase or a CO dehydrogenase subunit (Figure 6.16 and Appendix 1). The remaining read was identified as a dehydrogenase but had a higher similarity to xanthine dehydrogenase than CO dehydrogenase. On a phylogenetic level, eleven of these reads were closely associated to *Rhodobacteraceae*, ten of which were highly similar to sequences from the marine *Roseobacter* clade. Ten reads were derived from the ambient CO_2 treatment and had high sequence similarity to the genera *Roseobacter* (3 reads), *Sulfitobacter* (3 reads), *Jannaschia* (2 reads), *Sagittula* (1 read) and *Oxalobacteraceae* (1 read) from the *Betaproteobacteria*. In contrast, 3 reads were derived from the high CO_2 treatment with a high sequence similarity to the genera *Roseobacter*, *Ruegeria* and *Stappia* (which is not a classified as a marine *Roseobacter*).

Statistical analysis using a G test in the STAMP software package revealed a significant difference (P=<0.050) in the proportion of CO dehydrogenase reads between the ambient and high CO_2 mesocosms.

Table 6.4 Results of similarity analysis showing the top hit for each of the 13 reads assigned as carbon monoxide dehydrogenase identified by MG-RAST.[4]

Description	Max score	Total score	Query cover	E value	Ident	Accession	Align start	Align end	Library
Carbon monoxide dehydrogenase form I large subunit [Ruegeria sp. WHOI JT-08]	160	160	99%	1.00E-45	96%	AAW88347.1	287	367	High
Carbon monoxide dehydrogenase form II large subunit [Stappia sp. M8]	110	110	85%	7.00E-27	78%	AAP75596.1	149	217	High
Carbon monoxide dehydrogenase [Roseobacter sp. MED193]	80.1	182	98%	2.00E-31	92%	WP_009810137.1	260	297	High
Carbon monoxide dehydrogenase [Sulfitobacter sp. EE-36]	108	108	73%	1.00E-27	90%	WP_005849705.1	85	144	Ambient
Carbon monoxide dehydrogenase [Roseobacter sp. SK209-2-6]	120	120	91%	1.00E-30	81%	WP_008206634.1	167	238	Ambient
Carbon monoxide dehydrogenase subunit G [Jannaschia sp. CCS1]	125	125	97%	6.00E-35	95%	YP_510032.1	4	65	Ambient
Carbon monoxide dehydrogenase [Oxalobacteraceae bacterium IMCC9480]	87.4	87.4	80%	3.00E-18	73%	WP_009665216.1	640	680	Ambient
Carbon-monoxide dehydrogenase [Sagittula stellata]	115	115	98%	2.00E-29	84%	WP_005860860.1	85	159	Ambient
Carbon-monoxide dehydrogenase [Sulfitobacter sp. EE-36]	120	120	97%	8.00E-30	86%	WP_005853007.1	163	225	Ambient
Carbon monoxide dehydrogenase, large subunit [Jannaschia sp. CCS1]	169	169	98%	5.00E-47	99%	YP_510037.1	341	420	Ambient
Carbon monoxide dehydrogenase [Roseobacter sp. SK209-2-6]	148	148	99%	3.00E-43	89%	WP_008206629.1	3	81	Ambient
Carbon monoxide dehydrogenase [Sulfitobacter sp. EE-36]	112	112	100%	5.00E-29	83%	WP_005849705.1	49	134	Ambient
Dehydrogenase [Roseobacter denitrificans OCh 114]	110	110	99%	4.00E-26	64%	YP_682064.1	63	145	Ambient

[4] Reads were aligned in the NCBI using BLASTX (protein search against a translated nucleotide query) against the non-redundant protein database.

carbon monoxide dehydrogenase, large subunit [Jannaschia sp. CCS1]

Sequence ID: ref|YP_510037.1| **Length:** 808 **Number of Matches:** 1

Range 1: 341 to 420 GenPept Graphics ▼ Next Match ▲ Previous Match

Score	Expect	Method	Identities	Positives	Gaps	Frame
169 bits(427)	5e-47	Compositional matrix adjust.	79/80(99%)	80/80(100%)	0/80(0%)	-2

```
Query  242  FDACADPTKFPAGFMNICTGSYDIPTAYLEVDGVYTNKAPGGVSYRCSFRVTEAVYFIER  63
            FDACADPTKFPAGFMNICTGSYDIPTAYLEVDGVYTNKAPGGVSYRCSFRVTEAVYFIER
Sbjct  341  FDACADPTKFPAGFMNICTGSYDIPTAYLEVDGVYTNKAPGGVSYRCSFRVTEAVYFIER  400

Query  62   MIEVLAIELNMDSAELRRIN  3
            MIEVLAIELNMD+AELRRIN
Sbjct  401  MIEVLAIELNMDAAELRRIN  420
```

Figure 6.16 Sequence alignment of a read identified as carbon monoxide dehydrogenase by MG-RAST. The analysis was conducted in the NCBI using BLASTX against the non-redundant protein database.

6.3.3.4 Photoreaction centre subunits

Aerobic anoxygenic phototrophs (AAnPs) are a group of bacteria that use bacteriochlorophyll to support phototrophic electron transport, thereby supplementing cellular energy requirements and reducing the need for respiratory oxidation of organic substrates. The first AAnPs described belonged to the marine *Roseobacter* group (Shiba *et al.*, 1979) and for decades it was believed that this attribute was confined to species within the *Alphaproteobacteria* (Kolber *et al.*, 2001). However, metagenomic studies of the genes responsible for the synthesis of bacteriochlorophyll and the associated photosynthetic reaction centres indicated that uncultured *Gammaproteobacteria* included a significant number of AAnPs in bacterioplankton assemblages (Beja *et al.*, 2002, Moran and Miller, 2007).

An indicator of AAnPs is the presence of *puf* genes coding for the subunits of the light-harvesting complex (*pufB* and *pufA*) and the photosynthetic reaction centre complex (*pufC*, *pufL* and *pufM*) (Beja *et al.*, 2002). MG-RAST analysis of the metagenomic datasets revealed that 15 reads in total were assigned as being partial fragments of *puf* genes with 14 reads derived from the ambient CO_2 treatment and 1 read from the high CO_2 treatment (Table 6.5). BLAST analysis verified the metagenomic assignments with identities ranging from 65 – 100% on a protein level (Figure 6.17 and Appendix 1). In the ambient CO_2 treatment 11 out of the 14 sequences were closely associated with the

marine *Roseobacter* clade with a high similarity to sequences from the genera: *Roseobacter* (6 reads), *Thalassiobium* (3 reads), *Roseovarius* (1 read) and *Loktanella* (1 read). The remaining 3 reads were assigned as marine *Gammaproteobacteria* HTCC2080 in the OM60/NOR5 clade which is the first cultured marine *Gammaproteobacteria* known to possess genes for aerobic anoxygenic photosynthesis (Cho *et al.*, 2007). The only read derived from the high CO_2 treatment metagenome was assigned as a possible photosynthetic complex from the marine *Roseobacter* species *Roseobacter* sp. Azwk-3b.

A G test conducted using STAMP revealed a significant difference between the metagenomes in the proportions of all the *puf* genes (*pufC, pufL* and *pufM*) ($P=<0.05$).

Table 6.5 Results of similarity analysis showing the top hit for each of the 15 reads assigned as photoreaction centre subunits identified by MG-RAST.[5]

Description	Max score	Total score	Query cover	E value	Ident	Accession	Align start	Align end	Library
Possible photosynthetic co [Roseobacter sp. AzwK-3b]	112	112	96%	8.00E-29	65%	WP_007814221.	100	179	High
Photosynthetic reaction center subunit L [Roseovarius sp. TM1035]	134	134	98%	1.00E-36	93%	WP_008280384.1	166	248	Ambient
Photosynthetic reaction center cytochrome C subunit [Marine gamma proteobacterium HTCC2080]	179	179	98%	6.00E-53	100%	WP_007234725.1	224	303	Ambient
Photosynthetic reaction center cytochrome C subunit [Marine gamma proteobacterium HTCC2080]	105	105	80%	2.00E-25	67%	WP_007234725.1	258	323	Ambient
Photosynthetic reaction center M subunit, partial [Loktanella sp. RCC2642]	142	142	95%	5.00E-42	97%	AEV66157.1	3	73	Ambient
Photosynthetic reaction center subunit M [Marine gamma proteobacterium HTCC2080]	124	124	99%	1.00E-32	100%	WP_007234726.1	220	298	Ambient
Photosynthetic reaction center M subunit [Roseobacter sp. B11]	129	129	95%	8.00E-35	88%	ABX83042.1	125	209	Ambient
Photosynthetic reaction center cytochrome C subunit [Roseobacter sp. AzwK-3b]	130	130	98%	3.00E-34	76%	WP_007814237.1	236	313	Ambient
Photosynthetic reaction center subunit M [Thalassiobium sp. R2A62]	49.7	49.7	49%	2.00E-05	97%	WP_009159933.1	270	308	Ambient
Photosynthetic reaction center cytochrome c subunit [Roseobacter litoralis Och 149]	137	137	87%	4.00E-37	81%	YP_004716611.1	1	78	Ambient
Photosynthetic reaction center subunit M [Roseobacter denitrificans OCh 114]	79.7	79.7	65%	5.00E-16	97%	YP_680524.1	274	331	Ambient
Photosynthetic reaction center cytochrome c subunit [Roseobacter litoralis Och 149]]	76.3	132	98%	6.00E-23	80%	YP_004716611.1	122	161	Ambient
Photosynthetic complex assembly protein [Roseobacter denitrificans OCh 114]	40.4	78.2	53%	8.00E-07	53%	YP_680553.1	17	48	Ambient
Photosynthetic reaction center subunit L [Thalassiobium sp. R2A62]	155	155	98%	8.00E-45	98%	WP_009159999.1	152	233	Ambient
Photosynthetic reaction center subunit L [Thalassiobium sp. R2A62]	90.9	142	99%	7.00E-26	91%	WP_009159999.1	68	111	Ambient

[5] Reads were aligned in the NCBI using BLASTX (protein search against a translated nucleotide query) against the non-redundant protein database.

Photosynthetic reaction center cytochrome C subunit [marine gamma proteobacterium HTCC2080]
Sequence ID: ref|WP_007234725.1| **Length:** 382 **Number of Matches:** 1

Range 1: 224 to 303 GenPept Graphics ▼ Next Match ▲ Previous Match

Score	Expect	Method	Identities	Positives	Gaps	Frame
179 bits(454)	6e-53	Compositional matrix adjust.	80/80(100%)	80/80(100%)	0/80(0%)	-3

```
Query  241  LPNGNRSSVKQTEYIYSLMMHFSDSLGVNCTHCHNTRAFYDWEQSSPARVRAWHGIRMVR  62
            LPNGNRSSVKQTEYIYSLMMHFSDSLGVNCTHCHNTRAFYDWEQSSPARVRAWHGIRMVR
Sbjct  224  LPNGNRSSVKQTEYIYSLMMHFSDSLGVNCTHCHNTRAFYDWEQSSPARVRAWHGIRMVR  283

Query  61   EMNTKYVNQTTDWLPDHRKG  2
            EMNTKYVNQTTDWLPDHRKG
Sbjct  284  EMNTKYVNQTTDWLPDHRKG  303
```

Figure 6.17 Sequence alignment of a read identified as a photoreaction centre subunits by MG-RAST. The analysis was conducted in the NCBI using BLASTX against the non-redundant protein database.

In all the metabolic assignments investigated, it is worth noting that in all cases the genes being analyzed were present in significantly lower proportions in the high CO_2 treatment ($P<0.05$) (Figure 6.18). Furthermore, the number of gene related reads from the high CO_2 metagenome was exceptionally low for a dataset which contained ~47% more reads (31,520 versus 21,454 reads) than its ambient counterpart. We hypothesize that the decrease in gene abundance represents a reduction in marine *Roseobacter* cell numbers in the high CO_2 treatment caused by a reduction in primary production (Chapter 3 section 3.32).

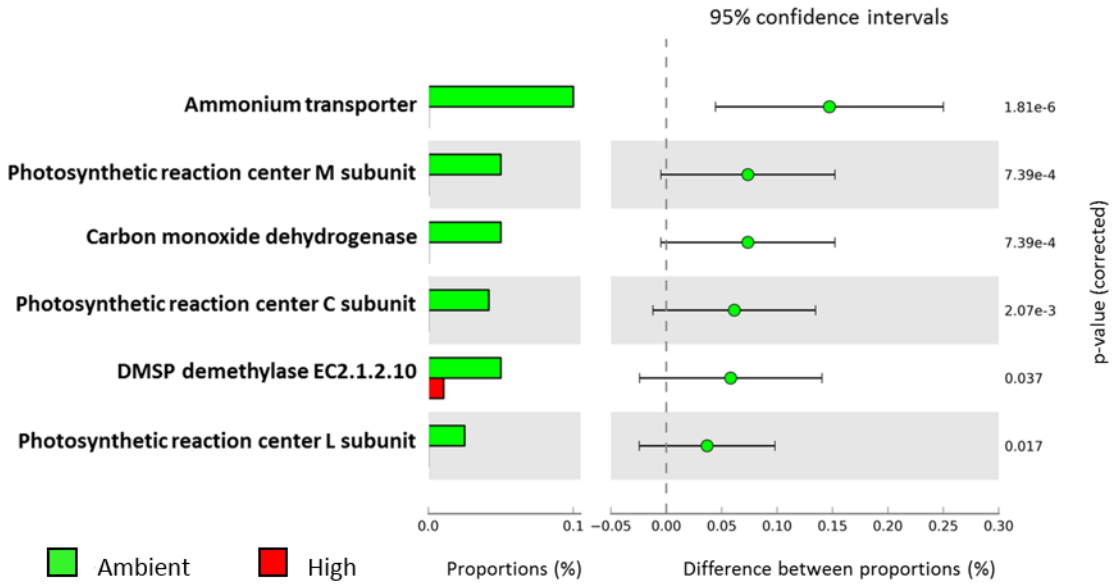

Figure 6.18 Statistical analysis of metabolic profiles identified in MG-RAST from the ambient and high CO_2 treatments. Genes overrepresented in the ambient CO_2 treatment (Green) are denoted as having a positive difference between proportions. The analysis was conducted in STAMP using a G-test with a 95% confidence level.

Members of the marine *Roseobacter* clade of *Alphaproteobacteria* are among the most abundant and ecologically relevant marine bacteria in the oceans playing a fundamental role in carbon and sulfur cycling as well as the global climate. Furthermore, these organisms are vital to the ecology of the oceans as they form symbiotic relationships with diverse marine organisms such as squid and cuttlefish (Grigioni *et al.*, 2000, Barbieri *et al.*, 2001), marine red algae (Ashen and Goff, 2000) and sponges (Althoff *et al.*, 1998, Webster *et al.*, 2004). The evidence presented in this study strongly suggests that the predicted decrease in ocean pH caused by increasing concentrations of atmospheric CO_2 will be accompanied by a significant decline in members of the *Rhodobacteraceae*. This could have important consequences for the marine sulfur cycle affecting the microbial food web and potentially global climate.

6.3.4 Potential consequences of a reduction in Rhodobacteraceae and marine Roseobacter abundance

DMSP is an organic sulfur compound synthesized by phytoplankton particularly dinophytes and haptophytes (Malin *et al.*, 1993) which serves multiple roles as an osmolyte, a cryoprotectant and an antioxidant (Karsten, 1996, Sunda *et al.*, 2002). It is also significant in the global sulfur cycle by supplying sulfur and carbon to heterotrophic bacteria (Kiene *et al.*, 2000) and transporting sulfur from the ocean to the atmosphere via its conversion to dimethylsulfide (DMS) (Bates *et al.*, 1987). There are two major biochemical routes for the degradation of DMSP. The first is the demethylation/demethiolation pathway (Kiene *et al.*, 2000) resulting in the production of 3- methylmercaptopropionate (MMPA) and MeSH which is a readily available source of reduced sulfur for microorganisms (Ledyard and Dacey, 1996, Kiene *et al.*, 1999). Only bacteria are known to express this pathway and therefore ultimately control the fate of DMSP (González *et al.*, 2003).

The alternate degradation route where DMSP is cleaved via the enzyme DMSP lyase to form DMS and acrylate is known as the lyase pathway (Cantoni and Anderson, 1956). Although some phytoplankton possess DMSP lyase, (Stefels and Dijkhuizen, 1996; Steinke *et al.*, 1996, Wolfe and Steinke, 1996, Steinke *et al.*, 1998, Niki *et al.*, 2000) bacteria are generally thought to dominate DMS production (Kiene, 1992). Both acrylate and the majority of DMS produced in the lyase pathway are utilized as substrates for microbial growth by specialised bacteria such as *Thiobacillus* and *Methylophaga* (Visscher and Van Gemerden, 1993, Schafer, 2007). Oxidation of DMS to dimethyl sulfoxide (DMSO) via microbial degradation is the largest sink for DMS in the marine environment with only 2 – 10% of DMS released to the atmosphere (Kiene and Bates, 1990; Archer *et al.*, 2002, Zubkov *et al.*, 2002). DMS is the most important source of natural sulfur to the atmosphere as it plays a major role in the sulfur cycle when it is transferred from marine to terrestrial environments via precipitation (Lovelock *et al.*, 1972). However, DMS derived sulfur also influences global temperature and climate dynamics through its effect on cloud cover (Moran *et al.*, 2012). When DMS enters the

atmosphere it is oxidized in to a variety of sulfur compound which serve as aerosols attracting water vapour around them. This increases the size and liquid content of the cloud which directly influences the global radiation budget by reducing the amount of short wave radiation reaching the lower atmosphere thereby cooling the Earth's surface (Korhonen *et al.*, 2008).

Globally, between 50 to 90% of DMSP produced by marine phytoplankton is degraded by bacterial demethylation which during an algal bloom may occur at rates exceeding 1000 nM d^{-1} (Van Duyl *et al.*, 1998; Kiene and Linn, 2000, Reisch *et al.*, 2011). If all of this was converted via the lyase pathway the gross production of DMS would increase by 2 – 20 fold (Kiene *et al.*, 2000). This is supported by the fact that metagenomic studies have revealed that genes involved in DMSP demethylation are two orders of magnitude more abundant in marine environments than DMSP lyase genes (Howard *et al.*, 2008; Todd *et al.*, 2009, Reisch *et al.*, 2011, Todd *et al.*, 2011). This is supported by this study, as only reads from the DMSP demethylation (11 reads) pathway were recovered from both metagenomes (ambient and high CO_2).

There is evidence supporting the theory that a homeostatic feedback cycle exists between phytoplankton and climate through the production of DMS. This has been formalised in the CLAW hypothesis (Charlson *et al.*, 1987), which proposes that certain phytoplankton species release DMS in response to increased solar radiation, and that DMS ultimately leads to increased cloud cover forming a negative feedback loop to stabilise global temperature.

Several studies have been carried out investigating the effects of ocean acidification on phytoplankton calcification rates and DMS production (Orr *et al.*, 2005; Wingenter *et al.*, 2007, McNeil and Matear, 2008), but few concerning the effects on bacterial populations (Joint *et al.*, 2010). However, it is known that the transfer of DMS from the ocean to the atmosphere is not simply a function of DMS production by phytoplankton but is also controlled by the competing pathways for DMSP degradation expressed by different groups of bacteria. Demethylation of DMSP exerts a major

biochemical control over DMS production and any perturbation impacting organisms catalysing this pathway could lead to increased DMS production. Currently, there are no quantitative data regarding the effect of elevated CO_2 on bacteria that degrade DMSP or DMS but such an effect could alter the DMS yield from DMSP (Vogt *et al.*, 2007).

The repression of *Roseobacter*-like bacteria by elevated CO_2 and relatively small decreases in seawater pH have important implications for the global climate system. There is strong evidence to support the importance of bacteria from the marine *Roseobacter* clade in DMSP degradation as they are present in significant numbers during phytoplankton blooms and possess diverse pathways for carbon and sulfur metabolism (González *et al.*, 1999; Miller and Belas, 2004, Vila *et al.*, 2004, Stoica and Herndl, 2007). The ability to use DMSP as a carbon and sulfur source explains their predominance in phytoplankton blooms and their dominant role in dictating the fate of DMSP. However, hitherto there has been no evaluation of the effects of climate change, including ocean acidification on these important bacteria. *Roseobacter*–like bacteria have been identified as the primary mediators of DMSP demethylation which directs sulfur compounds away from production of the climatically active gas DMS (Howard *et al.*, 2006). Lagrangian experiments conducted in the North Sea have shown a close correlation between the abundance of this bacterial group and both bacterial production and DMSP turnover which was not observed for other bacterial groups (Zubkov *et al.*, 2001).

Reduction in *Roseobacter* numbers could severely reduce the demethylation pathway resulting in increased production of DMS and enhancing the negative feedback on global thermoregulation mediated through cloud albedo.

It has been established that MeSH is the main source of sulfur for protein synthesis in marine bacterioplankton despite the high concentrations of sulfate in seawater (Kiene *et al.*, 1999, Kiene and Linn, 2000). Tracer experiments (Kiene *et al.*, 1999) reported a 30% incorporation of labelled sulfur in bacterioplankton macromolecules by amending seawater with <0.12 nM of [^{35}S] DMSP which was less

than 10% the natural concentration. Selected isolates of *Roseobacter*-like bacteria also incorporated sulfur from [^{35}S] DMSP but only if they were capable of degrading DMSP to MeSH, whereas sulfur from [^{35}S] MeSH was incorporated into all selected strains and natural populations obtained from seawater (Kiene *et al.*, 1999). These findings strongly suggest that bacterioplankton obtain sulfur from DMSP via MeSH instead of sulphate which is 10^7 fold more abundant (Kiene *et al.*, 1999). A reduction in the concentration of MeSH which would result from repression of *Roseobacter*-like bacteria will therefore not only have consequences for the climate feedback system but also for bacterial production as the decrease in organic sulfur availability will have to be made up from sulfate which contains sulfur in its most oxidized state (+VI). Consequently the use of sulfate represents an energy cost to bacteria both in the reduction of sulfate to thiol groups and in the methylation step during methionine synthesis (Kiene *et al.*, 1999). Our results demonstrate effects of elevated CO_2 on key organisms involved in the retention of organic sulfur in marine systems. However, it is the emergent effect of the changes in bacterial populations that we have observed which determines the significance of changes in bacterial transformations of DMSP.

It has been demonstrated that numerous members of the *Roseobacter* clade are able to both cleave and demethylate DMSP (González *et al.*, 2000) though the conditions in which one pathway is favoured over another has yet to be elucidated. Previous work suggests that the regulation of the competing pathways known as the bacterial switch is due to bacterial demand for carbon and sulfur (Kiene *et al.*, 2000, Simó, 2001). It is hypothesised that the demethylation pathway will be favoured when the demand for carbon and sulfur is high and dissolved DMSP ($DMSP_d$) concentration is low whereas the DMSP lyase pathway with be favoured when the demand for carbon and sulfur is low and $DMSP_d$ concentration is high.

A study by Levine *et al* (2012) quantified the abundance and transcription of key genes involved in DMSP breakdown. Using quantitative polymerase chain reaction (qPCR) they investigated the variability in the abundance of the DMSP demethylase gene *dmdA* and the DMSP lyase gene *dddP* over a 10 month time-series at the Bermuda

Atlantic Time-series Study station. The *dddP*, gene was chosen because it is an order of magnitude more abundant (along with *dddQ*) than *dddD, dddL, dddW* and *dddY* in the Sargasso Sea (Todd *et al.*, 2009). During the experiment it was estimated that ~33% of bacterioplankton cells contained a copy of *dmdA* and ~ 11% of cells contained a copy of *dddP*, based on total bacterial cell counts (Howard et al., 2008). They concluded that UV-A solar radiation plays an important role in global sulfur cycling both in phytoplankton and bacteria with bacterial demethylation occurring under low UV-A and bacterial DMSP cleavage occurring under elevated temperatures and moderate UV-A. Furthermore, no correlation was found between the demand for carbon and the availability of $DMSP_d$ in zones which had elevated DMSP demethylase activity and zones with elevated particulate DMS (DMSp) lyase activity (Levine *et al.*, 2012).

The PeECE III mesocosm experiment (2005) focussing on the effects of elevated CO_2 on DMSP transformation and DMS release demonstrated that the integrated average amount of DMS between days 0 -17 was significantly higher (26%) under conditions of elevated CO_2 similar to those used in our experiments (Wingenter *et al.*, 2007). However, a different group in the same study concluded that although more DMS was produced in the high CO_2 mesocosms in comparison to the ambient CO_2 mesocosms between days 0-22, it was not statistically significant (P=0.05) (Vogt *et al.*, 2007). This discrepancy is due to differences in data interpretation and the use of different statistical methods employed in the data analysis. Wingenter *et al* (2007) used a student's t-test at a 90% confidence level while Vogt *et al* (2007) used one-way ANOVA at a 95% confidence level in order to reduce type 1 errors (the incorrect rejection of the null hypothesis) and used a more stringent confidence criterion.

Increased DMS production in elevated CO_2 conditions was also observed in a mesocosm experiment off the coast of Korea (Kim *et al.*, 2010). The perturbation experiment was performed to investigate the effects of ocean acidification and global warming on DMS production. Mesocosms were set up to emulate three different environmental conditions: ambient control (ambient CO_2/ambient temperature), acidification only (~900 ppm CO_2/ambient temperature) and a greenhouse treatment

(~900 ppm CO_2/~3 °C warmer than ambient temperature). The results showed that the total DMS concentration accumulated over the entire experiment in the acidified and greenhouse mesocosms was 80% and 60% (respectively) higher than the ambient control mesocosms. Kim *et al* (2010) attributed the rise in DMS production to increased grazing of phytoplankton species by heterotrophic dinoflagellates as their abundance was considerably higher in the acidified and greenhouse mesocosms than in the control mesocosms. Grazing allows the mixing of DMSP and DMSP lyase enzymes that would otherwise be separated in the algal cells. However, statistical analysis using one-way ANOVA at a 95% confidence level reported the increases in DMS production to be only statistically marginal (P=0.05).

Hopkins *et al* (2009) analysed DMSP and DMS in the mesocosms that were used to prepare the *in situ* bottle incubations reported here. They reported 57% lower DMS concentrations under elevated CO_2 conditions for the bloom period of May 10^{th}-17^{th} (days 5 – 12), a 63% reduction post bloom period May 18^{th}-23^{rd} (days 13 - 18) and a 60% reduction over the entire experiment May 6^{th}-23^{rd} (days 1 – 18) (Hopkins *et al.*, 2009). This is contrary to our hypothesis that a decrease in the abundance of marine *Roseobacter*-like bacteria will result in a shift in the DMSP degradation pathway from the demethylation to the lyase pathway leading to a net increase in DMS concentration. However, the post bloom data reported by Hopkins *et al*. (2009), for the same period when a decrease in *Rhodobacteraceae* was observed, is based on measurements from mesocosms M3 and M4 reported to be high CO_2 and ambient CO_2 mesocosms respectively (Hopkins *et al.*, 2009). In fact, mesocosm M3 cannot be called a high CO_2 treatment in the post bloom stage of the experiment as CO_2 was not reintroduced into the system at the start of phase 2 in order to reduce the pH. Consequently, this mesocosm had a lower CO_2 concentration and a higher pH than mesocosms M1 and M2 which were subject to a further CO_2 treatment at the start of phase 2 (Chapter 3, Figure 3.1). For comparative analysis, it would be more logical to compare mesocosms M1 and M6 (high and ambient CO_2 respectively) which were used in this analysis, or data from mesocosms M2 and M5 (high and ambient CO_2 respectively) which were treated with ^{15}N-labelled nitrate. Water samples from these mesocosms were not used in the dark incubation

experiments of this study as the ^{15}N label may have interfered with $^{13}CO_2$ SIP experiments (Chapter 5). DMS data for mesocosms M1 and M2 and M5 and M6 obtained from unpublished data of Hopkins *et al* (2009) revealed that in the post bloom phase of the experiment, May 16th-22nd (days 11 – 17) DMS concentration in the elevated CO_2 treatment was only 6% lower when comparing M1 versus M6 (Figure 6.19A). Comparison of the ^{15}N-labelled treatments M2 versus M5 (Figure 6.19B) revealed that DMS concentration under elevated CO_2 was 46% higher over the same period. Interestingly, the high CO_2 mesocosm with the lowest pH and highest CO_2 concentration was mesocosm M2, which exhibited the highest levels of DMS. Statistical analysis of the data using a non-parametric Mann-Whitney test revealed no significant differences between the treatments with P= 0.81 (M1 v M6) and P=0.09 (M2 v M5). However, a significant difference was observed when comparing mesocosms M2 and M5 between days 14 -17 (P=0.03). Further examination of the graphs (Figure 6.19A/B) also shows that DMS concentration rises more steeply in the high CO_2 treatments (M1, M2) than their ambient CO_2 counterparts (M5, M6) towards the end of the experiment. We can only speculate as to what this rise means and more importantly is it significant? But it may be beneficial in future experiments to measure DMSP/DMS concentrations over a longer time period than the typical mesocosm experiment and to include a higher degree of true replication to permit less ambiguous interpretation of the data.

Community composition of the phytoplankton assemblage may play a significant role in controlling DMS as the link between the algal cell and atmospheric DMS is DMSP (Simó, 2001). Generally, haptophytes (including coccolithophorids and small flagellates) produce more DMSP than diatoms (Keller *et al.*, 1989, Liss *et al.*, 1993). In this study, the phytoplankton community was dominated by picoeukaryotes belonging to the order Mamiellales (*Micromonas* and *Bathycoccus*) whereas coccolithophores only represented ~3% of the total biomass (Hopkins *et al.*, 2009, Newbold *et al.*, 2012). However, the PeECE III mesocosm experiment conducted in 2005 was dominated during the bloom period by the coccolithophore *E. huxleyi* (Vogt *et al.*, 2007, Wingenter *et al.*, 2007), and it was suggested that phytoplankton community composition is the major factor in the evolution of DMS. In the PeECE III mesocosm experiment the maximum

DMS concentration for the 1xCO_2 mesocosms (ambient) was 29.5 nmol L^{-1} while in the 2xCO_2 and 3xCO_2 it was 27.4 nmol L^{-1} and 25.3 nmol L^{-1} respectively (Vogt *et al.*, 2007). In contrast, the maximum DMS concentration in this study was 12.8 nmol L^{-1}, 20.7 nmol L^{-1} and 10.6 nmol L^{-1} for the high mesocosms (M1, M2 and M3) and 31.4 nmol L^{-1}, 16.9 nmol L^{-1} and 11.6 nmol $^{-1}$ for the ambient mesocosm (M4, M5 and M6). In the Korean mesocosm experiment conducted by Kim *et al* (2010), it was the autotrophic nanoflagellates (which are known to be significant DMSP producers) which showed increased growth under elevated CO_2 conditions (Kim *et al.*, 2010). This was accompanied by significantly higher grazing rates which not only liberated the cytosolic DMSP into the surrounding environment but also released DMSP lyase enzymes (which are segregated in healthy cells) that are found in phytoplankton species such as *E. huxleyi* (Stefels *et al.*, 2007, Steinke *et al.*, 2007). It has been established that the lysis of algal cells can lead to the cleavage of DMSP into DMS and acrylic acid. Culture studies investigating DMSP cleavage on two axenic strains of *E. huxleyi* during viral lysis and grazing found that levels of DMS and acrylic acid were an order of magnitude higher during grazing as opposed to cell death by viral infection (Evans *et al.*, 2007). This shows that grazing is a more significant pathway in DMS production (at least in *E. huxleyi*) as viral infection in algal cells been found to decrease DMSP lyase activity in infected cultures (Evans *et al.*, 2007).

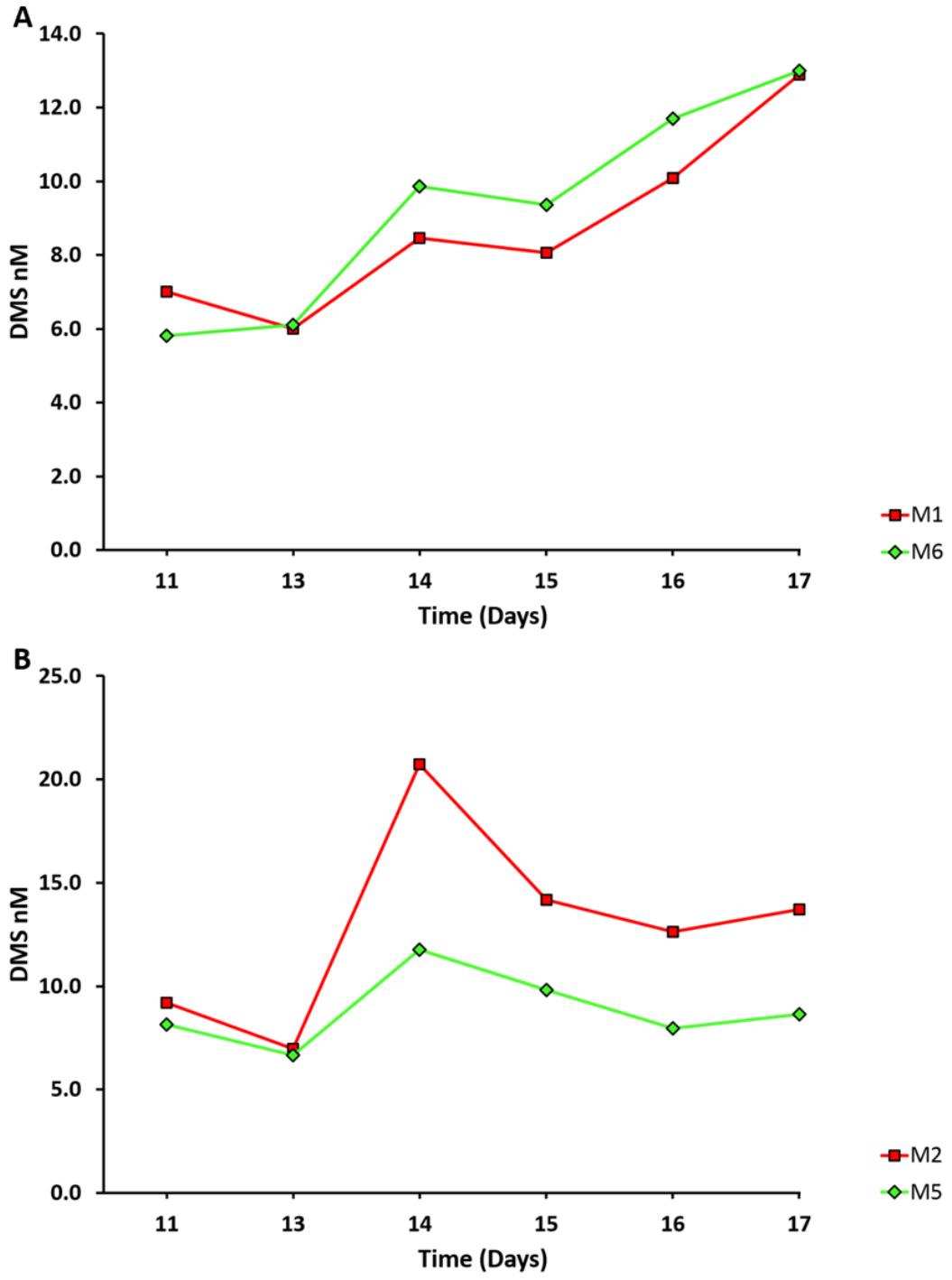

Figure 6.19. Temporal changes in DMS concentration for phase 2 (post bloom) of the mesocosm experiment (day 11 - 17 = May 16th– 22nd). High CO_2 treatment (M1) is depicted in red while ambient CO_2 treatment (M6) is in green (A). ^{15}N-labelled nitrate treatments with high CO_2 treatment (M2) depicted in red and ambient CO_2 treatment (M5) in green.

No analysis of specific bacterial populations involved in DMSP metabolism were made in those studies, however a reduction in the abundance of *Roseobacter*-like bacteria due to ocean acidification may have contributed to the increased DMS production observed in response to elevated CO_2 and seawater acidification.

DMSP flux (the rate in which it is released and consumed) can vary between several hours and a couple of days depending on bacterial sulfur demand which in turn is inextricably linked to heterotrophic bacterial production. Therefore, the higher the sulfur demand the more DMSP will be assimilated and less will be converted to DMS (Simó, 2001, Allgaier *et al.*, 2008). Clearly, it will be important to take account of the effect of ocean acidification on DMSP degradation pathways in global climate models. I believe that selection against bacteria that convert DMSP to MeSH and thus enhanced DMS release to the atmosphere may represent an important new negative feedback in the global climate system.

qPCR analysis (Chapter 4 section 4.3.5) revealed a decrease of ~56.4% in the abundance of 16S rRNA genes from *Rhodobacteraceae*-like bacteria from $8.85 \pm 0.9 \times 10^5$ copies/ml in the ambient CO_2 treatment to $3.86 \pm 0.3 \times 10^5$ copies/ml in the high CO_2 treatment. A decrease of 33.6% was also observed in the abundance of 16S rRNA genes from the *Flavobacteriaceae* with $4.08 \pm 0.1 \times 10^6$ copies/ml in the ambient CO_2 treatment to $2.71 \pm 0.28 \times 10^6$ in the high CO_2 treatment. In contrast, total bacterial 16S rRNA gene abundance was $5.51 \pm 0.37 \times 10^6$ copies/ml in the ambient CO_2 treatment which decreased to $4.00 \pm 0.43 \times 10^6$ copies/ml in the high CO_2 treatment (27.4% lower). Based on these numbers, *Flavobacteriaceae* represented 74% and 67.7% (respectively) of the total 16S rRNA gene abundance of the ambient and high CO_2 metagenomes, whereas the *Rhodobacteraceae* represented 16.1% and 9.3% (respectively). The substantially larger decrease of *Rhodobacteraceae* in relation to *Flavobacteriaceae* was reflected in the 16S rRNA gene clone libraries (Chapter 4 section 4.3.2). In these libraries, the abundance of *Flavobacteriaceae* relative to *Rhodobacteraceae* (16S rRNA clones) was 63.3% and 21.5% respectively in the ambient CO_2 library whereas in the high CO_2 it was 80.5% and 2.4% respectively. These libraries gave the impression that *Flavobacteriaceae* numbers

actually increased in response to elevated CO_2 when in fact what they actually depicted was an increase in abundance of *Flavobacteriaceae* relative to the *Rhodobacteraceae*.

6.4 Conclusions

The results of this study have established a link between a reduction in ocean pH and a significant decrease in representation of bacteria from the marine *Roseobacter* clade within the *Rhodobacteraceae*. We hypothesize that if the current trend in CO_2 emissions continues unabated the resulting decrease in ocean pH will initiate a cascade effect which could severely disrupt marine carbon and sulfur cycles as well as having a potential impact on DOM cycling. Consequently, marine organisms on all trophic levels will be severely affected as the flux of organic sulfur is diverted from the ocean to the atmosphere via conversion of DMSP to DMS rather than MeSH. This represents a novel negative feedback mechanism in the global climate system as enhanced atmospheric DMS would increase cloud formation and solar reflectance thereby decreasing the global temperature.

7. Summary and concluding remarks

7.1 Summary

There is substantial scientific evidence that human induced climate change will negatively impact marine biota, affecting whole ecosystems and biogeochemical cycles. Although there have been a great many studies investigating ocean acidification over the past decade, the majority have focused on the effects of calcification, photosynthesis and primary production. In this thesis I have attempted to address the balance and hopefully contributed to the missing gaps in our current knowledge. Firstly, I will provide a brief synopsis of the key points and results from each experiment. Secondly, I will make suggestions for future work and experimental improvements which may lead to a more complete understanding of the consequences of climate change.

7.2 Synopsis

7.2.1 Effects of elevated CO_2 and reduced pH on marine microbial communities

Analysis of the high and ambient CO_2 mesocosms revealed a reduction in primary production of 27.3% in the elevated CO_2 treatments. The largest decrease was observed in the large picoeukaryotes and *Synechococcus* which decreased by 64% and 74% respectively in comparison to the ambient CO_2 treatment. Coccolithophore abundance was also lower in the high CO_2 treatment by 45%. Bacterial abundance in both the mesocosms and dark incubation bottles was reduced in the high CO_2 treatments in phase 2 of the experiment (post-bloom). Over the five day incubation period bacterial abundance in the high CO_2 dark incubations was 10.9% that of the ambient CO_2 treatments.

7.2.2 Effects of CO_2 driven ocean acidification on microbial community composition

Distinct DGGE profiles of 16S ribosomal genes from mesocosm bacterial communities were observed which correlated with the effects of elevated CO_2 and reduced pH. Based on the reproducibility of the DGGE gels, samples were chosen for the construction 16S rRNA gene clone libraries and qPCR analysis. Libshuff analysis of

bacterial 16S rRNA gene clone libraries revealed significant differences in the community structure of the ambient and high CO_2 libraries. Phylogenetic analysis indicated that the majority of sequences were closely affiliated to two main families of bacteria; the *Rhodobacteraceae* within the class *Alphaproteobacteria* and the *Flavobacteriaceae* within the class *Flavobacteria*. Approximately 91% of *Rhodobacteraceae* sequences were derived from the ambient CO_2 clone library whereas the *Flavobacteriaceae* were more evenly distributed between both libraries. qPCR was employed to enumerate *Rhodobacteraceae* and *Flavobacteriaceae* species in the ambient and high CO_2 samples using 16S rRNA primers designed specifically to target these two groups. The results showed a significant reduction (P=0.001) in the abundance of *Rhodobacteraceae* 16S rRNA genes of 56.4% in response to elevated CO_2. qPCR analysis of total bacteria 16S rRNA genes showed that the ambient CO_2 library comprised of 74% *Flavobacteriaceae* and 16.1% *Rhodobacteraceae* whereas the high CO_2 library comprised of 67.7% *Flavobacteriaceae* and 9.6% *Rhodobacteraceae*.

7.2.3 Increased importance of CO_2 fixation by bacterial spp. from the Roseobacter clade in a marine mesocosm exposed to elevated CO_2

In order to examine the response of chemoautotrophic bacteria to elevated CO_2 and reduced pH, samples incubated with ^{13}C bicarbonate were subjected to stable isotope probing. The fractionation of the DNA was conducted in triplicate (3 x ambient CO_2, 3 x high CO_2) and the bacterial community investigated using DGGE analysis. Distinct profiles were observed from the ambient and high CO_2 treatments and based on the high degree of reproducibility they were pooled into their respective treatments. 16S rRNA gene clone libraries were constructed and selected clones sequenced. No chemoautotrophic bacteria were detected in any of the libraries suggesting that inorganic carbon uptake in this system was dominated by heterotrophic CO_2 fixation rather than autotrophic CO_2 fixation. The ^{13}C 16S rRNA gene clone libraries were dominated by *Rhodobacteraceae* both in the ^{13}C ambient and ^{13}C high CO_2 treatments with 61.4% and 45.7% of sequences respectively (n =96), suggesting that this particular group may play an important role in the assimilation of inorganic carbon. Metagenomic libraries

constructed from total DNA (not SIP) revealed that the majority of *Rhodobacteraceae* reads were closely associated with members of the marine *Roseobacter* clade which have been reported to fix CO_2 through anaplerotic pathways (Swingley *et al.*, 2007, Tang *et al.*, 2009).

7.2.4 Metagenomic assessment of the effect of ocean acidification on marine bacterioplankton

Analysis of ambient and high CO_2 metagenomic libraries confirmed that the treatments contained bacterial species primarily from the family *Rhodobacteraceae* and *Flavobacteriaceae*. The analysis also confirmed a decrease in the percentage of reads associated to *Rhodobacteraceae* with 37.7% in the ambient CO_2 metagenome and 8.8% in the high CO_2 metagenome. The majority of *Rhodobacteraceae* reads recovered were from members of the marine *Roseobacter* clade particularly species from the genera *Roseobacter*, *Ruegeria*, *Sulfitobacter*, *Loktanella* and *Roseovarius*. Analysis of functional assignments revealed a reduction in the number of reads associated with key metabolic processes of the marine *Roseobacter* clade. Reads associated with metabolic functions such as sulfur assimilation, carbon assimilation and aerobic anoxygenic phototrophy were lower in the high CO_2 metagenome compared to the ambient CO_2 metagenome. These decreases further support the repression of *Roseobacter*-like bacteria in elevated CO_2 and have important implications for the sulfur cycle and the global climate system. Furthermore, analysis of the DMSP data from the Bergen experiment revealed a significant increase in DMS production between days 14 – 17 in the high CO_2 treatment (M2) when compared to the ambient treatment (M5).

Although there may be some concern regarding the small size of the metagenomes, I believe this allowed for a more rigorous analysis as it allowed a more in depth analysis to be conducted in order to verify phylogenetic and functional assignments of sequence data.

7.3 Conclusions

Hypothesis I: Marine bacterial diversity will change in response to seawater pH.

The results presented in this thesis showed that elevated CO_2 reduced the abundance of *Alphaproteobacteria* from the marine *Roseobacter* clade which play important roles in carbon and sulfur cycles. In the mesocosm experiment we saw a reduction in primary production and associated change in community structure as a result of elevated CO_2. It has been established that changes in phytoplankton composition can alter bacteria community structure due to the availability of different algal primary products (Grossart *et al.*, 2006, Teeling *et al.*, 2012). Therefore, the decrease in the abundance of species from the marine *Roseobacter* clade was a consequence of elevated CO_2 reducing the quantity or quality of phytoplankton derived dissolved or particulate matter.

Hypothesis II: Decreasing seawater pH will alter biogeochemical cycling of carbon nitrogen and sulfur.

Members of the marine *Roseobacter* clade are considered to play primary roles in global carbon cycles, (Kolber *et al.*, 2001, Jiao *et al.*, 2007) sulfur cycles (Moran *et al.*, 2003, Howard *et al.*, 2006) and the climate system (Charlson *et al.*, 1987, Vallina and Simo, 2007). A reduction in marine *Roseobacter* species could potentially alter the flux of organic sulfur from the ocean to the atmosphere thereby promoting a negative feedback mechanism which would increase solar reflectance and decrease global temperature. The subsequent loss of reduced sulfur in the form of MeSH would have severe consequences on bacterial production which would affect marine organisms on higher trophic levels and impact DOM cycling.

7.4 Future work

A central governing body for climate change research is urgently required which would provide standard operating procedures for experimental design, collate data and

provide funding for researchers investigating all aspects of climate change. Research to date has generated data using various different experimental procedures such as; pH manipulation, different stress variables, duration of experiment and even different statistical analysis. Consequently, comparative analysis of ocean acidification impact studies has been difficult to interrupt (Liu *et al.*, 2010). Though a guide for the best practices in ocean acidification and data reporting has been published, it has yet to be widely adopted by the research community (Riebesell *et al.*, 2010). In order to make credible predictions of the effects of ocean acidification, experiments must be designed to simulate natural conditions as closely as possible. Larger *in situ* experiments are urgently required that can manipulate temperature as well as pH, thereby promoting stratification. Experimenters should allow for longer perturbations, firstly to introduce CO_2 gradually rather than the abrupt manner currently employed and secondly, to allow for potential acclimation or adaptation by marine organisms.

However, the consequences of ocean acidification are extremely difficult to predict as there are numerous interactive effects acting on a wide range of natural variables. It would take a great many years and numerous studies to simulate every possible scenario not to mention the logistics and cost of such a large endeavor. Therefore, mathematical modelling and computer simulations may be the way forward. Using these methods a multitude of different simulations could be ran *in silico* and the most likely scenarios tested in a fully automated mesocosm facility. Light, pH, temperature, salinity and nutrients could all be controlled by computers running the simulation and different phytoplankton blooms could be stimulated by the addition of cultured or wild type species from nursery areas within the facility. Naturally, the initial cost of building such a facility would be considerable however, if a consortium of major universities and marine laboratories was formed coupled with government grants and loans this may be achievable.

Alternatively, a mobile sea-going mesocosm facility could be constructed and conveyed to areas of the ocean such as CO_2 venting sites or coastal upwelling systems where pH and saturation state are lower than the accepted average (Feely *et al.*, 1988;

Feely *et al.*, 2008, Manzello *et al.*, 2008, Bates *et al.*, 2009, Manzello, 2010). However, the facility itself would at times be at the mercy of strong winds and unyielding waves making it a challenging work environment and costly to maintain.

Acinas, S. G., F. Rodríguez-Valera and C. Pedrós-Alió (1997). Spatial and temporal variation in marine bacterioplankton diversity as shown by RFLP fingerprinting of PCR amplified 16S rDNA. *FEMS Microbiology Ecology* **24**(1): 27-40.

Adkins, J. N., H. M. Mottaz, A. D. Norbeck, J. K. Gustin, J. Rue, T. R. W. Clauss, S. O. Purvine, K. D. Rodland, F. Heffron and R. D. Smith (2006). Analysis of the *Salmonella typhimurium* proteome through environmental response toward infectious conditions. *Molecular and Cellular Proteomics* **5**(8): 1450-1461.

Allaby, M. and R. Garratt (2002). *Encyclopedia of Weather and Climate: A-L*, Facts on File.

Allgaier, M., U. Riebesell, M. Vogt, R. Thyrhaug and H. P. Grossart (2008). Coupling of heterotrophic bacteria to phytoplankton bloom development at different pCO_2 levels: a mesocosm study. *Biogeosciences Discussions.* **5**(1): 317-359.

Allgaier, M., H. Uphoff, A. Felske and I. Wagner-Dobler (2003). Aerobic anoxygenic photosynthesis in *Roseobacter* clade bacteria from diverse marine habitats. *Applied and Environmental Microbiology* **69**(9): 5051-5059.

Alonso-Saez, L., P. E. Galand, E. O. Casamayor, C. Pedros-Alio and S. Bertilsson (2010). High bicarbonate assimilation in the dark by Arctic bacteria. *ISME Journal* **4**(12): 1581-1590.

Alonso, C., F. Warnecke, R. Amann and J. Pernthaler (2007). High local and global diversity of *Flavobacteria* in marine plankton. *Environmental Microbiology* **9**(5): 1253-1266.

Althoff, K., C. Schütt, R. Steffen, R. Batel and W. E. G. Müller (1998). Evidence for a symbiosis between bacteria of the genus *Rhodobacter* and the marine sponge *Halichondria panicea* : harbor also for putatively toxic bacteria? *Marine Biology* **130**(3): 529-536.

Altschul, S. F., W. Gish, W. Miller, E. W. Myers and D. J. Lipman (1990). Basic local alignment search tool. *Journal of Molecular Biology* **215**(3): 403-410.

Altschul, S. F., T. L. Madden, A. A. Schaffer, J. Zhang, Z. Zhang, W. Miller and D. J. Lipman (1997). Gapped BLAST and PSI-BLAST: a new generation of protein database search programs. *Nucleic Acids Research* **25**(17): 3389-3402.

Alvarez, L. W., W. Alvarez, F. Asaro and H. V. Michel (1980). Extraterrestrial cause for the Cretaceous-Tertiary extinction. *Science* **208**(4448): 1095-1108.

Archer, D., H. Kheshgi and E. Maier‐Reimer (1998). Dynamics of fossil fuel CO_2 neutralization by marine $CaCO_3$. *Global Biogeochemical Cycles* **12**(2): 259-276.

Archer, S. D., F. J. Gilbert, P. D. Nightingale, M. V. Zubkov, A. H. Taylor, G. C. Smith and P. H. Burkill (2002). Transformation of dimethylsulphoniopropionate to dimethyl sulphide during summer in the North Sea with an examination of key processes via a modelling approach. *Deep Sea Research Part II: Topical Studies in Oceanography* **49**(15): 3067-3101.

Arens, N. C. and A. H. Jahren (2000). Carbon isotope excursion in atmospheric CO_2 at the Cretaceous-Tertiary boundary: Evidence from terrestrial sediments. *Palaios* **15**(4): 314-322.

Arnone, J. A., P. S. J. Verburg, D. W. Johnson, J. D. Larsen, R. L. Jasoni, A. J. Lucchesi, C. M. Batts, C. von Nagy, W. G. Coulombe, D. E. Schorran, P. E. Buck, B. H. Braswell, J. S. Coleman, R. A. Sherry, L. L. Wallace, Y. Luo and D. S. Schimel (2008). Prolonged suppression of ecosystem carbon dioxide uptake after an anomalously warm year. *Nature* **455**(7211): 383-386.

Arthur, M. A., J. C. Zachos and D. S. Jones (1987). Primary productivity and the Cretaceous/Tertiary boundary event in the oceans. *Cretaceous Research* **8**(1): 43-54.

Artolozaga, I., M. Valcárcel, B. Ayo, A. Latatu and J. Iriberri (2002). Grazing rates of bacterivorous protists inhabiting diverse marine planktonic microenvironments. *Limnology and Oceanography* **47**(1): 142-150.

Ashelford, K. E., N. A. Chuzhanova, J. C. Fry, A. J. Jones and A. J. Weightman (2006). New screening software shows that most recent large 16S rRNA gene clone libraries contain chimeras. *Applied and Environmental Microbiology* **72**(9): 5734-5741.

Ashelford, K. E., A. J. Weightman and J. C. Fry (2002). PRIMROSE: a computer program for generating and estimating the phylogenetic range of 16S rRNA oligonucleotide probes and primers in conjunction with the RDP-II database. *Nucleic Acids Research* **30**(15): 3481-3489.

Ashen, J. B. and L. J. Goff (2000). Molecular and ecological evidence for species specificity and coevolution in a group of marine algal-bacterial symbioses. *Applied and Environmental Microbiology* **66**(7): 3024-3030.

Ashida, H., A. Danchin and A. Yokota (2005). Was photosynthetic RuBisCO recruited by acquisitive evolution from RuBisCO-like proteins involved in sulfur metabolism? *Research in Microbiology* **156**(5-6): 611-618.

Ayo, B., M. Unanue, I. Azúa, G. Gorsky, C. Turley and J. Iriberri (2001). Kinetics of glucose and amino acid uptake by attached and free-living marine bacteria in oligotrophic waters. *Marine Biology* **138**(5): 1071-1076.

Azam, F., T. Fenchel, J. Field, J. Gray, L. Meyer-Reil and F. Thingstad (1983). The ecological role of water-column microbes in the sea. *Marine Ecology Progress Series* **10**: 257-263.

Azam, F. and F. Malfatti (2007). Microbial structuring of marine ecosystems. *Nature Reviews Microbiology* **5**(10): 782-791.

Barbieri, E., B. J. Paster, D. Hughes, L. Zurek, D. P. Moser, A. Teske and M. L. Sogin (2001). Phylogenetic characterization of epibiotic bacteria in the accessory nidamental gland and egg capsules of the squid *Loligo pealei* (Cephalopoda:Loliginidae). *Environmental Microbiology* **3**(3): 151-167.

Barker, S., J. Higgins and H. Elderfield (2003). The future of the carbon cycle: review, calcification response, ballast and feedback on atmospheric CO_2. *Philosophical Transactions of the Royal Society of London. Series A: Mathematical, Physical and Engineering Sciences* **361**(1810): 1977-1999.

Barker, S. and A. Ridgwell (2012). Ocean Acidification. *Nature Education Knowledge* **3**(10).

Barnosky, A. D., N. Matzke, S. Tomiya, G. O. Wogan, B. Swartz, T. B. Quental, C. Marshall, J. L. McGuire, E. L. Lindsey and K. C. Maguire (2011). Has the Earth's sixth mass extinction already arrived? *Nature* **471**(7336): 51-57.

Barth, J. A., B. A. Menge, J. Lubchenco, F. Chan, J. M. Bane, A. R. Kirincich, M. A. McManus, K. J. Nielsen, S. D. Pierce and L. Washburn (2007). Delayed upwelling alters nearshore coastal ocean ecosystems in the northern California current. *Proceedings of the National Academy of Sciences* **104**(10): 3719-3724.

Bates, N. R., J. T. Mathis and L. W. Cooper (2009). Ocean acidification and biologically induced seasonality of carbonate mineral saturation states in the western Arctic Ocean. *Journal of Geophysical Research: Oceans* **114**(11).

Bates, T. S., J. D. Cline, R. H. Gammon and S. R. Kelly-Hansen (1987). Regional and seasonal variations in the flux of oceanic dimethylsulfide to the atmosphere. *Journal of Geophysical Research* **92**(C3): 2930-2938.

Bauer, M., M. Kube, H. Teeling, M. Richter, T. Lombardot, E. Allers, C. A. Wurdemann, C. Quast, H. Kuhl, F. Knaust, D. Woebken, K. Bischof, M. Mussmann, J. V. Choudhuri, F. Meyer, R. Reinhardt, R. I. Amann and F. O. Glockner (2006). Whole genome analysis of the marine Bacteroidetes '*Gramella forsetii*' reveals adaptations to degradation of polymeric organic matter. *Environmental Microbiology* **8**(12): 2201-2213.

Baumann, H., S. C. Talmage and C. J. Gobler (2012). Reduced early life growth and survival in a fish in direct response to increased carbon dioxide. *Nature Climate Change* **2**(1): 38-41.

Beardall, J. and M. Giordano (2002). Ecological implications of microalgal and cyanobacterial CO_2 concentrating mechanisms, and their regulation. *Functional Plant Biology* **29**(3): 335-347.

Beardall, J., S. Stojkovic and S. Larsen (2009). Living in a high CO_2 world: impacts of global climate change on marine phytoplankton. *Plant Ecology and Diversity* **2**(2): 191 - 205.

Beatty, J. T. (2002). On the natural selection and evolution of the aerobic phototrophic bacteria. *Photosynthesis Research* **73**: 109–114.

Bednarsek, N., G. A. Tarling, D. C. E. Bakker, S. Fielding, E. M. Jones, H. J. Venables, P. Ward, A. Kuzirian, B. Leze, R. A. Feely and E. J. Murphy (2012). Extensive dissolution of live pteropods in the Southern Ocean. *Nature Geoscience* **5**(12): 881-885.

Beerling, D. J., B. H. Lomax, D. L. Royer, G. R. Upchurch and L. R. Kump (2002). An atmospheric pCO_2 reconstruction across the Cretaceous-Tertiary boundary from leaf megafossils. *Proceedings of the National Academy of Sciences of the United States of America* **99**(12): 7836-7840.

Behrenfeld, M. J., R. T. O'Malley, D. A. Siegel, C. R. McClain, J. L. Sarmiento, G. C. Feldman, A. J. Milligan, P. G. Falkowski, R. M. Letelier and E. S. Boss (2006). Climate-driven trends in contemporary ocean productivity. *Nature* **444**(7120): 752-755.

Beja, O., M. T. Suzuki, J. F. Heidelberg, W. C. Nelson, C. M. Preston, T. Hamada, J. A. Eisen, C. M. Fraser and E. F. DeLong (2002). Unsuspected diversity among marine aerobic anoxygenic phototrophs. *Nature* **415**(6872): 630-633.

Belas, R., E. Horikawa, S. Aizawa and R. Suvanasuthi (2009). Genetic determinants of *Silicibacter* sp. TM1040 motility. *Journal of Bacteriology* **191**(14): 4502-4512.

Bell, T. G., M. T. Johnson, T. D. Jickells and P. S. Liss (2007). Ammonia/ammonium dissociation coefficient in seawater: a significant numerical correction. *Environmental Chemistry* **4**(3): 183-186.

Berg, G. M., M. Balode, I. Purina, S. Bekere, C. Béchemin and S. Maestrini (2003). Plankton community composition in relation to availability and uptake of oxidized and reduced nitrogen. *Aquatic Microbial Ecology* **30**(3): 263-274.

Berger, A. L. (1976). Obliquity and precession for the last 5,000,000 years. *Astronomy and Astrophysics* **51**(1): 127-135.

Berger, W. (2012). Milankovitch Theory-Hits and Misses. Technical report. La Jolla, California, USA, Scripps Institution of Oceanography**:** 36.

Berges, J. A. and P. G. Falkowski (1998). Physiological stress and cell death in marine phytoplankton: Induction of proteases in response to nitrogen or light limitation. *Limnology and Oceanography* **43**(1): 129-135.

Bergey's Manual Trust (2001). *Bergey's Manual of Systematic Bacteriology*. New York, Springer-Verlag.

Berner, R. A. and S. Honjo (1981). Pelagic sedimentation of aragonite: its geochemical significance. *Science* **211**(4485): 940-942.

Bernhard, G. H., J. Kathrin and G. D. Hans (1993). The Pearson product-moment correlation coefficient is better suited for identification of DNA fingerprint profiles than band matching algorithms. *Electrophoresis* **14**(1): 967-972.

Betzer, P. R., R. H. Byrne, J. G. Acker, C. S. Lewis, R. R. Jolley and R. A. Feely (1984). The oceanic carbonate system: A reassessment of biogenic controls. *Science* **226**(4678): 1074-1077.

Bird, D. F. and J. Kalff (1984). Empirical relationships between bacterial abundance and chlorophyll concentration in fresh and marine waters. *Canadian Journal of Fisheries and Aquatic Sciences* **41**(7): 1015-1023.

Birnie, G. D. and D. Rickwood (1978). *Centrifugal separations in molecular and cell biology*, Butterworth-Heinemann Limited.

Bjornsen, P. K. (1988). Phytoplankton exudation of organic matter: Why do healthy cells do it? *Limnology and Oceanography* **33**(1): 151-154.

Blackburn, T. J., P. E. Olsen, S. A. Bowring, N. M. McLean, D. V. Kent, J. Puffer, G. McHone, E. T. Rasbury and M. Et-Touhami (2013). Zircon U-Pb geochronology links theend-Triassic extinction with the central Atlantic magmatic province. *Science* **340**(6135): 941-945.

Blasing, T. J. and K. Smith. (2010). Recent greenhouse gas concentrations. *Oak Ridge National Laboratory, United State Department of Energy*, from http://cdiac.ornl.gov/pns/current_ghg.html.

Boden, T. A., G. Marland and R. J. Andres. (2010). Global, regional and national fossil-fuel CO_2 emissions. from http://cdiac.ornl.gov/trends/emis/tre_glob.html.

Bollmann, A., M. J. Bar-Gilissen and H. J. Laanbroek (2002). Growth at low ammonium concentrations and starvation response as potential factors involved in niche differentiation among ammonia-oxidizing bacteria. *Applied and Environmental Microbiology* **68**(10): 4751-4757.

Bollmann, A. and H. J. Laanbroek (2001). Continuous culture enrichments of ammonia-oxidizing bacteria at low ammonium concentrations. *FEMS Microbiology Ecology* **37**(3): 211-221.

Bond-Lamberty, B. and A. Thomson (2010). Temperature-associated increases in the global soil respiration record. *Nature* **464**(7288): 579-582.

Bopp, L., P. Monfray, O. Aumont, J. L. Dufresne, H. Le Treut, G. Madec, L. Terray and J. C. Orr (2001). Potential impact of climate change on marine export production. *Global Biogeochemical Cycles* **15**(1): 81-99.

Bothe, H., G. Jost, M. Schloter, B. B. Ward and K. P. Witzel (2000). Molecular analysis of ammonia oxidation and denitrification in natural environments. *FEMS Microbiology Reviews* **24**(5): 673-690.

Boyce, D. G., M. R. Lewis and B. Worm (2010). Global phytoplankton decline over the past century. *Nature* **466**(7306): 591-596.

Bradley, P. B., M. W. Lomas and D. A. Bronk (2010). Inorganic and organic nitrogen use by phytoplankton along Chesapeake Bay, measured using a flow cytometric sorting approach. *Estuaries and Coasts* **33**(4): 971-984.

Bratbak, G. and T. Thingstad (1985). Phytoplankton-bacteria interactions: an apparent paradox? Analysis of a model system with both competition and commensalism. *Marine Ecology Progress Series* **25**(1): 23-30.

Bricelj, V. M. and D. J. Lonsdale (1997). *Aureococcus anophagefferens*: Causes and ecological consequences of brown tides in U.S. Mid-Atlantic coastal waters. *Limnology and Oceanography* **42**(5): 1023-1038.

Brinkhoff, T., H.-A. Giebel and M. Simon (2008). Diversity, ecology, and genomics of the *Roseobacter* clade: a short overview. *Archives of Microbiology* **189**(6): 531-539.

Broecker, W. and E. Clark (2009). Ratio of coccolith CaCO3 to foraminifera CaCO3 in late Holocene deep sea sediments. *Paleoceanography* **24**(3): PA3205.

Brownlee, C. and A. R. Taylor (2002). Algal calcification and silification. *Encyclopedia of Life Sciences* Chichester, John Wiley & Sons , Ltd**:** 1-6.

Bruhn, J. B., L. Gram and R. Belas (2007). Production of antibacterial compounds and biofilm formation by *Roseobacter* species are iInfluenced by culture conditions. *Applied and Environmental Microbiology* **73(**2): 442-450.

Brussaard, C. P. D., A. A. M. Noordeloos, H. Witte, M. C. J. Collenteur, K. Schulz, A. Ludwig and U. Riebesell (2013). Arctic microbial community dynamics influenced by elevated CO_2 levels. *Biogeosciences* **10**(2): 719-731.

Buchan, A., J. M. Gonzalez and M. A. Moran (2005). Overview of the Marine *Roseobacter* Lineage. *Applied and Environmental Microbiology* **71**(10): 5665-5677.

Buckley, D. H., V. Huangyutitham, S. F. Hsu and T. A. Nelson (2007). Stable isotope probing with ^{15}N achieved by disentangling the effects of genome G+C content and isotope enrichment on DNA density. *Applied and environmental microbiology* **73**(10): 3189-3195.

Burgess, S. D., S. Bowring and S.-z. Shen (2014). High-precision timeline for Earth's most severe extinction. *Proceedings of the National Academy of Sciences* **111**(9): 3316-3321.

Caffrev, J. M., N. Harrington, I. Solem and B. B. Ward (2003). Biogeochemical processes in a small California estuary. 2. Nitrification activity, community structure and role in nitrogen budgets. *Marine Ecology Progress Series* **248**: 27-40.

Calbet, A. and M. R. Landry (2004). Phytoplankton growth, microzooplankton grazing, and carbon cycling in marine systems. *Limnology and Oceanography* **49**(1): 51-57.

Caldeira, K. (2007). What corals are dying to tell us about CO_2 and ocean acidification. *Oceanography* **20**: 188-195.

Caldeira, K. and M. E. Wickett (2003). Oceanography: Anthropogenic carbon and ocean pH. *Nature* **425**(6956): 365-365.

Caldeira, K. and M. E. Wickett (2005). Ocean model predictions of chemistry changes from carbon dioxide emissions to the atmosphere and ocean. *Journal of Geophysical Research: Oceans* **110**(C9).

Callister, S. J., M. A. Dominguez, C. D. Nicora, X. Zeng, C. L. Tavano, S. Kaplan, T. J. Donohue, R. D. Smith and M. S. Lipton (2006). Application of the accurate mass and time tag approach to the proteome analysis of sub-cellular fractions obtained from *Rhodobacter sphaeroides* 2.4.1. aerobic and photosynthetic cell cultures. *Journal of Proteome Research* **5**(8): 1940-1947.

Calvo, L. and L. J. Garcia-Gil (2004). Use of *amoB* as a new molecular marker for ammonia-oxidizing bacteria. *Journal of Microbiological Methods* **57**(1): 69-78.

Campisano, C. J. (2012). Milankovitch Cycles, paleoclimatic change, and hominin evolution. *Nature Education Knowledge* **4**(3).

Cantoni, G. L. and D. G. Anderson (1956). Enzymatic cleavage of dimethylpropiothetin by *Polysiphonia lanosa*. *Journal of Biological Chemistry* **222**(1): 171-177.

Caron, D. A., P. G. Davis, L. P. Madin and J. M. Sieburth (1982). Heterotrophic bacteria and bacterivorous protozoa in oceanic macroaggregates. *Science* **218**(4574): 795-797.

Carter, C., V. G. Britton and L. Haff (1983). CsTFA: A centrifugation medium for nucleic acid isolation. *Biotechniques* **1**: 142-147.

Charlson, R. J., J. E. Lovelock, M. O. Andreae and S. G. Warren (1987). Oceanic phytoplankton, atmospheric sulphur, cloud albedo and climate. *Nature* **326**(6114): 655-661.

Chaudhuri, R. R., N. J. Loman, L. A. Snyder, C. M. Bailey, D. J. Stekel and M. J. Pallen (2008). xBASE2: a comprehensive resource for comparative bacterial genomics. *Nucleic Acids Research* **36**(Database issue): 543-546.

Checkley, D. M., A. G. Dickson, M. Takahashi, J. A. Radich, N. Eisenkolb and R. Asch (2009). Elevated CO_2 enhances otolith growth in young fish. *Science* **324**(5935): 1683.

Chen, K. and L. Pachter (2005). Bioinformatics for whole-genome shotgun sequencing of microbial communities. *PLoS Computational Biology* **1**(2): 24.

Chen, X. and K. Gao (2003). Effect of CO_2 concentrations on the activity of photosynthetic CO_2 fixation and extracelluar carbonic anhydrase in the marine diatom *Skeletonema costatum*. *Chinese Science Bulletin* **48**(23): 2616-2620.

Chisholm, J. R. and J. Gattuso, P (1991). Validation of the alkalinity anomaly technique for investigating calcification and photosynthesis in coral reef communities. *Limnology and Oceanography* **36**(6): 1232-1239.

Cho, J., C and S. J. Giovannoni (2004). Cultivation and growth characteristics of a diverse group of oligotrophic Marine Gammaproteobacteria. *Applied and Environmental Microbiology* **70**(1): 432-440.

Cho, J., C, M. D. Stapels, R. M. Morris, K. L. Vergin, M. S. Schwalbach, S. A. Givan, D. F. Barofsky and S. J. Giovannoni (2007). Polyphyletic photosynthetic reaction centre genes in oligotrophic marine Gammaproteobacteria. *Environmental Microbiology* **9**(6): 1456-1463.

Chrost, R. H. and M. A. Faust (1983). Organic carbon release by phytoplankton: its composition and utilization by bacterioplankton. *Journal of Plankton Research* **5**(4): 477-493.

Clark, D. R. and K. J. Flynn (2000). The relationship between the dissolved inorganic carbon concentration and growth rate in marine phytoplankton. *Proceedings of the Royal Society of London. Series B: Biological Sciences* **267**(1447): 953-959.

Clarke, K. R. (1993). Non-parametric multivariate analyses of changes in community structure. *Australian Journal of Ecology* **18**(1): 117-143.

Coci, M., D. Riechmann, P. L. Bodelier, S. Stefani, G. Zwart and H. J. Laanbroek (2005). Effect of salinity on temporal and spatial dynamics of ammonia‐oxidising bacteria from intertidal freshwater sediment. *FEMS Microbiology Ecology* **53**(3): 359-368.

Cole, J. R., Q. Wang, E. Cardenas, J. Fish, B. Chai, R. J. Farris, A. S. Kulam-Syed-Mohideen, D. M. McGarrell, T. Marsh, G. M. Garrity and J. M. Tiedje (2009). The Ribosomal Database Project: improved alignments and new tools for rRNA analysis. *Nucleic Acids Research* **37**(suppl 1): 141-145.

Comeau, S., G. Gorsky, S. Alliouane and J. P. Gattuso (2010). Larvae of the pteropod *Cavolinia inflexa* exposed to aragonite undersaturation are viable but shell-less. *Marine Biology* **157**(10): 2341-2345.

Comeau, S., R. Jeffree, J. Teyssié, L and J. Gattuso, P (2010). Response of the Arctic pteropod *Limacina helicina* to projected future environmental conditions. *PLoS One* **5**(6): e11362.

Corfield, R. M. (1994). Palaeocene oceans and climate: An isotopic perspective. *Earth-Science Reviews* **37**(3-4): 225-252.

Cottrell, M. T. and D. L. Kirchman (2000). Natural assemblages of marine Proteobacteria and members of the *Cytophaga-Flavobacter* cluster consuming low and high molecular weight dissolved organic matter. *Applied and Environmental Microbiology* **66**(4): 1692-1697.

Cottrell, M. T., J. Ras and D. L. Kirchman (2010). Bacteriochlorophyll and community structure of aerobic anoxygenic phototrophic bacteria in a particle-rich estuary. *ISME Journal* **4**(7): 945-954.

Crawfurd, K. (2010). Marine phytoplankton in a high CO_2 world. PhD Thesis, University of Dundee.

Cunliffe, M. (2011). Correlating carbon monoxide oxidation with cox genes in the abundant Marine *Roseobacter* Clade. *ISME Journal* **5**(4): 685-691.

Cunliffe, M., A. S. Whiteley, L. Newbold, A. Oliver, H. Schafer and J. C. Murrell (2009). Comparison of bacterioneuston and bacterioplankton dynamics during a phytoplankton bloom in a fjord mesocosm. *Applied and Environmental Microbiology* **75**(22): 7173-7181.

Curson, A. R. J., J. D. Todd, M. J. Sullivan and A. W. B. Johnston (2011). Catabolism of dimethylsulphoniopropionate: microorganisms, enzymes and genes. *Nature Reviews Microbiology* **9**(12): 849-859.

D'Hondt, S., T. D. Herbert, J. King and C. Gibson (1996). Planktic foraminifera, asteroids and marine production: Death and recovery at the Cretaceous-Tertiary boundary. *Geological Society of America Special Papers* **307**: 303-317.

D'Hondt, S., M. E. Q. Pilson, H. Sigurdsson, A. K. Hanson, Jr. and S. Carey (1994). Surface-water acidification and extinction at the Cretaceous-Tertiary boundary. *Geology* **22**(11): 983-986.

D'Orgeville, M. and W. R. Peltier (2009). Implications of both statistical equilibrium and global warming simulations with CCSM3. Part I: On the decadal variability in the North Pacific basin. *Journal of Climate* **22**(20).

Dang, H. and C. R. Lovell (2000). Bacterial primary colonization and early succession on surfaces in marine waters as determined by amplified rRNA gene restriction analysis and sequence analysis of 16S rRNA Genes. *Applied and Environmental Microbiology* **66**(2): 467-475.

De Beer, D. and A. Larkum (2001). Photosynthesis and calcification in the calcifying algae *Halimeda discoidea* studied with microsensors. *Plant, Cell & Environment* **24**(11): 1209-1217.

De Kluijver, A., K. Soetaert, K. G. Schulz, U. Riebesell, R. G. J. Bellerby and J. J. Middelburg (2010). Phytoplankton-bacteria coupling under elevated CO_2 levels: a stable isotope labelling study. *Biogeosciences (BG)* **7**(11): 3783-3797.

De Vrind-de Jong, E. W. and J. P. M. De Vrind (1997). Algal deposition of carbonates and silicates. *Reviews in Mineralogy and Geochemistry* **35**(1): 267-307.

Dean, F. B., S. Hosono, L. Fang, X. Wu, A. F. Faruqi, P. Bray-Ward, Z. Sun, Q. Zong, Y. Du, J. Du, M. Driscoll, W. Song, S. F. Kingsmore, M. Egholm and R. S. Lasken (2002). Comprehensive human genome amplification using multiple displacement amplification. *Proceedings of the National Academy of Sciences of the United States of America* **99**(8): 5261-5266.

Dean, F. B., J. R. Nelson, T. L. Giesler and R. S. Lasken (2001). Rapid amplification of plasmid and phage DNA using Phi29 DNA polymerase and multiply-primed rolling circle amplification. *Genome Research* **11**(6): 1095-1099.

Dean, W. E. and E. Gorham (1998). Magnitude and significance of carbon burial in lakes, reservoirs, and peatlands. *Geology* **26**(6): 535-538.

DeConto, R. M. (2009). Plate Tectonics and Climate Change. *Encyclopedia of Paleoclimatology and Ancient Environments*. V. Gornitz. Netherlands, Springer**:** 784-797.

Del Giorgio, P. A. and C. M. Duarte (2002). Respiration in the open ocean. *Nature* **420**(6914): 379-384.

DeLong, E. F. (1992). Archaea in coastal marine environments. *Proceedings of the National Academy of Sciences. USA* **89**: 5685-5689.

DeLong, E. F. and O. Béjà (2010). The light-driven proton pump proteorhodopsin enhances bacterial survival during tough times. *PLoS Biology* **8**(4): e1000359.

DeLong, E. F., D. G. Franks and A. L. Alldredge (1993). Phylogenetic diversity of aggregatea attached vs. free-living marine bacterial assemblages. *Limnology and Oceanography* **38**(5): 924-934.

DeLorenzo, S., S. L. Bräuer, C. A. Edgmont, L. Herfort, B. M. Tebo and P. Zuber (2012). Ubiquitous dissolved inorganic carbon assimilation by marine bacteria in the Pacific northwest coastal Ocean as determined by stable isotope probing. *PLoS ONE* **7**(10): e46695.

DeSantis, T. Z., P. Hugenholtz, N. Larsen, M. Rojas, E. L. Brodie, K. Keller, T. Huber, D. Dalevi, P. Hu and G. L. Andersen (2006). Greengenes, a chimera-checked 16S rRNA gene database and workbench compatible with ARB. *Applied and Environmental Microbiology* **72**(7): 5069-5072.

Dijkhuizen, L. and W. Harder (1985). *Microbial Metabolism of Carbon Dioxide*. Oxford, Pergamon Press Ltd.

Ding, Y.-H. R., K. K. Hixson, C. S. Giometti, A. Stanley, A. Esteve-Núñez, T. Khare, S. L. Tollaksen, W. Zhu, J. N. Adkins, M. S. Lipton, R. D. Smith, T. Mester and D. R. Lovley (2006). The proteome of dissimilatory metal-reducing microorganism *Geobacter sulfurreducens* under various growth conditions. *Biochimica et Biophysica Acta (BBA) - Proteins and Proteomics* **1764**(7): 1198-1206.

Direito, S. O. L., E. Zaura, M. Little, P. Ehrenfreund and W. F. M. Röling (2014). Systematic evaluation of bias in microbial community profiles induced by whole genome amplification. *Environmental Microbiology*.

Dixson, D. L., P. L. Munday and G. P. Jones (2010). Ocean acidification disrupts the innate ability of fish to detect predator olfactory cues. *Ecology Letters* **13**(1): 68-75.

Dodge, J. D. and H. G. Marshall (1994). Biogeographic analysis of the armored planktonic dinoflagellate *Ceratium* in the North Atlantic and adjacent seas. *Journal of Phycology* **30**(6): 905-922.

Doney, S. C., V. J. Fabry, R. A. Feely and J. A. Kleypas (2009). Ocean Acidification: The other CO_2 problem. *Annual Review of Marine Science* **1**: 169-192.

Doronia, N. V. and Y. A. Trotsenko (1985). Levels of carbon dioxide assimilation in bacteria with different pathways of C1 metabolism. *Mikrobiologiya* **53**: 885 - 889.

Dortch, Q. (1990). The interaction between ammonium and nitrate uptake in phytoplankton. *Marine Ecology Progress Series.* **61**(1): 183-201.

Duarte, C. and Y. Prairie (2005). Prevalence of heterotrophy and atmospheric CO_2 emissions from aquatic ecosystems. *Ecosystems* **8**(7): 862-870.

Dupont, S., N. Dorey and M. Thorndyke (2010). What meta-analysis can tell us about vulnerability of marine biodiversity to ocean acidification? *Estuarine, Coastal and Shelf Science* **89**(2): 182-185.

DuRand, M. D., R. E. Green, H. M. Sosik and R. J. Olson (2002). Diel variations in optical properties of *Micromonas pusilla* (*prasinophyceae*). *Journal of Phycology* **38**(6): 1132-1142.

Edgar, R. C. (2004). MUSCLE: multiple sequence alignment with high accuracy and high throughput. *Nucleic Acids Research* **32**(5): 1792-1797.

Edwards, U., T. Rogall, H. Blocker, M. Emde and E. C. Bottger (1989). Isolation and direct complete nucleotide determination of entire genes. Characterization of a gene coding for 16S ribosomal RNA. *Nucleic Acids Research* **17**(19): 7843-7853.

Egge, J. K., T. F. Thingstad, A. Larsen, A. Engel, J. Wohlers, R. G. J. Bellerby and U. Riebesell (2009). Primary production during nutrient-induced blooms at elevated CO_2 concentrations. *Biogeosciences* **6**(5): 877-885.

Egleston, E. S., C. L. Sabine and F. M. Morel (2010). Revelle revisited: Buffer factors that quantify the response of ocean chemistry to changes in DIC and alkalinity. *Global Biogeochemical Cycles* **24**(1).

Eikrem, W. and J. Throndsen (1990). The ultrastructure of *Bathycoccus* gen. nov. and *B. prasino*s sp. nov., a non-motile picoplanktonic alga (Chlorophyta, *Prasinophyceae*) from the Mediterranean and Atlantic. *Phycologia* **29**(3): 344-350.

Elias, D., S. Tollaksen, D. Kennedy, H. Mottaz, C. Giometti, J. McLean, E. Hill, G. Pinchuk, M. Lipton, J. Fredrickson and Y. Gorby (2008). The influence of cultivation methods on *Shewanella oneidensis* physiology and proteome expression. *Archives of Microbiology* **189**(4): 313-324.

Engel, A., K. G. Schulz, U. Riebesell, R. Bellerby, B. Delille and M. Schartau (2008). Effects of CO_2 on particle size distribution and phytoplankton abundance during a mesocosm bloom experiment (PeECE II). *Biogeosciences* **5**(2): 509-521.

Engel, A., I. Zondervan, K. Aerts, L. Beaufort, A. Benthien, L. Chou, B. Delille, J. P. Gattuso, J. Harlay, C. Heemann, L. Hoffmann, S. Jacquet, J. Nejstgaard, M. D. Pizay, E. Rochelle-Newall, U. Schneider, A. Terbrueggen and U. Riebesell (2005). Testing the direct effect of CO_2 concentration on a bloom of the coccolithophorid *Emiliania huxleyi* in mesocosm experiments. *Limnology and Oceanography* **50**(2): 493-507.

Erlich, H. A., D. Gelfand and J. J. Sninsky (1991). Recent advances in the polymerase chain reaction. *Science* **252**(5013): 1643-1651.

Evans, C., S. V. Kadner, L. J. Darroch, W. H. Wilson, P. S. Liss and G. Malin (2007). The relative significance of viral lysis and microzooplankton grazing as pathways of dimethylsulfoniopropionate (DMSP) cleavage: An *Emiliania huxleyi* culture study. *Limnology and Oceanography* **52**(3): 1036.

Fabry, V. J. (1989). Aragonite production by pteropod molluscs in the subarctic Pacific. *Deep Sea Research Part A. Oceanographic Research Papers* **36**(11): 1735-1751.

Fabry, V. J., B. A. Seibel, R. A. Feely and J. C. Orr (2008). Impacts of ocean acidification on marine fauna and ecosystem processes. *ICES Journal of Marine Science* **65**(3): 414-432.

Falkowski, P., R. J. Scholes, E. Boyle, J. Canadell, D. Canfield, J. Elser, N. Gruber, K. Hibbard, P. Högberg, S. Linder, F. T. Mackenzie, B. Moore III, T. Pedersen, Y. Rosenthal, S. Seitzinger, V. Smetacek and W. Steffen (2000). The global carbon cycle: A test of our knowledge of Earth as a system. *Science* **290**(5490): 291-296.

Falkowski, P. G., R. T. Barber and V. Smetacek (1998). Biogeochemical controls and feedbacks on ocean primary production. *Science* **281**(5374): 200-206.

Falkowski, P. G., M. E. Katz, A. H. Knoll, A. Quigg, J. A. Raven, O. Schofield and F. J. R. Taylor (2004). The evolution of modern eukaryotic phytoplankton. *Science* **305**(5682): 354-360.

Fandino, L. B., L. Riemann, G. F. Steward and F. Azam (2005). Population dynamics of *Cytophaga-Flavobacteria* during marine phytoplankton blooms analyzed by real-time quantitative PCR. *Aquatic Microbial Ecology* **40**(3): 251-257.

Fasham, M. J. R., P. Boyd, W and G. Savidge (1999). Modeling the relative contributions of autotrophs and heterotrophs to carbon flow at a Lagrangian JGOFS station in the northeast Atlantic: the importance of DOC. *Limnology and Oceanography* **44**(1): 80-94.

Feely, R. A., R. H. Byrne, J. G. Acker, P. R. Betzer, C.-T. A. Chen, J. F. Gendron and M. F. Lamb (1988). Winter-summer variations of calcite and aragonite saturation in the Northeast Pacific. *Marine Chemistry* **25**(3): 227-241.

Feely, R. A., C. L. Sabine, J. M. Hernandez-Ayon, D. Ianson and B. Hales (2008). Evidence for upwelling of corrosive "acidified" water onto the continental shelf. *Science* **320**(5882): 1490-1492.

Feely, R. A., C. L. Sabine, K. Lee, W. Berelson, J. Kleypas, V. J. Fabry and F. J. Millero (2004). Impact of anthropogenic CO_2 on the $CaCO_3$ system in the oceans. *Science* **305**(5682): 362-366.

Feng, Y., M. E. Warner, Y. Zhang, J. Sun, F.-X. Fu, J. M. Rose and D. A. Hutchins (2008). Interactive effects of increased pCO_2, temperature and irradiance on the marine coccolithophore *Emiliania huxleyi* (*Prymnesiophyceae*). *European Journal of Phycology* **43**(1): 87-98.

Feng, Y. Y., C. E. Hare, K. Leblanc, J. M. Rose, Y. H. Zhang, G. R. DiTullio, P. A. Lee, S. W. Wilhelm, J. M. Rowe, J. Sun, N. Nemcek, C. Gueguen, U. Passow, I. Benner, C. Brown and D. A. Hutchins (2009). Effects of increased pCO_2 and temperature on the North Atlantic spring bloom. I. The phytoplankton community and biogeochemical response. *Marine Ecology Progress Series* **388**: 13-25.

Field, C. B., M. J. Behrenfeld, J. T. Randerson and P. Falkowski (1998). Primary production of the biosphere: Integrating terrestrial and oceanic components. *Science* **281**(5374): 237-240.

Flanagan, L. B. (2013). Warmer temperatures stimulate respiration and reduce net ecosystem productivity in a northern Great Plains grassland: Analysis of CO_2 exchange in automatic chambers. AGU Fall Meeting Abstracts.

Flynn, K. J., D. R. Clark and Y. Xue (2008). Modeling the release of dissolved organic matter ny phytoplankton. *Journal of Phycology* **44**(5): 1171-1187.

Fogg, G. (1983). The ecological significance of extracellular products of phytoplankton photosynthesis. *Botanica Marina* **26**(1): 3-14.

Food and Agriculture Organization (2008). The State of World Fisheries and Aquaculture - SOFIA. , Food and Agriculture Organization of the United Nations.

Forsgren, E., S. Dupont, F. Jutfelt and T. Amundsen (2013). Elevated CO_2 affects embryonic development and larval phototaxis in a temperate marine fish. *Ecology and Evolution* **3**(11): 3637-3646.

Forster, P., V. Ramaswamy, P. Artaxo, T. Berntsen, R. Betts, D. W. Fahey, J. Haywood, J. Lean, D. C. Lowe and G. Myhre (2007). Changes in atmospheric constituents and in radiative forcing. *Climate change* **20**.

Fraiberg, M., I. Borovok, R. M. Weiner and R. Lamed (2010). Discovery and characterization of cadherin domains in *Saccharophagus degradans* 2-40. *Journal of Bacteriology* **192**(4): 1066-1074.

Francis, C. A., G. D. O'Mullan and B. B. Ward (2003). Diversity of ammonia monooxygenase (*amoA*) genes across environmental gradients in Chesapeake Bay sediments. *Geobiology* **1**(2): 129-140.

Francois, R., S. Honjo, R. Krishfield and S. Manganini (2002). Factors controlling the flux of organic carbon to the bathypelagic zone of the ocean. *Global Biogeochemical Cycles* **16**(4): 1087.

Frankignoulle, M., M. Pichon and J.-P. Gattuso (1995). Aquatic calcification as a source of carbon dioxide. *Carbon Sequestration in the Biosphere*. M. Beran, Springer Berlin Heidelberg. **33:** 265-271.

Freitag, T. E., L. Chang and J. I. Prosser (2006). Changes in the community structure and activity of betaproteobacterial ammonia-oxidizing sediment bacteria along a freshwater-marine gradient. *Environmental Microbiology* **8**(4): 684-696.

Frommel, A. Y., R. Maneja, D. Lowe, A. M. Malzahn, A. J. Geffen, A. Folkvord, U. Piatkowski, T. B. Reusch and C. Clemmesen (2012). Severe tissue damage in Atlantic cod larvae under increasing ocean acidification. *Nature Climate Change* **2**(1): 42-46.

Fu, F. X., M. E. Warner, Y. Zhang, Y. Feng and D. A. Hutchins (2007). Effects of increased temperature and CO_2 on photosynthesis, growth and elemental ratios of marine *Synechococcus* and *Prochlorococcus* (cyanobacteria). *Journal of Phycology* **43**: 485-496.

Fuhrman, J. (1992). Bacterioplankton roles in cycling of organic matter: the microbial foodweb. *Bacterioplankton roles in cycling of organic matter: the microbial food web.* P. Falkowski and A. Woodhead. New York, Plenum Press**:** 361-383.

Fukuda, S.-y., Y. Suzuki and Y. Shiraiwa (2014). Difference in physiological responses of growth, photosynthesis and calcification of the coccolithophore *Emiliania huxleyi* to acidification by acid and CO_2 enrichment. *Photosynthesis Research* **121**(2): 299-309.

Gao, K., Y. Aruga, K. Asada, T. Ishihara, Akano, T., and M. Kiyohara (1993). Calcification in the articulated coralline alga *Corallina pilufera*, with special reference to the effect of elevated CO_2 concentration. *Marine Biology* **1**: 129-132.

Gao, K., J. Xu, G. Gao, Y. Li, D. A. Hutchins, B. Huang, L. Wang, Y. Zheng, P. Jin, X. Cai, D.-P. Hader, W. Li, K. Xu, N. Liu and U. Riebesell (2012). Rising CO_2 and increased light exposure synergistically reduce marine primary productivity. *Nature Climate Change* **2**(7): 519-523.

Garces, E., M. Vila, A. Rene, L. Alonso-Saez, S. Angles, A. Luglie, M. Maso and J. M. Gasol (2007). Natural bacterioplankton assemblage composition during blooms of *Alexandrium* spp. (*Dinophyceae*) in NW Mediterranean coastal waters. *Aquatic Microbial Ecology* **46**(1): 55-70.

Garrity, G. M., T. G. Lilburn and J. R. Cole (2007). *Taxonomic Outline of Bacteria and Archaea*, Michigan State University

Gasol, J. M. and X. A. Moran (1999). Effects of filtration on bacterial activity and picoplankton community structure as assessed by flow cytometry. *Aquatic Microbial Ecology* **16**(3): 251-264.

Gasol, J. M., U. L. Zweifel, F. Peters, J. A. Fuhrman and A. Hagstrom (1999). Significance of size and nucleic acid content heterogeneity as measured by flow cytometry in natural planktonic bacteria. *Applied and Environmental Microbiology* **65**(10): 4475-4483.

Gattuso, J., M. Pichon and M. Frankignoulle (1995). Biological control of air-sea CO_2 fluxes: effect of photosynthetic and calcifying marine organisms and ecosystems. *Marine Ecology Progress Series* **129**: 307-312.

Gehlen, M., N. Gruber, R. Gangsto, L. Bopp and A. Oschlies (2011). Biogeochemical consequences of ocean acidification and feedbacks to the earth system. *Ocean Acidification*: 230-248.

Geng, H. and R. Belas (2010). Molecular mechanisms underlying *roseobacter*-phytoplankton symbioses. *Current Opinion in Biotechnology* **21**(3): 332-338.

Geng, H., J. B. Bruhn, K. F. Nielsen, L. Gram and R. Belas (2008). Genetic dissection of tropodithietic acid biosynthesis by marine *roseobacters*. *Applied and Environmental Microbiology* **74**(5): 1535-1545.

Gerlach, T. (2011). Volcanic versus anthropogenic carbon dioxide. *Eos, Transactions American Geophysical Union* **92**(24): 201-202.

Giardina, E., I. Pietrangeli, C. Martone, S. Zampatti, P. Marsala, L. Gabriele, O. Ricci, G. Solla, P. Asili, G. Arcudi, A. Spinella and G. Novelli (2009). Whole genome amplification and real-time PCR in forensic casework. *BMC Genomics* **10**(1): 159.

Gifford, S. M., S. Sharma, M. Booth and M. A. Moran (2013). Expression patterns reveal niche diversification in a marine microbial assemblage. *ISME Journal* **7**(2): 281-298.

Giordano, M., J. Beardall and J. A. Raven (2005). CO_2 concentrating mechanisms in algae: Mechanisms, environmental modulation, and evolution. *Annual Review of Plant Biology* **56**(1): 99-131.

Giovannoni, S. J., H. J. Tripp, S. Givan, M. Podar, K. L. Vergin and D. Baptista (2005). Genome streamlining in a cosmopolitan oceanic bacterium. *Science* **309**: 1242-1245.

Gobler, C. J., D. A. Hutchins, N. S. Fisher, E. M. Cosper and S. A. Sanudo-Wilhelmy (1997). Release and bioavailability of C, N, P, Se, and Fe following viral lysis of a marine chrysophyte. *Limnology and Oceanography*: 1492-1504.

Gómez-Consarnau, L., N. Akram, K. Lindell, A. Pedersen, R. Neutze, D. L. Milton, J. M. González and J. Pinhassi (2010). Proteorhodopsin phototrophy promotes survival of marine bacteria during starvation. *PLoS Biology* **8**(4): e1000358.

Gomez-Consarnau, L., J. M. Gonzalez, M. Coll-Llado, P. Gourdon, T. Pascher, R. Neutze, C. Pedros-Alio and J. Pinhassi (2007). Light stimulates growth of proteorhodopsin-containing marine *Flavobacteria*. *Nature* **445**(7124): 210-213.

González, J. M., J. S. Covert, W. B. Whitman, J. R. Henriksen, F. Mayer, B. Scharf, R. Schmitt, A. Buchan, J. A. Fuhrman, R. P. Kiene and M. A. Moran (2003). *Silicibacter pomeroyi* sp. nov. and *Roseovarius nubinhibens* sp. nov., dimethylsulfoniopropionate-demethylating bacteria from marine environments. *International Journal of Systematic and Evolutionary Microbiology* **53**(5): 1261-1269.

González, J. M., B. Fernandez-Gomez, A. Fernandez-Guerra, L. Gomez-Consarnau, O. Sanchez, M. Coll-Llada, J. Del Campo, L. Escudero, R. Rodraguez-Martanez, L. Alonso-Saez, M. Latasa, I. Paulsen, O. Nedashkovskaya, I. Lekunberri, J. Pinhassi and C. Pedros-Alio (2008). Genome analysis of the proteorhodopsin-containing marine bacterium *Polaribacter* sp. MED152 (*Flavobacteria*). *Proceedings of the National Academy of Sciences* **105**(25): 8724-8729.

González, J. M., R. P. Kiene and M. A. Moran (1999). Transformation of sulfur compounds by an abundant lineage of marine bacteria in the alpha -subclass of the class Proteobacteria. *Applied and Environmental Microbiology* **65**(9): 3810-3819.

González, J. M., J. Pinhassi, B. Fernández-Gómez, M. Coll-Lladó, M. González-Velázquez, P. Puigbò, S. Jaenicke, L. Gómez-Consarnau, A. Fernàndez-Guerra and A. Goesmann (2011). Genomics of the proteorhodopsin-containing marine flavobacterium *Dokdonia* sp. strain MED134. *Applied and Environmental Microbiology* **77**(24): 8676-8686.

González, J. M., M. C. Portillo and C. Saiz-Jimenez (2005). Multiple displacement amplification as a pre-polymerase chain reaction (pre-PCR) to process difficult to amplify samples and low copy number sequences from natural environments. *Environmental Microbiology* **7**(7): 1024-1028.

González, J. M., R. Simo, R. Massana, J. S. Covert, E. O. Casamayor, C. Pedros-Alio and M. A. Moran (2000). Bacterial community structure associated with a dimethylsulfoniopropionate-producing North Atlantic algal bloom. *Applied and Environmental Microbiology* **66**(10): 4237-4246.

Good, I. J. (1953). The population frequencies of species and the estimation of population parameters. *Biometrika* **40**(3-4): 237-264.

Gordillo, F. J. L., C. Jiménez, F. L. Figueroa and F. X. Niell (2003). Influence of elevated CO_2 and nitrogen supply on the carbon assimilation performance and cell composition of the unicellular alga *Dunaliella viridis*. *Physiologia Plantarum* **119**(4): 513-518.

Gosink, J. J., C. R. Woese and J. T. Staley (1998). Polaribacter gen. nov., with three new species, *P. irgensii* sp. nov., *P. franzmannii* sp. nov. and *P. filamentus* sp. nov., gas vacuolate polar marine bacteria of the *Cytophaga-Flavobacterium-Bacteroides* group and reclassification of '*Flectobacillus glomeratus*' as *Polaribacter glomeratus* comb. nov. *International Journal of Systematic Bacteriology* **48**(1): 223-235.

Gotelli, N. J. and R. K. Colwell (2001). Quantifying biodiversity: procedures and pitfalls in the measurement and comparison of species richness. *Ecology Letters* **4**(4): 379-391.

Grigioni, S., R. Boucher-Rodoni, A. Demarta, M. Tonolla and R. Peduzzi (2000). Phylogenetic characterisation of bacterial symbionts in the accessory nidamental glands of the sepioid *Sepia officinalis* (Cephalopoda: Decapoda). *Marine Biology* **136**(2): 217-222.

Grossart, H.-P., F. Levold, M. Allgaier, M. Simon and T. Brinkhoff (2005). Marine diatom species harbour distinct bacterial communities. *Environmental Microbiology* **7**(6): 860-873.

Grossart, H. P., M. Allgaier, U. Passow and U. Riebesell (2006). Testing the effect of CO_2 concentration on dynamics of marine heterotrophic bacterioplankton. *Limnology and Oceanography* **51**: 1-11.

Grossart, H. P., T. Kiørboe, K. Tang and H. Ploug (2003). Bacterial colonization of particles: Growth and interactions. *Applied and Environmental Microbiology* **69**(6): 3500-3509.

Gurevitch, J. and L. V. Hedges (1999). Statistical issues in ecological meta-analyses. *Ecology* **80**(4): 1142-1149.

Gutowska, M. A., H. O. Pörtner and F. Melzner (2008). Growth and calcification in the cephalopod *Sepia officinalis* under elevated seawater pCO_2. *Marine Ecology Progress Series* **373**: 303-309.

Hall, T. A. (1999). BioEdit: a user-friendly biological sequence alignment editor and analysis program for Windows 95/98/NT *Nucleic Acids Symposium Series* **41**: 95-98.

Hammer, A., R. Schumann and H. Schubert (2002). Light and temperature acclimation of *Rhodomonas salina* (*Cryptophyceae*): photosynthetic performance. *Aquatic Microbial Ecology* **29**(3): 287-296.

Hammer, C. U., H. B. Clausen and W. Dansgaard (1980). Greenland ice sheet evidence of post-glacial volcanism and its climatic impact. *Nature* **288**(5788): 230-235.

Handelsman, J., M. R. Rondon, S. F. Brady, J. Clardy and R. M. Goodman (1998). Molecular biological access to the chemistry of unknown soil microbes: A new frontier for natural products. *Chemistry & Biology* **5**(10): 245-249.

Hansel, C. M. and C. A. Francis (2006). Coupled photochemical and enzymatic Mn(II) oxidation pathways of a planktonic *Roseobacter*-like bacterium. *Applied and Environmental. Microbiology* **72**(5): 3543-3549.

Hansell, D. A., Carlson, C.A., Repeta,D.j., Schlitzer,R. (2009). Dissolved organic matter in the ocean: A controversy stimulates new insights. *Oceanography* **22**(4).

Hansen, J. E., M. Sato, A. Lacis, R. Ruedy, I. Tegen and E. Matthews (1998). Climate forcings in the Industrial era. *Proceedings of the National Academy of Sciences of the United States of America* **95**(22): 12753-12758.

Harvey, B. P., D. Gwynn‐Jones and P. J. Moore (2013). Meta‐analysis reveals complex marine biological responses to the interactive effects of ocean acidification and warming. *Ecology and Evolution* **3**(4): 1016-1030.

Hays, G. C., A. J. Richardson and C. Robinson (2005). Climate change and marine plankton. *Trends in Ecology and Evolution* **20**(6): 337-344.

Hays, J. D., J. Imbrie and N. J. Shackleton (1976). Variations in the Earth's orbit: Pacemaker of the ice ages. *Science* **194**(4270): 1121-1132.

Head, I. M., J. R. Saunders and R. W. Pickup (1998). Microbial evolution, diversity, and ecology: A decade of ribosomal RNA analysis of uncultivated microorganisms. *Microbial Ecology* **35**(1): 1-21.

Healy, F. G., R. M. Ray, H. C. Aldrich, A. C. Wilkie, L. O. Ingram and K. T. Shanmugam (1995). Direct isolation of functional genes encoding cellulases from the microbial consortia in a thermophilic, anaerobic digester maintained on lignocellulose. *Applied Microbiology and Biotechnology* **43**(4): 667-674.

Hein, M. and K. Sand-Jensen (1997). CO_2 increases oceanic primary production. *Nature* **388**(6642): 526-527.

Helm, K. P., N. L. Bindoff and J. A. Church (2011). Observed decreases in oxygen content of the global ocean. *Geophysical Research Letters* **38**(23).

Hendriks, I. E., C. M. Duarte and M. Álvarez (2010). Vulnerability of marine biodiversity to ocean acidification: A meta-analysis. *Estuarine, Coastal and Shelf Science* **86**(2): 157-164.

Henriksen, J. R. (2004). webLIBSHUFF. from http://libshuff.mib.uga.edu.

Herrmann, A. D., M. E. Patzkowsky and D. Pollard (2003). Obliquity forcing with 8-12 times preindustrial levels of atmospheric pCO2 during the Late Ordovician glaciation. *Geology* **31**(6): 485-488.

Hixson, K. K., J. N. Adkins, S. E. Baker, R. J. Moore, B. A. Chromy, R. D. Smith, S. L. McCutchen-Maloney and M. S. Lipton (2006). Biomarker candidate identification in *Yersinia pestis* using organism-wide semiquantitative proteomics. *Journal of Proteome Research* **5**(11): 3008-3017.

Hold, G. L., E. A. Smith, M. S. Rappé, E. W. Maas, E. R. B. Moore, C. Stroempl, J. R. Stephen, J. I. Prosser, T. H. Birkbeck and S. Gallacher (2001). Characterisation of bacterial communities associated with toxic and non-toxic dinoflagellates: *Alexandrium* spp. and *Scrippsiella trochoidea*. *FEMS Microbiology Ecology* **37**(2): 161-173.

Holligan, P. M., E. Fernández, J. Aiken, W. M. Balch, P. Boyd, P. H. Burkill, M. Finch, S. B. Groom, G. Malin, K. Muller, D. A. Purdie, C. Robinson, C. C. Trees, S. M. Turner and P. van der Wal (1993). A biogeochemical study of the coccolithophore, *Emiliania huxleyi*, in the North Atlantic. *Global Biogeochemical Cycles* **7**(4): 879-900.

Hopkins, F. E., S. M. Turner, P. D. Nightingale, M. Steinke, D. Bakker and P. S. Liss (2009). Ocean acidification and marine trace gas emissions. *Proceedings of the National Academy of Sciences of the United States of America* **107**(2): 760-765.

Hopkinson, B. M., Y. Xu, D. Shi, P. J. McGinn and F. M. Morel (2010). The effect of CO_2 on the photosynthetic physiology of phytoplankton in the Gulf of Alaska. *Limnology and Oceanography* **55**(5): 2011.

Houghton, J., Y. Ding, D. Griggs, M. Noguer, P. Van der Linden, X. Dai, K. Maskell and C. Johnson (2001). IPCC, 2001: Climate Change 2001: The Scientific Basis. Contribution of Working Group I to the Third Assessment Report of the Intergovernmental Panel on Climate Change. Cambridge, United Kingdom, New York, USA. **881:** 9.

Houghton, J. T., B. A. Callander and S. K. Varney (1992). *Climate change 1992: the supplementary report to the IPCC scientific assessment*, Cambridge University Press.

Howard, E. C., J. R. Henriksen, A. Buchan, C. R. Reisch, H. Burgmann, R. Welsh, W. Ye, J. M. Gonzalez, K. Mace, S. B. Joye, R. P. Kiene, W. B. Whitman and M. A. Moran (2006). Bacterial taxa that limit sulfur flux from the Ocean. *Science* **314**(5799): 649-652.

Howard, E. C., S. Sun, E. J. Biers and M. A. Moran (2008). Abundant and diverse bacteria involved in DMSP degradation in marine surface waters. *Environmental Microbiology* **10**(9): 2397-2410.

Howard, M. D. A., W. P. Cochlan, N. Ladizinsky and R. M. Kudela (2007). Nitrogenous preference of toxigenic *Pseudo-nitzschia australis* (*Bacillariophyceae*) from field and laboratory experiments. *Harmful Algae* **6**(2): 206-217.

Hoyle, F. (1981). *Ice*, Hutchinson.

Hsu, K. J. (1980). Terrestrial catastrophe caused by cometary impact at the end of Cretaceous. *Nature* **285**(5762): 201-203.

Huesemann, M. H., A. D. Skillman and E. A. Crecelius (2002). The inhibition of marine nitrification by ocean disposal of carbon dioxide. *Marine Pollution Bulletin* **44**(2): 142-148.

Hugenholtz, P. (2002). Exploring prokaryotic diversity in the genomic era. *Genome Biology* **3**(2).

Hughes, L. (2000). Biological consequences of global warming: is the signal already apparent? *Trends in Ecology and Evolution* **15**(2): 56-61.

Human Microbiome Project Consortuim (2012). A framework for human microbiome research. *Nature* **486**(7402): 215-221.

Hunt, B., E. Pakhomov, G. Hosie, V. Siegel, P. Ward and K. Bernard (2008). Pteropods in southern ocean ecosystems. *Progress in Oceanography* **78**(3): 193-221.

Huson, D. H., A. F. Auch, J. Qi and S. C. Schuster (2007). MEGAN analysis of metagenomic data. *Genome Research*: 377 - 386.

Iglesias-Rodriguez, M. D., C. W. Brown, S. C. Doney, J. Kleypas, D. Kolber, Z. Kolber, P. K. Hayes and P. G. Falkowski (2002). Representing key phytoplankton functional groups in ocean carbon cycle models: Coccolithophorids. *Global Biogeochemical Cycles* **16**(4): 47-41.

Iglesias-Rodriguez, M. D., P. R. Halloran, R. E. M. Rickaby, I. R. Hall, E. Colmenero-Hidalgo, J. R. Gittins, D. R. H. Green, T. Tyrrell, S. J. Gibbs, P. von Dassow, E. Rehm, E. V. Armbrust and K. P. Boessenkool (2008). Phytoplankton Calcification in a High-CO_2 World. *Science* **320**(5874): 336-340.

Iglesias-Rodriguez, M. D., N. A. Nimer and M. J. Merrett (1998). Carbon dioxide-concentrating mechanism and the development of extracellular carbonic anhydrase in the marine picoeukaryote Micromonas pusilla. *New Phytologist* **140**(4): 685-690.

IPCC (2000). Emissions Scenarios - A Special Report of Working Group III of the Intergovernmental Panel on Climate Change. N. Nakicenovic and R. Swart. Cambridge**:** 599.

IPCC (2001). The Third assessment report of the Intergovernmental Panel on Climate Change (IPCC). Cambridge, UK & New York, USA.

IPCC. (2007). "Climate Change 2007" - Synthesis Report from http://www.ipcc.ch/publications_and_data/publications_ipcc_fourth_assessment_report_synthesis_report.htm.

Ivanova, I. A., J. R. Stephen, Y.-J. Chang, J. Brüggemann, P. E. Long, J. P. McKinley, G. A. Kowalchuk, D. C. White and S. J. Macnaughton (2000). A survey of 16S rRNA and *amoA* genes related to autotrophic ammonia-oxidizing bacteria of the β-subdivision of the class proteobacteria in contaminated groundwater. *Canadian Journal of Microbiology* **46**(11): 1012-1020.

Jain, A., D. Wuebbles and H. Kheshgi (1994). Integrated science model for assessment of climate change. Proceedings of Air and Waste Management Lawrence Livermore National Lab., CA (United States).

Jensen, L. M. (1983). Phytoplankton release of extracellular organic carbon, molecular weight composition and bacterial assimilation. *Marine Ecology Progress Series* **11**(1): 39-48.

Jeong, H. J., J. E. Song, N. S. Kang, S. Kim, Y. D. Yoo and J. Y. Park (2007). Feeding by heterotrophic dinoflagellates on the common marine heterotrophic nanoflagellate *Cafeteria sp*. *Marine Ecology Progress Series* **333**: 151.

Jiao, N., Y. Zhang, Y. Zeng, N. Hong, R. Liu, F. Chen and P. Wang (2007). Distinct distribution pattern of abundance and diversity of aerobic anoxygenic phototrophic bacteria in the global ocean. *Environmental Microbiology* **9**(12): 3091-3099.

Jitrapakdee, S., M. G. Nezic, A. Ian Cassady, Y. Khew-Goodall and J. C. Wallace (2002). Molecular cloning and domain structure of chicken pyruvate carboxylase. *Biochemical and Biophysical Research Communications* **295**(2): 387-393.

Johnson, K. S. (1982). Carbon dioxide hydration and dehydration kinetics in seawater. *Limnology and Oceanography* **27**(5): 849-855.

Joint, I., S. C. Doney and D. M. Karl (2010). Will ocean acidification affect marine microbes. *ISME Journal* **5**(1): 1-7.

Joint, I., P. Henriksen, G. A. Fonnes, D. Bourne, T. F. Thingstad and B. Riemann (2002). Competition for inorganic nutrients between phytoplankton and bacterioplankton in nutrient manipulated mesocosms. *Aquatic Microbial Ecology* **29**(2): 145-159.

Joint, I., M. Mühling and J. Querellou (2010). Culturing marine bacteria – an essential prerequisite for biodiscovery. *Microbial Biotechnology* **3**(5): 564-575.

Joint, I. and A. Pomroy (1983). Production of picoplankton and small nanoplankton in the Celtic Sea. *Marine Biology* **77**(1): 19-27.

Jordan, R. and J. Green (1994). A checklist of the extant haptophyta of the world. *Journal of the Marine Biological Association UK* **74**: 149-174.

Junier, P., O.-S. Kim, O. Hadas, J. F. Imhoff and K.-P. Witzel (2008). Evaluation of PCR Primer Selectivity and Phylogenetic Specificity by Using Amplification of 16S rRNA Genes from Betaproteobacterial Ammonia-Oxidizing Bacteria in Environmental Samples. *Applied and Environmental Microbiology* **74**(16): 5231-5236.

Kaiho, K., Y. Kajiwara, K. Tazaki, M. Ueshima, N. Takeda, H. Kawahata, T. Arinobu, R. Ishiwatari, A. Hirai and M. A. Lamolda (1999). Oceanic primary productivity and dissolved oxygen levels at the Cretaceous/Tertiary boundary: Their decrease, subsequent warming, and recovery. *Paleoceanography* **14**(4): 511-524.

Kaplan, A. and L. Reinhold (1999). CO_2 concentrating mechanisms in photosynthetic microorganisms. *Annual Review of Plant Biology* **50**(1): 539-570.

Kapustina, L. (1999). Recent dynamics of bacterioplankton in Lake Ladoga. *Boreal Environment Research* **4**: 263–267.

Karnovsky, N. J., K. A. Hobson, S. Iverson and G. Hunt (2008). Seasonal changes in diets of seabirds in the North Water Polynya: a multiple-indicator approach. *Marine Ecology Progress Series* **357**: 291.

Karsten, U., Kuck, K., Vogt, C., and Kirst, G.O. (1996). Dimethylsufoniopropionate production in phototrophic organisms and its physiological function as a cryoprotectant. *Biological environmental chemistry of DMSP and related sulfonium compounds, Plenum Press, New York*: 143–153.

Keeling, R. E., A. Kortzinger and N. Gruber (2010). Ocean deoxygenation in a warming world. *Annual Review of Marine Science* **2**: 199-229.

Keller, G. (2005). Impacts, volcanism and mass extinction: random coincidence or cause and effect? *Australian Journal of Earth Sciences* **52**: 725-757.

Keller, M. D., W. K. Bellows and R. R. L. Guillard (1989). Dimethyl sulfide production in marine phytoplankton. *ACS (American Chemical Society) Symposium Series*: 167-182.

Kembel, S. W., M. Wu, J. A. Eisen and J. L. Green (2012). Incorporating 16S gene copy number information improves estimates of microbial diversity and abundance. *PLoS Computational Biology* **8**(10): e1002743.

Khalil, M. A. K. (1999). Non-CO_2 greenhouse gases in the atmosphere. *Annual Review of Energy and the Environment* **24**(1): 645-661.

Khatiwala, S., F. Primeau and T. Hall (2009). Reconstruction of the history of anthropogenic CO_2 concentrations in the ocean. *Nature* **462**(7271): 346-349.

Kiene, R. P. (1992). Dynamics of dimethyl sulfide and dimethylsulfoniopropionate in oceanic water samples. *Marine Chemistry* **37**(1-2): 29-52.

Kiene, R. P. and T. S. Bates (1990). Biological removal of dimethyl sulphide from sea water. *Nature* **345**(6277): 702-705.

Kiene, R. P. and L. J. Linn (2000). The fate of dissolved dimethylsulfoniopropionate (DMSP) in seawater: tracer studies using 35S-DMSP. *Geochimica et Cosmochimica Acta* **64**(16): 2797-2810.

Kiene, R. P. and L. J. Linn (2000). Turnover of dissolved DMSP and its relationship with bacterial production in the Gulf of Mexico. *Limnology and Oceanography* **45**: 849–861.

Kiene, R. P., L. J. Linn and J. A. Bruton (2000). New and important roles for DMSP in marine microbial communities. *Journal of Sea Research* **43**(3-4): 209-224.

Kiene, R. P., L. J. Linn, J. González, M. A. Moran and J. A. Bruton (1999). Dimethylsulfoniopropionate and methanethiol are important precursors of methionine and protein-sulfur in marine bacterioplankton. *Applied and Environmental Microbiology* **65**(10): 4549-4558

Kiessling, W. and C. Simpson (2011). On the potential for ocean acidification to be a general cause of ancient reef crises. *Global Change Biology* **17**(1): 56-67.

Kim, J. M., K. Lee, E. J. Yang, K. Shin, J. H. Noh, K. Park, T, B. Hyun, H. Jeong, J, J. Kim, H, K. Kim, Y, M. Kim, H. Kim, C, P. Jang, G and M. Jang, C (2010). Enhanced production of oceanic dimethylsulfide resulting from CO_2-induced grazing activity in a high CO_2 world. *Environmental Science and Technology* **44**(21): 8140-8143.

Kim, O.-S., P. Junier, J. F. Imhoff and K.-P. Witzel (2008). Comparative analysis of ammonia monooxygenase (*amoA*) genes in the water column and sediment-water interface of two lakes and the Baltic Sea. *FEMS Microbiology Ecology* **66**(2): 367-378.

King, G. M. (2003). Molecular and culture-based analyses of aerobic carbon monoxide oxidizer diversity. *Applied and Environmental Microbiology* **69**(12): 7257-7265.

Kiørboe, T., H.-P. Grossart, H. Ploug and K. Tang (2002). Mechanisms and rates of bacterial colonization of sinking aggregates. *Applied and Environmental Microbiology* **68**(8): 3996-4006.

Kirchman, D. L. (2002). The ecology of *Cytophaga* & *Flavobacteria* in aquatic environments. *FEMS Microbiology Ecology* **39**(2): 91-100.

Kirchman, D. L. (2004). A primer on dissolved organic material and heterotrophic prokaryotes in the oceans. *The Ocean Carbon Cycle and Climate*, Springer**:** 31-63.

Kishimoto, N., F. Fukaya, K. Inagaki, T. Sugio, H. Tanaka and T. Tano (1995). Distribution of bacteriochlorophyll a among aerobic and acidophilic bacteria and light-enhanced CO_2-incorporation in *Acidiphilium rubrum*. *FEMS Microbiology Ecology* **16**(4): 291-296.

Klappenbach, J. A., P. R. Saxman, J. R. Cole and T. M. Schmidt (2001). rrndb: the Ribosomal RNA Operon Copy Number Database. *Nucleic Acids Research* **29**(1): 181-184.

Kleypas, J. A., R. A. Feely, V. J. Fabry, C. Langdon, C. L. Sabine and L. L. Robbins (2006). Impacts of ocean acidification on coral reefs and other marine calcifiers. A guide for future research. Report of a workshop sponsored by NSF, NOAA & USGS.

Knoll, A. H., R. K. Bambach, J. L. Payne, S. Pruss and W. W. Fischer (2007). Paleophysiology and end-Permian mass extinction. *Earth and Planetary Science Letters* **256**(3): 295-313.

Knorr, W., I. C. Prentice, J. I. House and E. A. Holland (2005). Long-term sensitivity of soil carbon turnover to warming. *Nature* **433**(7023): 298-301.

Koblížek, M., M. Mašín, J. Ras, A. J. Poulton and O. Prášil (2007). Rapid growth rates of aerobic anoxygenic phototrophs in the ocean. *Environmental Microbiology* **9**(10): 2401-2406.

Kolber, Z. S., F. G. Plumley, A. S. Lang, J. T. Beatty, R. E. Blankenship, C. L. VanDover, C. Vetriani, M. Koblizek, C. Rathgeber and P. G. Falkowski (2001). Contribution of aerobic photoheterotrophic bacteria to the carbon cycle in the ocean. *Science* **292**(5526): 2492-2495.

Koops, H.-P. and A. Pommerening-Röser (2001). Distribution and ecophysiology of the nitrifying bacteria emphasizing cultured species. *FEMS Microbiology Ecology* **37**(1): 1-9.

Korhonen, H., K. S. Carslaw, D. V. Spracklen, G. W. Mann and M. T. Woodhouse (2008). Influence of oceanic dimethyl sulfide emissions on cloud condensation nuclei concentrations and seasonality over the remote Southern Hemisphere oceans: A global model study. *Journal of Geophysical Research* **113**(D15): D15204.

Kornberg, H. L. (1966). Anaplerotic sequences and their role in metabolism. *Essays in Biochemistry*. P. N. Campbell and G. P. Greville. New York, Academic Press. **2:** 11-31.

Kowalchuk, G. A. and J. R. Stephen (2001). Ammonia-oxidizing bacteria: a model for molecular microbial ecology. *Annual Reviews in Microbiology* **55**(1): 485-529.

Kowalchuk, G. A., J. R. Stephen, W. De Boer, J. I. Prosser, T. M. Embley and J. W. Woldendorp (1997). Analysis of ammonia-oxidizing bacteria of the beta subdivision of the class Proteobacteria in coastal sand dunes by denaturing gradient gel electrophoresis and sequencing of PCR-amplified 16S ribosomal DNA fragments. *Applied and Environmental Microbiology* **63**(4): 1489-1497.

Kresge, N., R. D. Simoni and R. L. Hill (2005). The discovery of heterotrophic carbon dioxide fixation by Harland G. Wood. *Journal of Biological Chemistry*. **280**(18).

Kroeker, K. J., R. L. Kordas, R. Crim, I. E. Hendriks, L. Ramajo, G. S. Singh, C. M. Duarte and J.-P. Gattuso (2013). Impacts of ocean acidification on marine organisms: quantifying sensitivities and interaction with warming. *Global Change Biology* **19**(6): 1884-1896.

Kroeker, K. J., R. L. Kordas, R. N. Crim and G. G. Singh (2010). Meta-analysis reveals negative yet variable effects of ocean acidification on marine organisms. *Ecology Letters* **13**(11): 1419-1434.

Kusnetsov, H. L. and V. I. Romanenko (1966). Produktion der biomasse heterotropher bakterien und die Geschwindigkeit ihrer Vermehrung im rybinsk-Stansee. *Verhandlungen der Internationalen Vereinigung für Theoretische und Angewandte Limnologie* **16**: 1493-1500.

Lami, R., Z. Cuperova, J. Ras, P. Lebaron and M. Koblizek (2009). Distribution of free-living and particle-attached aerobic anoxygenic phototrophic bacteria in marine environments. *Aquatic Microbial Ecology* **55**(1): 31-38.

Lane, D. J., B. Pace, G. J. Olsen, D. A. Stahl, M. L. Sogin and N. R. Pace (1985). Rapid determination of 16S ribosomal RNA sequences for phylogenetic analyses. *Proceedings of the National Academy of Sciences of the United States of America* **82**(20): 6955-6959.

Langenheder, S. and K. Jurgens (2001). Regulation of bacterial biomass and community structure by metazoan and protozoan predation. *Limnology and Oceanography* **46**(1): 121-134.

Larsson, U. and A. Hagström (1979). Phytoplankton exudate release as an energy source for the growth of pelagic bacteria. *Marine Biology* **52**(3): 199-206.

Lasken, R. S. (2012). Genomic sequencing of uncultured microorganisms from single cells. *Nature Reviews Microbiology* **10**(9): 631-640.

Lassen, M. K., K. D. Nielsen, K. Richardson, K. Garde and L. Schlüter (2010). The effects of temperature increases on a temperate phytoplankton community - A mesocosm climate change scenario. *Journal of Experimental Marine Biology and Ecology* **383**(1): 79-88.

Lau, W. W. Y., R. G. Keil and E. V. Armbrust (2007). Succession and diel transcriptional response of the glycolate-utilizing component of the bacterial community during a spring phytoplankton bloom. *Applied and Environmental Microbiology* **73**(8): 2440-2450.

Learman, D. R., B. M. Voelker, A. I. Vazquez-Rodriguez and C. M. Hansel (2011). Formation of manganese oxides by bacterially generated superoxide. *Nature Geoscience* **4**(2): 95-98.

Lebaron, P., P. Servais, H. Agogue, C. Courties and F. Joux (2001). Does the high nucleic acid content of individual bacterial cells allow us to discriminate between active cells and inactive cells in aquatic systems? *Applied and Environmental Microbiology* **67**(4): 1775-1782.

Ledyard, K. M. and J. W. H. Dacey (1996). Microbial cycling of DMSP and DMS in coastal and oligotrophic seawater. *Limnology and Oceanography* **41**(1).

Lee, N., P. H. Nielsen, K. H. Andreasen, S. Juretschko, J. L. Nielsen, K.-H. Schleifer and M. Wagner (1999). Combination of fluorescent *In Situ* hybridization and microautoradiography-a new tool for structure-function analyses in microbial ecology. *Applied and Environmental Microbiology* **65**(3): 1289-1297.

Lee, S., Y.-C. Kang and J. Fuhrman (1995). Imperfect retention of natural bacterioplankton cells by glass fiber filters. *Marine Ecology Progress Series* **119**(1): 285-290.

Lee, Z. M.-P., C. Bussema and T. M. Schmidt (2009). rrnDB: documenting the number of rRNA and tRNA genes in bacteria and archaea. *Nucleic Acids Research* **37**(Supplement 1): 489-493.

Levine, N. M., V. A. Varaljay, D. A. Toole, J. W. Dacey, S. C. Doney and M. A. Moran (2012). Environmental, biochemical and genetic drivers of DMSP degradation and DMS production in the Sargasso Sea. *Environmental Microbiology* **14**(5): 1210-1223.

Lewis, E., D. Wallace and L. J. Allison (1998). *Program developed for CO_2 system calculations*, Carbon Dioxide Information Analysis Center, managed by Lockheed Martin Energy Research Corporation for the US Department of Energy.

Li, W. K. W. (1982). Estimating heterotrophic bacterial productivity by inorganic radiocarbon uptake: Importance of establishing time courses of uptake. *Marine Ecology Progress Series* **8**(2): 167-172.

Li, W. K. W. and P. M. Dickie (1991). Light and dark ^{14}C uptake in dimly-lit oligotrophic waters: relation to bacterial activity. *Journal of Plankton Research* **13**(supp1): 29-44.

Linley, E. A. S., R. C. Newell and M. I. Lucas (1983). Quantitative relationships between phytoplankton, bacteria and heterotrophic microflagellates in shelf waters. *Marine Ecology Progress Series* **12**(1): 77-89.

Liss, P., G. Malin and S. Turner (1993). Production of DMS by marine phytoplankton. *Dimethyl sulphide: oceans, atmosphere and climate*. Dordrecht, Kluwer Academic**:** 1-14.

Liu, J., M. G. Weinbauer, C. Maier, M. Dai and J. P. Gattuso (2010). Effect of ocean acidification on microbial diversity and on microbe-driven biogeochemistry and ecosystem functioning. *Aquatic Microbial Ecology* **61**(3): 291-305.

Lohbeck, K. T., U. Riebesell and T. B. Reusch (2012). Adaptive evolution of a key phytoplankton species to ocean acidification. *Nature Geoscience* **5**(5): 346-351.

López-Urrutia, Á., E. San Martin, R. P. Harris and X. Irigoien (2006). Scaling the metabolic balance of the oceans. *Proceedings of the National Academy of Sciences* **103**(23): 8739-8744.

Løvdal, T., C. Eichner, H.-P. Grossart, V. Carbonnel, L. Chou, V. Martin-Jézéquel and T. Thingstad (2008). Competition for inorganic and organic forms of nitrogen and phosphorous between phytoplankton and bacteria during an *Emiliania huxleyi* spring bloom. *Biogeosciences* **5**(2): 371-383.

Lovelock, J. E., R. J. Maggs and R. A. Rasmussen (1972). Atmospheric dimethyl sulphide and the natural sulphur cycle. *Nature* **237**(5356): 452-453.

Low-DÉCarie, E., G. F. Fussmann and G. Bell (2011). The effect of elevated CO_2 on growth and competition in experimental phytoplankton communities. *Global Change Biology* **17**(8): 2525-2535.

Ludwig, W., O. Strunk, R. Westram, L. Richter, H. Meier, Yadhukumar, A. Buchner, T. Lai, S. Steppi, G. Jobb, W. Forster, I. Brettske, S. Gerber, A. W. Ginhart, O. Gross, S. Grumann, S. Hermann, R. Jost, A. Konig, T. Liss, R. LuBmann, M. May, B. Nonhoff, B. Reichel, R. Strehlow, A. Stamatakis, N. Stuckmann, A. Vilbig, M. Lenke, T. Ludwig, A. Bode and K. H. Schleifer (2004). ARB: a software environment for sequence data. *Nucleic Acids Research* **32**: 1363 - 1371.

Lueders, T., M. Manefield and M. W. Friedrich (2004). Enhanced sensitivity of DNA and rRNA based stable isotope probing by fractionation and quantitative analysis of isopycnic centrifugation gradients. *Environmental Microbiology* **6**(1): 73-78.

Mackas, D. L. and M. D. Galbraith (2011). Pteropod time-series from the NE Pacific. *ICES Journal of Marine Science: Journal du Conseil* **69**(3): 448-459.

Malin, G. (2006). OCEANS: New pieces for the marine sulfur cycle jigsaw. *Science* **314**(5799): 607-608.

Malin, G., S. Turner, P. S. Liss, P. Holligan and D. Harbour (1993). Dimethyl sulfide and dimethylsulphoniopropionate in the Northeast Atlantic during the summer coccolithophore bloom. *Deep Sea Research* **40**: 1487–1508.

Malmstrom, R. R., M. T. Cottrell and D. A. Kirchman (2007). Diversity, abundance, and biomass production of bacterial groups in the western Arctic Ocean. *Aquatic Microbial Ecology* **47**(1): 45-55.

Maniatis, T., E. F. Fritsch and J. Sambrook, Eds. (1982). Purification of nucleic acids *Molecular Cloning: A Laboratory Manual*, Cold Spring Harbor Laboratory, Cold Spring Harbor, New York, p. 458.

Mann, H. B. and D. R. Whitney (1947). On a test of whether one of two random variables is stochastically larger than the other. *The Annals of Mathematical Statistics* **18**(1): 50-60.

Manton, I. and M. Parke (1960). Further observations on a small green flagellate with special reference to possible relatives of *Chromulina pusilla*. *Journal of the Marine Biological Association of the United Kingdom* **39**: 275-298.

Manz, W., R. Amann, W. Ludwig, M. Vancanneyt and K. H. Schleifer (1996). Application of a suite of 16S rRNA-specific oligonucleotide probes designed to investigate bacteria of the phylum cytophaga-flavobacter-bacteroides in the natural environment. *Microbiology* **142**(5): 1097-1106.

Manzello, D. P. (2010). Ocean acidification hot spots: Spatiotemporal dynamics of the seawater CO_2 system of eastern Pacific coral reefs. *Limnology and Oceanography* **55**(1): 239.

Manzello, D. P., J. A. Kleypas, D. A. Budd, C. M. Eakin, P. W. Glynn and C. Langdon (2008). Poorly cemented coral reefs of the eastern tropical Pacific: Possible insights into reef development in a high-CO_2 world. *Proceedings of the National Academy of Sciences* **105**(30): 10450-10455.

Marie, D., X. L. Shi, F. Rigaut-Jalabert and D. Vaulot (2010). Use of flow cytometric sorting to better assess the diversity of small photosynthetic eukaryotes in the English Channel. *FEMS Microbiology Ecology* **72**(2): 165-178.

Marie, D., F. Zhu, V. Balagué, J. Ras and D. Vaulot (2006). Eukaryotic picoplankton communities of the Mediterranean Sea in summer assessed by molecular approaches (DGGE, TTGE, QPCR). *FEMS Microbiology Ecology* **55**(3): 403-415.

Marsh, G. (2008) Seawater pH and anthropogenic carbon dioxide. Available at: http://arxiv.org/abs/0810.3596.

Marty, B. and I. N. Tolstikhin (1998). CO_2 fluxes from mid-ocean ridges, arcs and plumes. *Chemical Geology* **145**(3): 233-248.

Maruoka, T., C. Koeberl and B. F. Bohor (2007). Carbon isotopic compositions of organic matter across continental Cretaceous-Tertiary (K-T) boundary sections: Implications for paleoenvironment after the K-T impact event. *Earth and Planetary Science Letters* **253**(1-2): 226-238.

Mary, I., J. L. Heywood, B. M. Fuchs, R. Amann, G. A. Tarran and P. H. Burkill (2006). SAR11 dominance among metabolically active low nucleic acid bacterioplankton in surface waters along an Atlantic meridional transect. *Aquatic Microbial Ecology* **45**: 107-113.

Massana, R., V. Balagué, L. Guillou and C. Pedrós-Alió (2004). Picoeukaryotic diversity in an oligotrophic coastal site studied by molecular and culturing approaches. *FEMS Microbiology Ecology* **50**(3): 231-243.

Mayhew, P. J., G. B. Jenkins and T. G. Benton (2008). A long-term association between global temperature and biodiversity, origination and extinction in the fossil record. *Proceedings of the Royal Society B: Biological Sciences* **275**(1630): 47-53.

McClintock, I. (2009) Proof that CO_2 is not the cause of the current global warming. The Lavoisier Group

McMinn, A. (2011). Climate change in polar marine ecosystems. *Journal of Tropical Marine Ecosystem* **1**(1).

McNeil, B. (2006). Significance of the oceanic CO_2 sink for national carbon accounts. *Carbon Balance and Management* **1**(1): 5.

McNeil, B. I. and R. J. Matear (2008). Southern Ocean acidification: A tipping point at 450-ppm atmospheric CO_2. *Proceedings of the National Academy of Sciences* **105**(48): 18860-18864.

Meakin, N. G. and M. Wyman (2011). Rapid shifts in picoeukaryote community structure in response to ocean acidification. *The ISME journal* **5**(9): 1397-1405.

Melzner, F., M. Gutowska, M. Langenbuch, S. Dupont, M. Lucassen, M. C. Thorndyke, M. Bleich and H. Pörtner, O (2009). Physiological basis for high CO_2 tolerance in marine ectothermic animals: pre-adaptation through lifestyle and ontogeny? *Biogeosciences Discussions* **6**(3).

Meyer, F., D. Paarmann, M. D'Souza, R. Olson, E. M. Glass, M. Kubal, T. Paczian, A. Rodriguez, R. Stevens, A. Wilke, J. Wilkening and R. A. Edwards (2008). The metagenomics RAST server - a public resource for the automatic phylogenetic and functional analysis of metagenomes. *BMC Bioinformatics* **9**(1): 386.

Michaelidis, B., C. Ouzounis, A. Paleras and H. O. Pörtner (2005). Effects of long-term moderate hypercapnia on acid-base balance and growth rate in marine mussels Mytilus galloprovincialis. *Marine Ecology Progress Series* **293**(2): 109-118.

Middelboe, M., M. Søndergaard, Y. Letarte and N. H. Borch (1995). Attached and free-living bacteria: Production and polymer hydrolysis during a diatom bloom. *Microbial Ecology* **29**(3): 231-248.

Milankovitch, M. (1941). Canon of insolation and the ice-age problem. Royal Serbian Academy Sp. Publ. Belgrade, Engl. trans. 1969, Israel Program for Scientific Translations**:** 484.

Miller, T. R. and R. Belas (2004). Dimethylsulfoniopropionate metabolism by *Pfiesteria*-associated *Roseobacter* spp. *Applied and Environmental Microbiology* **70**(6): 3383-3391.

Miller, T. R. and R. Belas (2006). Motility is involved in *Silicibacter* sp. TM1040 interaction with dinoflagellates. *Environmental Microbiology* **8**(9): 1648-1659.

Miller, T. R., K. Hnilicka, A. Dziedzic, P. Desplats and R. Belas (2004). Chemotaxis of *Silicibacter* sp. strain TM1040 toward dinoflagellate products. *Applied and Environmental Microbiology* **70**(8): 4692-4701.

Millero, F. J., D. Pierrot, K. Lee, R. Wanninkhof, R. Feely, C. L. Sabine, R. M. Key and T. Takahashi (2002). Dissociation constants for carbonic acid determined from field measurements. *Deep Sea Research Part I: Oceanographic Research Papers* **49**: 1705-1723.

Mitchell, A. (2010). *Sea sick : the global ocean in crisis* Millers Point, N.S.W, Murdoch Books Australia.

Molina, V., O. Ulloa, L. Farias, H. Urrutia, S. Ramirez, P. Junier and K.-P. Witzel (2007). Ammonia-oxidizing β-Proteobacteria from the Oxygen Minimum Zone off Northern Chile. *Applied and Environmental Microbiology* **73**(11): 3547-3555.

Moore, L. R., A. F. Post, G. Rocap and S. W. Chisholm (2002). Utilization of different nitrogen sources by the marine cyanobacteria *Prochlorococcus* and *Synechococcus*. *Limnology and Oceanography* **47**(4): 989-996.

Moran, M. A., R. Belas, M. A. Schell, J. M. Gonzalez, F. Sun, S. Sun, B. J. Binder, J. Edmonds, W. Ye, B. Orcutt, E. C. Howard, C. Meile, W. Palefsky, A. Goesmann, Q. Ren, I. Paulsen, L. E. Ulrich, L. S. Thompson, E. Saunders and A. Buchan (2007). Ecological genomics of Marine *Roseobacters*. *Applied and Environmental Microbiology* **73**(14): 4559-4569.

Moran, M. A., A. Buchan, J. M. Gonzalez, J. F. Heidelberg, W. B. Whitman, R. P. Kiene, J. R. Henriksen, G. M. King, R. Belas, C. Fuqua, L. Brinkac, M. Lewis, S. Johri, B. Weaver, G. Pai, J. A. Eisen, E. Rahe, W. M. Sheldon, W. Ye, T. R. Miller, J. Carlton, D. A. Rasko, I. T. Paulsen, Q. Ren, S. C. Daugherty, R. T. Deboy, R. J. Dodson, A. S. Durkin, R. Madupu, W. C. Nelson, S. A. Sullivan, M. J. Rosovitz, D. H. Haft, J. Selengut and N. Ward (2004). Genome sequence of *Silicibacter pomeroyi* reveals adaptations to the marine environment. *Nature* **432**(7019): 910-913.

Moran, M. A., Gonz, aacute, J. M. lez and R. P. Kiene (2003). Linking a bacterial taxon to sulfur cycling in the sea: Studies of the Marine *Roseobacter* group. *Geomicrobiology Journal* **20**: 375-388.

Moran, M. A. and W. L. Miller (2007). Resourceful heterotrophs make the most of light in the coastal ocean. *Nature Reviews Microbiology* **5**(10): 792-800.

Moran, M. A., C. R. Reisch, R. P. Kiene and W. B. Whitman (2012). Genomic insights into bacterial DMSP transformations. *Annual Review of Marine Science* **4**(1).

Morán, X. A. G. (2007). Annual cycle of picophytoplankton photosynthesis and growth rates in a temperate coastal ecosystem: a major contribution to carbon fluxes. *Aquatic Microbial Ecology* **49**(3): 267-279.

Moriya, Y., M. Itoh, S. Okuda, A. C. Yoshizawa and M. Kanehisa (2007). KAAS: an automatic genome annotation and pathway reconstruction server. *Nucleic Acids Research* **35**(suppl 2): 182-185.

Morse, D., P. Salois, P. Markovic and J. W. Hastings (1995). A nuclear-encoded form II RuBisCO in dinoflagellates. *Science* **268**(5217): 1622-1624.

Mucci, A. (1983). The solubility of calcite and aragonite in seawater at various salinities, temperatures, and one atmosphere total pressure. *American Journal of Science* **283**(7): 780-799.

Munday, P. L., D. L. Dixson, J. M. Donelson, G. P. Jones, M. S. Pratchett, G. V. Devitsina and K. B. Døving (2009). Ocean acidification impairs olfactory discrimination and homing ability of a marine fish. *Proceedings of the National Academy of Sciences* **106**(6): 1848-1852.

Munoz, J. and M. J. Merrett (1989). Inorganic-carbon transport in some marine eukaryotic microalgae. *Planta* **178**(4): 450-455.

Müren, U., J. Berglund, K. Samuelsson and A. Andersson (2005). Potential effects of elevated sea-water temperature on pelagic food webs. *Hydrobiologia* **545**(1): 153-166.

Murray, A. E., C. M. Preston, R. Massana, L. T. Taylor, A. Blakis, K. Wu and E. F. DeLong (1998). Seasonal and spatial variability of bacterial and archaeal assemblages in the coastal waters near Anvers Island, Antarctica. *Applied and Environmental Microbiology* **64**(7): 2585-2595.

Muyzer, G., E. C. de Waal and A. G. Uitterlinden (1993). Profiling of complex microbial populations by denaturing gradient gel electrophoresis analysis of polymerase chain reaction-amplified genes coding for 16S rRNA. *Applied and Environmental Microbiology* **59**(3): 695-700.

Myklestad, S. M. (1995). Release of extracellular products by phytoplankton with special emphasis on polysaccharides. *Science of the Total Environment* **165**(1–3): 155-164.

Nagashima, K. V. P., A. Hiraishi, K. Shimada and K. Matsuura (1997). Horizontal transfer of genes coding for the photosynthetic reaction centers of purple bacteria. *Journal of Molecular Evolution* **45**(2): 131-136.

Nagata, T. (2000). Production mechanisms of dissolved organic matter. *Microbial Ecology of the Oceans*. D. Kirchman, Wiley-Liss**:** 121-152.

Neufeld, J. D., Yin Chen Marc G. Dumont J. Colin Murrell (2008). Marine methylotrophs revealed by stable-isotope probing, multiple displacement amplification and metagenomics. *Environmental Microbiology* **10**(6): 1526-1535.

Newbold, L. K., A. E. Oliver, T. Booth, B. Tiwari, T. DeSantis, M. Maguire, G. Andersen, C. J. van der Gast and A. S. Whiteley (2012). The response of marine picoplankton to ocean acidification. *Environmental Microbiology* **14**(9): 2293-2307.

Newton, R. J., L. E. Griffin, K. M. Bowles, C. Meile, S. Gifford, C. E. Givens, E. C. Howard, E. King, C. A. Oakley, C. R. Reisch, J. M. Rinta-Kanto, S. Sharma, S. Sun, V. Varaljay, M. Vila-Costa, J. R. Westrich and M. A. Moran (2010). Genome characteristics of a generalist marine bacterial lineage. *ISME Journal* **4**(6): 784-798.

Niki, T., M. Kunugi and A. Otsuki (2000). DMSP-lyase activity in five marine phytoplankton species: its potential importance in DMS production. *Marine Biology* **136**(5): 759-764.

Nimer, N. A. and M. J. Merrett (1996). The development of a CO_2-concentrating mechanism in *Emiliania huxleyi*. *New Phytologist* **133**(3): 383-389.

Norton, J. M. (2011). Diversity and environmental distribution of ammonia-oxidizing bacteria. *Nitrification*. B. B. Ward, M. G. Klotz and D. J. Arp. Washington, DC, ASM Press.

Not, F., M. Latasa, D. Marie, T. Cariou, D. Vaulot and N. Simon (2004). A single species, *Micromonas pusilla* (*Prasinophyceae*), dominates the eukaryotic picoplankton in the Western English Channel. *Applied and Environmental Microbiology* **70**(7): 4064-4072.

Novacek, M. J. (2001). *The Biodiversity Crisis: Losing What Counts*, New Press.

O'Mullan, G. D. and B. B. Ward (2005). Relationship of temporal and spatial variabilities of ammonia-oxidizing bacteria to nitrification rates in Monterey Bay, California. *Applied and Environmental Microbiology* **71**(2): 697-705.

Orr, J. C., V. J. Fabry, O. Aumont, L. Bopp, S. C. Doney, R. A. Feely, A. Gnanadesikan, N. Gruber, A. Ishida, F. Joos, R. M. Key, K. Lindsay, E. Maier-Reimer, R. Matear, P. Monfray, A. Mouchet, R. G. Najjar, G.-K. Plattner, K. B. Rodgers, C. L. Sabine, J. L. Sarmiento, R. Schlitzer, R. D. Slater, I. J. Totterdell, M.-F. Weirig, Y. Yamanaka and A. Yool (2005). Anthropogenic ocean acidification over the twenty-first century and its impact on calcifying organisms. *Nature* **437**(7059): 681-686.

Osenberg, C. W., O. Sarnelle, S. D. Cooper and R. D. Holt (1999). Resolving ecological questions through meta-analysis: goals, metrics, and models. *Ecology* **80**(4): 1105-1117.

Overbeck, J. (1972). Experimentelle Untersuchungen zur bestimmung der bakteriellen Produktion im See. *Verhandlungen der Internationalen Vereinigung für Theoretische und Angewandte Limnologie* **18**: 176--187.

Overbeck, J. (1979). Dark CO_2 uptake biochemical background and its relevance to *in situ* bacterial production. *Archiv für Hydrobiologie–Beiheft Ergebnisse der Limnologie* **12**(38): 38 - 47.

Overbeck, J. and R. J. Daley. (1973). Some precautionary comments on the Romanenko technique for estimating heterotrophic bacterial production. *Bulletins from the Ecological Research Committee (Stockholm)* **17**: 342-344.

Overbeek, R., T. Begley, R. M. Butler, J. V. Choudhuri, H.-Y. Chuang, M. Cohoon, V. de Crecy-Lagard, N. Diaz, T. Disz, R. Edwards, M. Fonstein, E. D. Frank, S. Gerdes, E. M. Glass, A. Goesmann, A. Hanson, D. Iwata-Reuyl, R. Jensen, N. Jamshidi, L. Krause, M. Kubal, N. Larsen, B. Linke, A. C. McHardy, F. Meyer, H. Neuweger, G. Olsen, R. Olson, A. Osterman, V. Portnoy, G. D. Pusch, D. A. Rodionov, C. Ruckert, J. Steiner, R. Stevens, I. Thiele, O. Vassieva, Y. Ye, O. Zagnitko and V. Vonstein (2005). The Subsystems Approach to Genome Annotation and its Use in the Project to Annotate 1000 Genomes. *Nucleic Acids Research* **33**(17): 5691-5702.

Paasche, E. (1964). A tracer study of the inorganic carbon uptake during coccolith formation and photosynthesis in the coccolithophorid *Coccolithus huxleyi*. *Physiologia plantarum* **3**: 82.

Paasche, E. (2002). A review of the coccolithophorid *Emiliania huxleyi* (*Prymnesiophyceae*), with particular reference to growth, coccolith formation, and calcification-photosynthesis interactions. *Phycologia* **40**(6): 503-529.

Pace, N. R., D. A. Stahl, D. J. Lane and G. J. Olsen (1985). Analyzing natural microbial populations by rRNA sequences. *American Society of Microbiology news* **51**: 4 - 12.

Paerl, H. W., J. Dyble, L. Twomey, J. L. Pinckney, J. Nelson and L. Kerkhof (2002). Characterizing man-made and natural modifications of microbial diversity and activity in coastal ecosystems. *Antonie Van Leeuwenhoek* **81**(1-4): 487-507.

Parker, L. M., P. M. Ross, W. A. O'Connor, H. O. Pörtner, E. Scanes and J. M. Wright (2013). Predicting the response of molluscs to the impact of ocean acidification. *Biology* **2**(2): 651-692.

Parks, D. H. and R. G. Beiko (2010). Identifying biologically relevant differences between metagenomic communities. *Bioinformatics* **26**(6): 715-721.

Pedrós-Alió, C., J. Gasol and R. Guerrero (1987). On the ecology of a *Cryptomonas phaseolus* population forming a metalimnetic bloom in Lake Cisó, Spain: Annual distribution and loss factors. *Limnology and Oceanography* **32**: 285-298.

Perez, R. C. and A. Matin (1982). Carbon dioxide assimilation by *Thiobacillus novellus* under nutrient-limited mixotrophic conditions. *Journal of Bacteriology* **150**(1): 46-51.

Pernthaler, A. and J. Pernthaler (2005). Diurnal variation of cell proliferation in three bacterial taxa from coastal North Sea Waters. *Applied and Environmental Microbiology* **71**(8): 4638-4644.

Perry, S. F. and K. M. Gilmour (2006). Acid-base balance and CO_2 excretion in fish: unanswered questions and emerging models. *Respiratory Physiology & Neurobiology* **154**(1-2): 199-215.

Peterson, J., S. Garges, M. Giovanni, P. McInnes, L. Wang, J. A. Schloss, V. Bonazzi, J. E. McEwen, K. A. Wetterstrand and C. Deal (2009). The NIH Human Microbiome Project. *Genome Research* **19**(12): 2317-2323.

Pettit, A. N. (1982). Cramer-von Misess statistic. *Encyclopedia of Statistical Sciences*. S. Kotz, N. L. Johnson and C. B. Read. New York, Wiley**:** 220–221.

Pettitt, A. N. (1976). Cramer-von Mises statistics for testing normality with censored samples. *Biometrika* **63**(3): 475-481.

Petty, G. W. (2008). *A first course in atmospheric thermodynamics*. Madison, WI, Sundog Publishing.

Pierce, S. D., J. A. Barth, R. E. Thomas and G. W. Fleischer (2006). Anomalously warm July 2005 in the northern California Current: Historical context and the significance of cumulative wind stress. *Geophysical Research Letters* **33**(22): L22S04.

Pinard, R., A. de Winter, G. Sarkis, M. Gerstein, K. Tartaro, R. Plant, M. Egholm, J. Rothberg and J. Leamon (2006). Assessment of whole genome amplification-induced bias through high-throughput, massively parallel whole genome sequencing. *BMC Genomics* **7**(1): 216.

Pinhassi, J., M. M. Sala, H. Havskum, F. Peters, O. Guadayol, A. Malits and C. Marrase (2004). Changes in bacterioplankton composition under different phytoplankton regimens. *Applied and Environmental Microbiology* **70**(11): 6753-6766.

Pinhassi, J., R. Simo, J. M. Gonzalez, M. Vila, L. Alonso-Saez, R. P. Kiene, M. A. Moran and C. Pedros-Alio (2005). Dimethylsulfoniopropionate turnover is linked to the composition and dynamics of the bacterioplankton assemblage during a microcosm phytoplankton bloom. *Applied and Environmental Microbiology* **71**(12): 7650-7660.

Piontek, J., C. Borchard, M. Sperling, K. G. Schulz, U. Riebesell and A. Engel (2012). Response of bacterioplankton activity in an Arctic fjord system to elevated pCO 2: results from a mesocosm perturbation study. *Biogeosciences Discussions* **9**(8): 10467-10511.

Plattner, G. K., F. Joos and T. F. Stocker (2002). Revision of the global carbon budget due to changing air - sea oxygen fluxes. *Global Biogeochemical Cycles* **16**(4): 43-41-43-12.

Pollack, J. B., O. B. Toon, T. P. Ackerman, C. P. McKAY and R. P. Turco (1983). Environmental effects of an impact-generated dust cloud: Implications for the Cretaceous-Tertiary extinctions. *Science* **219**(4582): 287-289.

Polz, M. F. and C. M. Cavanaugh (1998). Bias in template-to-product ratios in multitemplate PCR. *Applied and Environmental Microbiology* **64**(10): 3724-3730.

Pomeroy, L. R. (1974). The ocean's food web, a changing paradigm. *Bioscience* **24**(9): 499-504.

Pomeroy, L. R., P. J. Williams, F. Azam and E. A. Hobbie (2007). The microbial loop. *Oceanography* **20**: 28-33.

Pope, K. O., K. H. Baines, A. C. Ocampo and B. A. Ivanov (1997). Energy, volatile production, and climatic effects of the Chicxulub Cretaceous/Tertiary impact. *Journal of Geophysical Research* **102**(9): 21645-21664.

Pope, K. O., S. L. D'Hondt and C. R. Marshall (1998). Meteorite impact and the mass extinction of species at the Cretaceous/Tertiary boundary. *Proceedings of the National Academy of Sciences of the United States of America* **95**(19): 11028-11029.

Poussart, P. F., A. J. Weaver and C. R. Barnes (1999). Late Ordovician glaciation under high atmospheric CO_2: A coupled model analysis. *Paleoceanography* **14**(4): 542-558.

Prescott, J. M., R. S. Ragland and H. R. J. (1965). Utilization of CO_2 and acetate in amino acid synthesis by *Streptococcus bovis*. *Proceedings of the Society for Experimental Biology and Medicine* **119**: 1097-1102.

Puddu, A., A. Zoppini, S. Fazi, M. Rosati, S. Amalfitano and E. Magaletti (2003). Bacterial uptake of DOM released from P-limited phytoplankton. *FEMS Microbiology Ecology* **46**(3): 257-268.

Purkhold, U., A. Pommerening-Roser, S. Juretschko, M. C. Schmid, H.-P. Koops and M. Wagner (2000). Phylogeny of all recognized species of ammonia oxidizers based on comparative 16S rRNA and *amoA* sequence analysis: Implications for molecular diversity surveys. *Applied and Environmental Microbiology* **66**(12): 5368-5382.

Purkhold, U., M. Wagner, G. Timmermann, A. Pommerening-Röser and H.-P. Koops (2003). 16S rRNA and *amoA*-based phylogeny of 12 novel betaproteobacterial ammonia-oxidizing isolates: extension of the dataset and proposal of a new lineage within the nitrosomonads. *International Journal of Systematic and Evolutionary Microbiology* **53**(5): 1485-1494.

Raghunathan, A., H. R. Ferguson, Jr., C. J. Bornarth, W. Song, M. Driscoll and R. S. Lasken (2005). Genomic DNA amplification from a single bacterium. *Applied and Environmental Microbiology* **71**(6): 3342-3347.

Rampino, M. R. and K. Caldeira (2005). Major perturbation of ocean chemistry and a 'Strangelove Ocean' after the end-Permian mass extinction. *Terra Nova* **17**(6): 554-559.

Rappe, M. S., S. A. Connon, K. L. Vergin and S. J. Giovannoni (2002). Cultivation of the ubiquitous SAR11 marine bacterioplankton clade. *Nature* **418**: 630-633.

Rath, J., K. Y. Wu, G. J. Herndl and E. F. DeLong (1998). High phylogenetic diversity in a marine-snow-associated bacterial assemblage. *Aquatic Microbial Ecology* **14**(3): 261-269.

Raupach, M. R., G. Marland, P. Ciais, C. Le Quéré, J. G. Canadell, G. Klepper and C. B. Field (2007). Global and regional drivers of accelerating CO_2 emissions. *Proceedings of the National Academy of Sciences* **104**(24): 10288-10293.

Raven, J. A. (1986). Physiological consequences of extremely small size for autotrophic organisms in the sea. *In Photosynthetic Picoplankton*. T. Platt and W. K. W. Li. Ottawa, Canada, Canadian Bulletin of Fisheries and Aquatic Sciences. **214**.

Raven, J. A. (1993). Limits on growth rates. *Nature* **361**(6409): 209-210.

Raven, J. A., C. S. Cockell and C. L. De La Rocha (2008). The evolution of inorganic carbon concentrating mechanisms in photosynthesis. *Philosophical Transactions of the Royal Society B: Biological Sciences* **363**(1504): 2641-2650.

Reid, P. C., D. G. Johns, M. Edwards, M. Starr, M. Poulin and P. Snoeijs (2007). A biological consequence of reducing Arctic ice cover: arrival of the Pacific diatom Neodenticula seminae in the North Atlantic for the first time in 800 000 years. *Global Change Biology* **13**(9): 1910-1921.

Reinfelder, J. R. (2011). Carbon concentrating mechanisms in eukaryotic marine phytoplankton. *Annual Review of Marine Science* **3**(1): 291-315.

Reisch, C. R., M. A. Moran and W. B. Whitman (2011). Bacterial catabolism of dimethylsulfoniopropionate. *Frontiers in Microbiology* **2**.

Reisch, C. R., M. J. Stoudemayer, V. A. Varaljay, I. J. Amster, M. A. Moran and W. B. Whitman (2011). Novel pathway for assimilation of dimethylsulphoniopropionate widespread in marine bacteria. *Nature* **473**(7346): 208-211.

Retallack, G. J. (2001). A 300-million-year record of atmospheric carbon dioxide from fossil plant cuticles. *Nature* **411**(6835): 287-290.

Riclea, R., J. Gleitzmann, H. Bruns, C. Junker, B. Schulz and J. S. Dickschat (2012). Algicidal lactones from the Marine *Roseobacter* Clade bacterium *Ruegeria pomeroyi*. *Beilstein Journal of Organic Chemistry* **8**: 941-950.

Ridgwell, A. and R. E. Zeebe (2005). The role of the global carbonate cycle in the regulation and evolution of the Earth system. *Earth and Planetary Science Letters* **234**(3): 299-315.

Riebeek, H. (2010). Global Warming NASA Earth Observatory. from http://earthobservatory.nasa.gov/Features/GlobalWarming/page2.php.

Riebesell, U. (2004). Effects of CO_2 enrichment on marine phytoplankton. *Journal of Oceanography* **60**: 719-729.

Riebesell, U. (2007). Acid oceans. *Our Planet* Nairobi, Kenya, United Nations Environment Programme 1.

Riebesell, U., V. J. Fabry, L. Hansson and J. P. Gattuso (2010). Guide to best practices for ocean acidification research and data reporting., Publications Office of the European Union, Luxembourg.

Riebesell, U., D. A. Wolf-Gladrow and V. Smetacek (1993). Carbon dioxide limitation of marine phytoplankton growth rates. *Nature* **361**(6409): 249-251.

Riebesell, U., I. Zondervan, B. Rost, P. D. Tortell, R. E. Zeebe and F. M. M. Morel (2000). Reduced calcification of marine plankton in response to increased atmospheric CO_2. *Nature* **407**(6802): 364-367.

Riemann, L., G. F. Steward and F. Azam (2000). Dynamics of bacterial community composition and activity during a mesocosm diatom bloom. *Applied and Environmental Microbiology* **66**(2): 578-587.

Rink, B., S. Seeberger, T. Martens, C. D. Duerselen, M. Simon and T. Brinkhoff (2007). Effects of phytoplankton bloom in a coastal ecosystem on the composition of bacterial communities. *Aquatic Microbial Ecology* **48**(1): 47-60.

Rivkin, R. B. and L. Legendre (2001). Biogenic carbon cycling in the upper ocean: Effects of microbial respiration. *Science* **291**(5512): 2398-2400.

Robertson, J. E., C. Robinson, D. R. Turner, P. Holligan, A. J. Watson, P. Boyd, E. Fernandez and M. Finch (1994). The impact of a coccolithophore bloom on oceanic carbon uptake in the northeast Atlantic during summer 1991. *Deep Sea Research Part I: Oceanographic Research Papers* **41**(2): 297-314.

Robock, A. (2002). The Climatic Aftermath. *Science* **295**(5558): 1242-1244.

Rokitta, S. D. and B. Rost (2012). Effects of CO_2 and their modulation by light in the life-cycle stages of the coccolithophore *Emiliania huxleyi*. *Limnology & Oceanography* **57**(2): 607-618.

Romanenko, V. I. (1964). Heterotrophic assimilation of CO_2 by bacterial flora of water. *Microbiologiya* **33**: 610-614.

Ronaghi, M., M. Uhlzn and P. Nyrzn (1998). A sequencing method based on real-time pyrophosphate. *Science* **281**(5375): 363-365.

Rose, J. M., Y. Feng, C. J. Gobler, R. Gutierrez, C. E. Hare, K. Leblanc and D. A. Hutchins (2009). Effects of increased pCO_2 and temperature on the North Atlantic spring bloom. II. Microzooplankton abundance and grazing *Marine Ecology Progress Series* **388**: 27-40.

Rost, B. and U. Riebesell (2004). Coccolithophores and the biological pump: responses to environmental changes. *Coccolithophores - From Molecular Processes to Global Impact.* H. R. Thierstein and J. R. Young. New York, Springer Verlag**:** 76-99.

Rost, B., U. Riebesell, S. Burkhardt and D. Sültemeyer (2003). Carbon acquisition of bloom-forming marine phytoplankton. *Limnology and Oceanography* **48**(1): 55-67.

Rost, B., I. Zondervan and D. Wolf-Gladrow (2008). Sensitivity of phytoplankton to future changes in ocean carbonate chemistry: current knowledge, contradictions and research directions. *Marine Ecology Progress Series* **373**: 227-237.

Rotthauwe, J. H., K. P. Witzel and W. Liesack (1997). The ammonia monooxygenase structural gene *amoA* as a functional marker: molecular fine-scale analysis of natural ammonia-oxidizing populations. *Applied and Environmental Microbiology* **63**(12): 4704-4712.

Royal Society (2005). Ocean acidification due to increasing atmospheric carbon dioxide. Royal Society Policy Document, Royal Society.

Royer, D. L. (2006). CO_2 forced climate thresholds during the Phanerozoic. *Geochimica et Cosmochimica Acta* **70**(23): 5665-5675.

Rzhetsky, A. and M. Nei (1992). A simple method for estimating and testing minimumeEvolution trees. *Molecular Biology and Evolution* **9**(5): 945-967.

Sabine, C. L., R. A. Feely, N. Gruber, R. M. Key, K. Lee, J. L. Bullister, R. Wanninkhof, C. S. Wong, D. W. R. Wallace, B. Tilbrook, F. J. Millero, T.-H. Peng, A. Kozyr, T. Ono and A. F. Rios (2004). The Oceanic sink for anthropogenic CO_2. *Science* **305**(5682): 367-371.

Saitou, N. and M. Nei (1987). The neighbor-joining method: a new method for reconstructing phylogenetic trees. *Molecular Biology and Evolution* **4**(4): 406-425.

Samuelsson, K., J. Berglund, P. Haecky and A. Andersson (2002). Structural changes in an aquatic microbial food web caused by inorganic nutrient addition. *Aquatic Microbial Ecology* **29**(1): 29-38.

Sarthou, G., K. R. Timmermans, S. Blain and P. Tréguer (2005). Growth physiology and fate of diatoms in the ocean: a review. *Journal of Sea Research* **53**(1): 25-42.

Schafer, H. (2007). Isolation of *Methylophaga* spp. from marine dimethylsulfide-degrading enrichment cultures and identification of polypeptides induced during growth on dimethylsulfide. *Applied and Environmental Microbiology* **73**(8): 2580-2591.

Schäfer, H., B. Abbas, H. Witte and G. Muyzer (2002). Genetic diversity of 'satellite' bacteria present in cultures of marine diatoms. *FEMS Microbiology Ecology* **42**(1): 25-35.

Schippers, P., M. Lürling and M. Scheffer (2004). Increase of atmospheric CO_2 promotes phytoplankton productivity. *Ecology Letters* **7**(6): 446-451.

Schmidt, T. M., E. F. DeLong and N. R. Pace (1991). Analysis of a marine picoplankton community by 16S rRNA gene cloning and sequencing. *Journal of Bacteriology* **173**(14): 4371-4378.

Schmittner, A., J. C. H. Chiang and S. R. Hemming (2013). Introduction: The Ocean's Meridional Overturning Circulation. *Ocean Circulation: Mechanisms and Impacts—Past and Future Changes of Meridional Overturning*, American Geophysical Union**:** 1-4.

Schubert, H. L., R. M. Blumenthal and X. Cheng (2003). Many paths to methyltransfer: a chronicle of convergence. *Trends in Biochemical Sciences* **28**(6): 329-335.

Schuller, D. J., C. R. Reisch, M. A. Moran, W. B. Whitman and W. N. Lanzilotta (2012). Structures of dimethylsulfoniopropionate-dependent demethylase from the marine organism *Pelagabacter ubique*. *Protein science : a publication of the Protein Society* **21**(2): 289-298.

Schulte, P., L. Alegret, I. Arenillas, J. A. Arz, P. J. Barton, P. R. Bown, T. J. Bralower, G. L. Christeson, P. Claeys, C. S. Cockell, G. S. Collins, A. Deutsch, T. J. Goldin, K. Goto, J. M. Grajales-Nishimura, R. A. F. Grieve, S. P. S. Gulick, K. R. Johnson, W. Kiessling, C. Koeberl, D. A. Kring, K. G. MacLeod, T. Matsui, J. Melosh, A. Montanari, J. V. Morgan, C. R. Neal, D. J. Nichols, R. D. Norris, E. Pierazzo, G. Ravizza, M. Rebolledo-Vieyra, W. U. Reimold, E. Robin, T. Salge, R. P. Speijer, A. R. Sweet, J. Urrutia-Fucugauchi, V. Vajda, M. T. Whalen and P. S. Willumsen (2010). The Chicxulub asteroid impact and mass extinction at the Cretaceous-Paleogene boundary. *Science* **327**(5970): 1214-1218.

Schulz, K. G. and U. Riebesell (2013). Diurnal changes in seawater carbonate chemistry speciation at increasing atmospheric carbon dioxide. *Marine Biology* **160**(8): 1889-1899.

Selje, N., M. Simon and T. Brinkhoff (2004). A newly discovered *Roseobacter* cluster in temperate and polar oceans. *Nature* **427**(6973): 445-448.

Sheehan, P. M. (2001). The late Ordovician mass extinction. *Annual Review of Earth and Planetary Sciences* **29**(1): 331-364.

Sherr, E. B. and B. F. Sherr (2007). Heterotrophic dinoflagellates: a significant component of microzooplankton biomass and major grazers of diatoms in the sea. *Marine Ecology Progress Series* **352**: 187.

Shewan, J. M. and T. A. McMeekin (1983). Taxonomy (and Ecology) of Flavobacterium and related genera. *Annual Review of Microbiology* **37**(1): 233-252.

Shi, D., Y. Xu and F. M. M. Morel (2009). Effects of the pH/pCO_2 control method on medium chemistry and phytoplankton growth. *Biogeosciences* **6**(7): 1199-1207.

Shiba, T. (1984). Utilization of light energy by the strictly aerobic bacterium *Erythrobacter* sp OCH 114. *Journal of General and Applied Microbiology* **30**(3): 239-244.

Shiba, T., U. Simidu and N. Taga (1979). Distribution of aerobic bacteria which contain bacteriochlorophyll a. *Applied and Environmental Microbiology* **38**(1): 43-45.

Siegenthaler, U., T. F. Stocker, E. Monnin, D. Lüthi, J. Schwander, B. Stauffer, D. Raynaud, J.-M. Barnola, H. Fischer, V. Masson-Delmotte and J. Jouzel (2005). Stable carbon cycle–climate relationship during the late Pleistocene. *Science* **310**(5752): 1313-1317.

Sieracki, M. E., I. C. Gilg, E. C. Thier, N. J. Poulton and R. Goericke (2006). Distribution of planktonic aerobic anoxygenic photoheterotrophic bacteria in the northwest Atlantic. *Limnology and Oceanography* **51**(1): 38-46.

Simó, R. (2001). Production of atmospheric sulfur by oceanic plankton: biogeochemical, ecological and evolutionary links. *Trends in Ecology and Evolution* **16**(6): 287-294.

Simpson, S. D., P. L. Munday, M. L. Wittenrich, R. Manassa, D. L. Dixson, M. Gagliano and H. Y. Yan (2011). Ocean acidification erodes crucial auditory behaviour in a marine fish. *Biology letters* **7**(6): 917-920.

Singleton, D. R., M. A. Furlong, S. L. Rathbun and W. B. Whitman (2001). Quantitative comparisons of 16S rRNA gene sequence libraries from environmental samples. *Applied and Environmental Microbiology* **67**(9): 4374-4376.

Singleton, D. R., S. N. Powell, R. Sangaiah, A. Gold, L. M. Ball and M. D. Aitken (2005). Stable-isotope probing of bacteria capable of degrading salicylate, naphthalene or phenanthrene in a bioreactor treating contaminated soil. *Applied and Environmental Microbiology* **71**(3): 1202-1209.

Slightom, R. N. and A. Buchan (2009). Surface colonization by marine *roseobacters*: integrating genotype and phenotype. *Applied and Environmental Microbiology* **75**(19): 6027-6037.

Solomon, S., D. Qin, M. Manning, Z. Chen, M. Marquis, K. B. Averyt, M. Tignor and H. L. Miller (2007). Climate Change 2007. The Physical Science Basis. Intergovernmental Panel on Climatic Change.

Somerville, C. C., I. T. Knight, W. L. Straube and R. R. Colwell (1989). Simple, rapid method for direct isolation of nucleic acids from aquatic environments. *Applied and Environmental Microbiology* **55**(3): 548-554.

Sommer, U. and K. Lengfellner (2008). Climate change and the timing, magnitude and composition of the phytoplankton spring bloom. *Global Change Biology* **14**(6): 1199-1208.

Sonntag, K., J. Schwinde, A. A. Graaf, A. Marx, B. J. Eikmanns, W. Wiechert and H. Sahm (1995). ^{13}C NMR studies of the fluxes in the central metabolism of Corynebacterium glutamicum during growth and overproduction of amino acids in batch cultures. *Applied Microbiology and Biotechnology* **44**(3): 489-495.

Sorokin, D. Y. (2003). Oxidation of inorganic sulfur compounds by obligately organotrophic bacteria. *Microbiology* **72**(6): 641-653.

Sorokin, D. Y., H. Banciu, M. van Loosdrecht and J. G. Kuenen (2003). Growth physiology and competitive interaction of obligately chemolithoautotrophic, haloalkaliphilic, sulfur-oxidizing bacteria from soda lakes. *Extremophiles* **7**(3): 195-203.

Sorokin, J. I. (1966). On the carbon dioxide uptake during the cell synthesis by microorganisms. *Zeitschrift für allgemeine Mikrobiologie* **6**(1): 69-73.

Sowell, S. M., L. J. Wilhelm, A. D. Norbeck, M. S. Lipton, C. D. Nicora, D. F. Barofsky, C. A. Carlson, R. D. Smith and S. J. Giovanonni (2008). Transport functions dominate the SAR11 metaproteome at low-nutrient extremes in the Sargasso Sea. *ISME Journal* **3**(1): 93-105.

Spring, S., H. Lünsdorf, B. M. Fuchs and B. J. Tindall (2009). The photosynthetic apparatus and Its regulation in the aerobic gammaproteobacterium *Congregibacter litoralis* gen. nov., sp. nov. *PLoS ONE* **4**(3): e4866.

Stackebrandt, E., R. Pukall, G. Ulrichs and H. Rheims (1999). Analysis of 16S rDNA clone libraries: part of the big picture. *Proceedings of the 8th International Symposium on Microbial Ecology. Microbial biosystems: new frontiers* Halifax, Nova Scotia, Canada, Atlantic Canada Society for Microbial Ecology**:** 1-9.

Stahl, D. A., D. J. Lane, G. J. Olsen and N. R. Pace (1984). Analysis of hydrothermal vent-associated symbionts by ribosomal RNA sequences. *Science* **224**(4647): 409-411.

Staley, J. T. and A. Konopka (1985). Measurement of *in situ* activities of nonphotosynthetic microorganisms in aquatic and terrestrial habitats. *Annual Review of Microbiology* **39**(1): 321-346.

Stefels, J. and L. Dijkhuizen (1996). Characteristics of DMSP-lyase in *Phaeocystis* sp. (*Prymnesiophyceae*). *Marine Ecology Progress Series* **131**: 307-313.

Stefels, J., M. Steinke, S. Turner, G. Malin and S. Belviso (2007). Environmental constraints on the production and removal of the climatically active gas dimethylsulphide (DMS) and implications for ecosystem modelling. *Biogeochemistry* **83**(1): 245-275.

Stein, J. L., T. L. Marsh, K. Y. Wu, H. Shizuya and E. F. DeLong (1996). Characterization of uncultivated prokaryotes: isolation and analysis of a 40-kilobase-pair genome fragment from a planktonic marine archaeon. *Journal of Bacteriology* **178**(3): 591-599.

Steindler, L., M. S. Schwalbach, D. P. Smith, F. Chan and S. J. Giovannoni (2011). Energy starved *Candidatus Pelagibacter Ubique* substitutes light-mediated ATP production for endogenous carbon respiration. *PLoS ONE* **6**(5): e19725.

Steinke, M., C. Daniel and G. O. Kirst (1996). DMSP lyase in marine macro- and microalgae: intraspecific differences in cleavage activity. *Biological and Environmental Chemistry of DMSP and Related Sulfonium Compounds*. R. P. Kiene, P. T. Visscher, M. D. Keller and G. O. Kirst. New York, Plenum Press.

Steinke, M., C. Evans, G. Lee and G. Malin (2007). Substrate kinetics of DMSP-lyases in axenic cultures and mesocosm populations of *Emiliania huxleyi*. *Aquatic Sciences* **69**(3): 352-359.

Steinke, M., G. V. Wolfe and G. O. Kirst (1998). Partial characterisation of dimethylsulfoniopropionate (DMSP) lyase isozymes in 6 strains of *Emiliania huxleyi*. *Marine Ecology Progress Series* **175**: 215-225.

Stephen, J. R., A. E. McCaig, Z. Smith, J. I. Prosser and T. M. Embley (1996). Molecular diversity of soil and marine 16S rRNA gene sequences related to beta-subgroup ammonia-oxidizing bacteria. *Applied and Environmental Microbiology* **62**(11): 4147-4154.

Stocker, T. F., Q. Dahe and G.-K. Plattner (2013). Climate Change 2013: The Physical Science Basis. Working Group I Contribution to the Fifth Assessment Report of the Intergovernmental Panel on Climate Change. Summary for Policymakers.

Stoica, E. and G. Herndl (2007). Bacterioplankton community composition in nearshore waters of the NW Black Sea during consecutive diatom and coccolithophorid blooms. *Aquatic Sciences - Research Across Boundaries* **69**(3): 413-418.

Strengers, B., R. Leemans, B. Eickhout, B. de Vries and L. Bouwman (2004). The land-use projections and resulting emissions in the IPCC SRES scenarios scenarios as simulated by the IMAGE 2.2 model. *GeoJournal* **61**(4): 381-393.

Sun, J. D., X. Zhao and B. L. Hao (2010). Whole-genome based Archaea phylogeny and taxonomy: a composition vector approach. *Chinese Science Bulletin* **55**(22): 2323-2328

Sunda, W., D. J. Kieber, R. P. Kiene and S. Huntsman (2002). An antioxidant function for DMSP and DMS in marine algae. *Nature* **418**(6895): 317-320.

Suzuki, M. T. and S. J. Giovannoni (1996). Bias caused by template annealing in the amplification of mixtures of 16S rRNA genes by PCR. *Applied and Environmental Microbiology* **62**(2): 625-630.

Swan, B. K., M. Martinez-Garcia, C. M. Preston, A. Sczyrba, T. Woyke, D. Lamy, T. Reinthaler, N. J. Poulton, E. D. Masland, M. L. Gomez, M. E. Sieracki, E. F. DeLong, G. J. Herndl and R. Stepanauskas (2011). Potential for chemolithoautotrophy among ubiquitous bacteria lineages in the dark ocean. *Science* **333**(6047): 1296-1300.

Swingley, W. D., S. Sadekar, S. D. Mastrian, H. J. Matthies, J. Hao, H. Ramos, C. R. Acharya, A. L. Conrad, H. L. Taylor, L. C. Dejesa, M. K. Shah, M. E. O'Huallachain, M. T. Lince, R. E. Blankenship, J. T. Beatty and J. W. Touchman (2007). The complete genome sequence of *Roseobacter denitrificans* reveals a mixotrophic rather than photosynthetic metabolism. *Journal of Bacteriology* **189**(3): 683-690.

Takahashi, T., S. C. Sutherland, C. Sweeney, A. Poisson, N. Metzl, B. Tilbrook, N. Bates, R. Wanninkhof, R. A. Feely, C. Sabine, J. Olafsson and Y. Nojiri (2002). Global sea–air CO_2 flux based on climatological surface ocean pCO_2 and seasonal biological and temperature effects. *Deep Sea Research Part II: Topical Studies in Oceanography* **49**(9–10): 1601-1622.

Tamminen, T. (1995). Nitrate and ammonium depletion rates and preferences during a Baltic spring bloom. *Marine Ecology Progress Series* **120**(1): 123-133.

Tamura, K., J. Dudley, M. Nei and S. Kumar (2007). MEGA4: Molecular Evolutionary Genetics Analysis (MEGA) Software Version 4.0. *Molecular Biology and Evolution* **24**(8): 1596-1599.

Tang, K.-H., X. Feng, Y. J. Tang and R. E. Blankenship (2009). Carbohydrate metabolism and carbon fixation in *Roseobacter denitrificans OCh114*. *PLoS ONE* **4**(10): e7233.

Tang, K., H. Huang, N. Jiao and C. H. Wu (2010). Phylogenomic analysis of marine *Roseobacters*. *PLoS ONE* **5**(7): e11604.

Teeling, H., B. M. Fuchs, D. Becher, C. Klockow, A. Gardebrecht, C. M. Bennke, M. Kassabgy, S. Huang, A. J. Mann, J. Waldmann, M. Weber, A. Klindworth, A. Otto, J. Lange, J. Bernhardt, C. Reinsch, M. Hecker, J. Peplies, F. D. Bockelmann, U. Callies, G. Gerdts, A. Wichels, K. H. Wiltshire, F. O. Glöckner, T. Schweder and R. Amann (2012). Substrate-controlled succession of marine bacterioplankton populations induced by a phytoplankton bloom. *Science* **336**(6081): 608-611.

Teira, E., A. Fernández, X. A. Álvarez-Salgado, E. E. García-Martín, P. Serret and C. Sobrino (2012). Response of two marine bacterial isolates to high CO_2 concentration. *Marine Ecology Progress Series* **453**: 27-36.

Teira, E., J. M. Gasol, M. Aranguren-Gassis, A. Fernandez, J. Gonzalez, I. Lekunberri and X. A. Alvarez-Salgado (2008). Linkages between bacterioplankton community composition, heterotrophic carbon cycling and environmental conditions in a highly dynamic coastal ecosystem. *Environmental Microbiology* **10**(4): 906-917.

Temperton, B., D. Field, A. Oliver, B. Tiwari, M. Muhling, I. Joint and J. A. Gilbert (2009). Bias in assessments of marine microbial biodiversity in fosmid libraries as evaluated by pyrosequencing. *ISME Journal* **3**(7): 792-796.

Temperton, B., Oliver, A, Field, D, Tiwari, B, Muhling, M, Joint, I, and Gilbert, J. (2009). Bias in culture-independent assessments of microbial biodiversity in the global ocean *Nature Precedings*(2818.1).

Thole, S., D. Kalhoefer, S. Voget, M. Berger, T. Engelhardt, H. Liesegang, A. Wollherr, S. Kjelleberg, R. Daniel and M. Simon (2012). *Phaeobacter gallaeciensis* genomes from globally opposite locations reveal high similarity of adaptation to surface life. *ISME Journal* **6**(12): 2229-2244.

Thomas, C. D., A. Cameron, R. E. Green, M. Bakkenes, L. J. Beaumont, Y. C. Collingham, B. F. N. Erasmus, M. F. de Siqueira, A. Grainger, L. Hannah, L. Hughes, B. Huntley, A. S. van Jaarsveld, G. F. Midgley, L. Miles, M. A. Ortega-

Huerta, A. Townsend Peterson, O. L. Phillips and S. E. Williams (2004). Extinction risk from climate change. *Nature* **427**(6970): 145-148.

Thomsen, J., M. A. Gutowska, J. Saphörster, A. Heinemann, K. Trübenbach, J. Fietzke, C. Hiebenthal, A. Eisenhauer, A. Körtzinger, M. Wahl and F. Melzner (2010). Calcifying invertebrates succeed in a naturally CO_2 rich coastal habitat but are threatened by high levels of future acidification. *Biogeosciences* **7**(11): 3879-3891.

Thrash, J. C., J.-C. Cho, S. Ferriera, J. Johnson, K. L. Vergin and S. J. Giovannoni (2010). Genome sequences of strains HTCC2148 and HTCC2080, belonging to the OM60/NOR5 clade of the *Gammaproteobacteria*. *Journal of Bacteriology* **192**(14): 3842-3843.

Todd, J. D., A. R. J. Curson, C. L. Dupont, P. Nicholson and A. W. B. Johnston (2009). The *dddP* gene, encoding a novel enzyme that converts dimethylsulfoniopropionate into dimethyl sulfide, is widespread in ocean metagenomes and marine bacteria and also occurs in some Ascomycete fungi. *Environmental Microbiology* **11**(6): 1376-1385.

Todd, J. D., M. Kirkwood, S. Newton-Payne and A. W. B. Johnston (2011). *DddW*, a third DMSP lyase in a model *Roseobacter* marine bacterium, *Ruegeria pomeroyi* DSS-3. *ISME Journal*.

Tolli, J. D. (2003). Identity and dynamics of the microbial community responsible for carbon monoxide oxidation in marine environments. PhD. thesis.

Tolli, J. D. (2005). Biological CO-oxidation in the Sargasso Sea and in Vineyard Sound, Massachusetts. *Limnology and Oceanography* **50**: 1205-1212.

Tolli, J. D., S. M. Sievert and C. D. Taylor (2006). Unexpected diversity of bacteria capable of carbon monoxide oxidation in a coastal marine environment and contribution of the *Roseobacter*-associated clade to total CO oxidation. *Applied and Environmental Microbiology* **72**(3): 1966-1973.

Tourna, M., T. E. Freitag, G. W. Nicol and J. I. Prosser (2008). Growth, activity and temperature responses of ammonia‐oxidizing archaea and bacteria in soil microcosms. *Environmental Microbiology* **10**(5): 1357-1364.

Tringe, S. G., C. von Mering, A. Kobayashi, A. A. Salamov, K. Chen, H. W. Chang, M. Podar, J. M. Short, E. J. Mathur, J. C. Detter, P. Bork, P. Hugenholtz and E. M. Rubin (2005). Comparative metagenomics of microbial communities. *Science* **308**(5721): 554-557.

Tripathi, C. K. M., D. Tripathi, V. Praveen and V. Bihari (2007). Microbial diversity - biotechnological and industrial perspectives. *Indian Journal of Experimental Biology* **45**(4): 326-332.

Trouet, V., J. Esper, N. E. Graham, A. Baker, J. D. Scourse and D. C. Frank (2009). Persistent positive North Atlantic Oscillation mode dominated the medieval climate anomaly. *Science* **324**(5923): 78-80.

Twitchett, R. J. (2001). Incompleteness of the Permian–Triassic fossil record: a consequence of productivity decline? *Geological Journal* **36**(3‐4): 341-353.

Twitchett, R. J. (2006). The palaeoclimatology, palaeoecology and palaeoenvironmental analysis of mass extinction events. *Palaeogeography, Palaeoclimatology, Palaeoecology* **232**(2): 190-213.

Tyson, G. W., J. Chapman, P. Hugenholtz, E. E. Allen, R. J. Ram, P. M. Richardson, V. V. Solovyev, E. M. Rubin, D. S. Rokhsar and J. F. Banfield (2004). Community structure and metabolism through reconstruction of microbial genomes from the environment. *Nature* **428**(6978): 37-43.

Utter, M. F. and D. B. Keech (1963). Pyruvate Carboxylase. I. Nature of the reaction. *Journal of Biological Chemistry* **238**(8): 2603-2608.

Vallina, S. M. and R. Simo (2007). Strong relationship between DMS and the solar radiation dose over the global surface ocean. *Science* **315**(5811): 506-508.

Van de Waal, D. B., U. John, P. Ziveri, G.-J. Reichart, M. Hoins, A. Sluijs and B. Rost (2013). Ocean acidification reduces growth and calcification in a marine dinoflagellate. *PLoS ONE* **8**(6): e65987.

Van Duyl, F. C., W. W. C. Gieskes, A. J. Kop and W. E. Lewis (1998). Biological control of short-term variations in the concentration of DMSP and DMS during a Phaeocystis spring bloom. *Journal of Sea Research* **40**(3-4): 221-231.

Van Hannen, E. J., W. Mooij, M. P. van Agterveld, H. J. Gons and H. J. Laanbroek (1999). Detritus-dependent development of the microbial community in an experimental system: qualitative analysis by denaturing gradient gel electrophoresis. *Applied and Environmental Microbiology* **65**(6): 2478-2484.

Vellinga, M. and R. Wood (2002). Global climatic impacts of a collapse of the Atlantic thermohaline circulation. *Climatic Change* **54**(3): 251-267.

Venter, J. C. (2004). Environmental genome shotgun sequencing of the Sargasso Sea. *Science* **304**: 66-74.

Vila, M., R. Simo, R. P. Kiene, J. Pinhassi, J. M. Gonzalez, M. A. Moran and C. Pedros-Alio (2004). Use of microautoradiography combined with fluorescence *in stu* hybridization to determine dimethylsulfoniopropionate incorporation by marine bacterioplankton taxa. *Applied and Environmental Microbiology* **70**(8): 4648-4657.

Visscher, P. T. and H. Van Gemerden (1993). Sulfur cycling in laminated marine microbial ecosystems. *Biogeochemistry of Global Change: Radiatively Active Trace Gases* R. S. Oremland. New York, Chapman and Hall**:** 672-690.

Vogt, M., M. Steinke, S. Turner, A. Paulino, M. Meyerhöfer, U. Riebesell, C. LeQuéré and P. Liss (2007). Dynamics of dimethylsulphoniopropionate and dimethylsulphide under different CO_2 concentrations during a mesocosm experiment. *Biogeosciences Discussions* **4**(5): 3673-3699.

Wagner-Dobler, I. and H. Biebl (2006). Environmental biology of the marine *Roseobacter* lineage. *Annual Review of Microbiology* **60**(1): 255-280.

Waidner, L. A. and D. L. Kirchman (2007). Aerobic anoxygenic phototrophic bacteria attached to particles in turbid waters of the Delaware and Chesapeake estuaries. *Applied and Environmental Microbiology* **73**(12): 3936-3944.

Walker, H. H. (1932). Carbon dioxide as a factor affecting lag in bacterial growth. *Science* **76**: 602-604.

Walter, J. M., D. Greenfield, C. Bustamante and J. Liphardt (2007). Light-powering *Escherichia coli* with proteorhodopsin. *Proceedings of the National Academy of Sciences* **104**(7): 2408-2412.

Wanninkhof, R. and K. Thoning (1993). Measurement of fugacity of CO_2 in surface water using continuous and discrete sampling methods. *Marine Chemistry* **44**(2–4): 189-204.

Ward, D. M., R. Weller and M. M. Bateson (1990). 16S rRNA sequences reveal numerous uncultured microorganisms in a natural community. *Nature* **345**(6270): 63-65.

Ward, P., J. Haggart, E. Carter, D. Wilbur, H. Tipper and T. Evans (2001). Sudden productivity collapse associated with the Triassic-Jurassic boundary mass extinction. *Science* **292**(5519): 1148-1151.

Webster, G., T. M. Embley, T. E. Freitag, Z. Smith and J. I. Prosser (2005). Links between ammonia oxidizer species composition, functional diversity and nitrification kinetics in grassland soils. *Environmental Microbiology* **7**(5): 676-684.

Webster, N. S., A. P. Negri, M. M. Munro and C. N. Battershill (2004). Diverse microbial communities inhabit Antarctic sponges. *Environmental Microbiology* **6**(3): 288-300.

Whitman, W. B., D. C. Coleman and W. J. Wiebe (1998). Prokaryotes: The unseen majority. *Proceedings of the National Academy of Sciences* **95**(12): 6578-6583.

Whitney, S. M. and T. J. Andrews (1998). The CO_2/O_2 specificity of single-subunit ribulose-bisphosphate carboxylase from the dinoflagellate, *Amphidinium carterae*. *Australian Journal of Plant Physiology* **25**: 131-138.

Widdicombe, S. and J. I. Spicer (2008). Predicting the impact of ocean acidification on benthic biodiversity: what can animal physiology tell us? *Journal of Experimental Marine Biology and Ecology* **366**(1): 187-197.

Wignall, P. (2005). The link between large igneous province eruptions and mass extinctions. *Elements* **1**(5): 293-297.

Williamson, P., C. Turley, C. Brownlee, H. Findlay, S., A. Ridgwell, D. Scmidt, D. Shroeder, J. C. Blackford, T. Tyrrell and J. K. Pinnegar (2013). Impacts of climate change on ocean acidification. Marine Climate Change impacts Partnership.

Wingenter, O. W., K. B. Haase, M. Zeigler, D. R. Blake, F. S. Rowland, B. C. Sive, A. Paulino, R. Thyrhaug, A. Larsen, K. G. Schulz, M. Meyerhofer and U. Riebesell (2007). Unexpected consequences of increasing CO_2 and ocean acidity on marine production of DMS and CH_2ClI: Potential climate impacts. *Geophysical Research Letters* **34**(5).

Witt, V., C. Wild, K. R. Anthony, G. Diaz-Pulido and S. Uthicke (2011). Effects of ocean acidification on microbial community composition of and oxygen fluxes through, biofilms from the Great Barrier Reef. *Environmental Microbiology* **13**(11): 2976-2989.

Wittmann, A. C. and H.-O. Pörtner (2013). Sensitivities of extant animal taxa to ocean acidification. *Nature Climate Change* **3**(11): 995-1001.

Wolfe, G. V. and M. Steinke (1996). Grazing-activated production of dimethyl sulfide (DMS) by two clones of *Emiliania huxleyi*. *Limnology and Oceanography* **41**: 1151-1160.

Wood, H. G., C. Werkman, H., A. Hemingway and A. O. Nier (1941). Heavy carbon as a tracer in hetrotrophic carbon dioxide assimilation. *Journal of Biological Chemistry* **139**: 365-376.

Wood, H. G. and C. H. Werkman (1935). The utilization of CO_2 by the propionic acid bacteria in the dissimilation of glycerol. *Biochemical Journal* **332**: 332 (abstr.).

Wood, H. G. and C. H. Werkman (1936). The utilization of CO_2 in the dissimilation of glycerol by the propionic acid bacteria. *Biochemical Journal* **30**(418-53).

Wood, H. G., C. H. Werkman, A. Hemingway and A. O. Nier (1941). The position of carbon dioxide carbon in succinic acid synthesized by heterotrophic bacteria. *Journal of Biological Chemistry* **139**(1): 377-381.

Worden, A. Z. (2006). Picoeukaryote diversity in coastal waters of the Pacific Ocean. *Aquatic Microbial Ecology* **43**(2): 165-175.

Worden, A. Z., J. K. Nolan and B. Palenik (2004). Assessing the dynamics and ecology of marine picophytoplankton: The importance of the eukaryotic component. *Limnology and Oceanography* **49**(1): 168-179.

Wu, H., D. Zou and K. Gao (2008). Impacts of increased atmospheric CO_2 concentration on photosynthesis and growth of micro-and macro-algae. *Science in China Series C: Life Sciences* **51**(12): 1144-1150.

Wu, L., W. Cai, L. Zhang, H. Nakamura, A. Timmermann, T. Joyce, M. J. McPhaden, M. Alexander, B. Qiu, M. Visbeck, P. Chang and B. Giese (2012). Enhanced warming over the global subtropical western boundary currents. *Nature Climate Change* **2**(3): 161-166.

Wu, Y., K. Gao and U. Riebesell (2010). CO_2-induced seawater acidification affects physiological performance of the marine diatom *Phaeodactylum tricornutum*. *Biogeosciences* **7**(9): 2915-2923.

Yan, S., B. M. Fuchs, S. Lenk, J. Harder, J. Wulf, N.-Z. Jiao and R. Amann (2009). Biogeography and phylogeny of the NOR5/OM60 clade of *Gammaproteobacteria*. *Systematic and Applied Microbiology* **32**(2): 124-139.

Yapp, C. J. and H. Poths (1992). Ancient atmospheric CO_2 pressures inferred from natural goethites. *Nature* **355**(6358): 342-344.

Yapp, C. J. and H. Poths (1996). Carbon isotopes in continental weathering environments and variations in ancient atmospheric CO_2 pressure. *Earth and Planetary Science Letters* **137**(1-4): 71-82.

Yilmaz, S., M. Allgaier and P. Hugenholtz (2010). Multiple displacement amplification compromises quantitative analysis of metagenomes. *Nature Methods* **7**(12): 943-944.

Yoch, D. C. (2002). Dimethylsulfoniopropionate: Its sources,rRole in the marine food web, and biological degradation to dimethylsulfide. *Applied and Environmental Microbiology* **68**(12): 5804-5815.

Young, J. R. (1994). Functions of coccoliths. *Coccolithophores*. A. Winter and W. G. Siesser, Cambridge University Press, Cambridge**:** 63-82.

Yu, Y., M. Breitbart, P. McNairnie and F. Rohwer (2006). FastGroupII: A web-based bioinformatics platform for analyses of large 16S rDNA libraries. *BMC Bioinformatics* **7**(1): 57.

Yurkov, V. (1990). Biology of freshwater aerobic bacteria containing bacteriochlorophyll a. PhD, Academy of Sciences.

Yurkov, V. and J. T. Csotonyi (2008). New light on aerobic anoxygenic phototrophs. *The Purple Phototrophic Bacteria*. C. N. Hunter, F. Daldal, M. C. Thurnauer and J. T. Beatty, Springer Netherlands. **28:** 31-55.

Yurkov, V. V. and J. T. Beatty (1998). Aerobic anoxygenic phototrophic bacteria. *Microbiology and Molecular Biology Reviews* **62**(3): 695-724.

Yutin, N., M. T. Suzuki and O. Beja (2005). Novel primers reveal wider diversity among marine aerobic anoxygenic phototrophs. *Applied and Environmental Microbiology* **71**(12): 8958-8962.

Yutin, N., M. T. Suzuki, M. Rosenberg, D. Rotem, M. T. Madigan, J. Suling, J. F. Imhoff and O. Beja (2009). BchY-based degenerate primers target all types of anoxygenic photosynthetic bacteria in a single PCR. *Applied and Environmental Microbiology* **75**(23): 7556-7559.

Yvette, B.-S., K. Wen Hong Linda, C. Josef, Z. Lin, G. I. Roxann, S. Robert and W. S. Michael (2007). Reliability of high-throughput genotyping of whole genome amplified DNA in SNP genotyping studies. *Electrophoresis* **28**(16): 2812-2817.

Yvon-Durocher, G., J. I. Jones, M. Trimmer, G. Woodward and J. M. Montoya (2010). Warming alters the metabolic balance of ecosystems. *Philosophical Transactions of the Royal Society B: Biological Sciences* **365**(1549): 2117-2126.

Zachos, J. C., M. A. Arthur and W. E. Dean (1989). Geochemical evidence for suppression of pelagic marine productivity at the Cretaceous/Tertiary boundary. *Nature* **337**(6202): 61-64.

Zachos, J. C., G. R. Dickens and R. E. Zeebe (2008). An early Cenozoic perspective on greenhouse warming and carbon-cycle dynamics. *Nature* **451**(7176): 279-283.

Zeebe, R. E. and D. A. Wolf-Gladrow (2001). *CO_2 in Seawater: Equilibrium, Kinetics, Isotopes: Equilibrium, Kinetics, Isotopes*. Elsevier.

Zhang, K., A. C. Martiny, N. B. Reppas, K. W. Barry, J. Malek, S. W. Chisholm and G. M. Church (2006). Sequencing genomes from single cells by polymerase cloning. *Nature Biotechnology* **24**(6): 680-686.

Zhang, Y. and N. Jiao (2007). Dynamics of aerobic anoxygenic phototrophic bacteria in the East China Sea. *FEMS Microbiology Ecology* **61**(3): 459-469.

Zhu, F., R. Massana, F. Not, D. Marie and D. Vaulot (2005). Mapping of picoeucaryotes in marine ecosystems with quantitative PCR of the 18S rRNA gene. *FEMS Microbiology Ecology* **52**(1): 79-92.

Zubkov, M. V. (2009). Photoheterotrophy in marine prokaryotes. *Journal Of Plankton Research* **31**(9): 933-938.

Zubkov, M. V., B. M. Fuchs, S. D. Archer, R. P. Kiene, R. Amann and P. H. Burkill (2001). Linking the composition of bacterioplankton to rapid turnover of dissolved dimethylsulphoniopropionate in an algal bloom in the North Sea. *Environmental Microbiology* **3**(5): 304-311.

Zubkov, M. V., B. M. Fuchs, S. D. Archer, R. P. Kiene, R. Amann and P. H. Burkill (2002). Rapid turnover of dissolved DMS and DMSP by defined bacterioplankton communities in the stratified euphotic zone of the North Sea. *Deep Sea Research Part II: Topical Studies in Oceanography* **49**(15): 3017-3038.

Zubkov, M. V., B. M. Fuchs, P. H. Burkill and R. Amann (2001). Comparison of cellular and biomass specific activities of dominant bacterioplankton groups in stratified waters of the Celtic Sea. *Applied and Environmental Microbiology* **67**(11): 5210-5218.

9.1 Anaplerotic alignments

9.1.1 Malic enzyme

malic enzyme, partial [Oceanibulbus indolifex]
Sequence ID: ref|WP_007119057.1| Length: 551 Number of Matches: 1
Range 1: 445 to 522 GenPept Graphics ▼ Next Match ▲ Previous Match

Score	Expect	Method	Identities	Positives	Gaps	Frame
141 bits(356)	7e-38	Compositional matrix adjust.	64/78(82%)	74/78(94%)	0/78(0%)	-2

```
Query  235  RIVFAEGEDERVLRAAQAMLEETTERPILIGRPEVIEARIERAGLTIKMGERVDLVNPEN  56
            R+VFAEGEDERVLRAAQA++EET ERPILIGRPEVIE RIE+AGL +++G+ VDLVNPEN
Sbjct  445  RLVFAEGEDERVLRAAQAIIEETVERPILIGRPEVIERRIEKAGLNLQLGQNVDLVNPEN  504

Query  55   DPRYRDYWETYHNLMCRQ  2
            DPRYRDYWETYH+LMCR+
Sbjct  505  DPRYRDYWETYHSLMCRR  522
```

malic enzyme [Roseobacter sp. SK209-2-6]
Sequence ID: ref|WP_008205672.1| Length: 751 Number of Matches: 1
Range 1: 413 to 472 GenPept Graphics ▼ Next Match ▲ Previous Match

Score	Expect	Method	Identities	Positives	Gaps	Frame
107 bits(267)	5e-25	Compositional matrix adjust.	50/60(83%)	56/60(93%)	0/60(0%)	+2

```
Query  2    LESYELSLKSRMDPTASILSGINARARAAQARMIFAEGDDPRVLRAAVMYQRSGFGTALV  181
            +E+YE+SLK RMDPTASIL G+NARAR+AQ+RMIFAEGDDPRVLRAAV YQRSGFG ALV
Sbjct  413  MEAYEISLKGRMDPTASILRGLNARARSAQSRMIFAEGDDPRVLRAAVTYQRSGFGKALV  472
```

NADP-dependent malic enzyme [Ruegeria pomeroyi DSS-3]
Sequence ID: ref|YP_165285.1| Length: 751 Number of Matches: 1
Range 1: 491 to 547 GenPept Graphics ▼ Next Match ▲ Previous Match

Score	Expect	Method	Identities	Positives	Gaps	Frame
99.4 bits(246)	1e-22	Composition-based stats.	46/57(81%)	48/57(84%)	0/57(0%)	-2

```
Query  171  AAGELEVVNAANTEHLEDYKNYLYQRLQRKGFDTTDVHRLAARDRHVFGSLMLAHGH  1
            A  ELEVVNAANT HLE YK +LY RLQRKGFD  DVHRLAARDRHVF +LMLAHGH
Sbjct  491  AVRELEVVNAANTTHLETYKEFLYSRLQRKGFDNKDVHRLAARDRHVFSALMLAHGH  547
```

NADP-dependent malic enzyme [Silicibacter sp. TrichCH4B]
Sequence ID: ref|WP_009178264.1| Length: 751 Number of Matches: 1
Range 1: 700 to 749 GenPept Graphics ▼ Next Match ▲ Previous Match

Score	Expect	Method	Identities	Positives	Gaps	Frame
93.6 bits(231)	3e-20	Composition-based stats.	41/50(82%)	47/50(94%)	0/50(0%)	-3

```
Query  237  ASISVKLMQEMGGATVIGPILTGIDKPIQICSTVSSVNDILNMAAIAACN  88
            ASISVKLMQEMGGATV+GPIL+G+DKPIQICST S+ ND+LNMA +AACN
Sbjct  700  ASISVKLMQEMGGATVVGPILSGVDKPIQICSTTSTANDVLNMAVLAACN  749
```

NADP-dependent malic enzyme [Silicibacter sp. TrichCH4B]
Sequence ID: ref|WP_009178264.1| Length: 751 Number of Matches: 1
Range 1: 6 to 91 GenPept Graphics ▼ Next Match ▲ Previous Match

Score	Expect	Method	Identities	Positives	Gaps	Frame
137 bits(344)	2e-35	Compositional matrix adjust.	75/86(87%)	84/86(97%)	0/86(0%)	+2

```
Query  2    VTDADALAYHLEPTPGKFEITASVPMTTQRDLSLAYSPGVAVPCLAIADNPELAYDYTNK  181
            +T+ +ALA+HLEP+PGK+E+TA+VPMTTQRDLSLAYSPGVAVPC AIA+NPELAYDYTNK
Sbjct  6    ITNEEALAFHLEPSPGKWEVTATVPMTTQRDLSLAYSPGVAVPCEAIAENPELAYDYTNK  65

Query  182  GNLVAVISNGTAVlglgnlgalgSKP  259
            GNLVAVISNGTAVLGLGNLGALGSKP
Sbjct  66   GNLVAVISNGTAVLGLGNLGALGSKP  91
```

malic enzyme [Ruegeria sp. TM1040]

Sequence ID: ref|YP_614871.1| Length: 751 Number of Matches: 1

Range 1: 233 to 317 GenPept Graphics ▼ Next Match ▲ Previous Match

Score	Expect	Method	Identities	Positives	Gaps	Frame
161 bits(407)	2e-44	Compositional matrix adjust.	76/85(89%)	82/85(96%)	0/85(0%)	-3

```
Query  256  EGMNQWKSAHAVKTDLRSLKEAMHGADVFLGVSVKGAVTQEMVKNMADNPVIFAMANPDP  77
            EGMNQWKSAHAVKT+LRSL+EAM+GADVFLGVSVKGAVTQ+MVK+MADNPVIFAMANPDP
Sbjct  233  EGMNQWKSAHAVKTELRSLEEAMNGADVFLGVSVKGAVTQDMVKSMADNPVIFAMANPDP  292

Query  76   EITPEEAQEIRKDATVATGRSDYPN  2
            EITPEEA E+R DA VATGRSDYPN
Sbjct  293  EITPEEAHEVRVDAIVATGRSDYPN  317
```

malic enzyme [Paracoccus sp. N5]

Sequence ID: ref|WP_018000833.1| Length: 759 Number of Matches: 1

Range 1: 20 to 90 GenPept Graphics ▼ Next Match ▲ Previous Match

Score	Expect	Method	Identities	Positives	Gaps	Frame
133 bits(334)	3e-34	Compositional matrix adjust.	64/71(90%)	70/71(98%)	0/71(0%)	-3

```
Query  214  PKPGKLEIRATKPMANGRDLARAYSPGVAEACLEIKNDPSSAARYTARGNLVAVVSNGTA  35
            P+PGKLE+RATKP+ANGRDL+RAYSPGVAEACLEIK DP++AARYTARGNLVAVVSNGTA
Sbjct  20   PRPGKLEVRATKPLANGRDLSRAYSPGVAEACLEIKADPATAARYTARGNLVAVVSNGTA  79

Query  34   VLGLGNIGALA  2
            VLGLGNIGALA
Sbjct  80   VLGLGNIGALA  90
```

Malate dehydrogenase (oxaloacetate-decarboxylating) (NADP(+)) [Flavobacteria bacterium MS024-3C]

Sequence ID: ref|WP_008868122.1| Length: 765 Number of Matches: 1

Range 1: 336 to 419 GenPept Graphics ▼ Next Match ▲ Previous Match

Score	Expect	Method	Identities	Positives	Gaps	Frame
137 bits(345)	1e-35	Compositional matrix adjust.	83/84(99%)	84/84(100%)	0/84(0%)	-3

```
Query  253  TKINEAMKMAAVKALADLAKEPVPEQVNIAYGETRLAFSREYIIPKPFDPRLiseippai  74
            TKINEAMKMAAVKALADLAKEPVPEQVNIAYGETRLAFSREYIIPKPFDPRLISEIPPAI
Sbjct  336  TKINEAMKMAAVKALADLAKEPVPEQVNIAYGETRLAFSREYIIPKPFDPRLISEIPPAI  395

Query  73   araaieSGVAKEPIEDWDKYKEAL  2
            ARAA+ESGVAKEPIEDWDKYKEAL
Sbjct  396  ARAAMESGVAKEPIEDWDKYKEAL  419
```

Malate dehydrogenase (oxaloacetate-decarboxylating) (NADP+) [Flavobacterium psychrophilum

Sequence ID: ref|YP_001296987.1| Length: 771 Number of Matches: 1

Range 1: 19 to 80 GenPept Graphics ▼ Next Match ▲ Previous Match

Score	Expect	Method	Identities	Positives	Gaps	Frame
121 bits(303)	8e-30	Composition-based stats.	60/62(97%)	60/62(96%)	0/62(0%)	-2

```
Query  187  PGKIQVVPTTKYATQRDLSLAYSPGVAEPCLEIAKDVENVYKYTAKGNLVAVITNGTAVL  8
            PGKIQVVPT KYATQRDLSLAYSPGVAEPCLEIAKDV NVYKYTAKGNLVAVITNGTAVL
Sbjct  19   PGKIQVVPTKKYATQRDLSLAYSPGVAEPCLEIAKDVNNVYKYTAKGNLVAVITNGTAVL  78

Query  7    GL  2
            GL
Sbjct  79   GL  80
```

9.1.2 PEP Carboxykinase

Malate dehydrogenase (oxaloacetate-decarboxylating) (NADP(+)) [Flavobacteria bacterium MS024-3C]
Sequence ID: ref|WP_008868122.1| Length: 765 Number of Matches: 1

Range 1: 338 to 419 GenPept Graphics ▼ Next Match ▲ Previous Match

Score	Expect	Method	Identities	Positives	Gaps	Frame
137 bits(345)	1e-35	Compositional matrix adjust.	65/82(79%)	74/82(90%)	0/82(0%)	-1

```
Query  261  INEPMKMAAVKALAELTKKPVPEQVNIAYQETNLSFGREYIIPKPFDPRLIEEVPIAVAK  82
            INE MKMAAVKALA+L K+PVPEQVNIAY ET L+F REYIIPKPFDPRLI E+P A+A+
Sbjct  338  INEAMKMAAVKALADLAKEPVPEQVNIAYGETRLAFSREYIIPKPFDPRLISEIPPAIAR  397

Query  81   AAIESGVAKEPIEDWEKYREQL  16
            AA+ESGVAKEPIEDW+KY+E L
Sbjct  398  AAMESGVAKEPIEDWDKYKEAL  419
```

Malate dehydrogenase (oxaloacetate-decarboxylating) (NADP(+)) [Flavobacteria bacterium MS024-3C]
Sequence ID: ref|WP_008868122.1| Length: 765 Number of Matches: 1

Range 1: 229 to 305 GenPept Graphics ▼ Next Match ▲ Previous Match

Score	Expect	Method	Identities	Positives	Gaps	Frame
120 bits(301)	1e-29	Compositional matrix adjust.	61/77(79%)	66/77(85%)	0/77(0%)	+2

```
Query  2    DRSELSPEKSEFATHRKIDTLDEAMVDADVFVGLSVADIVTPSMLKSMAADPIVFAMANP  181
            DR  LS EK EFAT RKIDTLDEAM +ADVFVGLSVADIVTPSML SMA +PIVFAMANP
Sbjct  229  DRPNLSSEKEEFATARKIDTLDEAMENADVFVGLSVADIVTPSMLTSMADNPIVFAMANP  288

Query  182  NPEIEYQLACKTRDDII  232
            +PEI+Y+LA  TR DII
Sbjct  289  DPEIDYKLAMDTRKDII  305
```

9.1.2 PEP Carboxykinase

phosphoenolpyruvate carboxykinase [Roseobacter sp. MED193]
Sequence ID: ref|WP_009810791.1| Length: 532 Number of Matches: 1

Range 1: 441 to 525 GenPept Graphics ▼ Next Match ▲ Previous Match

Score	Expect	Method	Identities	Positives	Gaps	Frame
144 bits(364)	5e-39	Composition-based stats.	65/85(76%)	76/85(89%)	0/85(0%)	+3

```
Query  3    GSRMPIRATRALLTAAMNGILAASKFRKDPNFGFDVPVSVPGVADILLDPRRTWNDVNAY  182
            GSRMPIRATRALLTAA+ G LA  +FRKD NFGFDVPVSVPGVA++LLDPRRTW+D  AY
Sbjct  441  GSRMPIRATRALLTAALEGTLAQVEFRKDSNFGFDVPVSVPGVAEVLLDPRRTWDDQAAY  500

Query  183  DQQAKKLLEMFSRNFEKYLPFIDQD  257
            D+QA KL+EMFS NF++YLP+ID+D
Sbjct  501  DKQAAKLVEMFSNNFQQYLPYIDED  525
```

phosphoenolpyruvate carboxykinase [Roseobacter sp. SK209-2-6]
Sequence ID: ref|WP_008207589.1| Length: 532 Number of Matches: 2

Range 1: 420 to 472 GenPept Graphics ▼ Next Match ▲ Previous Match

Score	Expect	Method	Identities	Positives	Gaps	Frame
97.8 bits(242)	5e-34	Composition-based stats.	42/53(79%)	49/53(92%)	0/53(0%)	-2

```
Query  159  SNHGASCWLVNTGWTGGAYGIGSRMPIRATRALLTAAMNGILAASKFRKDPNF  1
            + HGA+CWLVNTGWTGGAYG+GSRMPIRATRALLTAA++G LA ++FRKD NF
Sbjct  420  AQHGATCWLVNTGWTGGAYGVGSRMPIRATRALLTAALDGSLAEAEFRKDSNF  472
```

phosphoenolpyruvate carboxykinase [Croceibacter atlanticus HTCC2559]

Sequence ID: ref|YP_003715097.1| **Length:** 536 **Number of Matches:** 1

Range 1: 141 to 232 GenPept Graphics ▼ Next Match ▲ Previous Match

Score	Expect	Method	Identities	Positives	Gaps	Frame
172 bits(435)	1e-48	Compositional matrix adjust.	78/92(85%)	88/92(95%)	0/92(0%)	-1

```
Query  278  FLRPTNEELKNFEQEWLVVNAPGFMANPELDGTRQHNFAILNFTKKIALIGGTGYTGEIK  99
            FLRP+ +ELKNF++EWL+VNAPGFMA+PE+DGTRQHNFAILNF KKIALIGGTGYTGEIK
Sbjct  141  FLRPSEDELKNFKEEWLIVNAPGFMADPEVDGTRQHNFAILNFGKKIALIGGTGYTGEIK  200

Query  98   KGIFSALNFILPVDKNTMPMHCSANVGKDGET  3
            KGIFSALNFILPV K T+PMHCSANVG+DG+T
Sbjct  201  KGIFSALNFILPVQKETLPMHCSANVGEDGDT  232
```

Phosphoenolpyruvate carboxykinase (ATP) [Dokdonia donghaensis MED134]

Sequence ID: gb|EAQ39883.1| **Length:** 537 **Number of Matches:** 1

Range 1: 275 to 361 GenPept Graphics ▼ Next Match ▲ Previous Match

Score	Expect	Method	Identities	Positives	Gaps	Frame
134 bits(337)	4e-35	Compositional matrix adjust.	66/87(76%)	73/87(83%)	1/87(1%)	-1

```
Query  258  CQGKSIS-QKKTKPDIYKAIKFGAILENVVMDDAGVVDFEDVSITQNTRVSYPIDHIENI  82
            C  K I+   + +PDIY AIK GAILENV++D+ G V FED SITQNTRVSYPIDHIENI
Sbjct  275  CYAKVINLSAENEPDIYNAIKPGAILENVILDEQGNVAFEDTSITQNTRVSYPIDHIENI  334

Query  81   QVPSIGTNPKNIFFLTADAFGVLPPIS  1
            QVPS+G NPKNIFFLTADAFGVLPPIS
Sbjct  335  QVPSLGKNPKNIFFLTADAFGVLPPIS  361
```

phosphoenolpyruvate carboxykinase [Maribacter sp. HTCC2170]

Sequence ID: ref|YP_003862438.1| **Length:** 528 **Number of Matches:** 1

Range 1: 361 to 444 GenPept Graphics ▼ Next Match ▲ Previous Match

Score	Expect	Method	Identities	Positives	Gaps	Frame
169 bits(429)	4e-48	Compositional matrix adjust.	79/84(94%)	83/84(98%)	0/84(0%)	-2

```
Query  253  HFISGYTAKVAGTEAGVNEPLPSFSACFGAPFMPLHPAKYAEMLSKKMQEAGVSVWLVNT  74
            HFISGYTAKVAGTEAGV EP+PSFSACFGAPFMPLHPAKYAEMLS+KMQEAGV+VWLVNT
Sbjct  361  HFISGYTAKVAGTEAGVVEPIPSFSACFGAPFMPLHPAKYAEMLSRKMQEAGVNVWLVNT  420

Query  73   GWTGGPYGVGTRMKLKYTRAMITA  2
            GWTGGPYGVGTRMKLKYTRAMI+A
Sbjct  421  GWTGGPYGVGTRMKLKYTRAMISA  444
```

9.1.3 Pyruvate carboxylase

pyruvate carboxylase [Roseobacter denitrificans OCh 114]

Sequence ID: ref|YP_683556.1| Length: 1146 Number of Matches: 1

Range 1: 471 to 553 GenPept Graphics ▼ Next Match ▲ Previous Match

Score	Expect	Method	Identities	Positives	Gaps	Frame
89.0 bits(219)	2e-18	Composition-based stats.	49/83(59%)	52/83(62%)	0/83(0%)	-1

```
Query  249  LTYIADITVNGHQR*KIVLVRELT*KTPRFQNPNLMHKWVPATYWSKKGPKAVADWMKTQ  70
            LTYIADITVNGH   K          K PR                +KGP+AVADWMK Q
Sbjct  471  LTYIADITVNGHPETKAHPRPPAHVKDPRPPKERAEPMMGTRNLLEQKGPQAVADWMKQQ  530

Query  69   KQLLITDTTMRDGHQSLLATRMR  1
            +QLLITDTTMRDGHQSLLATRMR
Sbjct  531  RQLLITDTTMRDGHQSLLATRMR  553
```

pyruvate carboxylase [Roseobacter sp. AzwK-3b]

Sequence ID: ref|WP_007814640.1| Length: 1146 Number of Matches: 1

Range 1: 777 to 858 GenPept Graphics ▼ Next Match ▲ Previous Match

Score	Expect	Method	Identities	Positives	Gaps	Frame
152 bits(383)	2e-40	Compositional matrix adjust.	70/82(85%)	75/82(91%)	0/82(0%)	-1

```
Query  247  PALGSIVEALAHTERDTGLDIAEIRKISSYWEQVRAQYSAFESGLQAPASEVYLHEMPGG  68
            P LGSIVEAL HTERDTG+DI  IR+IS+YWE VRAQY AFESGLQAPASEVYLHEMPGG
Sbjct  777  PCLGSIVEALMHTERDTGIDIERIREISNYWEHVRAQYVAFESGLQAPASEVYLHEMPGG  836

Query  67   QFTNLKAQARSLGLEDRWEDVA  2
            QFTNLKAQARS+GLED+W DVA
Sbjct  837  QFTNLKAQARSMGLEDKWPDVA  858
```

pyruvate carboxylase [Roseobacter sp. GAI101]

Sequence ID: ref|WP_008227983.1| Length: 1146 Number of Matches: 1

Range 1: 333 to 405 GenPept Graphics ▼ Next Match ▲ Previous Match

Score	Expect	Method	Identities	Positives	Gaps	Frame
147 bits(370)	7e-39	Compositional matrix adjust.	70/73(96%)	72/73(98%)	0/73(0%)	+3

```
Query  6    SQADIQLHGHALQTRITTEDPLNNFIPDYGRITAFREATGMGIRLDGGTAYSGGVITRYY  185
            SQAD+QL+GHALQTRITTEDP NNFIPDYGRITAFREATGMGIRLDGGTAYSGGVITRYY
Sbjct  333  SQADVQLNGHALQTRITTEDPQNNFIPDYGRITAFREATGMGIRLDGGTAYSGGVITRYY  392

Query  186  DSLLVKVTAKAQT  224
            DSLLVKVTAKAQT
Sbjct  393  DSLLVKVTAKAQT  405
```

pyruvate carboxylase [Rhodobacteraceae bacterium KLH11]

Sequence ID: ref|WP_008755952.1| Length: 1146 Number of Matches: 1

Range 1: 39 to 123 GenPept Graphics ▼ Next Match ▲ Previous Match

Score	Expect	Method	Identities	Positives	Gaps	Frame
168 bits(426)	3e-46	Compositional matrix adjust.	80/85(94%)	83/85(97%)	0/85(0%)	+1

```
Query  1    KLGLHRFKADEAYRIGKDLGPVAAYLSIEEMIRVAKASGADAVHPGYGLLSENPDFVDAC  180
            KLGLHRFKADEAYRIGKDLGPVAAYLSI+E+IRVAK SGADA+HPGYGLLSENPDFVDAC
Sbjct  39   KLGLHRFKADEAYRIGKDLGPVAAYLSIDEIIRVAKESGADAIHPGYGLLSENPDFVDAC  98

Query  181  AQNGITFIGPKADTMRALGDKASAR  255
            AQNGITFIGPKA TMRALGDKASAR
Sbjct  99   AQNGITFIGPKAQTMRALGDKASAR  123
```

pyruvate carboxylase [Roseovarius sp. TM1035]

Sequence ID: ref|WP_008282565.1| **Length:** 1167 **Number of Matches:** 1

Range 1: 246 to 325 GenPept Graphics ▼ Next Match ▲ Previous Match

Score	Expect	Method	Identities	Positives	Gaps	Frame
167 bits(423)	6e-46	Composition-based stats.	73/80(91%)	76/80(95%)	0/80(0%)	-1

```
Query  241  YHLFERDCSVQRRNQKVVERAPAPYLTNKQREEICRLGYKICKHVNYECAGTVEFLMDMN  62
            YHLFERDCSVQRRNQKVVERAPAPYL+  QREEIC+LGYKICKHVNYECAGTVEFLMDM+
Sbjct  246  YHLFERDCSVQRRNQKVVERAPAPYLSETQREEICQLGYKICKHVNYECAGTVEFLMDMD  305

Query  61   DEKFYFIEVNPRVQVEHTVT  2
              KFYFIEVNPRVQVEHTVT
Sbjct  306  TGKFYFIEVNPRVQVEHTVT  325
```

pyruvate carboxylase [Loktanella vestfoldensis]

Sequence ID: ref|WP_007205422.1| **Length:** 1147 **Number of Matches:** 1

Range 1: 410 to 492 GenPept Graphics ▼ Next Match ▲ Previous Match

Score	Expect	Method	Identities	Positives	Gaps	Frame
162 bits(409)	5e-44	Composition-based stats.	74/83(89%)	78/83(93%)	0/83(0%)	+1

```
Query  1    IARMDRALREFRIRGVSTNIAFVENLLKHPVFLNNEYHTKFIDETPSLFDFKARRDRATK  180
            IARMDRALREFRIRGVSTNIAFVENLLKHP FLNNEYHTKFIDETP LF+F  RRDRATK
Sbjct  410  IARMDRALREFRIRGVSTNIAFVENLLKHPTFLNNEYHTKFIDETPDLFNFTKRRDRATK  469

Query  181  LLTYIADITVNGHPETVGRAKPS  249
            +LTYIADITVNGHPET GRA+P+
Sbjct  470  ILTYIADITVNGHPETAGRARPA  492
```

pyruvate carboxylase [Rhodobacter sphaeroides ATCC 17025]

Sequence ID: ref|YP_001166888.1| **Length:** 1154 **Number of Matches:** 1

Range 1: 605 to 678 GenPept Graphics ▼ Next Match ▲ Previous Match

Score	Expect	Method	Identities	Positives	Gaps	Frame
157 bits(398)	1e-42	Composition-based stats.	70/74(95%)	73/74(98%)	0/74(0%)	+3

```
Query  3    PNLMTQMLLRASNGVGYTNYPDNVVQEFVRQAAETGVDLFRVFDSLNWVENMRVAMDAVI  182
            PN+MTQMLLRASNGVGYTNYPDNVVQEFVRQAAETGVD+FRVFDSLNWVENMRVAMDAVI
Sbjct  605  PNVMTQMLLRASNGVGYTNYPDNVVQEFVRQAAETGVDVFRVFDSLNWVENMRVAMDAVI  664

Query  183  ENGKICEGTICYTG  224
            E GK+CEGTICYTG
Sbjct  665  EAGKVCEGTICYTG  678
```

pyruvate carboxylase [Rhodobacterales bacterium HTCC2255]

Sequence ID: ref|WP_008034810.1| **Length:** 1148 **Number of Matches:** 1

Range 1: 608 to 696 GenPept Graphics ▼ Next Match ▲ Previous Match

Score	Expect	Method	Identities	Positives	Gaps	Frame
195 bits(495)	1e-55	Composition-based stats.	89/89(100%)	89/89(100%)	0/89(0%)	+1

```
Query  1    LMTQMLLRASNGVGYTNYPDNVVQEFVRQAAETGIDMFRVFDSLNWVENMRVAMDAVIEN  180
            LMTQMLLRASNGVGYTNYPDNVVQEFVRQAAETGIDMFRVFDSLNWVENMRVAMDAVIEN
Sbjct  608  LMTQMLLRASNGVGYTNYPDNVVQEFVRQAAETGIDMFRVFDSLNWVENMRVAMDAVIEN  667

Query  181  GKICEGSICYTGDILNPDRAKYNLNYYVK  267
            GKICEGSICYTGDILNPDRAKYNLNYYVK
Sbjct  668  GKICEGSICYTGDILNPDRAKYNLNYYVK  696
```

pyruvate carboxylase [Dokdonia donghaensis MED134]

Sequence ID: gb|EAQ40332.1| Length: 1150 Number of Matches: 1

Range 1: 218 to 306 GenPept Graphics ▼ Next Match ▲ Previous Match

Score	Expect	Method	Identities	Positives	Gaps	Frame
163 bits(412)	3e-44	Compositional matrix adjust.	74/89(83%)	83/89(93%)	0/89(0%)	-3

```
Query  268  DNHGNIRHLYERDCSVQRRHQKVVEIAPSFNISEEVKQNLYKYALAIAKQVNYNNIGTVE  89
            D HGNIRHLYERDCSVQRRHQKVVE+APS+N+S+ ++ NLYKYA+AIA +VNYNNIGTVE
Sbjct  218  DTHGNIRHLYERDCSVQRRHQKVVEMAPSYNLSQTLRDNLYKYAVAIATEVNYNNIGTVE  277

Query  88   FLVDNADNVYFIEVNPRIQVEHTVTEMVT  2
            FLVD  DN+YFIEVNPRIQVEHTVTEMVT
Sbjct  278  FLVDADDNIYFIEVNPRIQVEHTVTEMVT  306
```

pyruvate carboxylase [Dokdonia donghaensis MED134]

Sequence ID: gb|EAQ40332.1| Length: 1150 Number of Matches: 1

Range 1: 215 to 303 GenPept Graphics ▼ Next Match ▲ Previous Match

Score	Expect	Method	Identities	Positives	Gaps	Frame
162 bits(410)	5e-44	Compositional matrix adjust.	74/89(83%)	83/89(93%)	0/89(0%)	-3

```
Query  268  IVADNHGNIRHLYERDCSVQRRHQKVVEIAPSFNISEEVKQNLYKYALAIAKQVNYNNIG  89
            IVAD HGNIRHLYERDCSVQRRHQKVVE+APS+N+S+ ++ NLYKYA+AIA +VNYNNIG
Sbjct  215  IVADTHGNIRHLYERDCSVQRRHQKVVEMAPSYNLSQTLRDNLYKYAVAIATEVNYNNIG  274

Query  88   TVEFLVDNADNVYFIEVNPRIQVEHTVTE  2
            TVEFLVD  DN+YFIEVNPRIQVEHTVTE
Sbjct  275  TVEFLVDADDNIYFIEVNPRIQVEHTVTE  303
```

pyruvate carboxylase [Flavobacteriales bacterium ALC-1]

Sequence ID: ref|WP_008272439.1| Length: 1149 Number of Matches: 1

Range 1: 839 to 938 GenPept Graphics ▼ Next Match ▲ Previous Match

Score	Expect	Method	Identities	Positives	Gaps	Frame
166 bits(421)	3e-45	Compositional matrix adjust.	82/100(82%)	87/100(87%)	0/100(0%)	+2

```
Query  2    SNLRPQAYALGLGGRFDEVKKMYIEVNAMFGNIVKVTPSSKVVGDMAIFMVTNNLTPEGV  181
            SNLRPQA ALGLG RFDEVKKMY EVN MFGN+VKVTPSSKVVGDMAIFMVTNNLTPE V
Sbjct  839  SNLRPQAEALGLGDRFDEVKKMYAEVNKMFGNLVKVTPSSKVVGDMAIFMVTNNLTPEDV  898

Query  182  MENGEEISFPDSVIDFFKGDLGQPVGDFQKSFRK*ILKNQ  301
            M  GEEISFP+SVI+FFKGDLGQP G F K  +K ILKN+
Sbjct  899  MTRGEEISFPESVINFFKGDLGQPTGGFPKELQKIILKNK  938
```

9.1.4 PEP carboxylase

phosphoenolpyruvate carboxylase [Rhodobacterales bacterium Y4I]

Sequence ID: ref|WP_008557853.1| **Length:** 886 **Number of Matches:** 1

Range 1: 601 to 680 GenPept Graphics ▼ Next Match ▲ Previous Match

Score	Expect	Method	Identities	Positives	Gaps	Frame
101 bits(251)	8e-23	Compositional matrix adjust.	50/80(63%)	62/80(77%)	0/80(0%)	-3

```
Query  243  ISAQPEGTIEGMMRTTEQGEVVSAKYANRGTATAQIELLAASALLHTTKVTNDHVSPEFE  64
            I+AQP GTI G MR TEQGEVVS+KYANRGTA  Q+EL+A+S L H+ +      V+PE +
Sbjct  601  IAAQPAGTIAGRMRITEQGEVVSSKYANRGTALHQLELMASSVLRHSLQDDVPPVNPEHD  660

Query  63   SAFEALSGLSQTAYSALLNS  4
             AFEAL+G+SQ AYS LLN+
Sbjct  661  DAFEALAGMSQAAYSNLLNA  680
```

phosphoenolpyruvate carboxylase [Rhodobacteraceae bacterium HTCC2083]

Sequence ID: ref|WP_009827847.1| **Length:** 879 **Number of Matches:** 1

Range 1: 522 to 593 GenPept Graphics ▼ Next Match ▲ Previous Match

Score	Expect	Method	Identities	Positives	Gaps	Frame
98.2 bits(243)	6e-22	Composition-based stats.	56/72(78%)	60/72(83%)	0/72(0%)	-2

```
Query  218  RRSLNSRGRRMEIMLGYSDSNKDGGFICSTWELHSAQRNILQTLRSFNMKPAFFHGRGGS  39
            RRSL  +G R+E+MLGYSDSNKDGGFICSTWEL  AQR I QTL+     PAFFHGRGGS
Sbjct  522  RRSLKRQGSRIEVMLGYSDSNKDGGFICSTWELEQAQRKIKQTLQGLGFVPAFFHGRGGS  581

Query  38   VSRGGAPTGRAI  3
            VSRGGAPTGRAI
Sbjct  582  VSRGGAPTGRAI  593
```

phosphoenolpyruvate carboxylase [Flavobacteriales bacterium ALC-1]

Sequence ID: ref|WP_008270451.1| **Length:** 835 **Number of Matches:** 2

Range 1: 663 to 743 GenPept Graphics ▼ Next Match ▲ Previous Match

Score	Expect	Method	Identities	Positives	Gaps	Frame
121 bits(304)	9e-30	Compositional matrix adjust.	58/81(72%)	64/81(79%)	0/81(0%)	+2

```
Query  53   LKSDTFCGLLESVKTKRTWVFGVGTALKHYEDIGEFEKAQHLFKTSDFFKTLIENSMMSL  232
            L++  F G    +K      FGVGTALKHYED+GEFEK Q LFKTSDFFKTLIENSMMSL
Sbjct  663  LRAIPFVGSWSQLKQNVPGFFGVGTALKHYEDVGEFEKVQTLFKTSDFFKTLIENSMMSL  722

Query  233  SKSFFGLTKYMSEDPEYGAFW  295
            SKSFF LT+YM+EDPEYG FW
Sbjct  723  SKSFFDLTRYMAEDPEYGEFW  743
```

phosphoenolpyruvate carboxylase [Polaribacter]

Sequence ID: ref|WP_004569009.1| **Length:** 859 **Number of Matches:** 1

Range 1: 635 to 732 GenPept Graphics ▼ Next Match ▲ Previous Match

Score	Expect	Method	Identities	Positives	Gaps	Frame
175 bits(443)	6e-49	Compositional matrix adjust.	83/98(85%)	89/98(90%)	0/98(0%)	+2

```
Query  2    DIANTSYETYVAFKNHEKFLPYLEKMSTLQYYAKTNIGSRPSKRSQSDTLDFSDLRAIPF  181
            D+A TSYETYVAFKNH KFLPYLEKMSTL+YYAKTNIGSRPSKRS S TLDFS LRAIPF
Sbjct  635  DLAATSYETYVAFKNHPKFLPYLEKMSTLKYYAKTNIGSRPSKRSNSATLDFSALRAIPF  694

Query  182  VGSWSQLKQNVPGFYGVGTALKKYEDNGEFDKLIDFYN  295
            VGSWSQLKQNVPGF+GVGTALKKYED   F+++I FYN
Sbjct  695  VGSWSQLKQNVPGFFGVGTALKKYEDANRFEEVIAFYN  732
```

9.2 Metabolic enzyme alignments

9.2.1 DMSP demethylase

dimethyl sulfoniopropionate demethylase [Candidatus Pelagibacter sp. HTCC7211] Ambient CO_2

Sequence ID: ref|WP_008546106.1| Length: 381 Number of Matches: 1

Range 1: 7 to 60 GenPept Graphics ▼ Next Match ▲ Previous Match

Score	Expect	Method	Identities	Positives	Gaps	Frame
95.1 bits(235)	1e-21	Composition-based stats.	41/54(76%)	46/54(85%)	0/54(0%)	+2

```
Query  14   LNMSRRLRRTPYTDRVEQSGVRGFSVVNHMLLPKAFGSTVEEDYWHLRKHVQIW  175
            LNMSRR+RRTPYT+RVEQ GV  F+VVNHMLLPK F +TVEEDY HL K VQ+W
Sbjct  7    LNMSRRIRRTPYTNRVEQHGVSDFTVVNHMLLPKGFKNTVEEDYLHLSKEVQMW  60
```

dimethyl sulfoniopropionate demethylase [Ruegeria lacuscaerulensis] Ambient CO_2

Sequence ID: ref|WP_005983312.1| Length: 367 Number of Matches: 1

Range 1: 183 to 258 GenPept Graphics ▼ Next Match ▲ Previous Match

Score	Expect	Method	Identities	Positives	Gaps	Frame
154 bits(388)	3e-43	Composition-based stats.	69/76(91%)	72/76(94%)	0/76(0%)	-1

```
Query  230  FKADEMAIARSGYSKQGGFEIYVEGSDIGMPLWNALFAAGEDLNVRAGCPNLIERIEGGL  51
            F+  ++AIARSGYSKQGGFEIYVEGSDIGMPLWNALFAAG DL VRAGCPNLIERIEGGL
Sbjct  183  FEGRDLAIARSGYSKQGGFEIYVEGSDIGMPLWNALFAAGGDLQVRAGCPNLIERIEGGL  242

Query  50   LSYGNDMTDDNTPHEC  3
            LSYGNDMTDDNTPHEC
Sbjct  243  LSYGNDMTDDNTPHEC  258
```

dimethyl sulfoniopropionate demethylase [Ruegeria sp. TW15] Ambient CO_2

Sequence ID: ref|WP_010439960.1| Length: 364 Number of Matches: 1

Range 1: 218 to 263 GenPept Graphics ▼ Next Match ▲ Previous Match

Score	Expect	Method	Identities	Positives	Gaps	Frame
68.6 bits(166)	7e-12	Composition-based stats.	32/46(70%)	37/46(80%)	1/46(2%)	+3

```
Query  6    LFANGEDLFVRAGCPQGNERLESGLLSYGNDMDEFDTPFECGF-RF  140
            LFANG DL VRAGCP G ER+ESGLLS+G+DM   +TP+ECG  RF
Sbjct  218  LFANGRDLNVRAGCPNGIERIESGLLSFGSDMRRENTPYECGLERF  263
```

dimethyl sulfoniopropionate demethylase [Ruegeria sp. TM1040] Ambient CO_2

Sequence ID: ref|YP_613439.1| Length: 385 Number of Matches: 2

Range 1: 366 to 383 GenPept Graphics ▼ Next Match ▲ Previous Match

Score	Expect	Method	Identities	Positives	Gaps	Frame
35.0 bits(79)	0.004	Compositional matrix adjust.	16/18(89%)	16/18(88%)	0/18(0%)	-2

```
Query  56   LEVETPDGMRPALVREQF  3
            LEVETPDGMR ALVRE F
Sbjct  366  LEVETPDGMRTALVRENF  383
```

dimethyl sulfoniopropionate demethylase [Candidatus Pelagibacter sp. HTCC7211]

Sequence ID: ref|WP_008546106.1| Length: 381 Number of Matches: 1 Ambient CO_2

Range 1: 62 to 139 GenPept Graphics ▼ Next Match ▲ Previous Match

Score	Expect	Method	Identities	Positives	Gaps	Frame
113 bits(283)	3e-28	Composition-based stats.	51/78(65%)	63/78(80%)	0/78(0%)	+1

```
Query  1    VSCQRQVLINGLDAAALLQWMTPRDISKAKVGDCFYIPIIDPKAGLINDPVMLKLDEDRF  180
            VSCQRQV I G DAA L+Q +TPR I    +G CFYIP+++  AG+INDPV+LKLD+D F
Sbjct  62   VSCQRQVQICGPDAAKLIQKLTPRSIKDMTIGKCFYIPMLNENAGMINDPVLLKLDDDMF  121

Query  181  WLSIADSDVLLYAMGLAL  234
            W+SIADSD+LL+A GLAL
Sbjct  122  WISIADSDILLWAKGLAL  139
```

dimethyl sulfoniopropionate demethylase [Candidatus Pelagibacter ubique] High CO_2

Sequence ID: ref|WP_006997663.1| **Length:** 369 **Number of Matches:** 1

Range 1: 65 to 134 GenPept Graphics ▼ Next Match ▲ Previous Matc

Score	Expect	Method	Identities	Positives	Gaps	Frame
97.1 bits(240)	2e-22	Composition-based stats.	42/70(60%)	56/70(80%)	0/70(0%)	+3

```
Query  3    QVLINGLDAAALLQWMTPRDISKAKVGDCFYIPIIDPKAGLINDPVMLKLDEDRFWLSIA  182
            QV I+G D+A L+Q MT RD+SK+K+G C+Y PIID    LINDPV+LKLDE+++W+SIA
Sbjct  65   QVEISGKDSAELVQLMTCRDLSKSKIGRCYYCPIIDENGNLINDPVVLKLDENKWWISIA  124

Query  183  DSDVLLYCDG  212
            DSDV+ +  G
Sbjct  125  DSDVIFFAKG  134
```

aminomethyltransferase GcvT [Octadecabacter arcticus 238] Ambient CO_2

Sequence ID: ref|YP_007698959.1| **Length:** 384 **Number of Matches:** 1

Range 1: 17 to 103 GenPept Graphics ▼ Next Match ▲ Previous Match

Score	Expect	Method	Identities	Positives	Gaps	Frame
180 bits(456)	5e-53	Composition-based stats.	77/87(89%)	82/87(94%)	0/87(0%)	-3

```
Query  261  RKSPYSDAALRWGAKGFSVYNHMYIPRNFGDPIQNFWNLVNDAILCDVSVERQVEIKGPD  82
            RKSPYSDAALRWGAKGFSVYNHMYIPR+FG+P QNFWNL+N AILCDVSVERQVEIKGPD
Sbjct  17   RKSPYSDAALRWGAKGFSVYNHMYIPRDFGNPEQNFWNLINQAILCDVSVERQVEIKGPD  76

Query  81   AAKFVQYICCRDLSKCQIGQCKYVLIT  1
            AAKF QY+C RDLS C+IGQCKYVLIT
Sbjct  77   AAKFTQYLCSRDLSTCKIGQCKYVLIT  103
```

class V aminotransferase [Ruegeria pomeroyi DSS-3] Ambient CO_2

Sequence ID: ref|YP_167151.1| **Length:** 407 **Number of Matches:** 1

Range 1: 1 to 71 GenPept Graphics ▼ Next Match ▲ Previous Match

Score	Expect	Method	Identities	Positives	Gaps	Frame
134 bits(337)	1e-35	Compositional matrix adjust.	63/71(89%)	64/71(90%)	0/71(0%)	-2

```
Query  215  MKLDIDFVRSQFPAFSEPSLQGQAFFENAGGSYTCGAVIDRLTRFYTQRKVQPYAAYEAS  36
            M LDIDFVR QFPAF+EPSL GQAFFENAGGSYTC  VIDRLTRFYTQRKVQPYA YEAS
Sbjct  1    MALDIDFVRKQFPAFAEPSLHGQAFFENAGGSYTCQPVIDRLTRFYTQRKVQPYAPYEAS  60

Query  35   RLGGEEMDEAR  3
            RLGG EMDEAR
Sbjct  61   RLGGAEMDEAR  71
```

glycine cleavage system protein T [Loktanella vestfoldensis] Ambient CO_2

Sequence ID: ref|WP_007205555.1| **Length:** 379 **Number of Matches:** 1

Range 1: 70 to 147 GenPept Graphics ▼ Next Match ▲ Previous Match

Score	Expect	Method	Identities	Positives	Gaps	Frame
158 bits(399)	6e-45	Compositional matrix adjust.	74/78(95%)	77/78(98%)	0/78(0%)	+3

```
Query  3    GPDAAKFTQMLTCRDLSKMAVGQCKYILITNADGGILNDPILLRLAENHFWISLADSDIL  182
            GPDAA+FTQMLTCRDLSKMAVGQCKYILITNADGGILNDPILLRLAENHFWISLADSDIL
Sbjct  70   GPDAAQFTQMLTCRDLSKMAVGQCKYILITNADGGILNDPILLRLAENHFWISLADSDIL  129

Query  183  LWAQGVAVHSGLNVQIKE  236
            LWAQGVA+HSGLNV I+E
Sbjct  130  LWAQGVAIHSGLNVTIRE  147
```

DMSP demethylase transcriptional regulator [Thalassobacter arenae] High CO_2

Sequence ID: ref|WP_021100141.1| **Length:** 239 **Number of Matches:** 1

Range 1: 7 to 83 GenPept Graphics ▼ Next Match ▲ Previous Match

Score	Expect	Method	Identities	Positives	Gaps	Frame
125 bits(315)	1e-33	Compositional matrix adjust.	61/77(79%)	66/77(85%)	0/77(0%)	-3

```
Query  231  KKTDLSAQIAKDIRDSILSGALIVDERLPSEAELSDQFNVSRPTVREALKRLAAQNLIRT  52
            K  DLSAQIA  IRD+I++G LIVD RLPSEAEL++QFNVSRPTVREALKRLAAQ LIRT
Sbjct  7    KPADLSAQIAASIRDAIIAGELIVDARLPSEAELAEQFNVSRPTVREALKRLAAQALIRT  66

Query  51   QRGATGGAFVKRLRYED  1
            QRGATGGAFV  L Y D
Sbjct  67   QRGATGGAFVNHLTYPD  83
```

aminotransferase [Roseobacter denitrificans OCh 114] Ambient CO_2

Sequence ID: ref|YP_682561.1| **Length:** 407 **Number of Matches:** 1

Range 1: 173 to 235 GenPept Graphics ▼ Next Match ▲ Previous Match

Score	Expect	Method	Identities	Positives	Gaps	Frame
123 bits(308)	7e-32	Compositional matrix adjust.	57/63(90%)	60/63(95%)	0/63(0%)	+3

```
Query  3    VGHINPVTEITALAHASGAFVCVDGVSYAPHGFADVGALGPDIYLFSAYKTYGPHQGLMV  182
            VG +NPV EITALAHA+GAFVCVDGVSYAPHGF DVG+LGPDIYLFSAYKTYGPHQGLMV
Sbjct  173  VGEVNPVIEITALAHAAGAFVCVDGVSYAPHGFVDVGSLGPDIYLFSAYKTYGPHQGLMV  232

Query  183  IRR  191
            IRR
Sbjct  233  IRR  235
```

9.2.2 Ammonium transporters

ammonium transporter [Roseobacter sp. MED193]

Sequence ID: ref|WP_009810666.1| **Length:** 436 **Number of Matches:** 1

Range 1: 231 to 317 GenPept Graphics ▼ Next Match ▲ Previous Match

Score	Expect	Method	Identities	Positives	Gaps	Frame
133 bits(334)	6e-35	Compositional matrix adjust.	82/87(94%)	85/87(97%)	0/87(0%)	-1

```
Query  262  PGSNLALAXLGTFILWLGWFGFNGGSQLAMGTVGDVSDVSRIFantnmaaatgaiaALVL  83
            PGSNLALA LGTFILWLGWFGFNGGSQLAMGTVGDVSDVSRIFANTNMAAA GA+AAL+L
Sbjct  231  PGSNLALATLGTFILWLGWFGFNGGSQLAMGTVGDVSDVSRIFANTNMAAAAGAVAALIL  290

Query  82   TQLLYKKVDLTMVLNGALAGLVSITAE  2
            TQ+LYKKVDLTMVLNGALAGLVSITAE
Sbjct  291  TQVLYKKVDLTMVLNGALAGLVSITAE  317
```

ammonium transporter [gamma proteobacterium HTCC2207]

Sequence ID: ref|WP_007233085.1| **Length:** 436 **Number of Matches:** 1

Range 1: 145 to 221 GenPept Graphics ▼ Next Match ▲ Previous Match

Score	Expect	Method	Identities	Positives	Gaps	Frame
123 bits(309)	1e-31	Compositional matrix adjust.	72/77(94%)	74/77(96%)	0/77(0%)	-1

```
Query  232  AFAERMRFSAMLLFSALWLVVVYAPITHWVWDGGWLGEMGLLDFAGGTVVHITagvgalv  53
            AFAERMRFSAMLLFSALWLV VY+PITHWVW GGWLGEMGLLDFAGGTVVHITAGVGALV
Sbjct  145  AFAERMRFSAMLLFSALWLVAVYSPITHWVWGGGWLGEMGLLDFAGGTVVHITAGVGALV  204

Query  52   aalvlGNRRGFPNQAMP  2
            AALVLGNR+GFP QAMP
Sbjct  205  AALVLGNRKGFPQQAMP  221
```

ammonium transporter [Owenweeksia hongkongensis DSM 17368]

Sequence ID: ref|YP_004990125.1| **Length:** 425 **Number of Matches:** 2

Range 1: 299 to 347 GenPept Graphics ▼ Next Match ▲ Previous Match

Score	Expect	Method	Identities	Positives	Gaps	Frame
77.0 bits(188)	2e-25	Compositional matrix adjust.	35/49(71%)	44/49(89%)	0/49(0%)	-3

```
Query  272  AITPAAGFVNIGQSMFIGFIAAIISNYAIHLKNKTNVDDTLDVFQATGL  126
            AITPAAGFVNIGQS+ IGFIA+IISN+ IHL++K+ +DDTLDVF + G+
Sbjct  299  AITPAAGFVNIGQSVLIGFIASIISNWMIHLQHKSGIDDTLDVFPSHGI  347
```

ammonium transporter [Rhodobacteraceae bacterium HTCC2083]

Sequence ID: ref|WP_009828878.1| **Length:** 440 **Number of Matches:** 1

Range 1: 395 to 440 GenPept Graphics ▼ Next Match ▲ Previous Match

Score	Expect	Method	Identities	Positives	Gaps	Frame
86.3 bits(212)	4e-18	Compositional matrix adjust.	42/46(91%)	44/46(95%)	0/46(0%)	-2

```
Query  247  FAFGVSAVVWFILKATVGIRVSEEAEIMGLDTTELGMEAYPEFSKG  110
            FAFG+SA+VW ILKATVGIRVSEEAEI GLDTTELGMEAYPEFSKG
Sbjct  395  FAFGISAIVWSILKATVGIRVSEEAEISGLDTTELGMEAYPEFSKG  440
```

ammonium transporter [Croceibacter atlanticus HTCC2559]

Sequence ID: ref|YP_003716094.1| **Length:** 427 **Number of Matches:** 1

Range 1: 332 to 376 GenPept Graphics ▼ Next Match ▲ Previous Match

Score	Expect	Method	Identities	Positives	Gaps	Frame
73.9 bits(180)	7e-14	Composition-based stats.	33/45(73%)	40/45(88%)	0/45(0%)	-3

```
Query  177  LKNKTNVDDTLDVFPSHGVGGIVGMLLTAVFAKQVGLIYGQTDTF  43
            ++ + N+DDTLDVFPSHGVGGIVGM+LT V AK VGLIYG+T+TF
Sbjct  332  VQKQCNIDDTLDVFPSHGVGGIVGMILTGVLAKDVGLIYGETETF  376
```

ammonium transporter [marine gamma proteobacterium HTCC2080]

Sequence ID: ref|WP_007235465.1| **Length:** 435 **Number of Matches:** 1

Range 1: 1 to 71 GenPept Graphics ▼ Next Match ▲ Previous Match

Score	Expect	Method	Identities	Positives	Gaps	Frame
86.3 bits(212)	4e-18	Compositional matrix adjust.	62/71(87%)	65/71(91%)	0/71(0%)	-3

```
Query  215  MHVLRKsaflmlsalllpapalaaeisaADTSWLLTATALVLFMTLPGLSLFYGGLVRVR  36
            MHV RKSAF+ L A LLP PALA EIS+ADT+WLLTATALVLFMTLPGLSLFYGGLVRVR
Sbjct  1    MHVTRKSAFIALCAFLLPLPALAGEISSADTAWLLTATALVLFMTLPGLSLFYGGLVRVR  60

Query  35   NVLSVLMQCFA  3
            NVLSVLMQCFA
Sbjct  61   NVLSVLMQCFA  71
```

ammonium transporter [Phaeobacter gallaeciensis DSM 17395 = CIP 105210]

Sequence ID: ref|YP_006574316.1| **Length:** 446 **Number of Matches:** 1

Range 1: 64 to 149 GenPept Graphics ▼ Next Match ▲ Previous Match

Score	Expect	Method	Identities	Positives	Gaps	Frame
96.7 bits(239)	9e-22	Compositional matrix adjust.	75/86(87%)	80/86(93%)	0/86(0%)	-1

```
Query  258  LEAGLVRGKNVAMQLTKNMGLFSLAAIFYYLIGYNLMYPLGTWSIEgvlsgvwgvgvLEa  79
            LEAGLVR KNV MQLTKN+ LFSLAAIFYYLIGYNLMYPLGTWSIEGVLSGVWG GVLEA
Sbjct  64   LEAGLVRSKNVTMQLTKNVALFSLAAIFYYLIGYNLMYPLGTWSIEGVLSGVWGPGVLEA  123

Query  78   vgvtadaaddygyaatGSDFFFQLMF  1
            VG+T++ ADDY YA+TGSDFFFQLMF
Sbjct  124  VGITSEQADDYSYASTGSDFFFQLMF  149
```

ammonium transporter [Phaeobacter gallaeciensis]

Sequence ID: ref|WP_019296213.1| **Length:** 393 **Number of Matches:** 2

Range 1: 322 to 387 GenPept Graphics ▼ Next Match ▲ Previous Match

Score	Expect	Method	Identities	Positives	Gaps	Frame
55.5 bits(132)	2e-10	Compositional matrix adjust.	47/66(71%)	55/66(83%)	0/66(0%)	+1

```
Query  40   GSFGTIMIAVFGAGAWVAQIGSlvivgiftvvvtvvlvklvslvtplRVSEEDEYTGLDL  219
            G FGTIMIA+FGAGAW AQ+G+LVIVGIFTVVVT+ LVK+ +L+T LRV  E E  GLDL
Sbjct  322  GIFGTIMIAIFGAGAWAAQLGALVIVGIFTVVVTIALVKISALITSLRVDLESETNGLDL  381

Query  220  AAHGER  237
            + HGER
Sbjct  382  SVHGER  387
```

ammonium transporter [Roseovarius nubinhibens]

Sequence ID: ref|WP_009813814.1| **Length:** 441 **Number of Matches:** 1

Range 1: 136 to 204 GenPept Graphics ▼ Next Match ▲ Previous Match

Score	Expect	Method	Identities	Positives	Gaps	Frame
135 bits(340)	4e-36	Compositional matrix adjust.	65/69(94%)	65/69(94%)	0/69(0%)	+1

```
Query  10   RFFFQLMFCAATASIVSGALAERIKLWPFLAFVIVLVAVIYPIQASWKWGGGFLDAMGFQ  189
            FFFQLMFCAATASIVSGALAERIKLWPFLAF IVL AVIYPIQASWKWGGGFLDA GFQ
Sbjct  136  DFFFQLMFCAATASIVSGALAERIKLWPFLAFTIVLTAVIYPIQASWKWGGGFLDAAGFQ  195

Query  190  DFAGSTVVH  216
            DFAGSTVVH
Sbjct  196  DFAGSTVVH  204
```

ammonium transporter [marine gamma proteobacterium HTCC2080]

Sequence ID: ref|WP_007235465.1| **Length:** 435 **Number of Matches:** 1

Score	Expect	Method	Identities	Positives	Gaps	Frame
139 bits(351)	2e-37	Compositional matrix adjust.	83/85(98%)	84/85(98%)	0/85(0%)	+3

```
Query  3    LVTHLSAACGSLAWMTMEWLRHGKPSVLGIVTGMVAGLGTITpasgsvgpaaavvIGLTA  182
            LVTHLSAACGSLAWM MEW+RHGKPSVLGIVTGMVAGLGTITPASGSVGPAAAVVIGLTA
Sbjct  257  LVTHLSAACGSLAWMAMEWVRHGKPSVLGIVTGMVAGLGTITPASGSVGPAAAVVIGLTA  316

Query  183  GVVCYFATITLKNRLKIDDSLDVFP  257
            GVVCYFATITLKNRLKIDDSLDVFP
Sbjct  317  GVVCYFATITLKNRLKIDDSLDVFP  341
```

ammonium transporter [Cytophaga aurantiaca]

Sequence ID: ref|WP_018341692.1| **Length:** 414 **Number of Matches:** 1

Range 1: 70 to 119 GenPept Graphics ▼ Next Match ▲ Previous Match

Score	Expect	Method	Identities	Positives	Gaps	Frame
84.3 bits(207)	5e-18	Compositional matrix adjust.	42/50(84%)	45/50(90%)	0/50(0%)	-3

```
Query  151  FGIAYGNSNGWFAFDTGITTKDLGLGLTVSNKLFWFIQLGFAIAAISIVS  2
            FGIAYG SNGW+AFD GI   D+GLGLTVSNKLFWFIQ+GFAIAAISIVS
Sbjct  70   FGIAYGKSNGWWAFDFGIPEGDMGLGLTVSNKLFWFIQMGFAIAAISIVS  119
```

9.2.3 Carbon monoxide dehydrogenase

carbon monoxide dehydrogenase [Oxalobacteraceae bacterium IMCC9480] Ambient CO_2

Sequence ID: ref|WP_009665216.1| Length: 798 Number of Matches: 1

Range 1: 640 to 690 GenPept Graphics ▼ Next Match ▲ Previous Match

Score	Expect	Method	Identities	Positives	Gaps	Frame
87.4 bits(215)	3e-18	Composition-based stats.	37/51(73%)	42/51(82%)	0/51(0%)	-1

```
Query  189  HYRVTDFPFVFTNGAMAAHVEVDTATGFVKVLHFWAVEDCGRVINPLLVDE  37
            HY   DFPFVFTNG  A++VEVD  TGFVK+L  WAVEDCGR+INP+LVDE
Sbjct  640  HYAQRDFPFVFTNGVQASYVEVDVETGFVKLLKHWAVEDCGRIINPMLVDE  690
```

carbon monoxide dehydrogenase [Roseobacter sp. SK209-2-6] Ambient CO_2

Sequence ID: ref|WP_008206629.1| Length: 164 Number of Matches: 1

Range 1: 3 to 81 GenPept Graphics ▼ Next Match ▲ Previous Match

Score	Expect	Method	Identities	Positives	Gaps	Frame
148 bits(373)	3e-43	Compositional matrix adjust.	70/79(89%)	73/79(92%)	0/79(0%)	-3

```
Query  237  KKKHVTLNVNGKTEEFLAEPRELLIYTLRERLNITGPHIGCETSHCGACTVTINGKSVKS  58
            KK H+ L VNGK EEF AEPRELLIYTLRERLNITGPHIGCETSHCGACTVTINGKSVKS
Sbjct  3    KKMHIKLKVNGKDEEFFAEPRELLIYTLRERLNITGPHIGCETSHCGACTVTINGKSVKS  62

Query  57   CTMFAVQAEGAEITTIEGI  1
            CTMFA QA+GAE+TTIEGI
Sbjct  63   CTMFAAQADGAEVTTIEGI  81
```

carbon monoxide dehydrogenase [Sulfitobacter sp. EE-36] Ambient CO_2

Sequence ID: ref|WP_005849705.1| Length: 174 Number of Matches: 1

Range 1: 49 to 134 GenPept Graphics ▼ Next Match ▲ Previous Match

Score	Expect	Method	Identities	Positives	Gaps	Frame
112 bits(280)	5e-29	Compositional matrix adjust.	71/86(83%)	77/86(89%)	0/86(0%)	+1

```
Query  1    VQKVGPVKATFKGEVQITDLVPDTSMRIEgagkggaagfakggaDVRLVATEGGCELSYD  180
            VQKVGPVKATFKG+V +TD+VPD S++I G GKGGAAGFAKG ADV L A +GG ELSYD
Sbjct  49   VQKVGPVKATFKGQVTMTDMVPDQSIKISGEGKGGAAGFAKGEADVTLAAVDGGTELSYD  108

Query  181  VEAKVGGKLAQLGSRIIDGFAKKMAD  258
            VEAKVGGKLAQLGSRIIDGFAKKMAD
Sbjct  109  VEAKVGGKLAQLGSRIIDGFAKKMAD  134
```

dehydrogenase [Roseobacter denitrificans OCh 114] Ambient CO_2

Sequence ID: ref|YP_682064.1| Length: 765 Number of Matches: 1

Range 1: 63 to 145 GenPept Graphics ▼ Next Match ▲ Previous Match

Score	Expect	Method	Identities	Positives	Gaps	Frame
110 bits(275)	4e-26	Compositional matrix adjust.	53/83(64%)	66/83(79%)	0/83(0%)	+1

```
Query  1    VHAVYVAGDLETAGLKLGMRGAVMKNRDGSDGASPERPILAKSKLRFVGEPVAMILADTL  180
            VHAV  A DL+ AG+   M    +KNRDGS GA+P RPILA+ ++RFVGEPVA I+A+TL
Sbjct  63   VHAVLTADDLKAAGITKSMSAQTVKNRDGSMGAAPRRPILAEERMRFVGEPVAFIVAETL  122

Query  181  SQARDAAEMITLSYDDLPAKMNI  249
             QARDAAE+I LSY++LPAKM+I
Sbjct  123  DQARDAAELIDLSYEELPAKMDI  145
```

carbon monoxide dehydrogenase [Roseobacter sp. SK209-2-6] Ambient CO_2

Sequence ID: ref|WP_008206634.1| Length: 382 Number of Matches: 1

Range 1: 167 to 238 GenPept Graphics ▼ Next Match ▲ Previous Match

Score	Expect	Method	Identities	Positives	Gaps	Frame
120 bits(300)	1e-30	Compositional matrix adjust.	58/72(81%)	63/72(87%)	0/72(0%)	+3

```
Query  3    NHNIIWGTICFAGAVCSVHFLAMAGTNFAPEPAIAEFGPSMSNETLALGVIFFSFVIFGA  182
            N NI+ GT+CFA AVC+VHFLAM GTNF   P++AEFGP MSNETLALGVIFFSFVIFG
Sbjct  167  NRNILLGTLCFAIAVCAVHFLAMTGTNFVAVPSLAEFGPVMSNETLALGVIFFSFVIFGT  226

Query  183  CLWVSVTYLVVA  218
            CLWVSVTYLVVA
Sbjct  227  CLWVSVTYLVVA  238
```

carbon monoxide dehydrogenase, large subunit [Jannaschia sp. CCS1] — Ambient CO_2

Sequence ID: ref|YP_510037.1| **Length:** 808 **Number of Matches:** 1

Range 1: 341 to 420 GenPept Graphics — Next Match Previous Match

Score	Expect	Method	Identities	Positives	Gaps	Frame
169 bits(427)	5e-47	Compositional matrix adjust.	79/80(99%)	80/80(100%)	0/80(0%)	-2

```
Query  242  FDACADPTKFPAGFMNICTGSYDIPTAYLEVDGVYTNKAPGGVSYRCSFRVTEAVYFIER  63
            FDACADPTKFPAGFMNICTGSYDIPTAYLEVDGVYTNKAPGGVSYRCSFRVTEAVYFIER
Sbjct  341  FDACADPTKFPAGFMNICTGSYDIPTAYLEVDGVYTNKAPGGVSYRCSFRVTEAVYFIER  400

Query  62   MIEVLAIELNMDSAELRRIN  3
            MIEVLAIELNMD+AELRRIN
Sbjct  401  MIEVLAIELNMDAAELRRIN  420
```

carbon-monoxide dehydrogenase [Sulfitobacter sp. EE-36] — Ambient CO_2

Sequence ID: ref|WP_005853007.1| **Length:** 787 **Number of Matches:** 1

Range 1: 163 to 225 GenPept Graphics — Next Match Previous Match

Score	Expect	Method	Identities	Positives	Gaps	Frame
120 bits(300)	8e-30	Compositional matrix adjust.	54/63(86%)	60/63(95%)	0/63(0%)	+3

```
Query  3    LCYDWGFVEENKAATDKAFLDAAHVTSLELVNNRLVANPMEPRVALGEYSQGTDEHTLYT  182
            LCYDWGFVEENKAA DKAF DAAHVT+LELVNNRLVANPMEPRVA+G+Y++GT +HTLYT
Sbjct  163  LCYDWGFVEENKAAVDKAFDDAAHVTTLELVNNRLVANPMEPRVAVGDYARGTGDHTLYT  222

Query  183  TSQ  191
            TSQ
Sbjct  223  TSQ  225
```

carbon-monoxide dehydrogenase [Sagittula stellata] — Ambient CO_2

Sequence ID: ref|WP_005860860.1| **Length:** 274 **Number of Matches:** 1

Range 1: 85 to 159 GenPept Graphics — Next Match Previous Match

Score	Expect	Method	Identities	Positives	Gaps	Frame
115 bits(288)	2e-29	Compositional matrix adjust.	63/75(84%)	69/75(92%)	0/75(0%)	+1

```
Query  4    HATVAVEatsypalaataaHIGDPAVRNRGTIGGSLANNDPSACYPAAALASGATIVSNS  183
            HATVA EA +YPALAA A+ IGDPAVRNRGTIGGSLANNDPSACYPAAAL +GATIV+N+
Sbjct  85   HATVAAEAGAYPALAALASQIGDPAVRNRGTIGGSLANNDPSACYPAAALGTGATIVTNT  144

Query  184  REILADDFFQGMFTT  228
            REI ADD+FQGMFTT
Sbjct  145  REIAADDYFQGMFTT  159
```

carbon monoxide dehydrogenase subunit G [Jannaschia sp. CCS1] — Ambient CO_2

Sequence ID: ref|YP_510032.1| **Length:** 151 **Number of Matches:** 1

Range 1: 4 to 65 GenPept Graphics — Next Match Previous Match

Score	Expect	Method	Identities	Positives	Gaps	Frame
125 bits(315)	6e-35	Compositional matrix adjust.	59/62(95%)	61/62(98%)	0/62(0%)	-3

```
Query  188  SDEIVINAPKDRVYAALNDPEILRLCIPGCEELIKHSDTELEAKVVLKVGPVKARFNGDV  9
            +DEI+INAPKDRVYAALNDPEILR CIPGCEELIKHSDTELEAKVVLKVGPVKARFNGDV
Sbjct  4    ADEIIINAPKDRVYAALNDPEILRQCIPGCEELIKHSDTELEAKVVLKVGPVKARFNGDV  63

Query  8    QL  3
            QL
Sbjct  64   QL  65
```

carbon monoxide dehydrogenase [Sulfitobacter sp. EE-36] — Ambient CO_2

Sequence ID: ref|WP_005849705.1| **Length:** 174 **Number of Matches:** 1

Range 1: 85 to 144 GenPept Graphics — Next Match Previous Match

Score	Expect	Method	Identities	Positives	Gaps	Frame
108 bits(269)	1e-27	Compositional matrix adjust.	54/60(90%)	55/60(91%)	0/60(0%)	-3

```
Query  243  AGFAKGGADVRLVATEGGCELSYDVEAKVGGKLAQLGSRIIDGFAKKMADQFFNNLQETL  64
            AGFAKG ADV L A +GG ELSYDVEAKVGGKLAQLGSRIIDGFAKKMADQFFNNLQETL
Sbjct  85   AGFAKGEADVTLAAVDGGTELSYDVEAKVGGKLAQLGSRIIDGFAKKMADQFFNNLQETL  144
```

carbon monoxide dehydrogenase form II large subunit [Stappia sp. M8] High CO_2

Sequence ID: gb|AAP75596.1| Length: 407 Number of Matches: 1

Range 1: 149 to 217 GenPept Graphics ▼ Next Match ▲ Previous Matc

Score	Expect	Method	Identities	Positives	Gaps	Frame
110 bits(274)	7e-27	Compositional matrix adjust.	54/69(78%)	59/69(85%)	0/69(0%)	+3

```
Query  3    SFPHQTPVIMAYDSGDFDANLKQAQEAADVAGFAARKAEAASRGKLRGMGYSNYIEACGI  182
            SFPHQTPVIM YD+GD+DA L  A +AAD  GFAARKAEAASRGKLRG+G S YIEACGI
Sbjct  149  SFPHQTPVIMCYDAGDYDATLDAALKAADYDGFAARKAEAASRGKLRGIGLSCYIEACGI  208

Query  183  APSAAVEAL  209
            APSAAV +L
Sbjct  209  APSAAVGSL  217
```

carbon monoxide dehydrogenase form I large subunit [Ruegeria sp. WHOI JT-08] High CO_2

Sequence ID: gb|AAW88347.1| Length: 402 Number of Matches: 1

Range 1: 287 to 367 GenPept Graphics ▼ Next Match ▲ Previous Match

Score	Expect	Method	Identities	Positives	Gaps	Frame
160 bits(406)	1e-45	Compositional matrix adjust.	78/81(96%)	81/81(100%)	0/81(0%)	+1

```
Query  1    YGSRSTPVAGAATAMAGRKIRAKAQMIAAYLLEVHDNDVEFDVDRFIVKGAPEKFKTMKE  180
            YGSRSTPVAGAATAMAGRKIRAKAQMIAAYLLEVHD+DVEFDVDRF+VKGAPEKFKT+KE
Sbjct  287  YGSRSTPVAGAATAMAGRKIRAKAQMIAAYLLEVHDDDVEFDVDRFVVKGAPEKFKTIKE  346

Query  181  IAFAAYNQAIPGIEPGLEAVS  243
            IAFAAYNQAIPGIEPGLEAVS
Sbjct  347  IAFAAYNQAIPGIEPGLEAVS  367
```

carbon monoxide dehydrogenase [Roseobacter sp. MED193] High CO_2

Sequence ID: ref|WP_009810137.1| Length: 805 Number of Matches: 3

Range 1: 260 to 297 GenPept Graphics ▼ Next Match ▲ Previous Match

Score	Expect	Method	Identities	Positives	Gaps	Frame
80.1 bits(196)	2e-31	Composition-based stats.	35/38(92%)	37/38(97%)	0/38(0%)	+2

```
Query  2    SPDIGGGFGNKVGAYPGYVCSVVASIVTGKPVKWIEDR  115
            SPDIGGGFGNKVG YPGYVCS+VASIVTGKPVKW+EDR
Sbjct  260  SPDIGGGFGNKVGVYPGYVCSIVASIVTGKPVKWVEDR  297
```

9.2.4 Photoreaction centre subunits

Photosynthetic reaction center cytochrome C subunit [Roseobacter sp. AzwK-3b]

Sequence ID: ref|WP_007814237.1| **Length:** 372 **Number of Matches:** 1

Range 1: 236 to 313 GenPept Graphics ▼ Next Match ▲ Previous Match

Score	Expect	Method	Identities	Positives	Gaps	Frame
130 bits(326)	3e-34	Compositional matrix adjust.	59/78(76%)	63/78(80%)	0/78(0%)	-3

```
Query  235  IAVHSLESREDGVPGQDGYASIQQTERTYSLMNYFSNSLGVNCVFCHNSRAFYDGGQNTP  56
            I VH LESR  G+PG+DGY  IQQ ERTYSLMNY SNSLGVNCVFCHNSRAFYDG Q TP
Sbjct  236  IGVHDLESRVAGIPGEDGYPGIQQAERTYSLMNYVSNSLGVNCVFCHNSRAFYDGAQVTP  295

Query  55   QWSTASLGIAMVQSLNTD  2
            QW+T SLGI MV  +N D
Sbjct  296  QWATESLGIQMVLEMNND  313
```

photosynthetic reaction center M subunit, partial [Loktanella sp. RCC2642]

Sequence ID: gb|AEV66157.1| **Length:** 74 **Number of Matches:** 1

Range 1: 3 to 73 GenPept Graphics ▼ Next Match ▲ Previous Match

Score	Expect	Method	Identities	Positives	Gaps	Frame
142 bits(357)	5e-42	Compositional matrix adjust.	69/71(97%)	70/71(98%)	0/71(0%)	+2

```
Query  2    NPFHALSIAFLYGSALLFAMHGATILAVSRYGGEREIEQIVDRGTASERAALFWRWTMGF  181
            NPFHALSIAFLYGS LLFAMHGATILAVSR+GGEREIEQIVDRGTASERAALFWRWTMGF
Sbjct  3    NPFHALSIAFLYGSVLLFAMHGATILAVSRFGGEREIEQIVDRGTASERAALFWRWTMGF  62

Query  182  NATMEGIHRWA  214
            NATMEGIHRWA
Sbjct  63   NATMEGIHRWA  73
```

photosynthetic reaction center cytochrome c subunit PufC [Roseobacter litoralis Och 149]

Sequence ID: ref|YP_004716611.1| **Length:** 371 **Number of Matches:** 1

Range 1: 1 to 78 GenPept Graphics ▼ Next Match ▲ Previous Match

Score	Expect	Method	Identities	Positives	Gaps	Frame
137 bits(346)	4e-37	Compositional matrix adjust.	63/78(81%)	69/78(88%)	0/78(0%)	+3

```
Query  33   MLPKWFDKWNADNPTNVFGPAILVGVLGGAIFVAVLLVTWGNPAQTASMQTGPRGTGMSV  212
            M PKWFDKWNADNPTN+FGPAILVGVLG A+F A  +V+ GNPAQTASMQTGPRGTGMSV
Sbjct  1    MFPKWFDKWNADNPTNIFGPAILVGVLGVAVFGAAAIVSIGNPAQTASMQTGPRGTGMSV  60

Query  213  PEFDVARLAPDPTIDAYY  266
            PEF+VAR  PDPTI+ YY
Sbjct  61   PEFNVARFTPDPTIEGYY  78
```

Photosynthetic reaction center cytochrome C subunit [marine gamma proteobacterium HTCC2080]

Sequence ID: ref|WP_007234725.1| **Length:** 382 **Number of Matches:** 1

Range 1: 224 to 303 GenPept Graphics ▼ Next Match ▲ Previous Match

Score	Expect	Method	Identities	Positives	Gaps	Frame
179 bits(454)	6e-53	Compositional matrix adjust.	80/80(100%)	80/80(100%)	0/80(0%)	-3

```
Query  241  LPNGNRSSVKQTEYIYSLMMHFSDSLGVNCTHCHNTRAFYDWEQSSPARVRAWHGIRMVR  62
            LPNGNRSSVKQTEYIYSLMMHFSDSLGVNCTHCHNTRAFYDWEQSSPARVRAWHGIRMVR
Sbjct  224  LPNGNRSSVKQTEYIYSLMMHFSDSLGVNCTHCHNTRAFYDWEQSSPARVRAWHGIRMVR  283

Query  61   EMNTKYVNQTTDWLPDHRKG  2
            EMNTKYVNQTTDWLPDHRKG
Sbjct  284  EMNTKYVNQTTDWLPDHRKG  303
```

photosynthetic complex assembly protein [Roseobacter denitrificans OCh 114]

Sequence ID: ref|YP_680553.1| **Length:** 212 **Number of Matches:** 2

Range 1: 17 to 48 GenPept Graphics ▼ Next Match ▲ Previous Match

Score	Expect	Method	Identities	Positives	Gaps	Frame
40.4 bits(93)	8e-07	Compositional matrix adjust.	17/32(53%)	24/32(75%)	0/32(0%)	-1

```
Query  97   KAPKGEDILWRGKPSTLALARDALNLNWIIGY  2
            K PKGE+ILW+G+P    LA ++LN+ W+ GY
Sbjct  17   KPPKGENILWQGRPDWWRLAVESLNVKWVAGY  48
```

photosynthetic reaction center subunit L [Roseovarius sp. TM1035]

Sequence ID: ref|WP_008280384.1| **Length:** 279 **Number of Matches:** 1

Range 1: 166 to 248 GenPept Graphics ▼ Next Match ▲ Previous Match

Score	Expect	Method	Identities	Positives	Gaps	Frame
134 bits(338)	1e-36	Compositional matrix adjust.	77/83(93%)	81/83(97%)	0/83(0%)	-2

```
Query  250  IHFHYNPAHMlavtlfftttialaLHGGLILSAANPEKGEEAKTPDHEDTFFRDYIGYSV  71
            +HFHYNPAHMLAVTLFFTTT ALALHGGLILSAANPEKGEE KTPDHEDTFFRD+IGYSV
Sbjct  166  LHFHYNPAHMLAVTLFFTTTFALALHGGLILSAANPEKGEEMKTPDHEDTFFRDFIGYSV  225

Query  70   GTLGIHRVGYLLALNAVFFSAVC  2
            GTLGIHRVG+LLA+NAVFFSAVC
Sbjct  226  GTLGIHRVGFLLAINAVFFSAVC  248
```

Photosynthetic reaction center cytochrome C subunit [marine gamma proteobacterium HTCC2080]

Sequence ID: ref|WP_007234725.1| **Length:** 382 **Number of Matches:** 1

Range 1: 258 to 323 GenPept Graphics ▼ Next Match ▲ Previous Match

Score	Expect	Method	Identities	Positives	Gaps	Frame
105 bits(263)	2e-25	Compositional matrix adjust.	44/66(67%)	54/66(81%)	0/66(0%)	-2

```
Query  245  NSRAFGSWEESNSERVQAWHGQQMVKEMNNAYINPTNDWLPAHRQGPLGDAQKVNCATCH  66
            N+RAF  WE+S+  RV+AWHG +MV+EMN  Y+N T DWLP HR+GP+GD  KVNCATCH
Sbjct  258  NTRAFYDWEQSSPARVRAWHGIRMVREMNTKYVNQTTDWLPDHRKGPMGDPLKVNCATCH  317

Query  65   QGAYQP  48
            QGAY+P
Sbjct  318  QGAYKP  323
```

photosynthetic reaction center cytochrome c subunit PufC [Roseobacter litoralis Och 149]

Sequence ID: ref|YP_004716611.1| **Length:** 371 **Number of Matches:** 2

Range 1: 122 to 161 GenPept Graphics ▼ Next Match ▲ Previous Match

Score	Expect	Method	Identities	Positives	Gaps	Frame
76.3 bits(186)	6e-23	Composition-based stats.	32/40(80%)	36/40(90%)	0/40(0%)	+1

```
Query  82   SPEEGCAYCHGDVDLEEYGSDKIYTKVVARRMIQMTQSIN  201
            SPEEGC YCHG+ DLE YG+D +YTKVVARRMIQMTQ+IN
Sbjct  122  SPEEGCVYCHGEGDLETYGADDLYTKVVARRMIQMTQNIN  161
```

photosynthetic reaction center subunit M [Thalassiobium sp. R2A62]

Sequence ID: ref|WP_009159933.1| **Length:** 308 **Number of Matches:** 1

Range 1: 270 to 308 GenPept Graphics ▼ Next Match ▲ Previous Match

Score	Expect	Method	Identities	Positives	Gaps	Frame
49.7 bits(117)	2e-05	Compositional matrix adjust.	38/39(97%)	39/39(100%)	0/39(0%)	+3

```
Query  3    AWWFAVlttltggigilltgtVVDNWYVWAQDHGYAPLD  119
            AWWFAVLTTLTGGIGILLTGTVVDNW+VWAQDHGYAPLD
Sbjct  270  AWWFAVLTTLTGGIGILLTGTVVDNWFVWAQDHGYAPLD  308
```

photosynthetic reaction center subunit L [Thalassiobium sp. R2A62]

Sequence ID: ref|WP_009159999.1| **Length:** 276 **Number of Matches:** 1

Range 1: 152 to 233 GenPept Graphics ▼ Next Match ▲ Previous Match

Score	Expect	Method	Identities	Positives	Gaps	Frame
155 bits(393)	8e-45	Compositional matrix adjust.	80/82(98%)	81/82(98%)	0/82(0%)	+2

```
Query  2    FSHLDWVNNVGYAYGNFHYNPAHMIAItfffttCFALALHGSLVLSAVNPGKGKTIGTPD  181
            FSHLDWVNNVGYAYGNFHYNPAHMIAITFFFTTCFALALHGSLVLSAVNPG+GKTI TPD
Sbjct  152  FSHLDWVNNVGYAYGNFHYNPAHMIAITFFFTTCFALALHGSLVLSAVNPGRGKTIATPD  211

Query  182  HEDTYFRDLIGYSIGPLGIHRL  247
            HEDTYFRDLIGYSIGPLGIHRL
Sbjct  212  HEDTYFRDLIGYSIGPLGIHRL  233
```

photosynthetic reaction center M subunit [Roseobacter sp. B11]

Sequence ID: gb|ABX83042.1| **Length:** 238 **Number of Matches:** 1

Range 1: 125 to 209 GenPept Graphics ▼ Next Match ▲ Previous Match

Score	Expect	Method	Identities	Positives	Gaps	Frame
129 bits(324)	8e-35	Compositional matrix adjust.	75/85(88%)	80/85(94%)	0/85(0%)	-2

```
Query  256  VGCVTWWLRTYQLAQQHKMGKHlawafaallwlilvlglFRPVLMGSWSEAVPYGIFPHL  77
            V  +TWWLR+Y LAQQHKMGKH+AWAFA+ +WL LVLGLFRPVLMGSWSEAVPYGIFPHL
Sbjct  125  VSVMTWWLRSYLLAQQHKMGKHVAWAFASAIWLFLVLGLFRPVLMGSWSEAVPYGIFPHL  184

Query  76   DWTTAFSIRYGNLYYNPFHCLSIVF  2
            DWTTAFSIRYGNLYYNPFHCLSIVF
Sbjct  185  DWTTAFSIRYGNLYYNPFHCLSIVF  209
```

photosynthetic reaction center subunit M [Roseobacter denitrificans OCh 114]

Sequence ID: ref|YP_680524.1| **Length:** 331 **Number of Matches:** 1

Range 1: 274 to 331 GenPept Graphics ▼ Next Match ▲ Previous Match

Score	Expect	Method	Identities	Positives	Gaps	Frame
79.7 bits(195)	5e-16	Compositional matrix adjust.	56/58(97%)	58/58(100%)	0/58(0%)	+2

```
Query  2    WWFAvltpitggigilltgtvvDNWFIWAQEHNFAPMYDGAYGYEDYGSYEAFIGKEN  175
            WWFAVLTPITGGIGILLTGTVVDNWFIWAQEH+FAPMYDG+YGYEDYGSYEAFIGKEN
Sbjct  274  WWFAVLTPITGGIGILLTGTVVDNWFIWAQEHHFAPMYDGSYGYEDYGSYEAFIGKEN  331
```

photosynthetic reaction center subunit L [Thalassiobium sp. R2A62]

Sequence ID: ref|WP_009159999.1| **Length:** 276 **Number of Matches:** 2

Range 1: 68 to 111 GenPept Graphics ▼ Next Match ▲ Previous Match

Score	Expect	Method	Identities	Positives	Gaps	Frame
90.9 bits(224)	7e-26	Compositional matrix adjust.	40/44(91%)	44/44(100%)	0/44(0%)	-3

```
Query  134  NPPAIEVGLGVAPLAEGGLWQAITICATFAFLSWMMREVEICRK  3
            NPP++EVGLG+APLAEGGLWQAIT+CATFAFLSWMMREVEICRK
Sbjct  68   NPPSLEVGLGIAPLAEGGLWQAITVCATFAFLSWMMREVEICRK  111
```

photosynthetic reaction center subunit M [marine gamma proteobacterium HTCC2080]

Sequence ID: ref|WP_007234726.1| **Length:** 324 **Number of Matches:** 1

Range 1: 220 to 298 GenPept Graphics ▼ Next Match ▲ Previous Match

Score	Expect	Method	Identities	Positives	Gaps	Frame
124 bits(312)	1e-32	Compositional matrix adjust.	79/79(100%)	79/79(100%)	0/79(0%)	+3

```
Query  3    GATILAVSRYGGDREIDQVTDIGTAGERSMLYWRWCMGFNASMESIHRWAWWFAvltvit  182
            GATILAVSRYGGDREIDQVTDIGTAGERSMLYWRWCMGFNASMESIHRWAWWFAVLTVIT
Sbjct  220  GATILAVSRYGGDREIDQVTDIGTAGERSMLYWRWCMGFNASMESIHRWAWWFAVLTVIT  279

Query  183  ggigilltgtvvENWYLWG  239
            GGIGILLTGTVVENWYLWG
Sbjct  280  GGIGILLTGTVVENWYLWG  298
```

possible photosynthetic co [Roseobacter sp. AzwK-3b] **High CO_2**

Sequence ID: ref|WP_007814221.1| **Length:** 212 **Number of Matches:** 1

Range 1: 100 to 179 GenPept Graphics ▼ Next Match ▲ Previous Match

Score	Expect	Method	Identities	Positives	Gaps	Frame
112 bits(280)	8e-29	Compositional matrix adjust.	52/80(65%)	62/80(77%)	0/80(0%)	-1

```
Query  242  TVYTITSARIVMRIGAALTLTLNLPYRELGNASLKLHKDGSGTIALETTGNINLSYLVLW  63
            TVYTIT+ R+ MRIGAALT+TLNLP+ ++ NA L+LH+DG+GTIAL+  GN  LSYLV W
Sbjct  100  TVYTITNRRVAMRIGAALTVTLNLPFSQVRNADLRLHRDGTGTIALDLMGNTRLSYLVCW  159

Query  62   PHARAWRFSPAQPALRCIQD  3
            PH R W     QPALRCI D
Sbjct  160  PHVRPWVIRRTQPALRCIPD  179
```